ISSN 1007-9327 (print)
ISSN 2219-2840 (online)

World Journal of *Gastroenterology*

World J Gastroenterol 2018 March 7; 24(9): 957-1062

Published by Baishideng Publishing Group Inc

World Journal of Gastroenterology

Contents

Weekly Volume 24 Number 9 March 7, 2018

REVIEW

957 Quantitative and noninvasive assessment of chronic liver diseases using two-dimensional shear wave elastography

Xie LT, Yan CH, Zhao QY, He MN, Jiang TA

ORIGINAL ARTICLE

Basic Study

971 Can bacterial virulence factors predict antibiotic resistant *Helicobacter pylori* infection?

Brennan DE, Dowd C, O'Morain C, McNamara D, Smith SM

982 Dysregulation of PARP1 is involved in development of Barrett's esophagus

Zhang C, Ma T, Luo T, Li A, Gao X, Wang ZG, Li F

992 Autophagy activation by Jiang Zhi Granule protects against metabolic stress-induced hepatocyte injury

Zheng YY, Wang M, Shu XB, Zheng PY, Ji G

1004 Long noncoding RNA RP4 functions as a competing endogenous RNA through miR-7-5p sponge activity in colorectal cancer

Liu ML, Zhang Q, Yuan X, Jin L, Wang LL, Fang TT, Wang WB

Retrospective Study

1013 Quality indicators in pediatric colonoscopy in a low-volume center: Implications for training

Lee WS, Tee CW, Koay ZL, Wong TS, Zahraq F, Foo HW, Ong SY, Wong SY, Ng RT

1022 Prognostic value of lymph nodes count on survival of patients with distal cholangiocarcinomas

Lin HP, Li SW, Liu Y, Zhou SJ

Clinical Practice Study

1035 Phenotypic and genotypic characterization of inflammatory bowel disease in children under six years of age in China

Fang YH, Luo YY, Yu JD, Lou JG, Chen J

Randomized Controlled Trial

1046 Effect of polyglycolic acid sheet plus esophageal stent placement in preventing esophageal stricture after endoscopic submucosal dissection in patients with early-stage esophageal cancer: A randomized, controlled trial

Chai NL, Feng J, Li LS, Liu SZ, Du C, Zhang Q, Linghu EQ

CASE REPORT

1056 Four cancer cases after esophageal atresia repair: Time to start screening the upper gastrointestinal tract

Vergouwe FW, Gottrand M, Wijnhoven BP, IJsselstijn H, Piessen G, Bruno MJ, Wijnen RM, Spaander MC

Contents

World Journal of Gastroenterology
Volume 24 Number 9 March 7, 2018

ABOUT COVER

Editorial board member of *World Journal of Gastroenterology*, Sang Chul Lee, MD, PhD, Chief Doctor, Full Professor, Professor, Surgeon, Surgical Oncologist, Division of Colorectal Surgery, Department of General Surgery, Catholic University of Korea, Daejeon St. Mary's Hospital, Daejeon 34943, South Korea

AIMS AND SCOPE

World Journal of Gastroenterology (*World J Gastroenterol*, *WJG*, print ISSN 1007-9327, online ISSN 2219-2840, DOI: 10.3748) is a peer-reviewed open access journal. *WJG* was established on October 1, 1995. It is published weekly on the 7th, 14th, 21st, and 28th each month. The *WJG* Editorial Board consists of 642 experts in gastroenterology and hepatology from 59 countries.

The primary task of *WJG* is to rapidly publish high-quality original articles, reviews, and commentaries in the fields of gastroenterology, hepatology, gastrointestinal endoscopy, gastrointestinal surgery, hepatobiliary surgery, gastrointestinal oncology, gastrointestinal radiation oncology, gastrointestinal imaging, gastrointestinal interventional therapy, gastrointestinal infectious diseases, gastrointestinal pharmacology, gastrointestinal pathophysiology, gastrointestinal pathology, evidence-based medicine in gastroenterology, pancreatology, gastrointestinal laboratory medicine, gastrointestinal molecular biology, gastrointestinal immunology, gastrointestinal microbiology, gastrointestinal genetics, gastrointestinal translational medicine, gastrointestinal diagnostics, and gastrointestinal therapeutics. *WJG* is dedicated to become an influential and prestigious journal in gastroenterology and hepatology, to promote the development of above disciplines, and to improve the diagnostic and therapeutic skill and expertise of clinicians.

INDEXING/ABSTRACTING

World Journal of Gastroenterology (*WJG*) is now indexed in Current Contents®/Clinical Medicine, Science Citation Index Expanded (also known as SciSearch®), Journal Citation Reports®, Index Medicus, MEDLINE, PubMed, PubMed Central and Directory of Open Access Journals. The 2017 edition of Journal Citation Reports® cites the 2016 impact factor for *WJG* as 3.365 (5-year impact factor: 3.176), ranking *WJG* as 29th among 79 journals in gastroenterology and hepatology (quartile in category Q2).

NAME OF JOURNAL
World Journal of Gastroenterology

ISSN
ISSN 1007-9327 (print)
ISSN 2219-2840 (online)

LAUNCH DATE
October 1, 1995

FREQUENCY
Weekly

EDITORIAL OFFICE
Ze-Mao Gong, Director
World Journal of Gastroenterology
Baishideng Publishing Group Inc
7901 Stoneridge Drive, Suite 501,
Pleasanton, CA 94588, USA
Telephone: +1-925-2238242
Fax: +1-925-2238243
E-mail: editorialoffice@wjgnet.com
Help Desk: http://www.f6publishing.com/helpdesk
http://www.wjgnet.com

PUBLISHER
Baishideng Publishing Group Inc
7901 Stoneridge Drive, Suite 501,
Pleasanton, CA 94588, USA
Telephone: +1-925-2238242
Fax: +1-925-2238243
E-mail: bpgoffice@wjgnet.com
Help Desk: http://www.f6publishing.com/helpdesk
http://www.wjgnet.com

PUBLICATION DATE
March 7, 2018

INSTRUCTIONS TO AUTHORS
Full instructions are available online at http://www.wjgnet.com/bpg/gerinfo/204

ONLINE SUBMISSION
http://www.f6publishing.com

World Journal of Gastroenterology

Submit a Manuscript: http://www.f6publishing.com

World J Gastroenterol 2018 March 7; 24(9): 957-970

DOI: 10.3748/wjg.v24.i9.957

ISSN 1007-9327 (print) ISSN 2219-2840 (online)

REVIEW

Quantitative and noninvasive assessment of chronic liver diseases using two-dimensional shear wave elastography

Li-Ting Xie, Chun-Hong Yan, Qi-Yu Zhao, Meng-Na He, Tian-An Jiang

Li-Ting Xie, Chun-Hong Yan, Qi-Yu Zhao, Meng-Na He, Tian-An Jiang, Department of Ultrasound, The First Affiliated Hospital, College of Medicine, Zhejiang University, Hangzhou 310003, Zhejiang Province, China

ORCID number: Li-Ting Xie (0000-0002-0498-193X); Chun-Hong Yan (0000-0001-8084-4155); Qi-Yu Zhao (0000-0002-8732-8564); Meng-Na He (0000-0002-8178-3531); Tian-An Jiang (0000-0002-7672-8394).

Author contributions: Xie LT, Yan CH, Zhao QY, He MN and Jiang TA contributed to the research, and to drafting and editing of the manuscript; all authors approved the final draft submitted.

Conflict-of-interest statement: Authors declare no conflict of interests for this article.

Manuscript source: Unsolicited manuscript

Correspondence to: Tian-An Jiang, MD, PhD, Professor, Surgeon, Department of Ultrasound, The First Affiliated Hospital, College of Medicine, Zhejiang University, Qingchun Road, No.79, Hangzhou 310003, Zhejiang Province, China. tiananjiang@zju.edu.cn
Telephone: +86-18857127666

Received: December 28, 2017
Peer-review started: December 29, 2017
First decision: January 17, 2018
Revised: February 1, 2018
Accepted: February 9, 2018
Article in press: February 9, 2018
Published online: March 7, 2018

Abstract

Two-dimensional shear wave elastography (2D-SWE) is a rapid, simple and novel noninvasive method that has been proposed for assessing hepatic fibrosis in patients with chronic liver diseases (CLDs) based on measurements of liver stiffness. 2D-SWE can be performed easily at the bedside or in an outpatient clinic and yields immediate results with good reproducibility. Furthermore, 2D-SWE was an efficient method for evaluating liver fibrosis in small to moderately sized clinical trials. However, the quality criteria for the staging of liver fibrosis are not yet well defined. Liver fibrosis is the main pathological basis of liver stiffness and a key step in the progression from CLD to cirrhosis; thus, the management of CLD largely depends on the extent and progression of liver fibrosis. 2D-SWE appears to be an excellent tool for the early detection of cirrhosis and may have prognostic value in this context. Because 2D-SWE has high patient acceptance, it could be useful for monitoring fibrosis progression and regression in individual cases. However, multicenter data are needed to support its use. This study reviews the current status and future perspectives of 2D-SWE for assessments of liver fibrosis and discusses the technical advantages and limitations that impact its effective and rational clinical use.

Key words: Elastography; Shear wave; Chronic liver disease; Liver fibrosis

Core tip: There has been considerable research in recent years dedicated to the development of noninvasive methods of chronic liver diseases (CLDs). These include novel elastography methods. In this review, we outline the current state and future perspectives of the commonly used two-dimensional

shear wave elastography (2D-SWE) in CLDs. In particular, we discuss the applications and problems in chronic viral hepatitis, nonalcoholic fatty liver disease, alcoholic liver disease, liver transplantation, focal liver lesions, and autoimmune liver disease to synthesize existing evidence for the reader. This is the first full and complete review to assess various CLDs using 2D-SWE.

Xie LT, Yan CH, Zhao QY, He MN, Jiang TA. Quantitative and noninvasive assessment of chronic liver diseases using two-dimensional shear wave elastography. *World J Gastroenterol* 2018; 24(9): 957-970 Available from: URL: http://www.wjgnet.com/1007-9327/full/v24/i9/957.htm DOI: http://dx.doi.org/10.3748/wjg.v24.i9.957

INTRODUCTION

Liver fibrosis results from repetitive or sustained liver inflammation caused by chronic liver diseases (CLDs) and has serious long-term consequences in terms of patient morbidity and mortality due to the progression to cirrhosis. Patients with cirrhosis are at a higher risk of developing complications, including esophageal varices, ascites, liver failure and hepatocellular carcinoma (HCC), than healthy individuals[1,2]. Liver fibrosis is an important factor in the development of various CLDs and is mainly mediated by chronic liver injury, which leads to liver fibrosis characterized by increased extracellular matrix production by fibroblast-like cells and increased liver stiffness (LS)[3]. The precise assessment of the severity of liver fibrosis and reliable diagnosis of cirrhosis are vital steps in the management of CLDs, as they provide information that impacts therapeutic decisions[4,5].

Liver biopsy remains the reference standard for the staging of liver fibrosis, despite its limitations, including its invasivity and the pain experienced by patients, high cost, risk of bleeding and poor reproducibility, and contraindications, such as cases of massive ascites[6,7]. Furthermore, the accuracy of liver biopsy is influenced by several factors, including intra- and interobserver variability and sampling error[8,9]. Given these limitations, liver biopsy is not an ideal method for repeated assessments of disease progression as well.

The noninvasive assessment of liver fibrosis has recently become a research focus, leading to the introduction of new technologies. In particular, shear wave elastography (SWE), which is based on ultrasound (US) technology, has been widely applied and has gained acceptance. The latest guidelines on the clinical use of liver US elastography of the European Federation of Societies for Ultrasound in Medicine and Biology (EFSUMB)[10] and the guidelines on the evaluation of liver disease severity and prognosis of the European Association for the Study of the Liver- Asociación Latinoamericana para el Estudio del Hígado state that two-dimension (2D)-SWE is a valid and promising technique for noninvasive staging of liver fibrosis in viral hepatitis and seems to be at least equivalent to transient elastography (TE) and point SWE (pSWE)/acoustic radiation force impulse (ARFI)[11].

THE BASICS OF 2D-SWE

Comparison of elastography methods

Several elasticity imaging techniques have recently been developed for assessing the mechanical properties of liver tissues and staging the fibrosis level using different imaging modalities. In accordance with the Guidelines for the Basic Principles and Technology of EFSUMB[12], the available US-based elastography techniques include strain elastography (SE) and SWE; SWE can be further subdivided into three techniques - TE, pSWE and 2D-SWE - in addition to radiology-based magnetic resonance elastography (MRE).

Among these, TE is the most widely used elastography method. However, in a study of 13369 CLD patients over a 5-year period of using TE, unreliable results were obtained in 15.8% of cases[13]. The limitations of TE, such as the difficulty in measuring obese patients and patients with narrow intercostal spaces, the variations in operator experience, and the fact that it is not applicable in patients with ascites, were the primary factors contributing to these unreliable results. Importantly, the issue of obesity has been partially addressed by the introduction of specially designed XL probes that measure LS deeper than the standard M probes. It has also been reported that TE and ARFI elastography are inaccurate in the detection of early and intermediate fibrosis[14,15].

MRE can be used to quantitatively diagnose liver fibrosis with high accuracy and is mainly used for the diagnosis of advanced liver fibrosis and cirrhosis. The diagnostic accuracy of MRE increased when the liver fibrosis was getting serious, whereas the level of early fibrosis detected by MRE is inaccurate[16,17]. 2D-SWE is the latest elastography technology and can assess the elasticity of liver tissue easily and quickly, thus reflecting the degree of liver fibrosis. Table 1 demonstrates the comparison of currently available noninvasive methods in patients with CLD.

Principles of 2D-SWE

2D-SWE is a novel noninvasive method that has been proposed for assessing LS by measuring the velocity of elastic shear waves in the liver parenchyma[18]. In SWE, shear waves are created by US-generated pulses of an acoustic radiation force (Figure 1). The velocity of the shear wave is then estimated by a Doppler-like effect over a region of interest (ROI) and is related to the stiffness or elasticity of the medium[19]. This shear wave velocity can be used to calculate the tissue stiffness by the formula $E = \rho c^2$, where E is tissue elasticity (Young's modulus, kPa), ρ is tissue density (kg/m^3), and c is shear wave velocity (m/s)[20,21].

Table 1 Comparison of currently available noninvasive methods in patients with chronic liver disease

Content	Methods			
	TE	pSWE	2D-SWE	MRE
Technical principle	TE was the first commercially available elastography method developed for measuring liver stiffness using a dedicated device that includes an amplitude modulation (A) mode image for organ localization	pSWE can be implemented on a common ultrasound diagnostic system. It uses a regular ultrasonic probe to emit a single impulse of acoustic radiation force and generates a shear wave to detect the shear wave propagation velocity	2D-SWE is the combination of a radiation force applied to the tissues by focused ultrasonic beams and a very high frame rate US imaging sequence, which is able to capture the propagation of resulting the shear waves in real time	MRE enables the measurement of liver stiffness with an MRI-compatible generator; mechanical shear waves are delivered to the tissue and displayed as elastograms using phase-contrast image sequences
Reference point	▪Young's modulus (kPa)	▪Shear wave speed (m/s) ▪Young's modulus (kPa)	▪Shear wave speed (m/s) ▪Young's modulus (kPa)	▪Shear wave speed (m/s) ▪Young's modulus (kPa)
Selected example	▪FibroScan (Echosens, France)	▪VTQ using ARFI imaging (Siemens Healthcare, Germany) ▪ElastPQ (Philips Healthcare, Netherlands) ▪Shear Wave Measurement (Hitachi Aloka Medical, Japan)	▪SWE (SuperSonic Imagine, France) ▪Virtual Touch IQ (Siemens Healthcare, Germany) ▪Logiq E9 (GE Healthcare, United Kingdom) ▪Aplio 500 (Toshiba Medical Systems, United Kingdom)	▪MR Touch (GE Healthcare, United Kingdom) ▪MRE (Philips Healthcare, Netherlands; Siemens Healthcare, Germany)
Advantages	▪Most widely used and validated technique ▪Quality criteria well defined ▪ User friendly, rapid, easy to measure at the bedside ▪Good reproducibility ▪Good performance for noninvasive assessments of liver fibrosis staging ▪Excellent diagnostic accuracy for excluding liver cirrhosis ▪Prognostic value in cirrhosis	▪Can be performed using a regular US machine ▪ The ROI can be positioned under B-mode visualization ▪Higher applicability than TE (not limited by ascites or obesity) ▪pSWE is equal to the performance of TE for significant fibrosis and cirrhosis	▪Can be performed using a regular US machine ▪ Simple and fast to use ▪ The ROI can be positioned under B-mode visualization ▪ A larger ROI than that of TE and pSWE ▪Good applicability (not limited by ascites or obesity) ▪Good stability and reproducibility ▪Generates a real-time quantitative map of liver tissue stiffness ▪Can avoid large vessels and the gallbladder ▪ High performance for cirrhosis	▪Can be performed using a regular MRI machine ▪ Good stability and reproducibility ▪Scans the whole liver ▪Higher applicability than TE (not limited by ascites or obesity) ▪Excellent diagnostic accuracy for noninvasive staging of liver fibrosis and cirrhosis
Disadvantages	▪Requires a special device and probe ▪ ROI size is rather small and cannot be chosen ▪Lack of applicability (limited by ascites, severe obesity) ▪No B-mode orientation ▪ Cannot avoid large vessels or the gallbladder ▪Unable to distinguish between intermediate stages of liver fibrosis	▪ROI size is smaller than that of TE and cannot be modified ▪Quality criteria not yet well defined ▪Narrow range of values ▪Unable to distinguish between intermediate stages of liver fibrosis	▪Quality criteria not well defined ▪ No further prospective studies published ▪ Many factors cause failed measurements in clinical practice ▪Unable to distinguish between intermediate stages of liver fibrosis	▪Time-consuming ▪Even more costly than SWE and TE ▪ Failure can occur due to claustrophobia and iron overload ▪Affected by respiratory movement ▪ Hepatic MRE signal may be so low that waves cannot be adequately visualized with a gradient-echo based MRE sequence

2D-SWE: Two-dimensional shear wave elastography; MRE: Magnetic resonance elastography; MRI: Magnetic resonance imaging; pSWE: Point shear wave elastography; ROI: Region of interest; TE: Transient elastography; US: Ultrasound; VTQ: Virtual touch tissue quantification.

Elasticity is shown on a color-coded image displayed on a B-mode image. Then, with the ROI on the elasticity image, the mean, maximal and minimal LS values within the ROI can be visualized on a screen, along with the standard deviation (SD) of the measured elasticity[19,22]. The size and position of the ROI can be modified by the operator based on the specific goals of each liver assessment (Figure 2). In general, red areas indicate larger Young's modulus of stiffer tissues, while blue areas indicate smaller Young's modulus of softer tissues.

Examination technique

2D-SWE examination of the liver is performed by using convex US probes with integrated technological solutions allowing elasticity imaging and measurements, according to the World Federation for Ultrasound in Medicine and Biology[22,23] and the EFSUMB Guidelines for the Clinical Use of US Elastography[10,12], as well as the Society of Radiologists in Ultrasound Consensus Conference Statement regarding the assessment of liver fibrosis by elastography[24]. The proper examination procedure is described in Table 2, and the precautions

Table 2 Procedures of two-dimensional shear wave elastography

Key points	Procedures
Adequate preparation	▪ Fast and rest before the exam ▪ Perform in a supine position ▪ Train the patients on breathing
Accurate positioning	▪ Scan the 6/7/8 intercostal spaces of the right liver ▪ Acquire stable and high-quality images ▪ Instruct the patient to hold the breath for 3-5 s
Stable measurement	▪ Switch to SWE mode ▪ Freeze the image and adjust the position of the ROI ▪ Calculate the LS automatically ▪ Average the repeated measurement values

LS: Liver stiffness; ROI: Region of interest; SWE: Shear wave elastography.

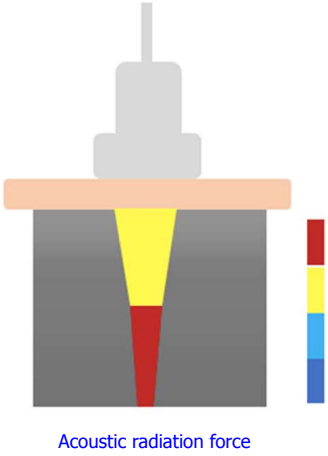

Figure 1 The principle of two-dimensional shear wave elastography. 2D-SWE is created by ultrasound-generated pulses from an acoustic radiation force that produce plane shear waves, and the propagation of the resulting shear waves can be captured in real time. 2D-SWE: Two-dimensional shear wave elastography.

and techniques of 2D-SWE in Table 3.

Normal value

"Normal" LS values have recently been studied in healthy subjects who have undergone a professional check-up and who have no overt causes of liver disease, with normal liver enzymes. Various results for normal LS values are shown in Table 4.

CLINICAL APPLICATIONS OF 2D-SWE

Diagnosis of chronic viral hepatitis

Viral hepatitis is a global public health issue, with approximately 248 million and 185 million people worldwide suffering from chronic hepatitis B (CHB) and hepatitis C (CHC), respectively[25-27]. Patients with advanced liver fibrosis from chronic viral hepatitis have a high risk of developing liver cancer and related complications, including portal hypertension (PH), esophageal and gastric variceal bleeding (EGVB), and liver failure. In these cases, prognosis and treatment are mainly affected by the degree of fibrosis, and the primary aim of treatment is controlling the progression of liver fibrosis[28,29]. The clinical practice guidelines for the management of CHB and CHC of the European Association for the Study of the Liver (EASL)[30,31], as well as the World Health Organization Guidelines for the Prevention, Care and Treatment of Persons with Chronic Hepatitis B Infection[32], recommend elastography as a routine method for clinically evaluating liver fibrosis to avoid the need for liver biopsy in some patients.

Recent studies performed worldwide have focused on 2D-SWE for determining the role of viral hepatitis in liver fibrosis. In one study, 454 CHB patients were examined by 2D-SWE and TE[33]. The results showed that 2D-SWE provided a more accurate correlation of liver elasticity with liver fibrosis stage than TE, especially for the identification of significant fibrosis (≥ F2). Bavu *et al*[18] examined 113 CHC patients and found that SWE performed better diagnostically for early, intermediate and advanced predicted levels of fibrosis than TE. Ferraioli *et al*[20] used biopsy as a reference to assess the accuracy of SWE and TE in 121 CHC patients; they found that real-time SWE was more accurate than TE for assessing significant fibrosis (≥ F2). These results were strongly supported by three meta-analyses published by other authors[34-36]. In addition, a recent large-sample meta-analysis concluded that SWE was more accurate for advanced fibrosis (≥ F3) and cirrhosis (F4)[37]. What's more, Grgurevic *et al*[38] evaluated the performance of real-time 2D-SWE for quantitatively assessing liver and spleen stiffness in patients with chronic viral hepatitis. They showed that real-time 2D-SWE can accurately identify various degrees of liver fibrosis and cirrhosis and demonstrated that liver and spleen stiffness continue to increase even after cirrhosis has developed. In fact, they noticed that spleen and liver stiffness tended to converge in more advanced stages of liver cirrhosis. This is an important study showing that 2D-SWE can be used to study the evolution of liver disease beyond cirrhosis.

As described above, SWE has high accuracy and specificity for assessing liver fibrosis due to chronic viral hepatitis, which makes it convenient for the real-time clinical monitoring of liver fibrosis. SWE technology is expected to replace biopsy, thereby eliminating the invasiveness and poor reproducibility of the latter technique. However, the quality criteria for the staging of liver fibrosis are not yet well defined. In addition, 2D-SWE has shown different diagnostic accuracies for liver fibrosis in patients with CHB and CHC. We suppose that this is probably due to the different etiologies of hepatitis B virus (HBV) and hepatitis C virus that lead to different tissue patterns and distributions of fibrosis development. Specifically, cirrhosis patients with HBV tend to produce larger regenerative nodules, which may result in different LS measurements if the ROI is placed in such an area. These findings suggest that assessments of the degree of liver fibrosis in different liver diseases cannot be based on the same diagnostic criteria, leading to

Table 3 Precautions and techniques of two-dimensional shear wave elastography

Key points	Precautions and techniques
Fasting and resting	▪ Patients should fast for a minimum of 2 h and rest for a minimum of 10 min before undergoing liver stiffness measurement with SWE
Position	▪ Measurement of liver stiffness by 2D-SWE should be performed in a supine position with the right arm maximally extended; this position ensures the best possible access for assessing the right liver lobe ▪ The transducer is placed in a right intercostal space to visualize the right liver lobe in B mode
Breathing train	▪ Instruct the patient not to breathe in or breathe out deeply in order to eliminate unreliable measurements induced by breathing movements ▪ It has been suggested that a breath hold for a few seconds during quiet breathing may lead to the best results
Clear 2D-US images	▪ Adequate B-mode liver image is a prerequisite for 2D-SWE measurements ▪ Must avoid the ribs, gas and other factors of routine ultrasound ▪ The appropriate pressure can be applied with the ultrasound probe to broaden the intercostal space and, thus, acquiring clear images. Contrary to the ordinary suggestion, this does not increase the liver's stiffness, as the intervening tissues prevent distortion of the liver surface
Scale	▪ Generally, the Young's modulus scale should not be less than 30 kPa and preferably not higher than 150 kPa
Depth	▪ Liver stiffness measured by 2D-SWE should be performed at least 10 mm under the liver capsule ▪ Measurements should not be performed too deep or too close, in order to avoid reverberation artifacts, insufficient penetration and acoustic shadow, as these factors will lead to incorrect results
Sampling frame	▪ The sampling frame should be placed in a well-visualized area of the right liver lobe, free of large vessels, the gallbladder, the liver capsule, and any other hollow organs ▪ In addition, the sampling frame should be placed in the center of the image
ROI	▪ For valid measurement quality of 2D-SWE, the ROI should be placed at a minimum of 1-2 cm and a maximum of 6 cm beneath the liver capsule ▪ The SWE acquisition is continued for 4-5 s once a stable SWE image is obtained ▪ The operator freezes the image, and the ROI should be placed in the most homogeneously colored area of the SWE ROI
Penetration mode	▪ When measuring patients with thick subcutaneous fat, fatty liver or advanced cirrhosis, SWE can be adjusted to "Pen" mode to improve the measurement success rate ▪ In 2D-SWE, if the signal is weak or unstable, the penetration mode can be activated

2D-SWE: Two-dimensional shear wave elastography; 2D-US: Two-dimensional ultrasound; Pen: Penetration; ROI: Region of interest; SWE: Shear wave elastography.

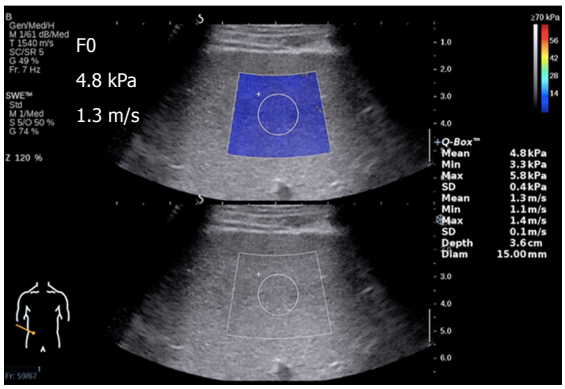

Figure 2 Example of two-dimensional shear wave elastography of the liver implemented using the Aixplorer US system (SuperSonic Imaging, France), which can be displayed simultaneously with the B-mode image. A 2D-SWE image from a 42-year-old male who had normal liver function with liver biopsy-proven fibrosis at METAVIR stage F0. The rectangular box is the area of view where the shear wave measurements were made and color-coded. The round circle is the ROI where the measurements were obtained. The system provides the mean, Max, Min, SD and Diam of the stiffness measurements within the ROI. For this case, the following measurements were made: Young's modulus: Mean = 4.8 kPa, Min = 3.3 kPa, Max = 5.8 kPa, SD = 0.4 kPa; shear wave velocity: Mean = 1.3 m/s, Min = 1.1 m/s, Max = 5.8 m/s, SD = 0.1 m/s, Depth = 3.6 cm, and Diam = 15.0 mm. 2D-SWE: Two-dimensional shear wave elastography; Diam: Diameter; Max: Maximum; Min: Minimum; ROI: Region of interest; SD: Standard deviation; US: Ultrasound.

the issue of how to establish diagnostic criteria for patients with multiple CLDs, *e.g.*, HBV patients with nonalcoholic fatty liver disease (NAFLD).

In the future, diagnosis and treatment in such situations will require personalization. The lack of specific criteria may also be due to the paucity of studies, small sample sizes, and diverse research areas; future developments will require more evidence-based medical data from large-scale, multicenter studies. Table 5 includes the cut-off values of LS assessed by 2D-SWE in various studies. Figure 3 shows 2D-SWE of liver fibrosis at METAVIR stages F1 through F4. Note that the LS gradually increases, and the color of the sampling frame gradually changes in the initial stages and incrementally increases in the later stages of fibrosis.

Diagnosis of NAFLD

NAFLD is the most prevalent CLD, representing a spectrum ranging from simple fatty liver (SFL) to nonalcoholic steatohepatitis (NASH)[39,40]. NAFLD has become a global health problem, with a prevalence comparable to the rates of metabolic syndrome, obesity, type 2 diabetes mellitus and dyslipidemia[41,42]. The morbidity and mortality of patients with NAFLD are related to the development of NASH, which may progress to fibrosis and cirrhosis, even resulting in an increased risk of HCC[43]. A meta-analysis[44] demonstrated that even SFL may result in fibrosis development, and fibrosis development was observed in approximately 30% of patients with SFL, as well as in patients with NASH. Liver fibrosis, but no other histological features, has been demonstrated as the

Table 4 Summary of the literature for two-dimensional shear wave elastography normal values

Ref.	Year	Country	Number	Mean age	Sex, female/male	Mean SWE, standard deviation, range	Remarks
Muller *et al*[19]	2009	France	15	NA	NA	2.6-6.2 kPa	No data available regarding age or sex of normal subjects
Ferraioli *et al*[79]	2012	Italy	42	34.8	13/29	4.92-5.39 kPa	
Sirli *et al*[82]	2013	Romania	82	26	56/26	6.0 ± 1.4 kPa	Female: 5.7 ± 1.3 kPa Male: 6.6 ± 1.5 kPa BMI ⩾ 25 kg/m²: 6.5 ± 1.5 kPa BMI < 25 kg/m²: 5.8 ± 1.3 kPa
Hudson *et al*[83]	2013	Canada	15	27	5/10	5.55 ± 0.74 kPa	
Wang *et al*[84]	2014	China	30	36.1 ± 14.7	14/16	4.29 kPa	
Suh *et al*[73]	2014	South Korea	196	29.2 ± 9.2	66/130	2.6-6.2 kPa	
Huang *et al*[85]	2014	China	502	37.9	310/192	5.10 ± 1.02 kPa	Female: 5.45 ± 1.02 kPa Male: 4.89 ± 0.96 kPa
Yoon *et al*[86]	2014	South Korea	122	NA	NA	5.12 ± 1.46 kPa (session Ⅰ) 4.95 ± 1.40 kPa (session Ⅱ)	No data available regarding age or sex of normal subjects
Leung *et al*[33]	2013	China	171	40.6 ± 10.8	103/68	5.5 ± 0.7 kPa	Female: 5.7 ± 0.5 kPa Male: 5.4 ± 0.7 kPa
Franchi-Abella *et al*[87]	2016	France	51	0-15	26/25	6.53 ± 1.38 kPa	No significant differences were observed between male and female patients, right and left lobes, or different breathing conditions

NA: Not available.

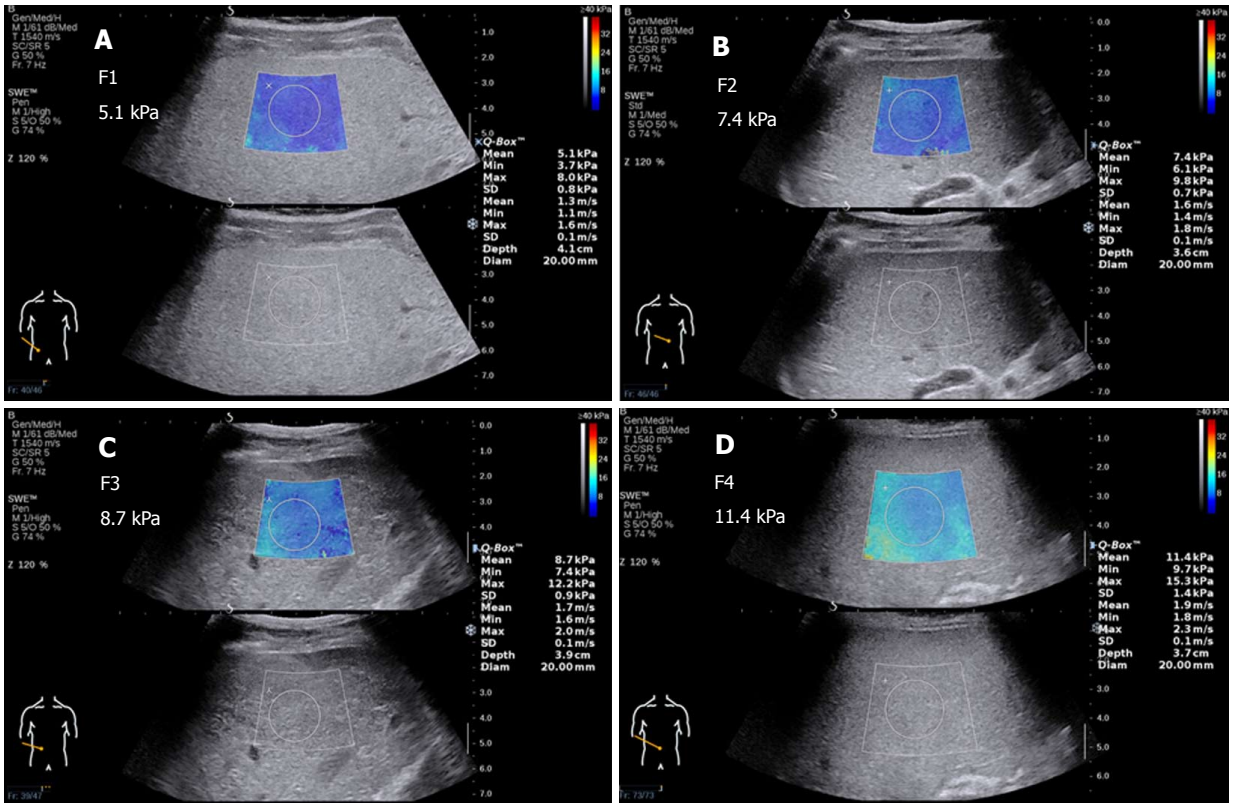

Figure 3 Two-dimensional shear wave elastography (Aixplorer US system, SuperSonic Imaging, France) of the liver in chronic hepatitis B patients with liver biopsy-proven fibrosis at METAVIR stages F1 through F4. A: F1 stage, mean Young's modulus = 5.1 kPa, mean shear wave velocity = 1.3 m/s; B: F2 stage, mean Young's modulus = 7.4 kPa, mean shear wave velocity = 1.4 m/s; C: F3 stage, mean Young's modulus = 8.7 kPa, mean shear wave velocity = 1.7 m/s; D: F4 stage, mean Young's modulus = 11.4 kPa, mean shear wave velocity = 1.9 m/s. Note the liver stiffness gradually increases, and the color of the sampling frame gradually changes in the initial stages and incrementally increases in the later stages of fibrosis. 2D-SWE: Two-dimensional shear wave elastography; US: Ultrasound.

single most crucial histological feature associated with the risk of liver-related complications and death in patients with NAFLD[45]. Therefore, the most important issue for patients with NAFLD is recognizing and assessing the stage of liver fibrosis, which is possible by using US elastography.

Table 5 Cut-off values of liver stiffness assessed with two-dimensional shear wave elastography in various studies

Ref.	Etiologies	Year	Country	Patients, *n*	⩾ F1 (fibrosis)		⩾ F2 (significant fibrosis)		⩾ F3 (severe fibrosis)		F4 (cirrhosis)	
					Cut-off, kPa	AUROC, %	Cut-off, kPa	AUROC, %	Cut-off, kPa	AUROC, %	Cut-off, kPa	AUROC, %
Leung *et al*[33]	HBV	2013	China	454	6.5	86	7.1	88	7.9	93	10.1	98
Herrmann *et al*[37]	HBV	2017	Germany	206	NA	NA	7.1	91	8.1	91	11.5	96
Zeng *et al*[29]	HBV	2014	China	303	NA	NA	7.2	92	9.7	95	11.7	95
Bavu *et al*[18]	HCV	2011	France	113	NA	NA	9.1	95	10.1	96	13.3	97
Ferraioli *et al*[20]	HCV	2012	Italy	121	NA	NA	7.1	92	8.7	98	10.4	98
Grgurevic *et al*[38]	CVH	2015	Croatia	123	NA	NA	8.1	99	NA	NA	10.8	95
Cassinotto *et al*[46]	NAFLD	2014	France	108	NA	NA	6.3	86	8.3	89	10.5	88
Garcovich *et al*[47]	NAFLD	2016	Italy	78	5.1	92	6.7	96	NA	NA	NA	NA
Thiele *et al*[51]	ALD	2016	Denmark	199	NA	NA	10.2	94	NA	NA	16.4	95

2D-SWE: Two-dimensional shear wave elastography; ALD: Alcoholic liver disease; AUROC: Area under the receiver operating characteristic curve; CVH: Chronic viral hepatitis; HBV: Hepatitis B virus; HCV: Hepatitis C virus; LS: Liver stiffness; NA: Not available; NAFLD: Nonalcoholic fatty liver disease.

Cassinotto *et al*[46] enrolled 291 patients with NAFLD and compared the performance of 2D-SWE, TE and Virtual Touch Quantification using liver biopsy as the reference method. They found that although obesity was related to an increased rate of failed LS measurements, these techniques, especially SWE, were valuable for diagnosing liver fibrosis in patients with NAFLD. The diagnostic performances of 2D-SWE for assessing liver fibrosis are as follows. For a sensitivity of at least 90% for diagnosing significant fibrosis (⩾ F2), severe fibrosis (⩾ F3) and cirrhosis (F4), the specificity is approximately 60%-70%; for a specificity of at least 90%, the sensitivity is approximately 50%-70%. 2D-SWE had areas under the receiver operating characteristic curves of 86%, 89% and 88% for the diagnosis of ⩾ F2, ⩾ F3 and F4, respectively. Furthermore, LS was mainly related to the fibrosis stage, and steatosis, inflammation and hepatocyte ballooning did not have significant influences on LS. Some NASH patients may have no fibrosis, and SWE may not be useful for the diagnosis of early-stage NASH without fibrosis. Hence, the next question became whether SWE can differentiate NASH from SFL, especially in the early stages of fibrosis. Probably not, and this is an area that relies on biochemical methods. Solutions to these problems will require multifaceted, prospective clinical studies to establish cut-off values for fibrosis staging.

In a study using SWE to identify the diagnostic accuracy of different degrees of fibrosis in 78 pediatric patients with biopsy-proven NASH[47], SWE was shown to be able to accurately evaluate significant liver fibrosis and, less efficiently, mild liver fibrosis in pediatric NAFLD patients. The study suggested that SWE can be used to assess liver fibrosis not only in adults but also in children and adolescents. However, few studies have focused on children; although fibrosis can be detected in children, the stage of fibrosis cannot yet be fully resolved, especially for fibrosis due to fatty liver. Consequently, the technique should be extended to all ages to further demonstrate the stability and reliability of the results.

Diagnosis of alcoholic liver disease

Alcoholic liver disease (ALD) is the most common liver disease in the Western world. Chronic and excessive alcohol consumption is responsible for the progression of alcoholic steatosis, hepatitis, fibrosis and cirrhosis. Complete therapy requires abstention from alcohol. Moreover, liver transplantation (LT) remains a life-saving treatment for patients with advanced ALD[48,49]. The EASL published clinical practice guidelines for the management of ALD in 2012[50]. The guidelines noted that elastography is a notable method for the early diagnosis of alcoholic cirrhosis.

A recent prospective study of 199 alcohol-overusing individuals with varying degrees of alcoholic liver fibrosis evaluated two elastography methods for the diagnosis of alcoholic fibrosis and cirrhosis, using liver biopsy as a reference[51]. The study found that 2D-SWE has a high accuracy (area under the curve ⩾ 0.92) for identifying subjects with significant fibrosis and cirrhosis, and the 2D-SWE cut-off values for optimal identification of significant fibrosis and cirrhosis were 10.2 kPa and 16.4 kPa. 2D-SWE was an extremely useful tool for diagnosing alcoholic fibrosis and, furthermore, was more appropriate for diagnosing early cirrhosis than for distinguishing

between early and advanced cirrhosis. However, the threshold values that will allow the accurate diagnosis of cirrhosis by SWE and obviate the need for liver biopsy in adults with ALD remain to be determined.

Patients with advanced ALD ultimately experience life-threatening complications, such as PH and ascites. These may lead to EGVB, which is among the most important causes of high mortality in patients with cirrhosis[52]. Therefore, assessing the severity of PH during follow-up is essential in patients with cirrhosis. The hepatic venous pressure gradient (HVPG) has been used to assess PH, but it is rarely used in clinical practice because of its invasiveness. A recent study found that LS measured by SWE is an independent predictor of the presence of HCC and esophageal and gastric varices in patients with CLD[53]. Another study demonstrated that SWE, as a promising tool to diagnose PH, has outstanding diagnostic accuracy, with a specificity and sensitivity ranging around 80%, and showed it to be superior to TE[54]; however, more than 30% of the clinically significant PH patients could not be conclusively diagnosed or ruled disease-free because their SWE values were between the cut-offs. Several recent studies have reported that LS measured by SWE in connection with HVPG is important for predicting clinically significant PH in patients with cirrhosis[55,56]. Thus, although 2D-SWE has exceptional clinical value for assessing HCC patients with PH and EGVB, it still cannot replace digestive endoscopy[52].

Assessment of end-stage liver disease after LT

LT is the only therapy for many patients who eventually progress to end-stage liver disease. However, LT is associated with a high rate of complications, which are difficult to identify in the early stages. One study reported a right lobe liver transplant recipient who experienced anastomotic stenosis of the right hepatic vein. SWE was quantitatively used to evaluate stiffness. The results suggested that SWE may be a noninvasive tool for assessing alterations in LS secondary to hepatic venous congestion after LT[57]. Another study showed that SWE may be useful during follow-up after LT. Liver rejection or hepatitis can be predicted at > 4 wk based on liver grafts that are stiffer than normal[58]. In a more recent study, SWE was successfully utilized to monitor the therapeutic effects of direct-acting antivirals in hepatitis C recurrence after LT; the median LS values decreased dramatically after treatment ($P < 0.001$). The study suggested that SWE is a valid diagnostic tool to follow-up hepatitis C patients undergoing LT[59].

From this study, we observed that SWE aids in the clinical diagnosis and detection of complications after LT, which represents great progress in SWE technology from diagnosis to monitoring. However, few studies have examined elastography in LT. This study represents the first step, although there is great potential for future research opportunities. Moreover, US elastography should be applied more for monitoring and predicting the complications of LT, particularly for assessing disease progression and prognosis.

Assessment of focal liver lesions

Focal liver lesions (FLLs) represent novel lesions for the field of US elastography and include those found in hemangioma, HCC, focal nodular hyperplasia (FNH), metastatic cancer and adenoma. Several studies have reported that 2D-SWE is a useful method for distinguishing FLLs, although it does not completely distinguish benign from malignant lesions[60-64]. The stiffness of lesions in liver malignancies is significantly higher than that of the liver parenchyma and is also higher than that of benign lesions[60,61] (Figure 4 shows HCC images of 2D-SWE). In malignant tumors, the hardness values of metastases were significantly higher than those found in HCC and cholangiocarcinoma[62]. In benign lesions, 2D-SWE has been regarded as a practical tool for distinguishing FNH from adenoma[63].

A recent study demonstrated the correct differentiation between benign and malignant FLLs by using real-time 2D-SWE in 96.1% of patients (area under the curve = 0.98)[64]. They used three elastography parameters, the mean stiffness of the FLL, the ratio between the minimal and maximum lesion stiffness, and the ratio between the stiffness of the FLL and the surrounding liver parenchyma to construct a new Liver Elastography Malignancy Prediction score based on a regression analysis. A simpler approach considering only mean lesion stiffness in a dichotomized fashion could be used to diagnose or rule-out malignancy with cut-off values of 14 kPa and 32.5 kPa, respectively.

Nonetheless, conclusions based on the current literature remain unclear. When 2D US and Doppler US suggest that a lesion is a benign tumor but elastography suggests malignancy, the lesion cannot therefore be diagnosed as malignant. Several technical limitations still exist. In situations in which the lesion is smaller than the ROI or located deep or near the heart, the shear wave propagation and imaging stability will be affected. Furthermore, lesion areas with necrotic liquefaction or calcification are not representative of the true lesion stiffness, which often leads to misdiagnosis.

Assessment of autoimmune liver disease

Autoimmune liver disease (AILDs) are intricate disorders resulting from the effects of multiple genes in association with environmental factors. The three major AILDs are primary biliary cirrhosis, primary sclerosing cholangitis and autoimmune hepatitis[65]. As they progress, these diseases may ultimately lead to chronic liver damage, liver fibrosis and cirrhosis. Zeng *et al*[66] used liver biopsy as the reference standard for determining the diagnostic accuracy of 2D-SWE for noninvasively assessing liver fibrosis in patients with AILD. Their results indicated that the optimal cut-off values for significant fibrosis (≥ F2), severe fibrosis (≥ F3) and cirrhosis (F4) were 9.7

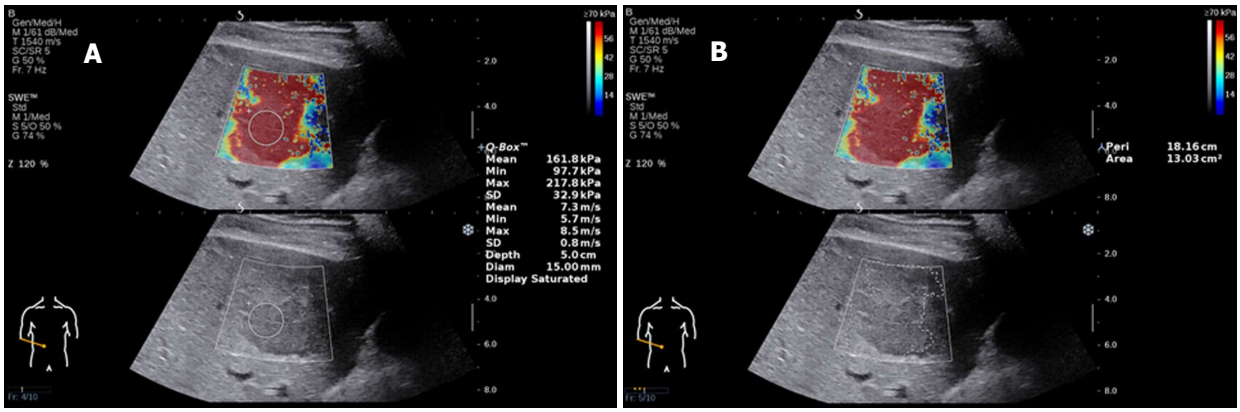

Figure 4 Two-dimensional shear wave elastography (Aixplorer US system, SuperSonic Imaging, France) images of a 69-year-old male with hepatocellular carcinoma based on the cirrhosis caused by hepatitis B virus. A: The mean Young's modulus is 161.8 kPa and the mean shear wave velocity is 7.3 m/s, which is obviously higher than the benign lesion; B: The area of the tumor is 13.03 cm^2. 2D-SWE: Two-dimensional shear wave elastography; HBV: Hepatitis B virus; HCC: Hepatocellular carcinoma; US: Ultrasound.

kPa, 13.2 kPa and 16.3 kPa, respectively. Moreover, the sensitivity and specificity ranged from 75% to 87% for all fibrosis stages. As these data show, SWE has high cut-off values in patients with AILD. The critical cut-off value was obviously higher than that for CHB/CHC. Therefore, different diseases have different thresholds, representing different developmental processes. AILD is relatively rare, and the current study was small; thus, further confirmation is necessary.

These results of LT, FLLs and AILD based on SWE cannot yet be clinically translated, as the research published to date is insufficient to definitively establish diagnostic criteria. However, elastography has shown promise for use in many research and development opportunities and future applications.

Future perspectives

Although there is evidence that 2D-SWE could become a crucial tool in end-stage liver disease, additional research and development are necessary. Additional work should focus on the role of SWE not only in cross-sectional diagnosis but also in longitudinal studies considering disease progression, regression and clinical outcomes[67]. Priority should be given to multicenter, large-scale verification research. Indeed, the longitudinal monitoring of fibrosis in patients with CLD may be a highly practical application for SWE. Preliminary research has revealed a remarkable decrease in LS values in patients with chronic viral hepatitis after continued antiviral treatment[68,69]. Given its high patient acceptance and good accessibility, SWE may also become a convenient tool for identifying patients with liver disease and a promising avenue for future research. However, several issues warrant further consideration.

The basic problem

1. Although alternative techniques, such as pSWE/ARFI or 2D-SWE, seem to overcome the limitations of TE, their quality criteria for the staging of liver fibrosis are not yet well defined.
   a. It remains unclear whether the shear wave Young's modulus or shear wave velocity is more representative.
   b. It remains unknown whether multiple measurements in one location are necessary when satisfactory measures of stiffness are obtained. Or, whether measurements in more than one location are needed.
   c. There is currently no agreement on objective quality criteria regarding what constitutes a valid measurement and what is an invalid measurement.
2. It remains unknown whether a simple semi-quantitative fibrosis score can adequately reflect the complexity of the pathophysiological process.

The clinical questions

1. In the era of promotion of precision medicine, can 2D-SWE accurately guide clinical work to aid in the design of an antiviral therapy for hepatitis B patients?
2. Can 2D-SWE be a reliable measurement of the prognosis of liver fibrosis?
3. Does a greater Young's modulus indicate more serious disease progression? Does a reduced Young's modulus indicate disease remission or effective treatment?
4. How do we diagnose the mixed types of liver disease?
5. In adult patients with NAFLD, what SWE LS cut-off value allows us to accurately diagnose the presence of cirrhosis and eliminate the need for liver biopsy?
6. In compensated cirrhosis of adult CLD, what 2D-SWE liver stiffness cut-off value allows us to avoid the need for gastroscopy?
7. Focal lesions can lead to erroneous results. How should these be resolved?

Patient follow-up questions

1. During follow-up monitoring, are there any definite cut-off values to weigh the progression, regression and outcome of liver disease?
2. What is a minimal time span for measuring LS over time? How often should measurements be performed?
3. How should elastography be used to predict the risk for HCC in patients with cirrhosis, regardless of etiology?

Here, we will address the first clinical issue. On the basis of the current study, we believe that SWE can guide clinical work to help develop a reasonable treatment strategy for patients with CLDs by measuring the degree of LS, which reflects the degree of liver fibrosis, and by monitoring the progress of the disease in real time. According to the EASL guidelines, it is of particular significance to identify patients with cirrhosis, as their treatment regimen and posttreatment surveillance must be adapted[27]. The latest report[70] from a European, 10-center, cohort study of 1951 adult Caucasian CHB patients found that HCC incidence distinctly dropped after the first 5 years of therapy, particularly in those with compensated cirrhosis. Furthermore, multivariable analysis showed that a LS $\geqslant$ 12 kPa at year 5 was related to greater HCC development after year 5, which likely represents valuable indirect markers of the severity of liver disease. Consequently, we believe that SWE can reflect liver fibrosis and guide therapy, thus decreasing the risk of HCC and remarkably improving the prognosis. This represents a major advancement in the treatment of CLD.

2D-SWE is known to be a multifactorial technique that factors in the anatomy of the liver, the physical characteristics and the underlying illness of the patient, the experience of the examiner, and differences in equipment. The following details include the factors associated with SWE reliability and ways to improve its performance in liver applications.

Anatomy of the liver

The liver is located in the upper abdomen, near the heart, lungs and gastrointestinal tract, and is particularly affected by respiratory movements as well as the heartbeat and gas in the gastrointestinal tract[71]. Measurements of the left liver lobe yield markedly higher values and are more variable than the right lobe; thus, LSM in the left liver lobe should be avoided whenever possible[72]. During the examination, the patient needs to cooperate by holding their breath (neither in the expiratory phase nor in the aspirated phase) to stabilize the 2D image measurement because stable 2D imaging is the basis of successful results[24].

Physical characteristics and underlying illness of the patient

Previous studies have reported that SWE measurements are not affected by a high body mass index, ascites or fatty liver[20,73], while in clinical practice, high measurement failure rates are due to obesity or ascites causing poor penetration[4]. Obese patients often have a fatty liver with a thick layer of subcutaneous fat and echo attenuation throughout the liver, which is not conducive to clear 2D imaging. In some very thin patients with a narrow intercostal space, especially patients who have entered the end-stage of liver cirrhosis, the right liver has been severely reduced to the extent that it affects elasticity measurements[33].

Using current methods, according to the patient's liver, the depth should be dropped, and the image should be appropriately enlarged while the areas of the sampling frame and ROI are adjusted to the shrinking liver. In addition, some factors influence the LS measured by elastography, leading to an overestimation of liver fibrosis[71,74-78]. Such factors include excessive alcohol intake, elevated central venous pressure, cardiac failure, intra- or extrahepatic cholestasis, alanine aminotransferase flare in acute or chronic hepatitis, and histological necroinflammation activity.

Operator experience

LS measurements by 2D-SWE should be made by an expert operator. It has been reported that experienced examiners have higher reproducibility of measurements than novice examiners[79,80]. It is advised that at least 50 supervised 2D-SWE measurements should be performed by beginners in order to acquire reliable results[79]. This issue therefore necessitates strict prejob training for operators to reduce the error caused by lack of experience and to improve the stability of clinical implementations (Figure 5 shows an analysis of failed measurements).

Differences in manufacturer equipment

There may be significant variation in the frequency of acoustic radiation forces used across manufacturers, although variations can even be observed across different equipment from the same manufacturer or due to different settings applied using the same equipment. Large differences among the measurements provided by different settings create obstacles to the clinical application of SWE that need be addressed in the future[81]. In summary, these techniques need to be performed using a standardized protocol with critically interpreted results, taking confounding factors into account.

CONCLUSION

In conclusion, 2D-SWE appears to be a valid, simple, rapid and reproducible method for the noninvasive assessment of liver fibrosis, with advantages including its low cost and widespread availability. As liver biopsies cannot be performed frequently, SWE can be used to regularly monitor liver fibrosis over the long term. SWE is a promising technology with potential clinical applications, including accurate quantification and therapeutic monitoring. We believe that with the popularity of US elastography, the noninvasive assessment of liver fibrosis will be further promoted. Most importantly, in the future, SWE may become a routine method of screening for patients with CLDs. Finally, large-scale, multicenter, multifield clinical studies are needed to explore the applications of SWE, as there may be variability in terms of demographics, disease and liver cancer incidence predictions. We are

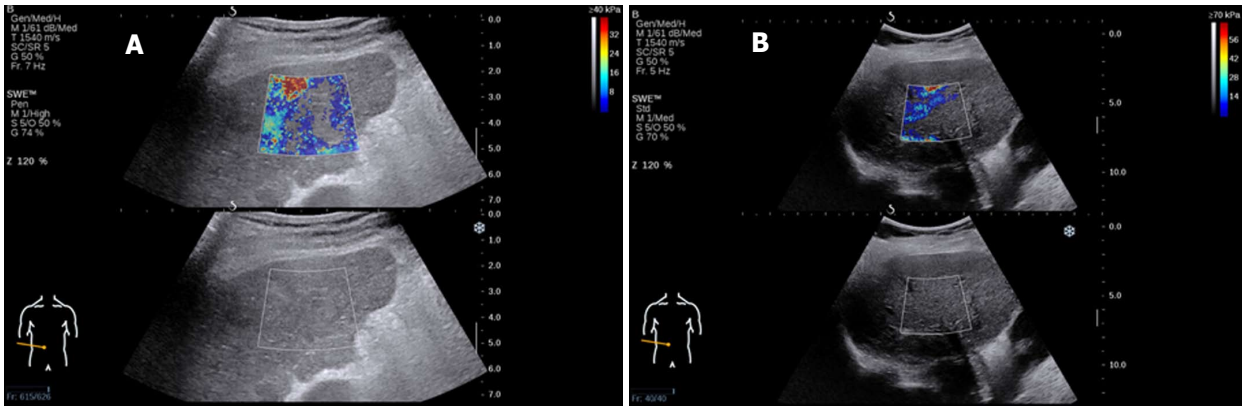

Figure 5 Analysis of failed measurements. A: A 69-year-old female who had right heart failure and could not hold her breath, causing the failed liver stiffness measurement; B: An image acquired by an inexperienced operator who did not set the standard parameters.

hopeful that SWE will continue to evolve and attain a utility equal to that of Doppler as a new mode of US imaging.

REFERENCES

1 **Singh S**, Muir AJ, Dieterich DT, Falck-Ytter YT. American Gastroenterological Association Institute Technical Review on the Role of Elastography in Chronic Liver Diseases. *Gastroenterology* 2017; **152**: 1544-1577 [PMID: 28442120 DOI: 10.1053/j.gastro.2017.03.016]

2 **GBD 2013 Mortality and Causes of Death Collaborators**. Global, regional, and national age-sex specific all-cause and cause-specific mortality for 240 causes of death, 1990-2013: a systematic analysis for the Global Burden of Disease Study 2013. *Lancet* 2015; **385**: 117-171 [PMID: 25530442 DOI: 10.1016/s0140-6736(14)61682-2]

3 **Lee YA**, Wallace MC, Friedman SL. Pathobiology of liver fibrosis: a translational success story. *Gut* 2015; **64**: 830-841 [PMID: 25681399 DOI: 10.1136/gutjnl-2014-306842]

4 **Friedrich-Rust M**, Poynard T, Castera L. Critical comparison of elastography methods to assess chronic liver disease. *Nat Rev Gastroenterol Hepatol* 2016; **13**: 402-411 [PMID: 27273167 DOI: 10.1038/nrgastro.2016.86]

5 **Stasi C**, Milani S. Non-invasive assessment of liver fibrosis: Between prediction/prevention of outcomes and cost-effectiveness. *World J Gastroenterol* 2016; **22**: 1711-1720 [PMID: 26819535 DOI: 10.3748/wjg.v22.i4.1711]

6 **Sharma S**, Khalili K, Nguyen GC. Non-invasive diagnosis of advanced fibrosis and cirrhosis. *World J Gastroenterol* 2014; **20**: 16820-16830 [PMID: 25492996 DOI: 10.3748/wjg.v20.i45.16820]

7 **Seeff LB**, Everson GT, Morgan TR, Curto TM, Lee WM, Ghany MG, Shiffman ML, Fontana RJ, Di Bisceglie AM, Bonkovsky HL, Dienstag JL; HALT-C Trial Group. Complication rate of percutaneous liver biopsies among persons with advanced chronic liver disease in the HALT-C trial. *Clin Gastroenterol Hepatol* 2010; **8**: 877-883 [PMID: 20362695 DOI: 10.1016/j.cgh.2010.03.025]

8 **Schiavon Lde L**, Narciso-Schiavon JL, de Carvalho-Filho RJ. Non-invasive diagnosis of liver fibrosis in chronic hepatitis C. *World J Gastroenterol* 2014; **20**: 2854-2866 [PMID: 24659877 DOI: 10.3748/wjg.v20.i11.2854]

9 **Cassinotto C**, Lapuyade B, Mouries A, Hiriart JB, Vergniol J, Gaye D, Castain C, Le Bail B, Chermak F, Foucher J, Laurent F, Montaudon M, De Ledinghen V. Non-invasive assessment of liver fibrosis with impulse elastography: comparison of Supersonic Shear Imaging with ARFI and FibroScan®. *J Hepatol* 2014; **61**: 550-557 [PMID: 24815876 DOI: 10.1016/j.jhep.2014.04.044]

10 **Dietrich CF**, Bamber J, Berzigotti A, Bota S, Cantisani V, Castera L, Cosgrove D, Ferraioli G, Friedrich-Rust M, Gilja OH, Goertz RS, Karlas T, de Knegt R, de Ledinghen V, Piscaglia F, Procopet B, Saftoiu A, Sidhu PS, Sporea I, Thiele M. EFSUMB Guidelines and Recommendations on the Clinical Use of Liver Ultrasound Elastography, Update 2017 (Long Version). *Ultraschall Med* 2017; **38**: e16-e47 [PMID: 28407655 DOI: 10.1055/s-0043-103952]

11 **European Association for Study of Liver**; Asociacion Latinoamericana para el Estudio del Higado. EASL-ALEH Clinical Practice Guidelines: Non-invasive tests for evaluation of liver disease severity and prognosis. *J Hepatol* 2015; **63**: 237-264 [PMID: 25911335 DOI: 10.1016/j.jhep.2015.04.006]

12 **Bamber J**, Cosgrove D, Dietrich CF, Fromageau J, Bojunga J, Calliada F, Cantisani V, Correas JM, D'Onofrio M, Drakonaki EE, Fink M, Friedrich-Rust M, Gilja OH, Havre RF, Jenssen C, Klauser AS, Ohlinger R, Saftoiu A, Schaefer F, Sporea I, Piscaglia F. EFSUMB guidelines and recommendations on the clinical use of ultrasound elastography. Part 1: Basic principles and technology. *Ultraschall Med* 2013; **34**: 169-184 [PMID: 23558397 DOI: 10.1055/s-0033-1335205]

13 **Castéra L**, Foucher J, Bernard PH, Carvalho F, Allaix D, Merrouche W, Couzigou P, de Lédinghen V. Pitfalls of liver stiffness measurement: a 5-year prospective study of 13,369 examinations. *Hepatology* 2010; **51**: 828-835 [PMID: 20063276 DOI: 10.1002/hep.23425]

14 **Friedrich-Rust M**, Ong MF, Martens S, Sarrazin C, Bojunga J, Zeuzem S, Herrmann E. Performance of transient elastography for the staging of liver fibrosis: a meta-analysis. *Gastroenterology* 2008; **134**: 960-974 [PMID: 18395077 DOI: 10.1053/j.gastro.2008.01.034]

15 **Haque M**, Robinson C, Owen D, Yoshida EM, Harris A. Comparison of acoustic radiation force impulse imaging (ARFI) to liver biopsy histologic scores in the evaluation of chronic liver disease: A pilot study. *Ann Hepatol* 2010; **9**: 289-293 [PMID: 20720270]

16 **Singh S**, Venkatesh SK, Wang Z, Miller FH, Motosugi U, Low RN, Hassanein T, Asbach P, Godfrey EM, Yin M, Chen J, Keaveny AP, Bridges M, Bohte A, Murad MH, Lomas DJ, Talwalkar JA, Ehman RL. Diagnostic performance of magnetic resonance elastography in staging liver fibrosis: a systematic review and meta-analysis of individual participant data. *Clin Gastroenterol Hepatol* 2015; **13**: 440-451.e6 [PMID: 25305349 DOI: 10.1016/j.cgh.2014.09.046]

17 **Huwart L**, Sempoux C, Vicaut E, Salameh N, Annet L, Danse E, Peeters F, ter Beek LC, Rahier J, Sinkus R, Horsmans Y, Van Beers BE. Magnetic resonance elastography for the noninvasive staging of liver fibrosis. *Gastroenterology* 2008; **135**: 32-40 [PMID: 18471441 DOI: 10.1053/j.gastro.2008.03.076]

18 **Bavu E**, Gennisson JL, Couade M, Bercoff J, Mallet V, Fink M, Badel A, Vallet-Pichard A, Nalpas B, Tanter M, Pol S. Noninvasive in vivo liver fibrosis evaluation using supersonic shear imaging: a clinical study on 113 hepatitis C virus patients. *Ultrasound Med*

Biol 2011; **37**: 1361-1373 [PMID: 21775051 DOI: 10.1016/j.ultrasmedbio.2011.05.016]
19 **Muller M**, Gennisson JL, Deffieux T, Tanter M, Fink M. Quantitative viscoelasticity mapping of human liver using supersonic shear imaging: preliminary in vivo feasibility study. *Ultrasound Med Biol* 2009; **35**: 219-229 [PMID: 19081665 DOI: 10.1016/j.ultrasmedbio.2008.08.018]
20 **Ferraioli G**, Tinelli C, Dal Bello B, Zicchetti M, Filice G, Filice C; Liver Fibrosis Study Group. Accuracy of real-time shear wave elastography for assessing liver fibrosis in chronic hepatitis C: a pilot study. *Hepatology* 2012; **56**: 2125-2133 [PMID: 22767302 DOI: 10.1002/hep.25936]
21 **Poynard T**, Munteanu M, Luckina E, Perazzo H, Ngo Y, Royer L, Fedchuk L, Sattonnet F, Pais R, Lebray P, Rudler M, Thabut D, Ratziu V. Liver fibrosis evaluation using real-time shear wave elastography: applicability and diagnostic performance using methods without a gold standard. *J Hepatol* 2013; **58**: 928-935 [PMID: 23321316 DOI: 10.1016/j.jhep.2012.12.021]
22 **Shiina T**, Nightingale KR, Palmeri ML, Hall TJ, Bamber JC, Barr RG, Castera L, Choi BI, Chou YH, Cosgrove D, Dietrich CF, Ding H, Amy D, Farrokh A, Ferraioli G, Filice C, Friedrich-Rust M, Nakashima K, Schafer F, Sporea I, Suzuki S, Wilson S, Kudo M. WFUMB guidelines and recommendations for clinical use of ultrasound elastography: Part 1: basic principles and terminology. *Ultrasound Med Biol* 2015; **41**: 1126-1147 [PMID: 25805059 DOI: 10.1016/j.ultrasmedbio.2015.03.009]
23 **Ferraioli G**, Filice C, Castera L, Choi BI, Sporea I, Wilson SR, Cosgrove D, Dietrich CF, Amy D, Bamber JC, Barr R, Chou YH, Ding H, Farrokh A, Friedrich-Rust M, Hall TJ, Nakashima K, Nightingale KR, Palmeri ML, Schafer F, Shiina T, Suzuki S, Kudo M. WFUMB guidelines and recommendations for clinical use of ultrasound elastography: Part 3: liver. *Ultrasound Med Biol* 2015; **41**: 1161-1179 [PMID: 25800942 DOI: 10.1016/j.ultrasmedbio.2015.03.007]
24 **Barr RG**, Ferraioli G, Palmeri ML, Goodman ZD, Garcia-Tsao G, Rubin J, Garra B, Myers RP, Wilson SR, Rubens D, Levine D. Elastography Assessment of Liver Fibrosis: Society of Radiologists in Ultrasound Consensus Conference Statement. *Radiology* 2015; **276**: 845-861 [PMID: 26079489 DOI: 10.1148/radiol.2015150619]
25 **Schweitzer A**, Horn J, Mikolajczyk RT, Krause G, Ott JJ. Estimations of worldwide prevalence of chronic hepatitis B virus infection: a systematic review of data published between 1965 and 2013. *Lancet* 2015; **386**: 1546-1555 [PMID: 26231459 DOI: 10.1016/s0140-6736(15)61412-x]
26 **Petruzziello A**, Marigliano S, Loquercio G, Cozzolino A, Cacciapuoti C. Global epidemiology of hepatitis C virus infection: An up-date of the distribution and circulation of hepatitis C virus genotypes. *World J Gastroenterol* 2016; **22**: 7824-7840 [PMID: 27678366 DOI: 10.3748/wjg.v22.i34.7824]
27 **European Association for the Study of the Liver**. Electronic address: easloffice@easloffice.eu.; European Association for the Study of the Liver. EASL 2017 Clinical Practice Guidelines on the management of hepatitis B virus infection. *J Hepatol* 2017; **67**: 370-398 [PMID: 28427875 DOI: 10.1016/j.jhep.2017.03.021]
28 **Rockey DC**. Noninvasive assessment of liver fibrosis and portal hypertension with transient elastography. *Gastroenterology* 2008; **134**: 8-14 [PMID: 18166342 DOI: 10.1053/j.gastro.2007.11.053]
29 **Zeng J**, Liu GJ, Huang ZP, Zheng J, Wu T, Zheng RQ, Lu MD. Diagnostic accuracy of two-dimensional shear wave elastography for the non-invasive staging of hepatic fibrosis in chronic hepatitis B: a cohort study with internal validation. *Eur Radiol* 2014; **24**: 2572-2581 [PMID: 25027837 DOI: 10.1007/s00330-014-3292-9]
30 **European Association For The Study Of The Liver**. EASL clinical practice guidelines: Management of chronic hepatitis B virus infection. *J Hepatol* 2012; **57**: 167-185 [PMID: 22436845 DOI: 10.1016/j.jhep.2012.02.010]
31 **European Association for Study of Liver**. EASL Clinical Practice Guidelines: management of hepatitis C virus infection. *J Hepatol* 2014; **60**: 392-420 [PMID: 24331294 DOI: 10.1016/j.jhep.2013.11.003]
32 **WHO Guidelines Approved by the Guidelines Review Committee**. Guidelines for the Prevention, Care and Treatment of Persons with Chronic Hepatitis B Infection. Geneva: World Health Organization Copyright (c) World Health Organization 2015, 2015
33 **Leung VY**, Shen J, Wong VW, Abrigo J, Wong GL, Chim AM, Chu SH, Chan AW, Choi PC, Ahuja AT, Chan HL, Chu WC. Quantitative elastography of liver fibrosis and spleen stiffness in chronic hepatitis B carriers: comparison of shear-wave elastography and transient elastography with liver biopsy correlation. *Radiology* 2013; **269**: 910-918 [PMID: 23912619 DOI: 10.1148/radiol.13130128]
34 **Feng JC**, Li J, Wu XW, Peng XY. Diagnostic Accuracy of SuperSonic Shear Imaging for Staging of Liver Fibrosis: A Meta-analysis. *J Ultrasound Med* 2016; **35**: 329-339 [PMID: 26795041 DOI: 10.7863/ultra.15.03032]
35 **Li C**, Zhang C, Li J, Huo H, Song D. Diagnostic Accuracy of Real-Time Shear Wave Elastography for Staging of Liver Fibrosis: A Meta-Analysis. *Med Sci Monit* 2016; **22**: 1349-1359 [PMID: 27102449 DOI: 10.12659/msm.895662]
36 **Jiang T**, Tian G, Zhao Q, Kong D, Cheng C, Zhong L, Li L. Diagnostic Accuracy of 2D-Shear Wave Elastography for Liver Fibrosis Severity: A Meta-Analysis. *PLoS One* 2016; **11**: e0157219 [PMID: 27300569 DOI: 10.1371/journal.pone.0157219]
37 **Herrmann E**, de Lédinghen V, Cassinotto C, Chu WC, Leung VY, Ferraioli G, Filice C, Castera L, Vilgrain V, Ronot M, Dumortier J, Guibal A, Pol S, Trebicka J, Jansen C, Strassburg C, Zheng R, Zheng J, Francque S, Vanwolleghem T, Vonghia L, Manesis EK, Zoumpoulis P, Sporea I, Thiele M, Krag A, Cohen-Bacrie C, Criton A, Gay J, Deffieux T, Friedrich-Rust M. Assessment of biopsy-proven liver fibrosis by two-dimensional shear wave elastography: An individual patient data-based meta-analysis. *Hepatology* 2018; **67**: 260-272 [PMID: 28370257 DOI: 10.1002/hep.29179]
38 **Grgurevic I**, Puljiz Z, Brnic D, Bokun T, Heinzl R, Lukic A, Luksic B, Kujundzic M, Brkljacic B. Liver and spleen stiffness and their ratio assessed by real-time two dimensional-shear wave elastography in patients with liver fibrosis and cirrhosis due to chronic viral hepatitis. *Eur Radiol* 2015; **25**: 3214-3221 [PMID: 25903706 DOI: 10.1007/s00330-015-3728-x]
39 **Haga Y**, Kanda T, Sasaki R, Nakamura M, Nakamoto S, Yokosuka O. Nonalcoholic fatty liver disease and hepatic cirrhosis: Comparison with viral hepatitis-associated steatosis. *World J Gastroenterol* 2015; **21**: 12989-12995 [PMID: 26675364 DOI: 10.3748/wjg.v21.i46.12989]
40 **Younossi ZM**, Koenig AB, Abdelatif D, Fazel Y, Henry L, Wymer M. Global epidemiology of nonalcoholic fatty liver disease-Meta-analytic assessment of prevalence, incidence, and outcomes. *Hepatology* 2016; **64**: 73-84 [PMID: 26707365 DOI: 10.1002/hep.28431]
41 **Williams CD**, Stengel J, Asike MI, Torres DM, Shaw J, Contreras M, Landt CL, Harrison SA. Prevalence of nonalcoholic fatty liver disease and nonalcoholic steatohepatitis among a largely middle-aged population utilizing ultrasound and liver biopsy: a prospective study. *Gastroenterology* 2011; **140**: 124-131 [PMID: 20858492 DOI: 10.1053/j.gastro.2010.09.038]
42 **Sanyal AJ**, Brunt EM, Kleiner DE, Kowdley KV, Chalasani N, Lavine JE, Ratziu V, McCullough A. Endpoints and clinical trial design for nonalcoholic steatohepatitis. *Hepatology* 2011; **54**: 344-353 [PMID: 21520200 DOI: 10.1002/hep.24376]
43 **Vernon G**, Baranova A, Younossi ZM. Systematic review: the epidemiology and natural history of non-alcoholic fatty liver disease and non-alcoholic steatohepatitis in adults. *Aliment Pharmacol Ther* 2011; **34**: 274-285 [PMID: 21623852 DOI: 10.1111/j.1365-2036.2011.04724.x]
44 **Singh S**, Allen AM, Wang Z, Prokop LJ, Murad MH, Loomba R. Fibrosis progression in nonalcoholic fatty liver vs nonalcoholic steatohepatitis: a systematic review and meta-analysis of paired-biopsy studies. *Clin Gastroenterol Hepatol* 2015; **13**: 643-54.e1-9; quiz e39-40 [PMID: 24768810 DOI: 10.1016/j.cgh.2014.04.014]
45 **Angulo P**, Kleiner DE, Dam-Larsen S, Adams LA, Bjornsson ES, Charatcharoenwitthaya P, Mills PR, Keach JC, Lafferty HD,

Stahler A, Haflidadottir S, Bendtsen F. Liver Fibrosis, but No Other Histologic Features, Is Associated With Long-term Outcomes of Patients With Nonalcoholic Fatty Liver Disease. *Gastroenterology* 2015; **149**: 389-97.e10 [PMID: 25935633 DOI: 10.1053/j.gastro.2015.04.043]

46 **Cassinotto C**, Boursier J, de Lédinghen V, Lebigot J, Lapuyade B, Cales P, Hiriart JB, Michalak S, Bail BL, Cartier V, Mouries A, Oberti F, Fouchard-Hubert I, Vergniol J, Aubé C. Liver stiffness in nonalcoholic fatty liver disease: A comparison of supersonic shear imaging, FibroScan, and ARFI with liver biopsy. *Hepatology* 2016; **63**: 1817-1827 [PMID: 26659452 DOI: 10.1002/hep.28394]

47 **Garcovich M**, Veraldi S, Di Stasio E, Zocco MA, Monti L, Tomà P, Pompili M, Gasbarrini A, Nobili V. Liver Stiffness in Pediatric Patients with Fatty Liver Disease: Diagnostic Accuracy and Reproducibility of Shear-Wave Elastography. *Radiology* 2017; **283**: 820-827 [PMID: 27982761 DOI: 10.1148/radiol.2016161002]

48 **Rehm J**, Samokhvalov AV, Shield KD. Global burden of alcoholic liver diseases. *J Hepatol* 2013; **59**: 160-168 [PMID: 23511777 DOI: 10.1016/j.jhep.2013.03.007]

49 **Mueller S**, Seitz HK, Rausch V. Non-invasive diagnosis of alcoholic liver disease. *World J Gastroenterol* 2014; **20**: 14626-14641 [PMID: 25356026 DOI: 10.3748/wjg.v20.i40.14626]

50 **European Association for the Study of Liver**. EASL clinical practical guidelines: management of alcoholic liver disease. *J Hepatol* 2012; **57**: 399-420 [PMID: 22633836 DOI: 10.1016/j.jhep.2012.04.004]

51 **Thiele M**, Detlefsen S, Sevelsted Møller L, Madsen BS, Fuglsang Hansen J, Fialla AD, Trebicka J, Krag A. Transient and 2-Dimensional Shear-Wave Elastography Provide Comparable Assessment of Alcoholic Liver Fibrosis and Cirrhosis. *Gastroenterology* 2016; **150**: 123-133 [PMID: 26435270 DOI: 10.1053/j.gastro.2015.09.040]

52 **Tripathi D**, Stanley AJ, Hayes PC, Patch D, Millson C, Mehrzad H, Austin A, Ferguson JW, Olliff SP, Hudson M, Christie JM; Clinical Services and Standards Committee of the British Society of Gastroenterology. U.K. guidelines on the management of variceal haemorrhage in cirrhotic patients. *Gut* 2015; **64**: 1680-1704 [PMID: 25887380 DOI: 10.1136/gutjnl-2015-309262]

53 **Kasai Y**, Moriyasu F, Saito K, Hara T, Kobayashi Y, Nakamura I, Sugimoto K. Value of shear wave elastography for predicting hepatocellular carcinoma and esophagogastric varices in patients with chronic liver disease. *J Med Ultrason (2001)* 2015; **42**: 349-355 [PMID: 26576786 DOI: 10.1007/s10396-014-0603-3]

54 **Jansen C**, Bogs C, Verlinden W, Thiele M, Möller P, Görtzen J, Lehmann J, Praktiknjo M, Chang J, Krag A, Strassburg CP, Francque S, Trebicka J. Algorithm to rule out clinically significant portal hypertension combining Shear-wave elastography of liver and spleen: a prospective multicentre study. *Gut* 2016; **65**: 1057-1058 [PMID: 26896458 DOI: 10.1136/gutjnl-2016-311536]

55 **Procopet B**, Berzigotti A, Abraldes JG, Turon F, Hernandez-Gea V, García-Pagán JC, Bosch J. Real-time shear-wave elastography: applicability, reliability and accuracy for clinically significant portal hypertension. *J Hepatol* 2015; **62**: 1068-1075 [PMID: 25514554 DOI: 10.1016/j.jhep.2014.12.007]

56 **Maruyama H**, Kobayashi K, Kiyono S, Sekimoto T, Kanda T, Yokosuka O. Two-dimensional shear wave elastography with propagation-based reliability assessment for grading hepatic fibrosis and portal hypertension. *J Hepatobiliary Pancreat Sci* 2016; **23**: 595-602 [PMID: 27440720 DOI: 10.1002/jhbp.379]

57 **Wang HK**, Lai YC, Tseng HS, Lee RC, Loong CC, Lin NC, Chou YH, Chiou HJ, Chang CY. Hepatic venous congestion after living donor liver transplantation: quantitative assessment of liver stiffness using shear wave elastography--a case report. *Transplant Proc* 2012; **44**: 814-816 [PMID: 22483503 DOI: 10.1016/j.transproceed.2012.01.035]

58 **Yoon JH**, Lee JY, Woo HS, Yu MH, Lee ES, Joo I, Lee KB, Yi NJ, Lee YJ, Han JK, Choi BI. Shear wave elastography in the evaluation of rejection or recurrent hepatitis after liver transplantation. *Eur Radiol* 2013; **23**: 1729-1737 [PMID: 23300037 DOI: 10.1007/s00330-012-2748-z]

59 **Korda D**, Lenard ZM, Gerlei Z, Jakab Z, Haboub-Sandil A, Wagner L, Varga M, Cseprekal O, Marton A, Horvathy D, Takacs S, Doros A, Mathe Z. Shear-wave elastography for the assessment of liver fibrosis in liver transplant recipients treated for hepatitis C virus recurrence. *Eur J Gastroenterol Hepatol* 2018; **30**: 27-32 [PMID: 29049126 DOI: 10.1097/MEG.0000000000001003]

60 **Conti CB**, Cavalcoli F, Fraquelli M, Conte D, Massironi S. Ultrasound elastographic techniques in focal liver lesions. *World J Gastroenterol* 2016; **22**: 2647-2656 [PMID: 26973405 DOI: 10.3748/wjg.v22.i9.2647]

61 **Park HS**, Kim YJ, Yu MH, Jung SI, Jeon HJ. Shear Wave Elastography of Focal Liver Lesion: Intraobserver Reproducibility and Elasticity Characterization. *Ultrasound Q* 2015; **31**: 262-271 [PMID: 26086459 DOI: 10.1097/RUQ.0000000000000175]

62 **Lu Q**, Ling W, Lu C, Li J, Ma L, Quan J, He D, Liu J, Yang J, Wen T, Wu H, Zhu H, Luo Y. Hepatocellular carcinoma: stiffness value and ratio to discriminate malignant from benign focal liver lesions. *Radiology* 2015; **275**: 880-888 [PMID: 25636031 DOI: 10.1148/radiol.14131164]

63 **Brunel T**, Guibal A, Boularan C, Ducerf C, Mabrut JY, Bancel B, Boussel L, Rode A. Focal nodular hyperplasia and hepatocellular adenoma: The value of shear wave elastography for differential diagnosis. *Eur J Radiol* 2015; **84**: 2059-2064 [PMID: 26299323 DOI: 10.1016/j.ejrad.2015.07.029]

64 **Grgurevic I**, Bokun T, Salkic NN, Brkljacic B, Vukelić-Markovic M, Stoos-Veic T, Aralica G, Rakic M, Filipec-Kanizaj T, Berzigotti A. Liver elastography malignancy prediction score for noninvasive characterization of focal liver lesions. *Liver Int* 2017; Epub ahead of print [PMID: 29028279 DOI: 10.1111/liv.13611]

65 **Carbone M**, Neuberger JM. Autoimmune liver disease, autoimmunity and liver transplantation. *J Hepatol* 2014; **60**: 210-223 [PMID: 24084655 DOI: 10.1016/j.jhep.2013.09.020]

66 **Zeng J**, Huang ZP, Zheng J, Wu T, Zheng RQ. Non-invasive assessment of liver fibrosis using two-dimensional shear wave elastography in patients with autoimmune liver diseases. *World J Gastroenterol* 2017; **23**: 4839-4846 [PMID: 28765706 DOI: 10.3748/wjg.v23.i26.4839]

67 **Grgurević I**, Bokun T, Mustapić S, Trkulja V, Heinzl R, Banić M, Puljiz Ž, Lukšić B, Kujundžić M. Real-time two-dimensional shear wave ultrasound elastography of the liver is a reliable predictor of clinical outcomes and the presence of esophageal varices in patients with compensated liver cirrhosis. *Croat Med J* 2015; **56**: 470-481 [PMID: 26526884 DOI: 10.3325/cmj.2015.56.470]

68 **Marcellin P**, Gane E, Buti M, Afdhal N, Sievert W, Jacobson IM, Washington MK, Germanidis G, Flaherty JF, Aguilar Schall R, Bornstein JD, Kitrinos KM, Subramanian GM, McHutchison JG, Heathcote EJ. Regression of cirrhosis during treatment with tenofovir disoproxil fumarate for chronic hepatitis B: a 5-year open-label follow-up study. *Lancet* 2013; **381**: 468-475 [PMID: 23234725 DOI: 10.1016/S0140-6736(12)61425-1]

69 **Hartl J**, Denzer U, Ehlken H, Zenouzi R, Peiseler M, Sebode M, Hübener S, Pannicke N, Weiler-Normann C, Quaas A, Lohse AW, Schramm C. Transient elastography in autoimmune hepatitis: Timing determines the impact of inflammation and fibrosis. *J Hepatol* 2016; **65**: 769-775 [PMID: 27238753 DOI: 10.1016/j.jhep.2016.05.023]

70 **Papatheodoridis GV**, Idilman R, Dalekos GN, Buti M, Chi H, van Boemmel F, Calleja JL, Sypsa V, Goulis J, Manolakopoulos S, Loglio A, Siakavellas S, Keskın O, Gatselis N, Hansen BE, Lehretz M, de la Revilla J, Savvidou S, Kourikou A, Vlachogiannakos I, Galanis K, Yurdaydin C, Berg T, Colombo M, Esteban R, Janssen HLA, Lampertico P. The risk of hepatocellular carcinoma decreases after the first 5 years of entecavir or tenofovir in Caucasians with chronic hepatitis B. *Hepatology* 2017; **66**: 1444-1453 [PMID: 28622419 DOI: 10.1002/hep.29320]

71 **Cosgrove D**, Piscaglia F, Bamber J, Bojunga J, Correas JM, Gilja OH, Klauser AS, Sporea I, Calliada F, Cantisani V, D'Onofrio M, Drakonaki EE, Fink M, Friedrich-Rust M, Fromageau J, Havre RF, Jenssen C, Ohlinger R, Săftoiu A, Schaefer F, Dietrich CF; EFSUMB. EFSUMB guidelines and recommendations

on the clinical use of ultrasound elastography. Part 2: Clinical applications. *Ultraschall Med* 2013; **34**: 238-253 [PMID: 23605169 DOI: 10.1055/s-0033-1335375]
72 **Karlas T**, Pfrepper C, Wiegand J, Wittekind C, Neuschulz M, Mössner J, Berg T, Tröltzsch M, Keim V. Acoustic radiation force impulse imaging (ARFI) for non-invasive detection of liver fibrosis: examination standards and evaluation of interlobe differences in healthy subjects and chronic liver disease. *Scand J Gastroenterol* 2011; **46**: 1458-1467 [PMID: 21916815 DOI: 10.3109/00365521.2011.610004]
73 **Suh CH**, Kim SY, Kim KW, Lim YS, Lee SJ, Lee MG, Lee J, Lee SG, Yu E. Determination of normal hepatic elasticity by using real-time shear-wave elastography. *Radiology* 2014; **271**: 895-900 [PMID: 24555633 DOI: 10.1148/radiol.14131251]
74 **Mueller S**, Millonig G, Sarovska L, Friedrich S, Reimann FM, Pritsch M, Eisele S, Stickel F, Longerich T, Schirmacher P, Seitz HK. Increased liver stiffness in alcoholic liver disease: differentiating fibrosis from steatohepatitis. *World J Gastroenterol* 2010; **16**: 966-972 [PMID: 20180235 DOI: 10.3748/wjg.v16.i8.966]
75 **Millonig G**, Friedrich S, Adolf S, Fonouni H, Golriz M, Mehrabi A, Stiefel P, Pöschl G, Büchler MW, Seitz HK, Mueller S. Liver stiffness is directly influenced by central venous pressure. *J Hepatol* 2010; **52**: 206-210 [PMID: 20022130 DOI: 10.1016/j.jhep.2009.11.018]
76 **Millonig G**, Reimann FM, Friedrich S, Fonouni H, Mehrabi A, Büchler MW, Seitz HK, Mueller S. Extrahepatic cholestasis increases liver stiffness (FibroScan) irrespective of fibrosis. *Hepatology* 2008; **48**: 1718-1723 [PMID: 18836992 DOI: 10.1002/hep.22577]
77 **Arena U**, Vizzutti F, Corti G, Ambu S, Stasi C, Bresci S, Moscarella S, Boddi V, Petrarca A, Laffi G, Marra F, Pinzani M. Acute viral hepatitis increases liver stiffness values measured by transient elastography. *Hepatology* 2008; **47**: 380-384 [PMID: 18095306 DOI: 10.1002/hep.22007]
78 **Fraquelli M**, Rigamonti C, Casazza G, Donato MF, Ronchi G, Conte D, Rumi M, Lampertico P, Colombo M. Etiology-related determinants of liver stiffness values in chronic viral hepatitis B or C. *J Hepatol* 2011; **54**: 621-628 [PMID: 21146243 DOI: 10.1016/j.jhep.2010.07.017]
79 **Ferraioli G**, Tinelli C, Zicchetti M, Above E, Poma G, Di Gregorio M, Filice C. Reproducibility of real-time shear wave elastography in the evaluation of liver elasticity. *Eur J Radiol* 2012; **81**: 3102-3106 [PMID: 22749107 DOI: 10.1016/j.ejrad.2012.05.030]
80 **Zhuang Y**, Ding H, Zhang Y, Sun H, Xu C, Wang W. Two-dimensional Shear-Wave Elastography Performance in the Noninvasive Evaluation of Liver Fibrosis in Patients with Chronic Hepatitis B: Comparison with Serum Fibrosis Indexes. *Radiology* 2017; **283**: 873-882 [PMID: 27982760 DOI: 10.1148/radiol.2016160131]
81 **Piscaglia F**, Salvatore V, Mulazzani L, Cantisani V, Colecchia A, Di Donato R, Felicani C, Ferrarini A, Gamal N, Grasso V, Marasco G, Mazzotta E, Ravaioli F, Ruggieri G, Serio I, Sitouok Nkamgho JF, Serra C, Festi D, Schiavone C, Bolondi L. Differences in liver stiffness values obtained with new ultrasound elastography machines and Fibroscan: A comparative study. *Dig Liver Dis* 2017; **49**: 802-808 [PMID: 28365330 DOI: 10.1016/j.dld.2017.03.001]
82 **Sirli R**, Bota S, Sporea I, Jurchis A, Popescu A, Gradinaru-Tascău O, Szilaski M. Liver stiffness measurements by means of supersonic shear imaging in patients without known liver pathology. *Ultrasound Med Biol* 2013; **39**: 1362-1367 [PMID: 23743106 DOI: 10.1016/j.ultrasmedbio.2013.03.021]
83 **Hudson JM**, Milot L, Parry C, Williams R, Burns PN. Inter- and intra-operator reliability and repeatability of shear wave elastography in the liver: a study in healthy volunteers. *Ultrasound Med Biol* 2013; **39**: 950-955 [PMID: 23453379 DOI: 10.1016/j.ultrasmedbio.2012.12.011]
84 **Wang CZ**, Zheng J, Huang ZP, Xiao Y, Song D, Zeng J, Zheng HR, Zheng RQ. Influence of measurement depth on the stiffness assessment of healthy liver with real-time shear wave elastography. *Ultrasound Med Biol* 2014; **40**: 461-469 [PMID: 24361224 DOI: 10.1016/j.ultrasmedbio.2013.10.021]
85 **Huang Z**, Zheng J, Zeng J, Wang X, Wu T, Zheng R. Normal liver stiffness in healthy adults assessed by real-time shear wave elastography and factors that influence this method. *Ultrasound Med Biol* 2014; **40**: 2549-2555 [PMID: 25282481 DOI: 10.1016/j.ultrasmedbio.2014.05.008]
86 **Yoon JH**, Lee JM, Han JK, Choi BI. Shear wave elastography for liver stiffness measurement in clinical sonographic examinations: evaluation of intraobserver reproducibility, technical failure, and unreliable stiffness measurements. *J Ultrasound Med* 2014; **33**: 437-447 [PMID: 24567455 DOI: 10.7863/ultra.33.3.437]
87 **Franchi-Abella S**, Corno L, Gonzales E, Antoni G, Fabre M, Ducot B, Pariente D, Gennisson JL, Tanter M, Corréas JM. Feasibility and Diagnostic Accuracy of Supersonic Shear-Wave Elastography for the Assessment of Liver Stiffness and Liver Fibrosis in Children: A Pilot Study of 96 Patients. *Radiology* 2016; **278**: 554-562 [PMID: 26305193 DOI: 10.1148/radiol.2015142815]

P- Reviewer: Grgurevic I, Tahiri M, Tantau M **S- Editor**: Gong ZM
L- Editor: Filipodia **E- Editor**: Huang Y

World Journal of Gastroenterology

Submit a Manuscript: http://www.f6publishing.com

World J Gastroenterol 2018 March 7; 24(9): 971-981

DOI: 10.3748/wjg.v24.i9.971

ISSN 1007-9327 (print) ISSN 2219-2840 (online)

ORIGINAL ARTICLE

Basic Study

Can bacterial virulence factors predict antibiotic resistant *Helicobacter pylori* infection?

Denise E Brennan, Colin Dowd, Colm O'Morain, Deirdre McNamara, Sinéad M Smith

Denise E Brennan, Colin Dowd, Colm O'Morain, Deirdre McNamara, Sinéad M Smith, Department of Clinical Medicine, School of Medicine, Trinity College Dublin, Dublin D2, Ireland

ORCID number: Denise E Brennan (0000-0001-8200-3181); Colin Dowd (0000-0003-0608-0585); Colm O'Morain (0000-0002-1847-6782); Deirdre McNamara (0000-0003-2324-3382); Sinéad M Smith (0000-0003-3460-3590).

Author contributions: McNamara D and Smith SM contributed equally to the study; McNamara D and Smith SM designed the study and coordinated the research; Brennan DE, Dowd C and Smith SM performed experiments and analysed data; O'Morain C and McNamara D recruited patients; Brennan DE, McNamara D and Smith SM wrote the paper; all authors provided critical input into the final manuscript.

Supported by the Health Research Board (HRA-POR-2014-526).

Institutional review board statement: The study was reviewed and approved by the Adelaide and Meath Hospital Research Ethics Committee.

Conflict-of-interest statement: None to declare.

Data sharing statement: There is no additional data to share.

Manuscript source: Invited manuscript

Correspondence to: Sinéad M Smith, PhD, Ussher Assistant Professor in Applied and Translational Medicine, Rm 1.46, Department of Clinical Medicine, Trinity Centre, Adelaide and Meath Hospital, Tallaght, Dublin D24, Ireland. smithsi@tcd.ie
Telephone: +353-1-8963844
Fax: +353-1-8962988

Received: January 10, 2018
Peer-review started: January 10, 2018
First decision: January 18, 2018
Revised: February 5, 2018
Accepted: February 8, 2018
Article in press: February 8, 2018
Published online: March 7, 2018

Abstract

AIM

To evaluate the association between virulence factor status and antibiotic resistance in *Helicobacter pylori* (*H. pylori*)-infected patients in Ireland.

METHODS

DNA was extracted from antral and corpus biopsies obtained from 165 *H. pylori*-infected patients. Genotyping for clarithromycin and fluoroquinolone-mediating mutations was performed using the Genotype HelicoDR assay. *cagA* and *vacA* genotypes were investigated using PCR.

RESULTS

Primary, secondary and overall resistance rates for clarithromycin were 50.5% (*n* = 53/105), 78.3% (*n* = 47/60) and 60.6% (*n* = 100/165), respectively. Primary, secondary and overall resistance rates for fluoroquinolones were 15.2% (*n* = 16/105) and 28.3% (*n* = 17/60) and 20% (*n* = 33/165), respectively. Resistance to both antibiotics was 12.4% (*n* = 13/105) in treatment-naïve patients, 25% (*n* = 15/60) in those previously treated and 17% (*n* = 28/165) overall. A *cagA*-positive genotype was detected in 22.4% (*n* = 37/165) of patient samples. The dominant *vacA* genotype was S1/M2 at 44.8% (*n* = 74/165), followed by S2/M2 at 26.7% (*n* = 44/165), S1/M1 at 23.6% (*n*

= 39/165) and S2/M1 at 4.8% (*n* = 8/165). Primary clarithromycin resistance was significantly lower in *cagA*-positive strains than in *cagA*-negative strains [32% (*n* = 8/25) *vs* 56.3% (*n* = 45/80); *P* = 0.03]. Similarly, in patients infected with more virulent *H. pylori* strains bearing the *vacA* s1 genotype, primary clarithromycin resistance was significantly lower than in those infected with less virulent strains bearing the *vacA* s2 genotype, [41% (*n* = 32/78) *vs* 77.8% (*n* = 21/27); *P* = 0.0001]. No statistically significant association was found between primary fluoroquinolone resistance and virulence factor status.

CONCLUSION

Genotypic *H. pylori* clarithromycin resistance is high and *cagA*-negative strains are dominant in our population. Less virulent (*cagA*-negative and *vacA* S2-containing) strains of *H. pylori* are associated with primary clarithromycin resistance.

Key words: *Helicobacter pylori*; Antibiotic resistance; Fluoroquinolone; Clarithromycin; Virulence factor; VacA; CagA

Core tip: The management of *Helicobacter pylori* (*H. pylori*) infection is challenging, largely due to the emergence of antibiotic resistance. A greater understanding of local antibiotic resistance rates is important in determining the most appropriate treatment regimen in a given population. Furthermore, insight into the virulence of the infecting strains and the association between virulence and antibiotic resistance could potentially be an avenue to explore in the effort to improve eradication rates. This study provides and update on the prevalence of clarithromycin and fluoroquinolone resistance in Ireland and demonstrates that less virulent strains of *H. pylori* are predictive of primary clarithromycin resistance.

Brennan DE, Dowd C, O'Morain C, McNamara D, Smith SM. Can bacterial virulence factors predict antibiotic resistant *Helicobacter pylori* infection? *World J Gastroenterol* 2018; 24(9): 971-981 Available from: URL: http://www.wjgnet.com/1007-9327/full/v24/i9/971.htm DOI: http://dx.doi.org/10.3748/wjg.v24.i9.971

INTRODUCTION

Helicobacter pylori (*H. pylori*) infection causes acute and chronic gastritis, gastric and duodenal ulcers, and in rare cases gastric adenocarcinoma and MALT (mucosa-associated lymphoid tissue) lymphoma[1]. While its prevalence in the developed world has generally decreased, it is still high in indigenous populations and the developing world[2]. The Maastricht consensus recommends that all symptomatic *H. pylori*-infected adults are treated[1]. There are many different treatment options available, however the most common treatment for first-line eradication of *H. pylori* is triple therapy, which consists of two antibiotics (clarithromycin and amoxicillin) and a proton pump inhibitor, taken for 7-14 d. An efficacious therapy for *H. pylori* eradication is one that achieves an eradication rate of over 80%[1]. However, in many countries, the eradication rate for standard triple therapy has fallen below 80%. Indeed in a recent study in Ireland, the eradication rates of standard seven-day triple therapy were just 56.8% and 61% by intention-to-treat and per-protocol analysis, respectively[3]. There are several factors that impact the efficacy of treatment for *H. pylori*; high bacterial load, high gastric acidity and poor patient compliance. However, undoubtedly the most important is the rapid emergence of antimicrobial resistant strains of *H. pylori*, particularly to clarithromycin[4-6]. Resistance to clarithromycin can decrease the success rate of clarithromycin-based triple therapy by up to 70%[7]. One study found that the presence of clarithromycin resistant strains in a patient infected with *H. pylori* predicted treatment failure almost perfectly[8].

H. pylori is a highly heterogeneous bacterium and its virulence varies geographically. Virulence factors not only contribute to the pathogenicity of the bacteria but may play a role in determining treatment outcome[9]. The most commonly studied virulence factors in *H. pylori* are encoded by the cytotoxin associated gene A (*cagA*) and the vacuolating associated gene A (*vacA*). There are at least 4 variable regions in the *vacA* gene; in the signal (s) region, of which one of two alleles can be present: s1 or s2, and in the middle (m) region, of which one of two alleles can be present; m1 or m2[10]. These variable regions display different levels of toxicity to host cells, with *vacA* s1/m1 being most cytotoxic, followed by s1/m2. The s2/m2 genotype has been found to induce little or no toxicity[11]. A possible relationship between virulence factors and antimicrobial resistance has been suggested. A study conducted in 2009 in Ireland reported that the absence of *cagA* may be a risk factor for developing metronidazole resistance[12]. This study aimed to provide an update on the prevalence of virulence factor genotypes and antibiotic resistance in Irish *H. pylori* strains and assess the relationship between clarithromycin and fluoroquinolone resistance with virulence factor status.

MATERIALS AND METHODS

Study design and ethics

A prospective study was carried out in a tertiary referral teaching hospital (Adelaide and Meath Hospital, Dublin, Ireland) affiliated with Trinity College Dublin. Patients who had been referred to the endoscopy clinic were included from August 2014 until June 2017. The study received ethical approval from the Adelaide and Meath

Table 1 Polymerase chain reaction primers used in this study

Primer	Primer sequence	Gene	Product size (bp)
CAGA-F	5′-GATAACAGGCAAGCTTTTGATG-3′	*cagA*	349
CAGA-R	5′-CTGCAAAAGATTGTTTGGCAGA-3′		
VA1-F	5′- ATGGAAATACAACAACAAACACAC-3′	*vacA* signal region	259/286 (s1/s2)
VA1-R	5′ – CTGCTTGAATGCGCCAAAC-3′		
VAG-F	5′ – CAATCTGTCCAATCAAGCGAG-3′	*vacA* middle region	567/642 (m1/m2)
VAG-R	5′- GCTTCAAAATAATTCCAAGG-3′		

Hospital Research Ethics Committee. Informed consent was obtained from all patients before enrolment.

Study population

Inclusion criteria were (1) ability and willingness to participate in the study and to provide informed consent, and (2) confirmed *H. pylori* infection as indicated by a positive rapid urease test (TRI-MED Distributors, PTY LTD, Washington, United States) at 30 min and by histology.

Exclusion criteria were (1) age less than 18 years, (2) pregnancy or lactation, (3) severe inter-current illness, (4) current PPI use or recent antibiotic use (within 4 wk); and (5) bleeding problems or use of blood thinning drugs.

Sample collection

A single corpus and antrum biopsy from each patient were placed into collection tubes and stored at -20 ℃ until processed for genomic DNA isolation using the QIAamp DNA Mini Kit (Qiagen GmbH, Hilden, Germany) according to manufacturer's instructions. All isolated DNA was stored -20 ℃ until genotyping was performed.

Antimicrobial susceptibility genotyping

Genotyping for clarithromycin and fluoroquinolone-mediating mutations was performed using the Genotype HelicoDR assay (Hain Lifescience GmbH, Nehren, Germany) according to the manufacturer's instructions. Briefly, multiplex amplification of DNA regions of interest was performed using biotinylated primers supplied in the GenoType HelicoDR kit and the Hotstart Taq DNA polymerase kit (Qiagen). PCR products were reverse hybridised to DNA strips containing probes for gene regions of interest, developed and interpreted according to the manufacturers' instructions[13].

Virulence factor genotyping

To determine virulence factor genotype, PCR was performed as previously described by Taneike *et al*[12] using the primers described in Table 1. C*agA* and *vacA* genotypes were evaluated by performing gel electrophoresis on the PCR products using 1% agarose gel.

Statistical analysis

Statistical analysis was carried out using GraphPad Prism (GraphPad Software Inc., CA, United States). Continuous variables are presented as arithmetic mean and SD. *P* values for continuous variables were calculated and compared using the two-tailed independent *t*-test. *P* values for categorical variables were calculated using the Fisher's exact test/Pearson χ^2-test. In all cases, a *P* value less than 0.05 was considered significant.

RESULTS

Prevalence of genotypic antimicrobial resistance

Samples from a total of 165 *H. pylori*-infected patients were analysed in the study. Patient demographics and clinical characteristics are shown in Table 2. 63.6% (*n* = 105) of patients had not been treated for *H. pylori* infection previously, while 36.4% (*n* = 60) had undergone at least one eradication treatment regimen (Table 2).

Primary resistance rates for clarithromycin and fluoroquinolones were 50.5% (*n* = 53/105; Table 3) and 15.2% (*n* = 16/105; Table 4), respectively. In those previously treated for *H. pylori* infection, the resistance rates for both clarithromycin and fluoroquinolones were higher at 78.3% (*n* = 47/60; Table 3) and 28.3% (*n* = 17/60; Table 4), respectively. Overall resistance rates, regardless of treatment history, were 60.6% (*n* = 100/165; Table 3) and 20% (*n* = 33/165; Table 4) for clarithromycin and fluoroquinolones, respectively. Among patients infected with a clarithromycin-resistant strain, the most common point mutation was A2147G, at 78% (*n* = 78/100; Table 3). The most common point mutation conferring resistance to fluoroquinolones in resistant patients was *gyr*91 D91Y, at 54.5% (*n* = 18/33; Table 4).

Dual resistance rates for clarithromycin and fluoroquinolones were 12.4% (*n* = 13/105) in the treatment naïve, 25% (*n* = 15/60) in those previously treated and 17% (*n* = 28/165) in all patients included (Table 5). The overall rate of dual susceptibility among the patients was 36.4% (*n* = 60/165; Table 5). Dual susceptibility was significantly higher in treatment-naïve patients versus those previously treated (46.6%, *n* = 49/105 versus 18.3%, *n* = 11/60; $P < 0.05$; Fisher's exact test).

Distribution of H. pylori virulence-factor genotype

Table 6 illustrates the distribution of *H. pylori* virulence factor genotype in infected patients. Overall, 22.4% (*n*

Table 2 Demographic and clinical characteristics of *Helicobacter pylori*-infected patients included in the study

	Number of gastric biopsy specimens *n* (%)		
	All patients 165 (100)	Treatment Naïve 105 (63.6)	Previously treated 60 (36.4)
Gender			
Female	69 (41.8)	31 (29.5)	38 (63.3)
Male	96 (58.2)	74 (70.5)	22 (36.7)
Age			
mean ± SD	49.2 ± 15.8	50.3 ± 16.3	47.4 ± 14.7
Histology findings			
Chronic gastritis	130 (78.8)	78 (74.3)	52 (86.7)
Intestinal metaplasia	23 (13.9)	16 (15.2)	7 (11.7)
No data available	11 (6.7)	10 (9.5)	1 (1.7)
Normal mucosa	1 (0.6)	1 (1.0)	0 (0.0)
Endoscopic findings			
Gastritis	92 (55.8)	57 (54.3)	35 (58.3)
Normal	32 (19.4)	19 (18.1)	13 (21.7)
Gastric/duodenal ulcer	21 (12.7)	15 (14.3)	6 (10.0)
No data available	17 (10.3)	11 (10.5)	6 (10.0)
Atrophic mucosa	1 (0.6)	1 (1.0)	0 (0.0)
Other[1]	2 (1.2)	2 (1.9)	0 (0.0)

[1]Other endoscopic findings: 1 intestinal metaplasia and erosion: 1 portal hypertensive gastropathy.

Table 3 Clarithromycin resistance rates and the distribution of resistance-mediating mutations

Genotype	Number of gastric biopsy specimens *n* (%)			*P* value[1]
	All patients 165 (100)	Treatment Naïve 105 (63.6)	Previously treated 60 (36.4)	
Clarithromycin^S (WT)	65 (39.4)	52 (49.5)	13 (21.7)	< 0.001
Clarithromycin^R	100 (60.6)	53 (50.5)	47 (78.3)	
Point mutations				
A2147G	78 (78)	44 (83)	34 (72.3)	NS
A2146G	8 (8)	3 (5.7)	5 (10.6)	NS
A2146C	6 (6)	3 (5.7)	3 (6.4)	NS
A2146C + A2147G	5 (5)	3 (5.7)	2 (4.3)	NS
A2146G + A2147G	2 (2)	0 (0)	2 (4.3)	NS
A2146G + A2146C	1 (1)	0 (0)	1 (2.1)	NS

[1]Treatment-naïve versus previously treated patients (Fisher's exact test). Clarithromycin^S: Sensitive to clarithromycin; Clarithromycin^R: Resistant to clarithromycin.

= 37/165) of patients were infected with strains that were *cagA* positive and 77.6% (*n* = 128/165) that were *cagA* negative. The most prevalent *vacA* allele was S1/M2 at 44.8% (*n* = 74/165), followed by S2/M2, S1/M1 and S2/M1 at 26.7% (*n* = 44/165), 23.6% (*n* = 39/165) and 4.8% (*n* = 8/165), respectively (Table 6). Interestingly, the frequency of the *vacA* S1 genotype (the more virulent S region genotype) was significantly lower in those previously treated than the treatment-naïve group [58.3% (*n* = 35/60) *vs* 74.3% (*n* = 78/105) respectively; *P* < 0.05; Fisher's exact test]. Additionally, the frequency of the S2/M2 genotype (the least virulent genotype) was significantly higher in those patients who have been treated previously [36.7% (*n* = 22/60) *vs* 21% (*n* = 22/105) respectively; *P* < 0.05; Fisher's exact test; Table 6].

Less virulent strains of H. pylori are associated with primary clarithromycin resistance

Next, the relationship between antibiotic resistance and virulence factor genotype was assessed. Analysis of all recruited patients revealed that genotypic resistance to clarithromycin was significantly lower in *cagA*-positive strains than in *cagA*-negative strains [40.5% (*n* = 15/37) *vs* 66.4% (*n* = 85/128); χ^2 = 8.04; *P* = 0.004; Pearson χ^2 test; Figure 1A]. When patients were sub-grouped into treatment-naïve (Figure 1B) and those previously treated (Figure 1C), clarithromycin resistance was also lower in *cagA*-positive strains compared to *cagA*-negative strains, although this only reached statistical significance in the treatment-naïve cohort [32% (*n* = 8/25) *vs* 56.3% (*n* = 45/80); χ^2 = 4.5; *P* = 0.03; Pearson χ^2 test; Figure 1B]. Similarly, in patients infected with more virulent *H. pylori* strains bearing the *vacA* s1 genotype, clarithromycin resistance was significantly lower than in those infected with less virulent strains bearing the *vacA* s2 genotype, when all patients were included [52.2% (*n* = 59/113) *vs* 78.8% (*n* = 41/52); χ^2 = 10.6; *P* = 0.001; Pearson χ^2 test; Figure 2A] and in those that were treatment-naïve [41% (*n* = 32/78) *vs* 77.8% (*n* = 21/27); χ^2 = 10.8; *P* = 0.0001; Pearson χ^2 test; Figure 2B], but not in patients that were previously treated (Figure 2C).

Table 4 Fluoroquinolone resistance rates and the distribution of resistance-mediating mutations

Genotype	Number of gastric biopsy specimens *n* (%)			*P* value[1]
	All patients 165 (100)	Treatment Naïve 105 (63.6)	Previously treated 60 (36.4)	
Fluoroquinolone^{S} (WT)	132 (80.0)	89 (84.8)	43 (71.7)	
Fluoroquinolone^{R}	33 (20.0)	16 (15.2)	17 (28.3)	NS
Point mutations				
*gyr*91 D91Y	18 (54.5)	10 (62.5)	8 (47.1)	NS
*gyr*91 D91N	6 (18.2)	2 (12.5)	4 (23.5)	NS
*gyr*91 D91G	2 (6.1)	0 (0.0)	2 (11.8)	NS
*gyr*91 D91N + *gyr*91 D91G	2 (6.1)	1 (6.3)	1 (5.9)	NS
*gyr*91 D91N +*gyr*91 D91Y	2 (6.1)	1 (6.3)	1 (5.9)	NS
*gyr*87 N87K	1 (3.0)	1 (6.3)	0 (0.0)	NS
*gyr*87 N87K + *gyr*91 D91N + *gyr*91 D91G	1 (3.0)	0 (0.0)	1 (5.9)	NS
*gyr*87 N87K + *gyr*91 D91N + *gyr*91 D91G + *gyr*91 D91Y	1 (3.0)	1 (6.3)	0 (0.0)	NS

[1]Treatment-naïve versus previously treated patients (Fisher's exact test). Fluoroquinolone^{S}: Sensitive to fluoroquinolones; Fluoroquinolone^{R}: Resistant to fluoroquinolones.

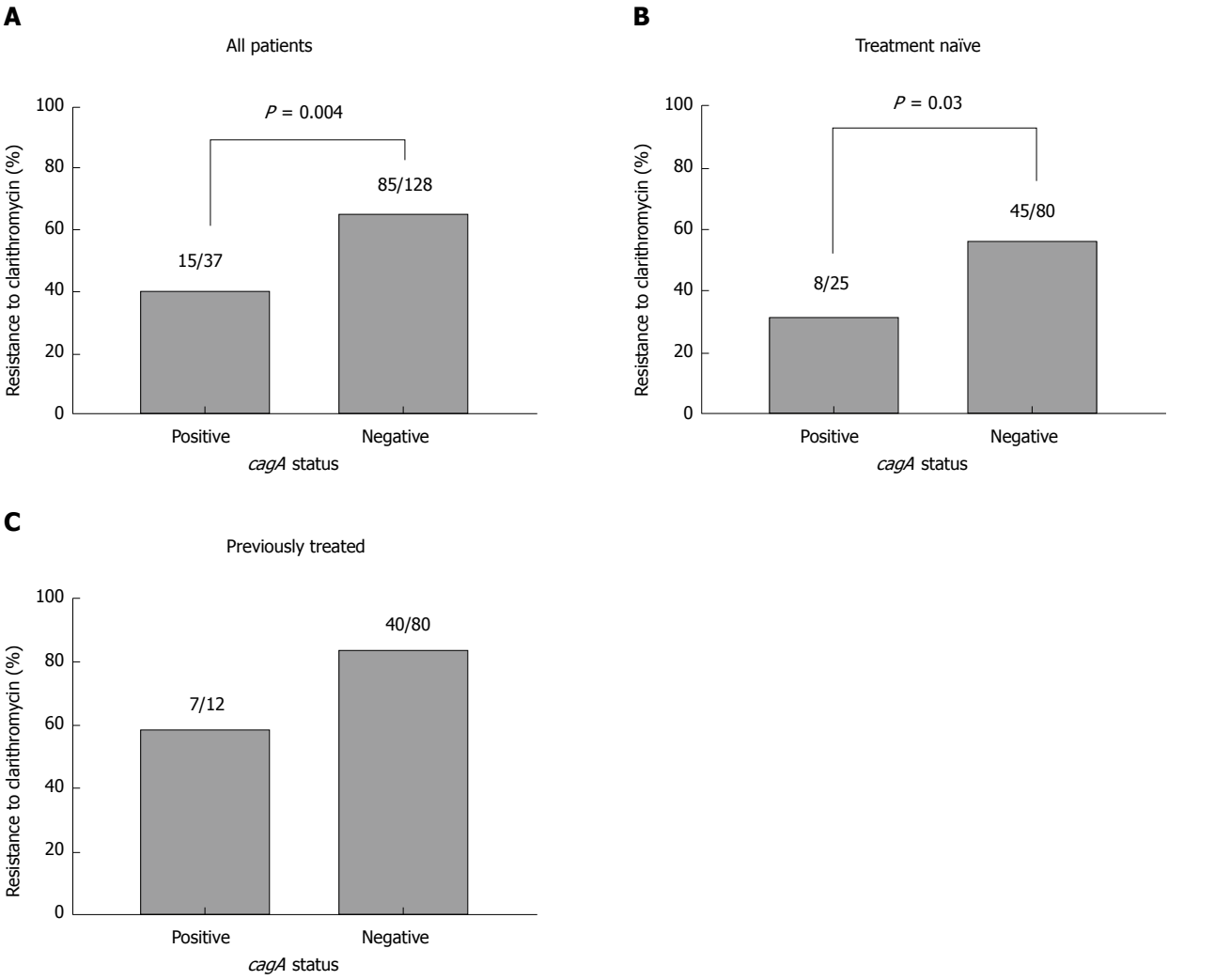

Figure 1 Prevalence of clarithromycin-resistance according to *cagA* genotype. A: All patients; B: Treatment naïve patients; C: Previously treated patients.

The frequency of resistance to fluoroquinolones in each virulence factor genotype was also examined. *CagA* status was not significantly associated with fluoroquinolone resistance when all patients were analysed (Figure 3A) or when the patients were sub-divided into those with primary infections (Figure 3B) and those previously treated (Figure 3C). While there was a significant association between the less virulent *vacA* s2 genotype and fluoroquinolone resistance when all patients were included [15% (*n* = 17/113) *vs* 30.8% (*n* = 16/52); χ^2 = 5.5; *P* = 0.02; Pearson χ^2 test; Figure 4A], this did not reach statistical

Table 5 Antimicrobial susceptibility results for both clarithromycin and fluoroquinolone

Genotype	Number of gastric biopsy specimens *n* (%)			*P* value[1]
	All patients 165 (100)	Treatment Naïve 105 (63.6)	Previously treated 60 (36.4)	
Susceptible (to both)	60 (36.4)	49 (46.6)	11 (18.3)	< 0.05
Resistant (to at least one)	105 (63.6)	56 (53.3)	49 (81.6)	
Susceptible/resistant to one	137 (83.0)	92 (87.6)	45 (75.0)	
Resistant to both	28 (17.0)	13 (12.4)	15 (25.0)	0.05

[1]Treatment-naïve versus previously treated patients (Fisher's exact test).

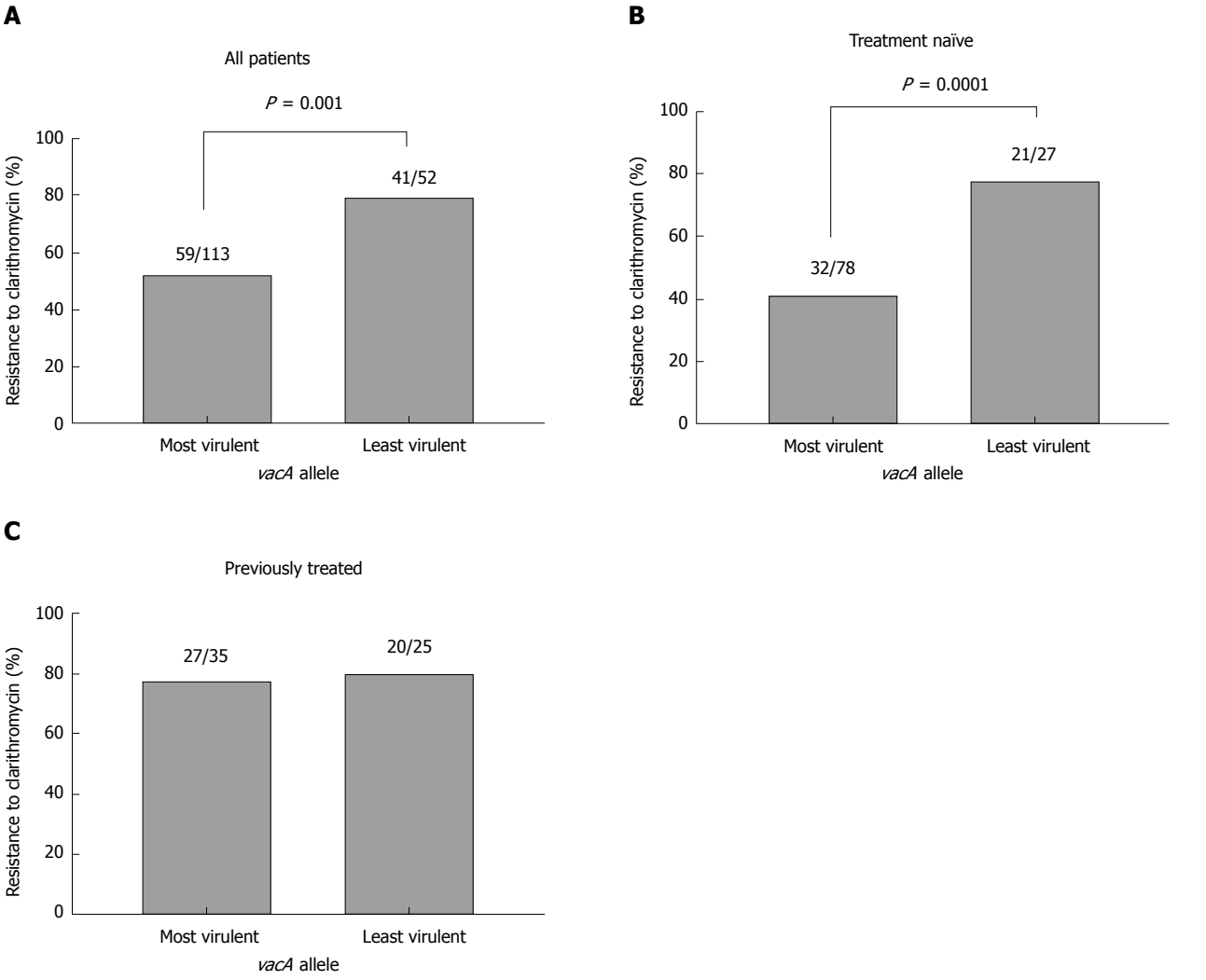

Figure 2 Prevalence of clarithromycin resistance according to *vacA* genotype. A: All patients; B: Treatment naïve patients; C: Previously treated patients. Most virulent: S1/M1, S1/M2; Least virulent: S2/M1; S2/M2.

significance in treatment naïve patients (Figure 4B) or those previously treated (Figure 4C).

Taken together, these findings indicate that the absence of *cagA* and the less virulent *vacA* genotypes (S2/M1 and S2/M2) may be predictors of primary clarithromycin resistance in treatment-naïve patients.

DISCUSSION

This study aimed to provide an update on the prevalence of antibiotic resistance and distribution of virulence factor genotypes in *H. pylori* strains in Ireland. In addition we investigated whether virulence factor genotypes are associated with antibiotic susceptibility. Primary clarithromycin resistance among our patients was high at 50.5% and even higher in those previously treated at 78%. Among patients infected with a resistant strain, the most common point mutation conferring clarithromycin resistance was A2147G, in keeping with other studies[14-19]. Our primary clarithromycin resistance rate is high compared to rates reported in Europe, Asia Pacific and other countries[5,19-21]. Variations

Table 6 Distribution of *Helicobacter pylori* virulence-factor genotypes among infected patients in Ireland *n* (%)

Genotype	Overall (*n* = 165)	Treatment naïve (*n* = 105)	Previous treatment (*n* = 60)	*P* value[1]
cagA status				
Positive	37 (22.4)	25 (23.8)	12 (20)	NS
Negative	128 (77.6)	80 (76.2)	48 (80)	
vacA allele				
S1	113 (68.5)	78 (74.3)	35 (58.3)	
S2	52 (31.5)	27 (25.7)	25 (41.7)	< 0.05
M1	47 (28.5)	31 (29.5)	16 (26.7)	
M2	118 (71.5)	74 (70.5)	44 (73.3)	NS
S1/M1	39 (23.6)	26 (24.8)	13 (21.7)	NS
S1/M2	74 (44.8)	52 (49.5)	22 (36.7)	NS
S2/M1	8 (4.8)	5 (4.8)	3 (5.0)	NS
S2/M2	44 (26.7)	22 (21.0)	22 (36.7)	< 0.05

[1]Treatment-naïve versus previously treated patients (Fisher's exact test).

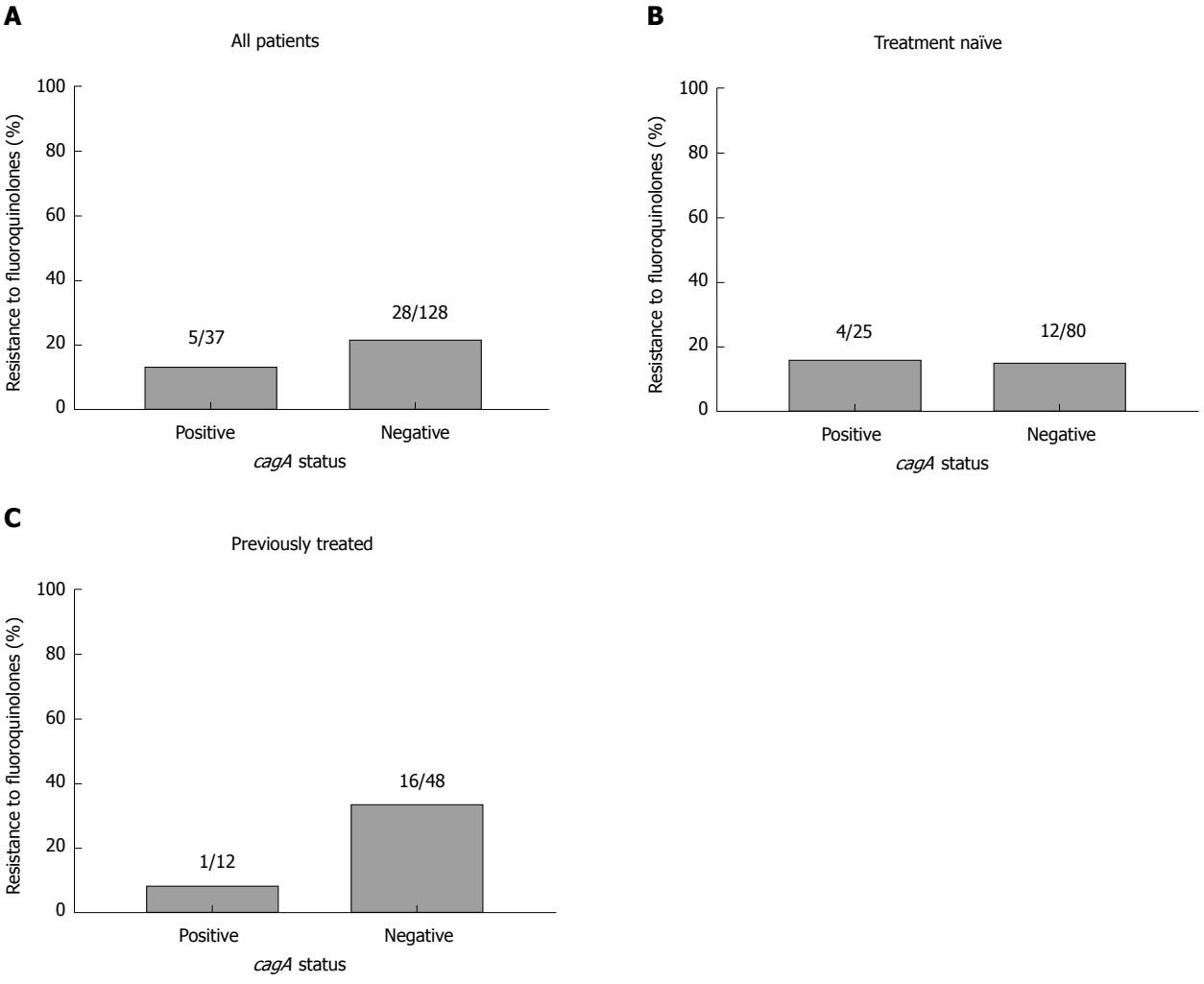

Figure 3 Prevalence of fluoroquinolone-resistance according to *cagA* genotype. A: All patients; B: Treatment naïve patients; C: Previously treated patients.

in *H. pylori* antibiotic resistance rates among different populations are influenced by previous antibiotic use, with studies demonstrating that previous exposure to macrolides increases the risk of clarithromycin resistant *H. pylori* infection[5,22]. The sharp increase in primary clarithromycin resistance from 3.9% in 1997 to 9.3% in 2008[23], to the current rate of 50.5% in 2017 is a cause for concern and is reflected in the poor eradication rate (56.8% ITT) for 7 days clarithromycin-based triple therapy recently reported from our centre[3]. In an effort to address increasing antibiotic resistance and falling eradication rates, the Irish *H. pylori* Working Group

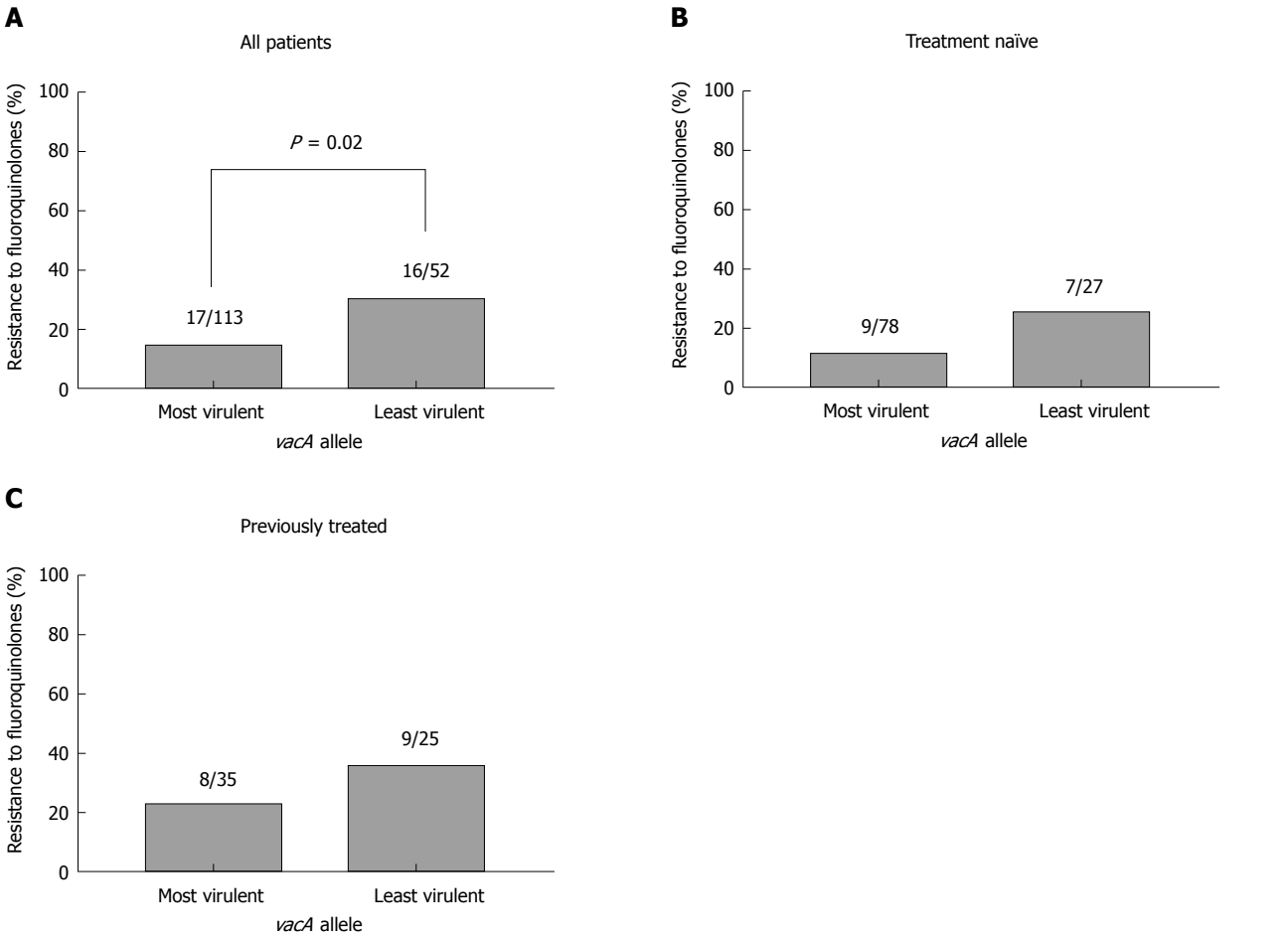

Figure 4 Prevalence of fluoroquinolone-resistance according to *vacA* genotype. A: All patients; B: Treatment naïve patients; C: Previously treated patients. Most virulent: S1/M1, S1/M2; Least virulent: S2/M1; S2/M2.

have recently highlighted the need for more widespread antibiotic resistance surveillance and extended *H. pylori* treatment durations[24]. It should be noted that antibiotic resistance was determined at the genetic level in the current study compared to culture and Etests in the earlier Irish surveys.

The primary and secondary rates of fluoroquinolone resistance were 15.2% and 28.3%, respectively. The primary rate of levofloxacin resistance has only risen slightly since the last Irish survey in 2008-2009, which reported a rate of 12%[25], and is in keeping with the 14.1% rate reported in Europe[5]. The most common point mutation conferring resistance to fluoroquinolones in our patients was *gyr91* D91Y. This contrasts with other studies in which *gyr91* D91N and *gyr87* N87K mutations were reported with highest frequency[14,16-18].

In our cohort, the overall frequency of *H. pylori* infections with strains containing the *cagA* gene was 22.4%. This has decreased since the distribution of the *cagA* genotype was last investigated in Ireland in 2009, with a frequency of 68% reported[12]. It is also lower than distributions reported in Cuba and Iran[26,27]. There is a well-known association between *cagA*-positive strains of *H. pylori* and peptic ulcer disease[28,29]. This relatively low frequency of *cagA*-positive genotype is not surprising given that the prevalence of peptic ulcer disease was also low in our cohort at 12.7% (Table 2), which is a decrease on the prevalence of peptic ulcer disease reported in the previous Irish study (17%[12]). The most prevalent *vacA* genotype in our cohort was S1/M2, followed by S2/M2, S1/M1 and S2/M1. This pattern is similar to the pattern reported in Ireland in 2009 as well as the studies mentioned above[12,26,27].

Interestingly, the frequency of the more virulent S1 genotype was significantly lower in those previously treated than the treatment-naïve group (58.3% *vs* 74.3%). Additionally, the frequency of the least virulent S2/M2 genotype was significantly higher in those previously treated previously (36.7% *vs* 21%). This is in accordance with a hypothesis described previously which suggests that more virulent strains elicit a stronger inflammatory response, enabling increased blood flow to the site of infection, therefore enhancing delivery of antibiotics and the potential for successful eradication[30]. Another potential explanation is that a more virulent strain of *H. pylori* may replicate faster and is therefore more susceptible to antibiotics, whose mechanisms of action are to inhibit bacterial replication[31].

We found an inverse relationship between the

virulence of the infecting strain and the presence of clarithromycin resistance: the absence of *cagA,* and the less virulent *vacA* genotypes (S2/M1 and S2/M2), may be indicators of clarithromycin resistance, in particular in treatment-naïve patients. The association between virulence factors and antibiotic resistance in *H. pylori* has been evaluated in other studies, with controversial results. Absence of *cagA* was found to be a risk factor for metronidazole resistance[12] and other studies have found an association between clarithromycin resistance mutations and the less virulent *vacA* genotypes[32,33]. Another report revealed that *cagE* and *vacA* S1 correlated with clarithromycin and metronidazole resistance[34], while others found that neither *cagA* nor *vacA* was associated with resistance[29,35-37]. There may be no direct causation involving the presence of less virulent strains of *H. pylori* and antibiotic resistance. Rather, the presence or absence of virulence factors may cause physiological effects which create an environment in which antibiotic resistant strains of *H. pylori* can flourish as outlined above[31]. As less virulent strains are less immunogenic, an inadequate delivery of antibiotics may reach infected areas in the stomach and as a result, antimicrobial resistant strains may be selected for in the population of less virulent strains. It has been shown that a *cagA*- strain may tend to acquire drug resistance *in vitro*[12]. Indeed, studies have shown that virulence factor genotype may also influence treatment outcome. A number of studies have reported the presence or absence of *cagA* and *vacA* as predictors of eradication of *H. pylori*[36,38-40]. Wang *et al*[39] conducted a meta-analysis of 25 studies and found that infection with *cagA* positive, *vacA* S1 strains were associated with *H. pylori* eradication.

In conclusion, this study found that the *cagA* negative and *vacA* S1/M2 genotypes were the most dominant in *H. pylori* strains in Ireland. A surprisingly high rate of primary genotypic clarithromycin resistance was observed (50.5%), with a primary genotypic fluoroquinolone resistance rate of 15.2%. It was also found that there is a relationship between the less virulent strains of *H. pylori* (*cagA*-negative and *vacA* S2) and primary clarithromycin resistance. It is well known that the prevalence of antibiotic resistance is increasing worldwide while eradication rates of *H. pylori* are decreasing. The relationship between less virulent strains of *H. pylori* and presence of antibiotic resistance found herein could potentially be an avenue to explore in the effort to improve eradication rates.

ARTICLE HIGHLIGHTS

Research background

Helicobacter pylori (H. pylori) causes chronic gastritis, gastric and duodenal ulcers, gastric adenocarcinoma and mucosa-associated lymphoid tissue lymphoma. Disease outcome is related to both host and bacterial factors. Eradication is recommended in all symptomatic patients and those at risk of gastric cancer. However, eradication rates for current therapies are falling due to the emergence of antibiotic resistant *H. pylori* strains. *H. pylori* is a highly heterogeneous bacterium and its virulence varies geographically. Virulence factors contribute to the pathogenicity of the bacteria and have been suggested to influence treatment outcome.

Research motivation

In response to the increasing problem of *H. pylori* antibiotic resistance, local antibiotic resistance surveillance is recommended to guide clinicians in their choice of *H. pylori* therapy. Knowledge of local antimicrobial resistance rates and the prevalence of virulent infections will influence strategies for optimising the management of *H. pylori* infection.

Research objectives

This study aimed to provide an update on the prevalence of antibiotic resistance in Ireland, in particular for the antibiotics clarithromycin and fluoroquinolones. The virulence of the infecting strains was assessed by investigating *cagA* and *vacA* status. In addition the relationship between virulence factor status and antibiotic resistance was evaluated.

Research methods

DNA was extracted from antral and corpus biopsies obtained from *H. pylori*-infected patients. Genotyping for clarithromycin and fluoroquinolone-mediating mutations was performed using the Genotype HelicoDR assay. *CagA* and *vacA* genotypes were investigated using PCR and agarose gel electrophoresis.

Research results

Primary resistance to clarithromycin was high at 50.5%. Primary resistance to fluoroquinolones was 15.2%. Primary resistance to both antibiotics was 12.4%. A *cagA*-positive genotype was detected in 22.4% of patient samples. The dominant *vacA* genotype was S1/M2 at 44.8%, followed by S2/M2 at 26.7%, S1/M1 at 23.6% and S2/M1 at 4.8%. Primary clarithromycin resistance was significantly lower in *cagA*-positive strains than in *cagA*-negative strains (32% *vs* 56.3%). Similarly, in patients infected with more virulent *H. pylori* strains bearing the *vacA* s1 genotype, primary clarithromycin resistance was significantly lower than in those infected with less virulent strains bearing the *vacA* s2 genotype, (41% *vs* 77.8%). In summary, genotypic *H. pylori* clarithromycin resistance is high and *cagA*-negative strains are dominant in our population. Less virulent (*cagA*-negative and *vacA* S2-containing) strains of *H. pylori* are associated with primary clarithromycin resistance.

Research perspectives

Given the high rate of primary clarithromycin resistance detected in our study, the use of alternatives to clarithromycin-based triple therapy should be considered for first line *H. pylori* treatment in our cohort. In order to validate the association between less virulent strains and clarithromycin resistance, the influence of virulence factor genotype on treatment outcome should be assessed.

ACKNOWLEDGMENTS

The authors would like to acknowledge Mark Feighery, Ciara Treacy and Edwin Fahy for technical assistance.

REFERENCES

1 **Malfertheiner P**, Megraud F, O'Morain CA, Gisbert JP, Kuipers EJ, Axon AT, Bazzoli F, Gasbarrini A, Atherton J, Graham DY, Hunt R, Moayyedi P, Rokkas T, Rugge M, Selgrad M, Suerbaum S, Sugano K, El-Omar EM; European Helicobacter and Microbiota Study Group and Consensus panel. Management of Helicobacter pylori infection-the Maastricht V/Florence Consensus Report. *Gut* 2017; **66**: 6-30 [PMID: 27707777 DOI: 10.1136/gutjnl-2016-312288]

2 **Leja M**, Axon A, Brenner H. Epidemiology of Helicobacter pylori infection. *Helicobacter* 2016; **21** Suppl 1: 3-7 [PMID: 27531531 DOI: 10.1111/hel.12332]

3 **Haider RB**, Brennan DE, Omorogbe J, Holleran G, Hall B, O'Morain C, Breslin N, O'Connor HJ, Smith SM, McNamara

D. A randomized-controlled study to compare the efficacy of sequential therapy with standard triple therapy for Helicobacter pylori eradication in an Irish population. *Eur J Gastroenterol Hepatol* 2015; **27**: 1265-1269 [PMID: 26287955 DOI: 10.1097/MEG.0000000000000457]

4 **Graham DY**, Fischbach L. Helicobacter pylori treatment in the era of increasing antibiotic resistance. *Gut* 2010; **59**: 1143-1153 [PMID: 20525969 DOI: 10.1136/gut.2009.192757]

5 **Megraud F**, Coenen S, Versporten A, Kist M, Lopez-Brea M, Hirschl AM, Andersen LP, Goossens H, Glupczynski Y; Study Group participants. Helicobacter pylori resistance to antibiotics in Europe and its relationship to antibiotic consumption. *Gut* 2013; **62**: 34-42 [PMID: 22580412 DOI: 10.1136/gutjnl-2012-302254]

6 **Smith SM**, O'Morain C, McNamara D. Antimicrobial susceptibility testing for Helicobacter pylori in times of increasing antibiotic resistance. *World J Gastroenterol* 2014; **20**: 9912-9921 [PMID: 25110421 DOI: 10.3748/wjg.v20.i29.9912]

7 **Fischbach L**, Evans EL. Meta-analysis: the effect of antibiotic resistance status on the efficacy of triple and quadruple first-line therapies for Helicobacter pylori. *Aliment Pharmacol Ther* 2007; **26**: 343-357 [PMID: 17635369 DOI: 10.1111/j.1365-2036.2007.03386.x]

8 **Broutet N**, Tchamgoué S, Pereira E, Lamouliatte H, Salamon R, Mégraud F. Risk factors for failure of Helicobacter pylori therapy--results of an individual data analysis of 2751 patients. *Aliment Pharmacol Ther* 2003; **17**: 99-109 [PMID: 12492738 DOI: 10.1046/j.1365-2036.2003.01396.x]

9 **Uotani T**, Miftahussurur M, Yamaoka Y. Effect of bacterial and host factors on Helicobacter pylori eradication therapy. *Expert Opin Ther Targets* 2015; **19**: 1637-1650 [PMID: 26245678 DOI: 10.1517/14728222.2015.1073261]

10 **Atherton JC**, Cao P, Peek RM Jr, Tummuru MK, Blaser MJ, Cover TL. Mosaicism in vacuolating cytotoxin alleles of Helicobacter pylori. Association of specific vacA types with cytotoxin production and peptic ulceration. *J Biol Chem* 1995; **270**: 17771-17777 [PMID: 7629077 DOI: 10.1074/jbc.270.30.17771]

11 **Rhead JL**, Letley DP, Mohammadi M, Hussein N, Mohagheghi MA, Eshagh Hosseini M, Atherton JC. A new Helicobacter pylori vacuolating cytotoxin determinant, the intermediate region, is associated with gastric cancer. *Gastroenterology* 2007; **133**: 926-936 [PMID: 17854597 DOI: 10.1053/j.gastro.2007.06.056]

12 **Taneike I**, Nami A, O'Connor A, Fitzgerald N, Murphy P, Qasim A, O'Connor H, O'Morain C. Analysis of drug resistance and virulence-factor genotype of Irish Helicobacter pylori strains: is there any relationship between resistance to metronidazole and cagA status? *Aliment Pharmacol Ther* 2009; **30**: 784-790 [PMID: 19604178 DOI: 10.1111/j.1365-2036.2009.04095.x]

13 **Brennan DE**, Omorogbe J, Hussey M, Tighe D, Holleran G, O'Morain C, Smith SM, McNamara D. Molecular detection of Helicobacter pylori antibiotic resistance in stool vs biopsy samples. *World J Gastroenterol* 2016; **22**: 9214-9221 [PMID: 27895408 DOI: 10.3748/wjg.v22.i41.9214]

14 **Pastukh N**, Binyamin D, On A, Paritsky M, Peretz A. GenoType ® HelicoDR test in comparison with histology and culture for Helicobacter pylori detection and identification of resistance mutations to clarithromycin and fluoroquinolones. *Helicobacter* 2017; **22** [PMID: 29058343 DOI: 10.1111/hel.12447]

15 **Cambau E**, Allerheiligen V, Coulon C, Corbel C, Lascols C, Deforges L, Soussy CJ, Delchier JC, Megraud F. Evaluation of a new test, genotype HelicoDR, for molecular detection of antibiotic resistance in Helicobacter pylori. *J Clin Microbiol* 2009; **47**: 3600-3607 [PMID: 19759218 DOI: 10.1128/JCM.00744-09]

16 **Lee JW**, Kim N, Nam RH, Park JH, Choi YJ, Kim JM, Kim JS, Jung HC. GenoType HelicoDR test in the determination of antimicrobial resistance of Helicobacter pylori in Korea. *Scand J Gastroenterol* 2014; **49**: 1058-1067 [PMID: 24957849 DOI: 10.3109/00365521.2014.894117]

17 **Miendje Deyi VY**, Burette A, Bentatou Z, Maaroufi Y, Bontems P, Lepage P, Reynders M. Practical use of GenoType® HelicoDR, a molecular test for Helicobacter pylori detection and susceptibility testing. *Diagn Microbiol Infect Dis* 2011; **70**: 557-560 [PMID: 21696906 DOI: 10.1016/j.diagmicrobio.2011.05.002]

18 **Sanches BS**, Martins GM, Lima K, Cota B, Moretzsohn LD, Ribeiro LT, Breyer HP, Maguilnik I, Maia AB, Rezende-Filho J, Meira AC, Pinto H, Alves E, Mascarenhas R, Passos R, de Souza JD, Trindade OR, Coelho LG. Detection of Helicobacter pylori resistance to clarithromycin and fluoroquinolones in Brazil: A national survey. *World J Gastroenterol* 2016; **22**: 7587-7594 [PMID: 27672279 DOI: 10.3748/wjg.v22.i33.7587]

19 **Tanih NF**, Ndip RN. Molecular Detection of Antibiotic Resistance in South African Isolates of Helicobacter pylori. *Gastroenterol Res Pract* 2013; **2013**: 259457 [PMID: 23710166 DOI: 10.1155/2013/259457]

20 **Macías-García F**, Llovo-Taboada J, Díaz-López M, Bastón-Rey I, Domínguez-Muñoz JE. High primary antibiotic resistance of Helicobacter Pylori strains isolated from dyspeptic patients: A prevalence cross-sectional study in Spain. *Helicobacter* 2017; **22** [PMID: 28913872 DOI: 10.1111/hel.12440]

21 **Kuo YT**, Liou JM, El-Omar EM, Wu JY, Leow AHR, Goh KL, Das R, Lu H, Lin JT, Tu YK, Yamaoka Y, Wu MS; Asian Pacific Alliance on Helicobacter and Microbiota. Primary antibiotic resistance in Helicobacter pylori in the Asia-Pacific region: a systematic review and meta-analysis. *Lancet Gastroenterol Hepatol* 2017; **2**: 707-715 [PMID: 28781119 DOI: 10.1016/S2468-1253(17)30219-4]

22 **McNulty CA**, Lasseter G, Shaw I, Nichols T, D'Arcy S, Lawson AJ, Glocker E. Is Helicobacter pylori antibiotic resistance surveillance needed and how can it be delivered? *Aliment Pharmacol Ther* 2012; **35**: 1221-1230 [PMID: 22469191 DOI: 10.1111/j.1365-2036.2012.05083.x]

23 **O'Connor A**, Taneike I, Nami A, Fitzgerald N, Murphy P, Ryan B, O'Connor H, Qasim A, Breslin N, O'Moráin C. Helicobacter pylori resistance to metronidazole and clarithromycin in Ireland. *Eur J Gastroenterol Hepatol* 2010; **22**: 1123-1127 [PMID: 20354442 DOI: 10.1097/MEG.0b013e328338e43d]

24 **Smith S**, Boyle B, Brennan D, Buckley M, Crotty P, Doyle M, Farrell R, Hussey M, Kevans D, Malfertheiner P, Megraud F, Nugent S, O'Connor A, O'Morain C, Weston S, McNamara D. The Irish Helicobacter pylori Working Group consensus for the diagnosis and treatment of H. pylori infection in adult patients in Ireland. *Eur J Gastroenterol Hepatol* 2017; **29**: 552-559 [PMID: 28350745 DOI: 10.1097/MEG.0000000000000822]

25 **O'Connor A**, Taneike I, Nami A, Fitzgerald N, Ryan B, Breslin N, O'Connor H, McNamara D, Murphy P, O'Morain C. Helicobacter pylori resistance rates for levofloxacin, tetracycline and rifabutin among Irish isolates at a reference centre. *Ir J Med Sci* 2013; **182**: 693-695 [PMID: 23625165 DOI: 10.1007/s11845-013-0957-3]

26 **Feliciano O**, Gutierrez O, Valdés L, Fragoso T, Calderin AM, Valdes AE, Llanes R. Prevalence of Helicobacter pylori vacA, cagA, and iceA Genotypes in Cuban Patients with Upper Gastrointestinal Diseases. *Biomed Res Int* 2015; **2015**: 753710 [PMID: 25945344 DOI: 10.1155/2015/753710]

27 **Pajavand H**, Alvandi A, Mohajeri P, Bakhtyari S, Bashiri H, Kalali B, Gerhard M, Najafi F, Abiri R. High Frequency of vacA s1m2 Genotypes Among Helicobacter pylori Isolates From Patients With Gastroduodenal Disorders in Kermanshah, Iran. *Jundishapur J Microbiol* 2015; **8**: e25425 [PMID: 26862378 DOI: 10.5812/jjm.25425]

28 **van Doorn LJ**, Schneeberger PM, Nouhan N, Plaisier AP, Quint WG, de Boer WA. Importance of Helicobacter pylori cagA and vacA status for the efficacy of antibiotic treatment. *Gut* 2000; **46**: 321-326 [PMID: 10673291 DOI: 10.1136/gut.46.3.321]

29 **Godoy AP**, Ribeiro ML, Benvengo YH, Vitiello L, Miranda Mde C, Mendonça S, Pedrazzoli J Jr. Analysis of antimicrobial susceptibility and virulence factors in Helicobacter pylori clinical isolates. *BMC Gastroenterol* 2003; **3**: 20 [PMID: 12911839 DOI: 10.1186/1471-230X-3-20]

30 **Khan A**, Farooqui A, Manzoor H, Akhtar SS, Quraishy MS, Kazmi SU. Antibiotic resistance and cagA gene correlation: a looming crisis of Helicobacter pylori. *World J Gastroenterol* 2012; **18**: 2245-2252 [PMID: 22611319 DOI: 10.3748/wjg.v18.i18.2245]

31 **Sugimoto M**, Yamaoka Y. Virulence factor genotypes of Helicobacter pylori affect cure rates of eradication therapy. *Arch Immunol Ther Exp* (Warsz) 2009; **57**: 45-56 [PMID: 19219527 DOI: 10.1007/s00005-009-0007-z]

32 **Boyanova L**, Markovska R, Yordanov D, Gergova G, Mitov I. Clarithromycin Resistance Mutations in Helicobacter pylori in Association with Virulence Factors and Antibiotic Susceptibility of the Strains. *Microb Drug Resist* 2016; **22**: 227-232 [PMID: 26618567 DOI: 10.1089/mdr.2015.0199]

33 **Elviss NC**, Owen RJ, Xerry J, Walker AM, Davies K. Helicobacter pylori antibiotic resistance patterns and genotypes in adult dyspeptic patients from a regional population in North Wales. *J Antimicrob Chemother* 2004; **54**: 435-440 [PMID: 15243025 DOI: 10.1093/jac/dkh343]

34 **Karabiber H**, Selimoglu MA, Otlu B, Yildirim O, Ozer A. Virulence factors and antibiotic resistance in children with Helicobacter pylori gastritis. *J Pediatr Gastroenterol Nutr* 2014; **58**: 608-612 [PMID: 24792628 DOI: 10.1097/MPG.0000000000000273]

35 **López-Brea M**, Martínez MJ, Domingo D, Sánchez I, Alarcón T. Metronidazole resistance and virulence factors in Helicobacter pylori as markers for treatment failure in a paediatric population. *FEMS Immunol Med Microbiol* 1999; **24**: 183-188 [PMID: 10378418 DOI: 10.1111/j.1574-695X.1999.tb01280.x]

36 **Liou JM**, Chang CY, Chen MJ, Chen CC, Fang YJ, Lee JY, Wu JY, Luo JC, Liou TC, Chang WH, Tseng CH, Wu CY, Yang TH, Chang CC, Wang HP, Sheu BS, Lin JT, Bair MJ, Wu MS; Taiwan Gastrointestinal Disease and Helicobacter Consortium. The Primary Resistance of Helicobacter pylori in Taiwan after the National Policy to Restrict Antibiotic Consumption and Its Relation to Virulence Factors-A Nationwide Study. *PLoS One* 2015; **10**: e0124199 [PMID: 25942450 DOI: 10.1371/journal.pone.0124199]

37 **van Doorn LJ**, Glupczynski Y, Kusters JG, Mégraud F, Midolo P, Maggi-Solcà N, Queiroz DM, Nouhan N, Stet E, Quint WG. Accurate prediction of macrolide resistance in Helicobacter pylori by a PCR line probe assay for detection of mutations in the 23S rRNA gene: multicenter validation study. *Antimicrob Agents Chemother* 2001; **45**: 1500-1504 [PMID: 11302817 DOI: 10.1128/AAC.45.5.1500-1504.2001]

38 **Suzuki T**, Matsuo K, Sawaki A, Ito H, Hirose K, Wakai K, Sato S, Nakamura T, Yamao K, Ueda R, Tajima K. Systematic review and meta-analysis: importance of CagA status for successful eradication of Helicobacter pylori infection. *Aliment Pharmacol Ther* 2006; **24**: 273-280 [PMID: 16842453 DOI: 10.1111/j.1365-2036.2006.02994.x]

39 **Wang D**, Li Q, Gong Y, Yuan Y. The association between vacA or cagA status and eradication outcome of Helicobacter pylori infection: A meta-analysis. *PLoS One* 2017; **12**: e0177455 [PMID: 28493953 DOI: 10.1371/journal.pone.0177455]

40 **Figura N**, Moretti E, Vaglio L, Langone F, Vernillo R, Vindigni C, Giordano N. Factors modulating the outcome of treatment for the eradication of Helicobacter pylori infection. *New Microbiol* 2012; **35**: 335-340 [PMID: 22842603]

P- Reviewer: Chiba T, Rodrigo L, Sugimoto M **S- Editor**: Wang XJ
L- Editor: A **E- Editor**: Huang Y

World Journal of Gastroenterology

Submit a Manuscript: http://www.f6publishing.com

World J Gastroenterol 2018 March 7; 24(9): 982-991

DOI: 10.3748/wjg.v24.i9.982

ISSN 1007-9327 (print) ISSN 2219-2840 (online)

ORIGINAL ARTICLE

Basic Study

Dysregulation of PARP1 is involved in development of Barrett's esophagus

Chao Zhang, Teng Ma, Tao Luo, Ang Li, Xiang Gao, Zhong-Gao Wang, Fei Li

Chao Zhang, Tao Luo, Ang Li, Xiang Gao, Zhong-Gao Wang, Fei Li, Department of General Surgery, Xuanwu Hospital, Capital Medical University, Beijing 100053, China

Teng Ma, Beijing Institute of Radiation Medicine, Beijing 100053, China

Zhong-Gao Wang, Department of Gastroesophageal Reflux Disease, Second Artillery General Hospital of Chinese People's Liberation Army, Beijing 100088, China

ORCID number: Chao Zhang (0000-0002-1825-0097); Teng Ma (0000-0002-8360-1543); Tao Luo (0000-0002-4641-0027); Ang Li (0000-0003-4795-8374); Xiang Gao (0000-0003-2297-903X); Zhong-Gao Wang (0000-0003-4436-3770); Fei Li (0000-0002-1713-967X).

Author contributions: Zhang C, Ma T and Luo T are co-first authors; Zhang C, Ma T, Luo T and Li F designed and performed the research; Ma T, Li A and Gao X contributed the analytical tools; Zhang C and Luo T analyzed the data; Zhang C and Ma T wrote the manuscript; Luo T and Li F revised the manuscript; all authors read and approved the final manuscript.

Supported by the National Natural Science Foundation of China, No. 81470587; and Beijing Municipal Natural Science Foundation of China, No. 7162076.

Institutional review board statement: The study was reviewed and approved by the Second Artillery General Hospital of Chinese People's Liberation Army and the Xuanwu Hospital Institutional Review Boards.

Institutional animal care and use committee statement: Approval from the animal care and use committee of Xuanwu Hospital was obtained for this study.

Conflict-of-interest statement: The authors declare that they have no conflicts of interest.

Data sharing statement: There are no additional data available.

ARRIVE guidelines statement: This study meets the requirements of the ARRIVE guidelines.

Manuscript source: Unsolicited manuscript

Correspondence to: Fei Li, MD, PhD, Chief Doctor, Professor, Department of General Surgery, Xuanwu Hospital of Capital Medical University, No. 45, Changchun Street, Xicheng District, Beijing 100053, China. feili35@126.com
Telephone: +86-10-83198731
Fax: +86-10-83198868

Received: December 9, 2017
Peer-review started: December 9, 2017
First decision: December 20, 2017
Revised: December 26, 2017
Accepted: January 23, 2018
Article in press: January 23, 2018
Published online: March 7, 2018

Abstract

AIM

To investigate the potential role of poly(ADP-ribose) polymerase 1 (PARP1) in the development of Barrett's esophagus (BE).

METHODS

A BE mouse model was established to examine the esophageal morphological changes and molecular changes. Microarray analysis was performed to compare the gene expression profiles between BE patients and healthy controls. qPCR was used to examine the PARP1 expression in cell lines after treatment with H_2O_2 and

bile acids (pH 4). Immunofluorescence staining, comet assay, and annexin V staining were used to evaluate the impact of PARP1 activity on cell survival and DNA damage response after oxidative stress.

RESULTS

The gene expression profile in normal and BE esophageal epithelial cells showed that PARP1, the major poly(ADP-ribose) polymerase, was overexpressed in BE. In the mouse model of BE, positive staining for NF-κB, γH2AX, and poly(ADP-ribose) (PAR) was observed. H_2O_2 and bile acids (pH 4) increased the PARP1 mRNA expression level in normal esophageal epithelial cells. Using shRNA-PARP1 to suppress PARP1 activity decreased the cell viability after treatment with H_2O_2 and bile acids (pH 4), and increased the oxidative damage as demonstrated by an increase in the levels of H_2O_2, intracellular reactive oxygen species (ROS), oxidative DNA damage, double-strand breaks, and apoptosis ($P < 0.01$).

CONCLUSION

The dysfunction of PARP1 in esophageal epithelial cells increases the levels of ROS and oxidative DNA damage, which could be common risk factors for BE and esophageal adenocarcinoma.

Key words: PARP1; Barrett's esophagus; DNA repair; Oxidative damage; Bile acids

Core tip: In this study, we compared the gene expression profile in normal esophagus and Barrett's esophagus (BE), and found that poly(ADP-ribose) polymerase 1 (PARP1) was overexpressed in BE. In a BE model, positive staining for NF-κB, γH2AX, and PAR was observed. H_2O_2 and bile acids (pH 4) increased the PARP1 mRNA expression level in normal esophageal epithelial cells. PARP1 inhibition could decrease the cell viability after bile acids treatment, and increased the oxidative damage, double-strand breaks, and apoptosis. Thus, our study demonstrates a novel molecular mechanism for the role of PARP1 in the process of Barrett's metaplasia, which sheds a potential therapeutic role for PARP1 inhibitor in BE.

Zhang C, Ma T, Luo T, Li A, Gao X, Wang ZG, Li F. Dysregulation of PARP1 is involved in development of Barrett's esophagus. *World J Gastroenterol* 2018; 24(9): 982-991 Available from: URL: http://www.wjgnet.com/1007-9327/full/v24/i9/982.htm DOI: http://dx.doi.org/10.3748/wjg.v24.i9.982

INTRODUCTION

Gastro-esophageal reflux disease (GERD) is known as reflux of gastric acid, usually mixed with bile acids, into the lower esophagus[1-3]. GERD-associated chronic mucosal injury and inflammation are major risk factors for the development of Barrett's esophagus (BE), a premalignant condition closely associated with the development of esophageal adenocarcinoma. BE is present in 10%-20% of patients with GERD[4,5]. Although the leading cause of BE is formerly considered a chronic inflammation, increasing evidence suggests that oxidative stress-induced DNA damage induces the apoptosis of esophageal epithelial cells during the pathogenesis of BE. However, it is unclear why esophageal epithelial cells are sensitive to oxidative damage.

Oxidative DNA damage is usually induced by reactive oxygen species (ROS) primarily generated from normal intracellular metabolism in mitochondria and peroxisomes[6,7]. A number of external hazards such as ionizing radiation, chemicals, and solar ultraviolet light can also trigger ROS production. These active free radicals attack double-strand DNA, inducing various types of DNA lesions, including DNA single-strand breaks (SSBs) and DNA double-strand breaks (DSBs), which may lead to genomic instability[6,8]. To cope with these threats, cells have evolved DNA damage response systems to detect and repair DNA lesions. As one of the earliest alarm systems and regulators in DNA damage response, poly(ADP-ribose) (PAR) participates in the repair of numerous types of DNA damage including SSBs and DSBs[9]. Thus, the cellular metabolism of PAR is critical for DNA damage response and genomic stability. The reaction of poly(ADP-ribosyl)ation (PARylation) is catalyzed by a group of PAR polymerases (PARPs). Using NAD+ as the substrate, PARPs covalently adds ADP-ribose to the side chains of arginine, aspartic acid, and glutamic acid residues in target proteins. After catalyzing the first ADP-ribose onto the proteins, other ADP-riboses can be covalently linked and the continuous reactions produce both linear and branched polymers known as PAR[10]. The structure of PAR has been well characterized: the ADP-ribose unit in the polymer is linked by glycosidic ribose-ribose 1'-2' bonds. The chain length is heterogeneous and can reach around 200 units with 20-50 units in each branch[11].

Although PARylation has been examined both *in vivo* and *in vitro*, the function of PARP1 in esophageal epithelial cells remains elusive. In this study, we hypothesized that PARP1 may be involved in the oxidative damage in the development of BE. We aimed to investigate the potential role of PARP1 and PARylation-related DNA damage in the process of BE in GERD through using a BE mouse model and BE cell lines. Elucidating the role of PARP1 in BE will provide a novel therapeutic strategy for this condition.

MATERIALS AND METHODS

GERD model preparation and BE verification

Experiments in 20 male C57Bl/6 mice with a mean weight of 29 g (27-31 g) were performed. All

Table 1 Baseline patient characteristics

Patient characteristic	*n* = 20
Age (mean ± SD), yr	56.0 ± 12.5
Gender, male, *n* (%)	16 (80)
Body mass index (mean ± SD), kg/m^2	26.5 ± 3.1
Barrett's length (median, IQR), cm	4.7 (3.8-5.5)
Circumferential extent (C)	100%

mice adapted to the environment 7 d to 10 d after purchase, and then water was banned for 24 h before the operation. Chloral hydrate (10%; 3 mL/kg) was administered intraperitoneally for anesthesia. The lower end of the esophagus was separated and a longitudinal cut (about 1-1.5 cm) was performed at the gastroesophageal junction without vascular region. The anti-reflux barrier of the gastroesophageal junction was damaged by the operation.

Hematoxylin and eosin staining and immunohistochemical staining

Animals were sacrificed 3 mo after surgery. Samples were taken in the operating room of the animal facility immediately after the animal sacrifice. The entire stomach and esophagus were removed and immediately fixed in formalin for at least 24 h. Subsequently, samples were processed for paraffin embedding and 7 μmol/L sections were obtained through a microtome and put on positive charged slides. Sections of the lower esophagus were then stained with HE following a standardized protocol and observed under a light microscope. The same samples were subjected for immunohistochemistry. For immunohistochemical staining, sections were placed on polylysine-coated slides. After deparaffinization in xylene and rehydration through graded alcohol, each section was treated with 1% hydrogen peroxide for 20 min, and then blocking serum was applied for 20 min. The slides were incubated overnight with the primary antibody (γH2AX and NF-κB at 1:300 and PAR at 1:500) at 4 ℃ in a closed chamber. Immunohistochemical staining was performed by the streptoavidin-biotin-peroxidase complex technique (Histofine SAB-PO(M) Kit; Nichirei Corp., Tokyo, Japan). Staining was done with 3,3′-diaminobenzidine followed by light counterstaining with methyl green and dehydration.

Cell isolation and culture

Immortalised BE cell lines BAR-T and CP-A (American Type Culture Collection, ATCC, Manassas, VA, United States) were cultured with epithelial cell medium 2 (ScienCell, Carlsbad, CA, United States), supplemented with 5% fetal bovine serum and antibiotics on primaria plates and flasks (BD Biosciences, Bedford, MA, United States). The immortalised human esophageal epithelia cell lines HET1A and EPC2 were obtained from ATCC. HET1A cell line was cultured in Dulbecco's modified Eagle's medium (DMEM) supplemented with 10% fetal bovine serum and antibiotics (Invitrogen). EPC2 cells were grown in keratinocyte SFM medium supplemented with 40 mg/mL bovine pituitary extract and 1.0 ng/mL epidermal growth factor (Invitrogen, Carlsbad, California, United States). All cell lines were grown at 37 ℃ in 5% carbon dioxide.

Patients

Tissue samples of the lower esophagus from 39 individuals, consisting of esophageal squamous epithelia from 19 healthy subjects and 20 specimens from patients with BE, were obtained from the pathological center of the Xuanwu Hospital or the Second Artillery General Hospital of Chinese People's Liberation Army in China. The baseline characteristics of patients are shown in Table 1. Gene expression was examined by whole-human-genome microarrays (Affymetrix, Santa Clara, CA, United States). Normal healthy esophageal biopsies were collected from patients with esophageal pain but diagnosed with normal squamous epithelia without pathological changes.

All samples were snap-frozen in liquid nitrogen and stored at -80 ℃. We obtained tissue specimens from all subjects with informed written consent (approved by the local ethics committees of the Xuanwu Hospital and the Second Artillery General Hospital of Chinese People's Liberation Army. Each single specimen included in this study was histopathologically approved according to grading and staging results by an experienced pathologist.

Microarray

Preparation of labeled cRNA and hybridization were done using the gene chip hybridization, wash, and stain kit (Affymetrix, Santa Clara, CA, United States). Two cycle labeling was applied to all samples. In total, 28 chip data were collected using Gene Chip Operation Software (GCOS, Affymetrix, United States). The 39 specimens analyzed consisted of 20 BE and 19 normal esophageal samples. To obtain the relative gene expression measurements, probe set-level data extraction was performed with the GCRMA (Robust Multiarray Average) normalization algorithm implemented in GeneSpring GX10.2 (Agilent). All data were log2 transformed.

RNA extraction and qRT-PCR

RNA extraction was carried out using the RNeasy Mini Kit (Qiagen, Valencia, CA, United States). Total RNA quality and yield were assessed using a bioanalyzer system (Agilent 2100 Bioanalyzer; Agilent Technologies, CA, United States) and a spectrophotometer (NanoDrop ND-1000; NanoDrop Technologies, DE, United States). Only RNA with an RNA integrity number > 9.0 was used for microarray analysis.

For quantification of mRNA expression, qRT-PCR was performed for three genes plus one control, using pre-designed gene-specific TaqMan probes and primer

sets purchased from Applied Biosystems.

Comet assays

Single-cell gel electrophoretic comet assays were performed under alkaline conditions. Briefly, cells were treated with 100 μmol/L H_2O_2 at 37 ℃. For cellular lysis, the slides were immersed in the alkaline lysis solution overnight in the dark. Next, the slides were subjected to electrophoresis at 20 V (0.6 V/cm) for 25 min and stained in 2.5 mg/mL propidium iodide for 20 min. All images were taken with a fluorescence microscope and analyzed with Comet Assay IV software.

Immunofluorescence staining

After treatment with H_2O_2, cells were fixed in 3% paraformaldehyde and permeabilized in 0.5% Triton X-100 for 30 min at room temperature. Samples were blocked with 5% goat serum and then incubated in primary antibody for 1 h. Samples were then washed with PBS three times and incubated with secondary antibody for 30 min. After PBS washing, the nuclei were stained with Hoechst 33258. The signals were visualized by fluorescence microscopy. We calculated the number of γH2AX foci per nucleus, and for quantitative analysis, 15 nuclear foci were selected to count in each group. For the immunofluorescence assay of anti-8-oxoguanine (8-OXOG), cells were exposed to bile acids cocktail (0.1 mmol/L; pH 4) for 60 min. Cells were then incubated with primary antibody against 8-OXOG (mouse, 1:200; Millipore) overnight at 48 ℃, followed by incubation with secondary goat anti-mouse antibody conjugated with TRITC (1:1000) at room temperature for 45 min. The slides were mounted using Vectashield with DAPI (Vector Laboratories, Burlingame, CA, United States) and viewed under a fluorescence microscope.

Western blot analysis

Cells were harvested and lysed with 100 μL of NETN 300 lysis buffer unless otherwise specified. Soluble fractions were subjected to Western blot analysis.

Statistical analysis

All experiments were performed in triplicate unless indicated otherwise. Student's *t*-test was used for statistical analyses, and $P < 0.05$ was considered statistically significant.

RESULTS

Increased DNA damage response and inflammation in the mouse BE model

During the surgical operation, the mortality rate of mice was 10%, the perioperative mortality rate was 15%, and 1 wk later, the mortality rate was 10%. The lower esophagus from the BE mouse model was processed for staining for γH2AX, NF-κB, and PAR. In the mouse BE model, esophagitis with esophageal erosions and squamous epithelial thickening with basal cell layer hyperplasia were seen. Esophagitis was accompanied by the development of papillary hyperplasia of the squamous epithelia (Figure 1A). Columnar intestinal-type metaplasia resembling that of human BE was seen with erosive esophagitis. No adenocarcinoma or squamous cell carcinoma was seen. In the immunohistochemistry staining, more positive staining for γH2AX, NF-κB, and PAR was observed, suggesting the DNA damage response and inflammation in the BE epithelium.

PARP1 expression is upregulated in the esophageal epithelial cells of BE

To investigate the gene expression changes during the development of BE, samples from BE patients and normal esophagus controls were subjected to microarray analysis. 20 BE lesions for microarray analysis were resected from 20 patients with a mean age of 56 ± 12 years between February 2013 and January 2016. Main patient characteristics are presented in Table 1.

As shown in Figure 2A, PARP1 was one of the up-regulated genes. Representative expression profile of PARP1 between the BE patients and normal controls was also showed in Figure 2B. Besides, PARP1 expression in normal esophageal epithelial cell lines (HET1A and EPC2) and BE epithelial cell lines (CP-A and BAR-T) was also examined. PAPR1 was increased in CP-A and BAR-T cell lines.

To investigate whether PARP1 expression levels can be upregulated by exposure to H_2O_2 and acidic bile acids, we exposed HET1A cells to H_2O_2 (100 μmol/L) and bile acids (0.1 mmol/L; pH 4) for 30 min. Following this exposure, cells were washed in PBS and cultured in regular medium for 30 min, 1 h, 2 h, 4 h, or 8 h, and mRNA levels were measured by RT-PCR. In response to this treatment, significant upregulation of the mRNA levels of PARP1 was observed at 2 h for H_2O_2 and at 4 h and 8 h for both H_2O_2 and bile acids (Figure 2C).

PARP1 protects the epithelial cells of BE from H_2O_2-induced oxidative stress

We next tested the protective effect of PARP1 against H_2O_2-induced oxidative stress. The knockdown of PARP1 in BAR-T cells (Figure 3A) led to a significantly lower cell viability following exposure to H_2O_2, compared with controls ($P < 0.01$ for 100 μmol/L, 200 μmol/L, and 400 μmol/L H_2O_2; Figure 3B), suggesting that the downregulation of endogenous PARP1 sensitized the BAR-T cells to H_2O_2-induced oxidative stress. To further examine the oxidative DNA damage effect after H_2O_2 treatment, we performed comet assay analysis. As shown in Figure 3C, BAR-T cells with PARP1 knockdown displayed a significantly severe DNA damage signal upon exposure to 200 μmol/L H_2O_2 for 2 h (4.3 ± 0.8 *vs*

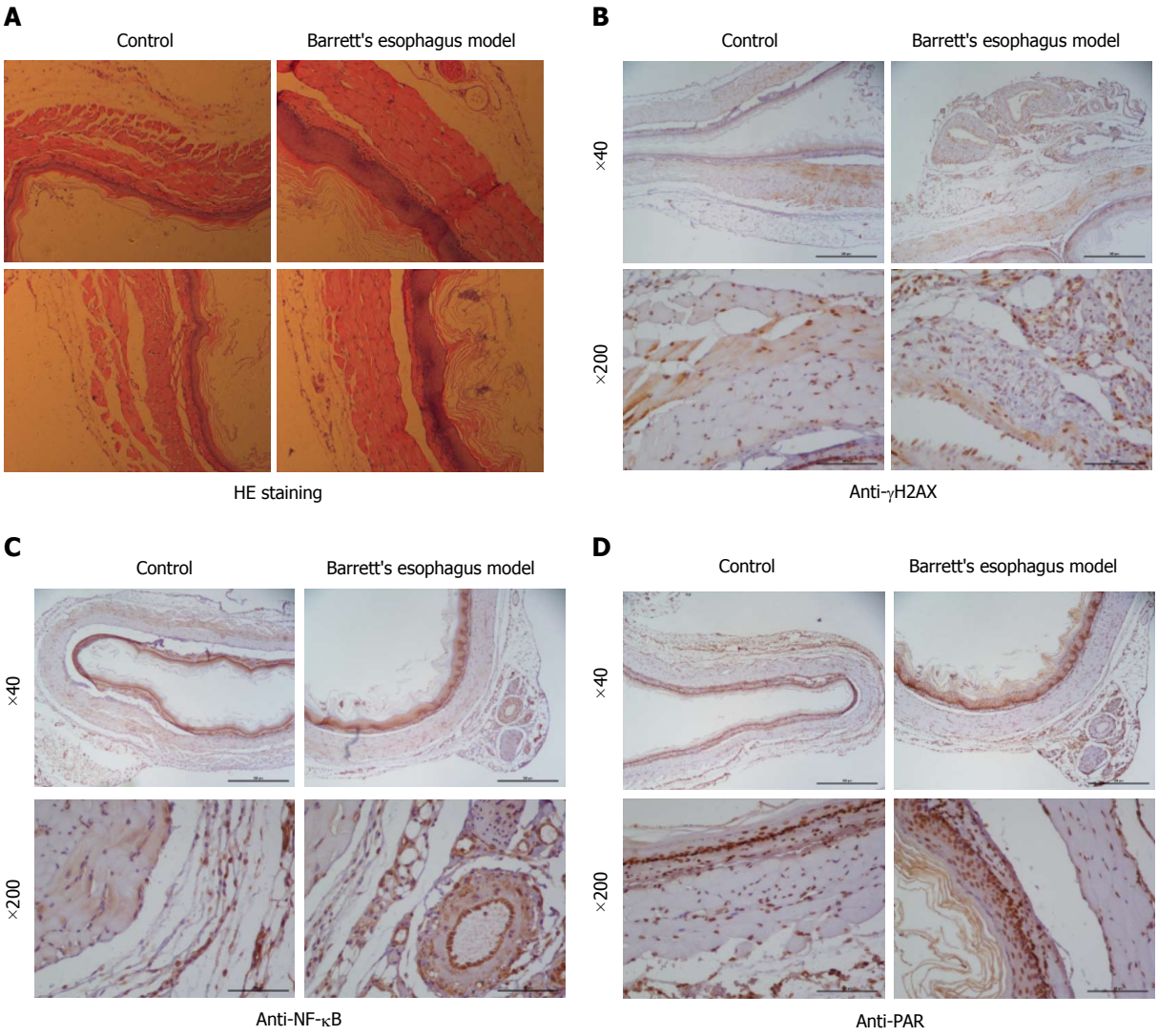

Figure 1 Establishment of a Barrett's esophagus mouse model. A: HE staining; B: γH2AX staining; C: NF-κB staining; D: Poly(ADP-ribose) staining.

8.6 ± 1.4, $P < 0.01$).

PARP1 knockdown leads to increased acidic bile acid-induced H_2O_2 level

We exposed BE epithelial cells to a bile acids cocktail adjusted to pH 4 and performed the Amplex UltraRed H_2O_2 assay to measure H_2O_2 levels. BAR-T cells with knockdown of endogenous PARP1 displayed higher H_2O_2 levels than control cells transfected with scrambled shRNA (Figure 4A).

PARP1 protects the epithelial cells of BE from acidic bile acid-induced oxidative DNA damage

We used immunofluorescence staining for 8-OXOG, one of the most identified oxidative DNA damage sites. On exposure of BAR-T cells with PARP1 knockdown to bile acids (pH 4), more oxidative DNA damage was observed than control cells exposed to acidic bile acids (Figure 4B).

PARP1 protects esophageal epithelial cells from acidic bile acid-induced DNA damage

Gastric acid, particularly in combination with bile acids, has been shown to induce DSBs in esophageal epithelial cells. The immunocytochemical staining for γH2AX, a reliable marker for DSBs, demonstrated significantly high levels of positive γH2AX sites following knockdown of PARP1 in BAR-T cells (19.8% ± 0.3% *vs* 42.6% ± 7.2%, $P < 0.01$, Figure 4C) than in control cells.

PARP1 protects esophageal epithelial cells from acidic bile acid-induced apoptosis

Because PARP1 expression protected cells from acidic bile acid-induced DNA damage, it may protect the epithelial cells of BE from acidic bile acid-induced apoptosis. BAR-T cells were treated with bile acids (pH 4) for 10 min or 30 min, followed by replacement with a regular culture medium for 24 h. The ATP-Glo cell

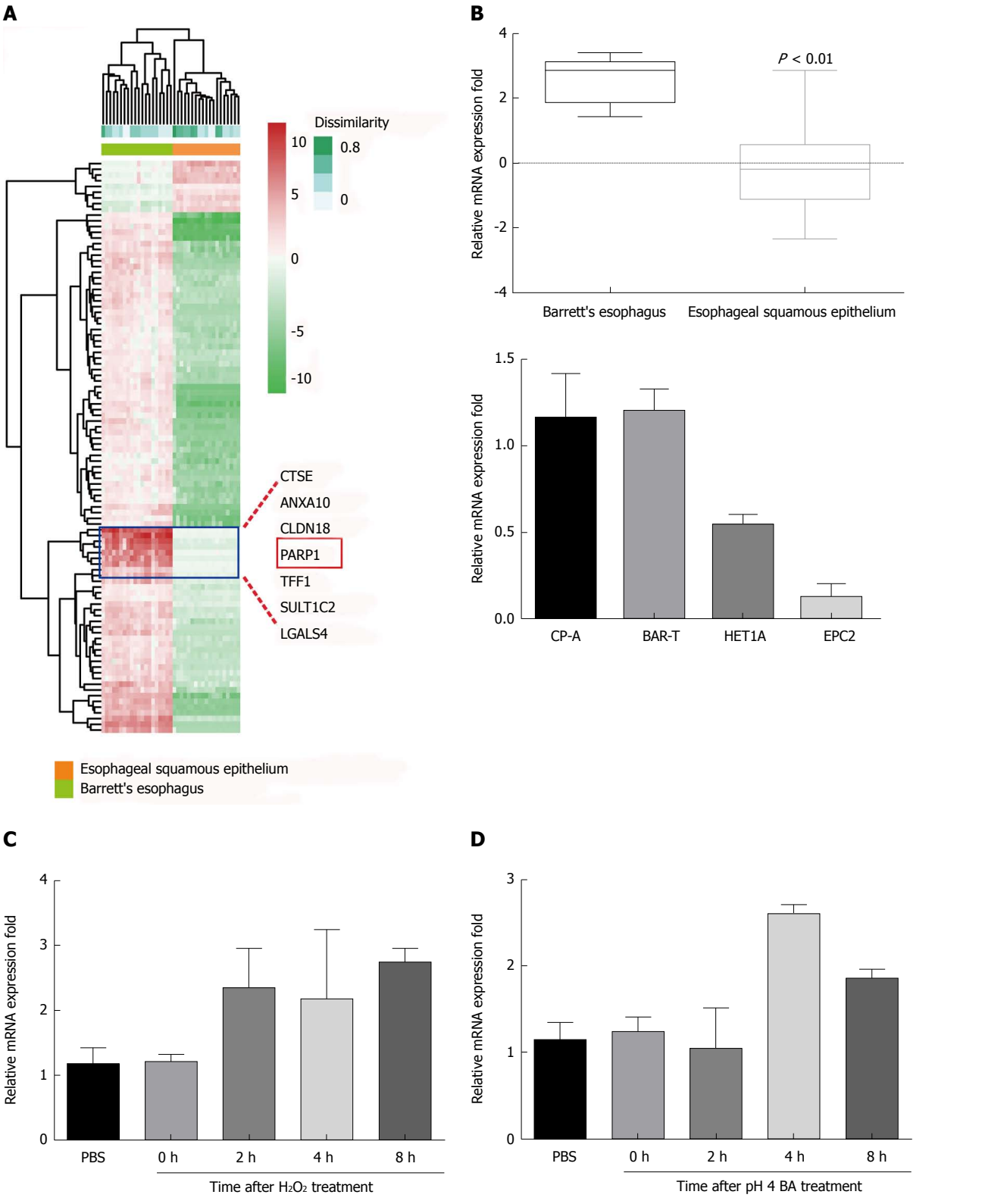

Figure 2 PARP1 is aberrantly expressed in Barrett's esophagus. A: Microarray profiling of gene expression between esophageal squamous epithelium and Barrett's esophagus; B: PARP1 is overexpressed in Barrett's esophagus and Barrett's esophagus cell lines; C: H_2O_2 increased PARP1 expression; D: BAs (pH 4) increased PARP1 expression.

viability assay was then used to determine cell viability at this 24 h time point. As shown in Figure 4D, the short-term exposure (10 min) did not change the cell viability at 24 h. However, the exposure for 30 min demonstrated a significant reduction in cell viability in BAR-T cells lacking PARP1 (82.5% ± 2.2% *vs* 63.0% ± 1.6%, $P < 0.05$). Consistent with this finding, the cells with PARP1 knockdown displayed significantly more

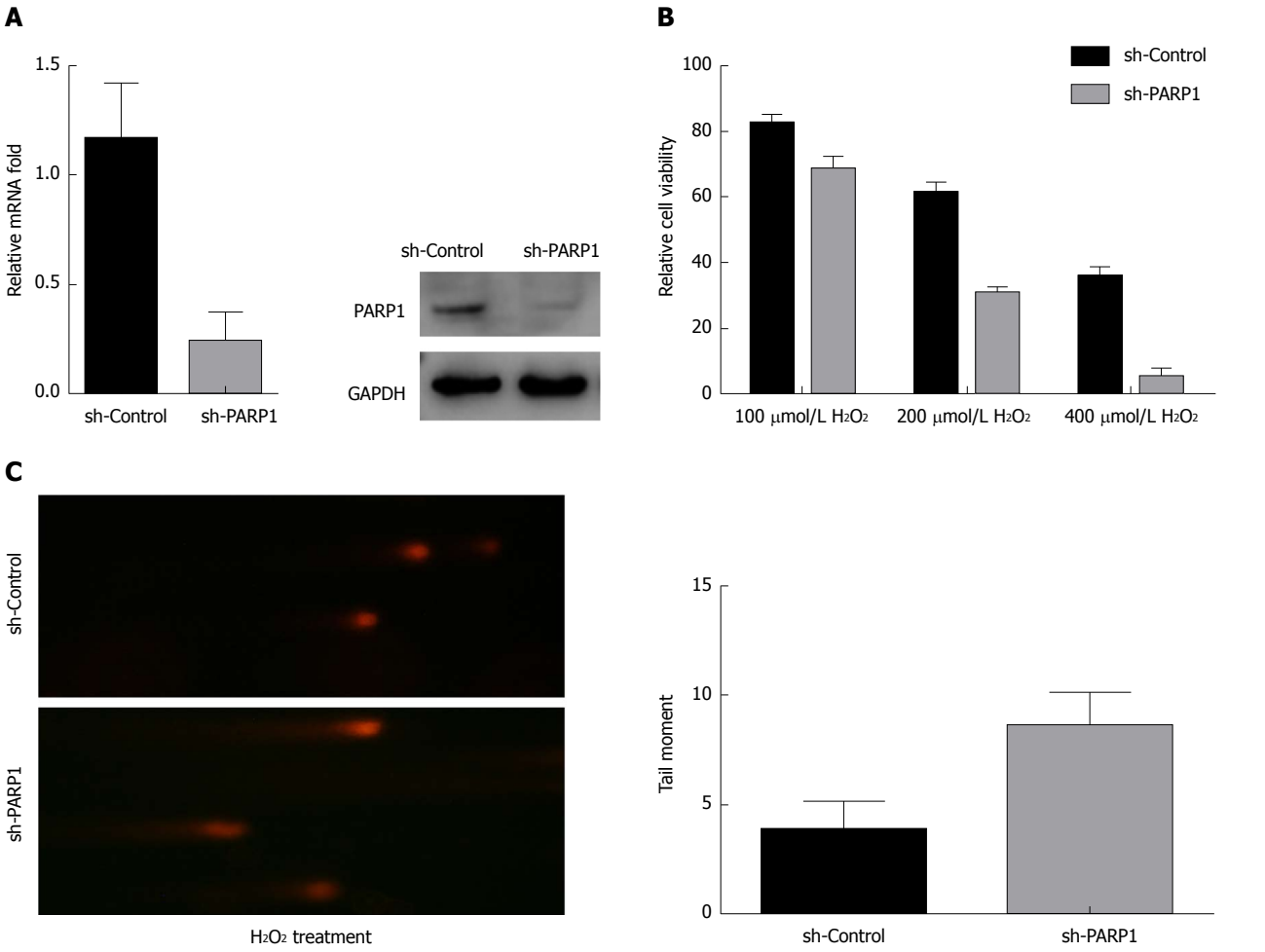

Figure 3 PARP1 protects Barrett's esophagus cells from H_2O_2-induced oxidative damage. A: Knockdown of PARP1 in BAR-T cells; B: BAR-T cells were more sensitive to H_2O_2-induced cell death after PARP1 knockdown; C: BAR-T cells were more sensitive to H_2O_2-induced DNA damage after PARP1 knockdown.

apoptosis after acidic bile acid exposure as indicated by annexin V assay ($P < 0.05$, 10 min: 2.1 ± 0.2 *vs* 6.3 ± 0.8; 30 min: 2.3 ± 0.1 *vs* 8.5 ± 1.2, Figure 4E).

DISCUSSION

During pathological events such as excessive and unrepairable oxidant DNA damage, highly activated PARPs synthesize large amounts of PAR in a few seconds. Our results showed that excessive PARP1 expression may probably a resistance factor of BE epithelial cells to H_2O_2 or bile acid-induced oxidative damage and cell death. In recent years, PARP1 inhibitors have shown promising therapeutic effects on ovarian cancer, breast cancer[12], and neurological diseases[13], and this effect is mainly associated with the induction of DSBs. Interestingly, pharmacological inhibition of PARP1 provides significant benefits in animal models of cardiovascular disorders[14]. It is also reported that PARP1 was identified as a direct target gene of miR-223, which is overexpressed in BE-associated esophageal adenocarcinoma[15]. Here, we demonstrated that PARP1 contributes to genomic stability and oxidative stress injury, and positively regulates the viability of esophageal epithelial cells, which reveals a potential therapeutic strategy for BE.

GERD is a chronic inflammation of the esophagus stimulated by repeated acid/bile acids. Esophagitis, of course, is clinically the major pathological manifestation as the result from GERD, which is also characterized with BE[16]. It is known that metaplasia is a pathological condition that commonly occurs in the presence of chronic inflammation[17], including typical Barrett's metaplasia[18]. In our mouse BE model, esophagitis and papillary hyperplasia of the squamous epithelia was observed, suggesting that the manifestation of GERD occurred. Furthermore, chronic inflammation is likely to carry an increased risk of cancer via oxidative damage pathways[19]. Thus, there is a strong association between GERD-induced ROS accumulation, chronic inflammatory infiltration, and BE formation.

Moreover, the BE mouse model also showed increased positivity for NF-κB, which is a transcription factor that has been established to play an active role in inflammation[20], and there is evidence that it serves as a key determinant of mucosal inflammation

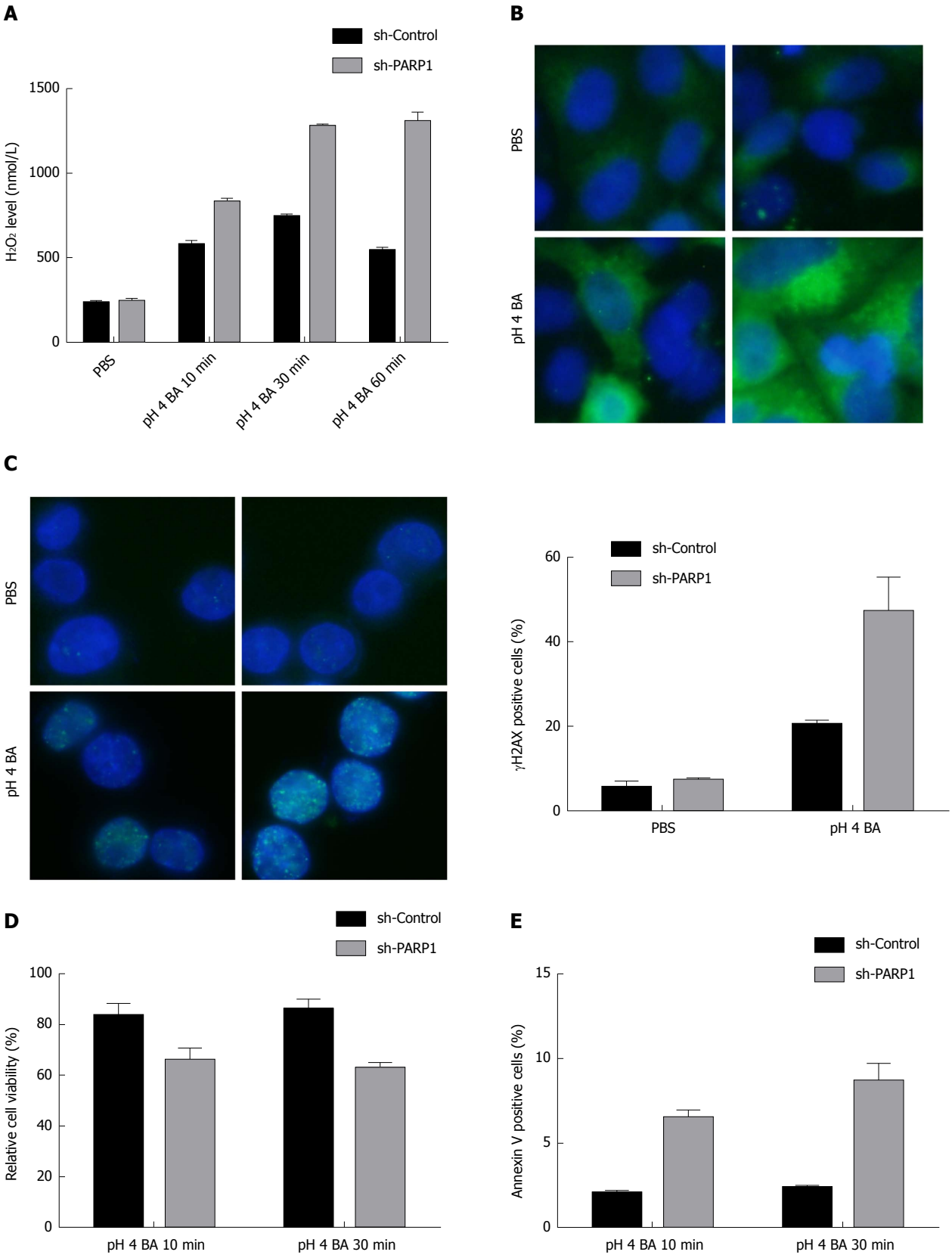

Figure 4 PARP1 protects Barrett's esophagus cells from BA (pH 4)-induced oxidative damage. A: H_2O_2 levels in PARP1-depleted BAR-T cells; B: 8-OXOG staining in PARP1-depleted BAR-T cells; C: γH2AX staining in PARP1- depleted BAR-T cells; D and E: Decreased cell viability in PARP1-depleted BAR-T cells.

and protection[21]. In particular, NF-κB expression has been found in 40%-60% of biopsy specimens of Barrett metaplasia and in 61%-80% of Barrett's adenocarcinomas, but in only 13% of reflux-injured squamous epithelia[22,23]. The level of NF-κB activation is correlated with the process from Barrett's mucosal

metaplasia to carcinogenesis, and indirectly proves that an inflammatory response might contribute to carcinogenesis[23]. This suggests the possibility that inflammation-mediated activation of the NF-κB pathway in a portion of cells, which may regulate the expression of NF-κB downstream proteins to replace the normal squamous cells for metaplasia and carcinogenesis.

Both the immunohistochemistry staining results and cell line results demonstrated that elevated expression of PARP1 is involved in the pathogenesis of BE. More importantly, PARP1 is known to be a co-activator of NF-κB and play a key role in pro-inflammation to contribute to inflammatory processes through the regulation of transcription factors[24,25]: NF-κB is one of the first mediators of inflammation to be identified as a target for PARP activity, which was proved to be a binding partner and also to be PARylated by PARP1. Further, NF-κB activity was greatly abrogated independent of upstream activation of NF-κB in PARP-/- mice and cell lines[26], and PARP1 inhibition reduced the extent of inflammation by modulating oxidative stress and impairing the activation of NF-κB and activator protein-1 in an inflammation model[27]. Both PAR and NF-κB staining increased in the BE mouse model, indicating the possible correlation between PARP1 activity and NF-κB. Further molecular mechanistic study in cells could clarify whether PARP1 regulates NF-κB activity in the oxidative damage-induced BE.

In conclusion, our study suggests that a high level of endogenous PARP1 in esophageal epithelial cells impairs oxidative DNA damage repair, inducing the death of esophageal epithelial cells during the process of BE formation. PARP inhibition treatment suppresses PARP activity and facilitates DNA damage repair in esophageal epithelial cells by prolonging PARylation. Thus, PARP1 acts as a mediator of esophageal disease, and PARylation may play a pivotal protective role as an antioxidant defense mechanism by maintaining esophageal epithelial cell function under pathological conditions of oxidative stress. Hence, PARP inhibitors may provide a novel clinical treatment for suppressing BE caused by oxidative damage.

ARTICLE HIGHLIGHTS

Research background

Barrett's esophagus is a major complication of gastro-esophageal reflux disease (GERD) and an important precursor lesion for the development of esophageal adenocarcinoma. However, the cellular and molecular mechanisms of Barrett's metaplasia remain unclear. It has been demonstrated that poly(ADP-ribose) polymerases (PARPs)-associated ADP-ribosylation plays an important role in DNA damage and inflammatory response. Although PARP1-associated ADP-ribosylation has been examined both *in vivo* and *in vitro*, the function of PARP1 in esophageal epithelial cells and Barrett's esophagus has not been illustrated.

Research motivation

In this study, the potential role of PARP1 and PARP1-related oxidative damage in Barrett's esophagus was investigated.

Research objectives

The study investigated the potential role of PARP1 in oxidative damage in Barrett's esophagus, which is urgent and essential for developing therapeutic targets.

Research methods

Expression of PARP1 gene was analyzed using microarray analysis in patient esophageal tissue samples. A Barrett's esophagus mouse model was established to examine the esophageal morphological changes and molecular changes. qPCR was used to examine the PARP1 expression in cell lines after treatment with H_2O_2 and bile acids (pH 4). To evaluate the impact of PARP1 activity on cell survival and DNA damage response after oxidative stress, immunofluorescence staining, comet assay, and annexin V staining were used.

Research results

High expression of PARP1 was associated with Barrett's esophagus. Positive staining for NF-κB, γH2AX, and poly(ADP-ribose) was observed in the mouse model of Barrett's esophagus. Knockdown of PARP1 decreased the cell viability following treatment with H_2O_2 and bile acids (pH 4). We further demonstrated that PARP1 inhibition could increase the oxidative damage as demonstrated by an increase in the levels of H_2O_2, intracellular reactive oxygen species, oxidative DNA damage, double-strand breaks, and apoptosis.

Research conclusions

The dysfunction of PARP1 in esophageal epithelial cells increases the levels of reactive oxygen species and oxidative DNA damage, and downregulation of PARP1 or PARP1 inhibitor may be a potential therapeutic strategy for Barrett's esophagus.

Research perspectives

This study will provide an example for investigating the relationship between the oxidative DNA damage and Barrett's metaplasia, and the underlying role of the PARP1 in Barrett's esophagus. The direction of the future research is to provide more evidence for developing novel strategies by targeting PARP1 in Barrett's esophagus. In our future research, the PARP1-related downstream signaling pathway (inflammation or DNA damage) will be tested in Barrett's esophagus epithelial cells or animal models to observe the inhibitory effect of PARP1.

REFERENCES

1 **Nehra D**, Howell P, Williams CP, Pye JK, Beynon J. Toxic bile acids in gastro-oesophageal reflux disease: influence of gastric acidity. *Gut* 1999; **44**: 598-602 [PMID: 10205192 DOI: 10.1136/gut.44.5.598]

2 **Herregods TV**, Bredenoord AJ, Smout AJ. Pathophysiology of gastroesophageal reflux disease: new understanding in a new era. *Neurogastroenterol Motil* 2015; **27**: 1202-1213 [PMID: 26053301 DOI: 10.1111/nmo.12611]

3 **Tack J**, Pandolfino JE. Pathophysiology of Gastroesophageal Reflux Disease. *Gastroenterology* 2018; **154**: 277-288 [PMID: 29037470 DOI: 10.1053/j.gastro.2017.09.047]

4 **Eluri S**, Shaheen NJ. Barrett's esophagus: diagnosis and management. *Gastrointest Endosc* 2017; **85**: 889-903 [PMID: 28109913 DOI: 10.1016/j.gie.2017.01.007]

5 **Shaheen NJ**. New Directions in Barrett's Esophagus. *Gastrointest Endosc Clin N Am* 2017; **27**: xv-xvi [PMID: 28577775 DOI: 10.1016/j.giec.2017.04.001]

6 **Cadet J**, Wagner JR. Oxidatively generated base damage to cellular DNA by hydroxyl radical and one-electron oxidants: similarities and differences. *Arch Biochem Biophys* 2014; **557**: 47-54 [PMID: 24820329 DOI: 10.1016/j.abb.2014.05.001]

7 **Finkel T**, Holbrook NJ. Oxidants, oxidative stress and the biology of ageing. *Nature* 2000; **408**: 239-247 [PMID: 11089981 DOI: 10.1038/35041687]

8 **Olinski R**, Gackowski D, Foksinski M, Rozalski R, Roszkowski

K, Jaruga P. Oxidative DNA damage: assessment of the role in carcinogenesis, atherosclerosis, and acquired immunodeficiency syndrome. *Free Radic Biol Med* 2002; **33**: 192-200 [PMID: 12106815 DOI: 10.1016/S0891-5849(02)00878-X]

9 **Li M**, Yu X. Function of BRCA1 in the DNA damage response is mediated by ADP-ribosylation. *Cancer Cell* 2013; **23**: 693-704 [PMID: 23680151 DOI: 10.1016/j.ccr.2013.03.025]

10 **Schreiber V**, Dantzer F, Ame JC, de Murcia G. Poly(ADP-ribose): novel functions for an old molecule. *Nat Rev Mol Cell Biol* 2006; **7**: 517-528 [PMID: 16829982 DOI: 10.1038/nrm1963]

11 **Kim MY**, Zhang T, Kraus WL. Poly(ADP-ribosyl)ation by PARP-1: 'PAR-laying' NAD+ into a nuclear signal. *Genes Dev* 2005; **19**: 1951-1967 [PMID: 16140981 DOI: 10.1101/gad.1331805]

12 **Lesueur P**, Chevalier F, Austry JB, Waissi W, Burckel H, Noël G, Habrand JL, Saintigny Y, Joly F. Poly-(ADP-ribose)-polymerase inhibitors as radiosensitizers: a systematic review of pre-clinical and clinical human studies. *Oncotarget* 2017; **8**: 69105-69124 [PMID: 28978184 DOI: 10.18632/oncotarget.19079]

13 **Sriram CS**, Jangra A, Kasala ER, Bodduluru LN, Bezbaruah BK. Targeting poly(ADP-ribose)polymerase1 in neurological diseases: A promising trove for new pharmacological interventions to enter clinical translation. *Neurochem Int* 2014; **76**: 70-81 [PMID: 25049175 DOI: 10.1016/j.neuint.2014.07.001]

14 **Xu S**, Bai P, Little PJ, Liu P. Poly(ADP-ribose) polymerase 1 (PARP1) in atherosclerosis: from molecular mechanisms to therapeutic implications. *Med Res Rev* 2014; **34**: 644-675 [PMID: 24002940 DOI: 10.1002/med.21300]

15 **Streppel MM**, Pai S, Campbell NR, Hu C, Yabuuchi S, Canto MI, Wang JS, Montgomery EA, Maitra A. MicroRNA 223 is upregulated in the multistep progression of Barrett's esophagus and modulates sensitivity to chemotherapy by targeting PARP1. *Clin Cancer Res* 2013; **19**: 4067-4078 [PMID: 23757351 DOI: 10.1158/1078-0432.CCR-13-0601]

16 **Vaezi MF**, Richter JE. Role of acid and duodenogastroesophageal reflux in gastroesophageal reflux disease. *Gastroenterology* 1996; **111**: 1192-1199 [PMID: 8898632 DOI: 10.1053/gast.1996.v111.pm8898632]

17 **V. Kumar AKA,** N Fausto, R Mitchell. Robbins Basic Pathology. 8th ed: Elsevier Saunders, 2007

18 **Colleypriest BJ**, Palmer RM, Ward SG, Tosh D. Cdx genes, inflammation and the pathogenesis of Barrett's metaplasia. *Trends Mol Med* 2009; **15**: 313-322 [PMID: 19564133 DOI: 10.1016/j.molmed.2009.05.001]

19 **Farinati F**, Piciocchi M, Lavezzo E, Bortolami M, Cardin R. Oxidative stress and inducible nitric oxide synthase induction in carcinogenesis. *Dig Dis* 2010; **28**: 579-584 [PMID: 21088405 DOI: 10.1159/000320052]

20 **Baeuerle PA**. IkappaB-NF-kappaB structures: at the interface of inflammation control. *Cell* 1998; **95**: 729-731 [PMID: 9865689 DOI: 10.1016/S0092-8674(00)81694-3]

21 **Jobin C**, Sartor RB. The I kappa B/NF-kappa B system: a key determinant of mucosalinflammation and protection. *Am J Physiol Cell Physiol* 2000; **278**: C451-C462 [PMID: 10712233 DOI: 10.1152/ajpcell.2000.278.3.C451]

22 **Abdel-Latif MM**, O'Riordan J, Windle HJ, Carton E, Ravi N, Kelleher D, Reynolds JV. NF-kappaB activation in esophageal adenocarcinoma: relationship to Barrett's metaplasia, survival, and response to neoadjuvant chemoradiotherapy. *Ann Surg* 2004; **239**: 491-500 [PMID: 15024310 DOI: 10.1097/01.sla.0000118751.95179.c6]

23 **O'Riordan JM**, Abdel-latif MM, Ravi N, McNamara D, Byrne PJ, McDonald GS, Keeling PW, Kelleher D, Reynolds JV. Proinflammatory cytokine and nuclear factor kappa-B expression along the inflammation-metaplasia-dysplasia-adenocarcinoma sequence in the esophagus. *Am J Gastroenterol* 2005; **100**: 1257-1264 [PMID: 15929754 DOI: 10.1111/j.1572-0241.2005.41338.x]

24 **Hassa PO**, Hottiger MO. A role of poly (ADP-ribose) polymerase in NF-kappaB transcriptional activation. *Biol Chem* 1999; **380**: 953-959 [PMID: 10494847 DOI: 10.1515/bc.1999.118]

25 **Liu L**, Ke Y, Jiang X, He F, Pan L, Xu L, Zeng X, Ba X. Lipopolysaccharide activates ERK-PARP-1-RelA pathway and promotes nuclear factor-κB transcription in murine macrophages. *Hum Immunol* 2012; **73**: 439-447 [PMID: 22391342 DOI: 10.1016/j.humimm.2012.02.002]

26 **Oliver FJ**, Ménissier-de Murcia J, Nacci C, Decker P, Andriantsitohaina R, Muller S, de la Rubia G, Stoclet JC, de Murcia G. Resistance to endotoxic shock as a consequence of defective NF-kappaB activation in poly (ADP-ribose) polymerase-1 deficient mice. *EMBO J* 1999; **18**: 4446-4454 [PMID: 10449410 DOI: 10.1093/emboj/18.16.4446]

27 **Brunyánszki A**, Hegedus C, Szántó M, Erdélyi K, Kovács K, Schreiber V, Gergely S, Kiss B, Szabó E, Virág L, Bai P. Genetic ablation of PARP-1 protects against oxazolone-induced contact hypersensitivity by modulating oxidative stress. *J Invest Dermatol* 2010; **130**: 2629-2637 [PMID: 20613774 DOI: 10.1038/jid.2010.190]

P- Reviewer: Zhao JB **S- Editor**: Wang JL
L- Editor: Wang TQ **E- Editor**: Huang Y

World Journal of Gastroenterology

Submit a Manuscript: http://www.f6publishing.com

World J Gastroenterol 2018 March 7; 24(9): 992-1003

DOI: 10.3748/wjg.v24.i9.992

ISSN 1007-9327 (print) ISSN 2219-2840 (online)

ORIGINAL ARTICLE

Basic Study

Autophagy activation by Jiang Zhi Granule protects against metabolic stress-induced hepatocyte injury

Yi-Yuan Zheng, Miao Wang, Xiang-Bing Shu, Pei-Yong Zheng, Guang Ji

Yi-Yuan Zheng, Miao Wang, Xiang-Bing Shu, Pei-Yong Zheng, Guang Ji, Institute of Digestive Disease, Longhua Hospital, Shanghai University of Traditional Chinese Medicine, Shanghai 200032, China

ORCID number: Yi-Yuan Zheng (0000-0001-9487-3766); Miao Wang (0000-0002-0344-7575); Xiang-Bing Shu (0000-0002-4096-8281); Pei-Yong Zheng (0000-0003-1084-5317); Guang Ji (0000-0003-0842-3676).

Author contributions: Zheng YY and Wang M contributed equally as co-first authors; Zheng YY and Wang M performed the majority of experiments and drafted the article; Shu XB established the animal model; Zheng PY analyzed the data; Ji G designed the research; all authors approved the final version of the article to be published.

Supported by the National Natural Science Foundation of China, No. 81370092.

Institutional review board statement: This study was reviewed and approved by the Institutional Review Board of Institute of Digestive Disease, Shanghai University of Traditional Chinese Medicine, Shanghai, China.

Institutional animal care and use committee statement: All procedures involving animals were reviewed and approved by the Institutional Animal Care and Use Committee of Shanghai University of Traditional Chinese Medicine (IACUC protocol number Approval number: SZY201508004).

Conflict-of-interest statement: All authors declare that they have no conflicts of interest.

Data sharing statement: No additional data are available.

Manuscript source: Unsolicited manuscript

Correspondence to: Guang Ji, PhD, Chief Doctor, Professor, Institute of Digestive Disease, Longhua Hospital, Shanghai University of Traditional Chinese Medicine, No. 725 South Wanping Road, Shanghai 200032, China. jiliver@vip.sina.com
Telephone: +86-21-64385700
Fax: +86-21-64385700

Received: November 9, 2017
Peer-review started: November 10, 2017
First decision: December 13, 2017
Revised: December 22, 2017
Accepted: January 1, 2018
Article in press: January 1, 2018
Published online: March 7, 2018

Abstract

AIM

To elucidate the potential role of autophagy and the protective effects of Jiang Zhi Granule (JZG) in metabolic stress-induced hepatocyte injury.

METHODS

An *in vitro* and *in vivo* approach was used in this study. HepG2 cells were incubated in culture medium containing palmitate (PA; 0, 0.1, 0.2, 0.3, 0.4 or 0.5 mmol/L) and treated with or without JZG (100 μg/mL) for 24 h or 48 h, and the progression of autophagy was visualized by stable fluorescence-expressing cell lines LC3 and p62. Western blot analyses were performed to examine the expression of LC3-Ⅱ/LC3-Ⅰ, p62, mTOR and PI3K, while mitochondrial integrity and oxidative stress were observed by fluorescence staining of JC-1 and reactive oxygen species. C57BL/6 mice

were divided into three groups: control group (n = 10), high fat (HF) group (n = 13) and JZG group (n = 13); and, histological staining was carried out to detect inflammation and lipid content in the liver.

RESULTS

The cell trauma induced by PA was aggravated in a dose- and time-dependent manner, and hepatic function was improved by JZG. PA had dual effects on autophagy by activating autophagy induction and blocking autophagic flux. The PI3K-AKT-mTOR signaling pathway and the fusion of isolated hepatic autophagosomes and lysosomes were critically involved in this process. JZG activated autophagy progression by either induction of autophagosomes or co-localization of autophagosomes and lysosomes as well as degradation of autolysosomes to protect against PA-induced hepatocyte injury, and protected mitochondrial integrity against oxidative stress in PA-induced mitochondrial dysfunction. In addition, JZG ameliorated lipid droplets and inflammation induced by HF diet *in vivo*, leading to improved metabolic disorder and associated liver injury in a mouse model of non-alcoholic fatty liver disease (NAFLD).

CONCLUSION

Metabolic stress-induced hepatocyte injury exhibited dual effects on autophagy and JZG activated the entire process, resulting in beneficial effects in NAFLD.

Key words: Autophagy; PI3K-AKT-mTOR signaling pathway; Autophagic flux; Oxidative stress; Hepatocyte injury; Non-alcoholic fatty liver disease

Core tip: Non-alcoholic fatty liver disease (NAFLD), which is mainly characterized by the accumulation of lipids and energy metabolism dysfunction, is now one of the most common risk factors worldwide. As studies have demonstrated that autophagy is important in the maintenance of normal hepatocyte function and in the response to pathogenic changes, we examined the potential role of autophagy in metabolic stress-induced hepatocyte injury. The results showed that metabolic stress had dual effects on autophagy, resulting in autophagy induction and autophagic flux inhibition. The Chinese herbal formula Jiang Zhi Granule activated the autophagy process to protect against metabolic stress-induced hepatocyte injury in NAFLD.

Zheng YY, Wang M, Shu XB, Zheng PY, Ji G. Autophagy activation by Jiang Zhi Granule protects against metabolic stress-induced hepatocyte injury. *World J Gastroenterol* 2018; 24(9): 992-1003 Available from: URL: http://www.wjgnet.com/1007-9327/full/v24/i9/992.htm DOI: http://dx.doi.org/10.3748/wjg.v24.i9.992

INTRODUCTION

Fatty liver disease (FLD), which is mainly characterized by the accumulation of lipids in hepatocytes and energy metabolism dysfunction, is clinically classified into two broad categories: alcoholic (A)FLD and non-alcoholic (NA)FLD[1]. NAFLD is currently much more prevalent than AFLD, which accounts for 75% of all chronic liver diseases, and is increasingly recognized as one of the most common risk factors worldwide[2]. NAFLD has a wide clinical pathological spectrum, ranging from simple steatosis non-alcoholic fatty liver to non-alcoholic steatohepatitis, which includes fibrosis and cirrhosis[3]. And, in the meantime, it often occurs with other metabolic diseases, such as obesity and diabetes[4].

The pathogenesis of NAFLD is still unknown; however, the "two hits" hypothesis is now widely accepted[5]. A disturbance in metabolic homeostasis is one of the key events during the occurrence of NAFLD and typical pathological features, including steatosis, inflammation, fibrosis and cirrhosis, are considered to be related to oxidative stress resulting from lipid accumulation and reactive oxygen species (ROS) generation[6].

Oxidative stress is a stimulus for autophagy, which is important for metabolic homeostasis in the liver[7], as it can prompt nutrient recycling, remove abnormal organelles and toxic protein aggregates and alter the level of metabolic factors, thus contributing to the maintenance of normal hepatocyte function and the response to pathogenic changes in the liver[8,9]. Hepatic autophagy occurs at a basal level and can be elevated under stress conditions[10], such as oxidative stress.

Studies have shown that autophagy is a highly selective process and can modulate cellular energy stores, such as carbohydrates and lipids[11,12], and recent research has demonstrated that autophagy assists in the degradation of triglycerides in the liver[13]. Autophagy regulators, such as rapamycin and carbamazepine, have been proven effective to improve hepatic function[14]. However, no effective therapeutic approach has been accepted as the standard option for NAFLD and its complications. Thus, new treatments are still urgently needed to prevent or delay the onset as well as the progression of NAFLD.

Jiang Zhi Granule (JZG), which is composed of *Herba gynostemmatis, Radix salviae, Rhizoma polygoni cuspidati, Herba artemisiae scopariae* and *Folium nelumbinis*, is a clinically used herbal formula designed to treat patients with NAFLD[15]. JZG had a positive drug safety evaluation and has been approved for clinical trials by the State Food and Drug Administration (SFDA; Authorization Number: Z10960082). Our preliminary studies indicated that JZG had beneficial effects in improving hepatic fat accumulation in both cell lines and animals[16], and the efficacy of JZG in patients with

NAFLD was also confirmed[17]. As previous studies on JZG have indicated its antisteatotic effect, we conducted this study to determine the underlying mechanism of JZG.

MATERIALS AND METHODS

Animal models

Male C57BL/6 mice aged 6 wk were purchased from SLAC Animal Laboratories (Shanghai, China). After 1-wk acclimatization, the mice were divided into three groups: the control group (n = 10) received a 12-wk standard diet (STD); the high fat (HF) group (n = 13) received a HF diet (HFD; consisting of 10% lard oil, 2% cholesterol and 88% STD) supplemented with 1% DSS (MP Biomedicals, Solon, OH, United States) in drinking water; and, the JZG group (n = 13) also received a HF-DSS diet, but were also given JZG which had been dissolved in saline and was administered daily by oral gavage at a dose of 994 mg/kg daily (approximately 12 times that of the standard dose used in clinical practice). DSS was given in cycles; each cycle consisted of 7 d DSS administration followed by a 10-d interval with normal drinking water[18]. At the end of the experimental period, blood samples were drawn from the heart, while the mice were under anesthesia, livers were excised, and samples were either immediately snap-frozen in liquid nitrogen or fixed in 4% PFA.

Cell culture

HepG2 cells were obtained from the Cell Bank of the Chinese Academy of Sciences (Shanghai, China), and were cultured in DMEM supplemented with 10% fetal bovine serum, 100 U/mL penicillin and 100 μg/mL streptomycin. Saturated palmitic acid (PA) and JZG were used in this study. HepG2 cells were incubated in culture medium containing PA (0, 0.1, 0.2, 0.3, 0.4 or 0.5 mmol/L) and treated with or without JZG (100 μg/mL) for 24 h or 48 h, as described previously[16].

Western blot

Western blot analyses were performed as described previously[19]. Rabbit antibodies against LC3 (monoclonal ab192890), SQSTM1/p62 (monoclonal ab109012), p-mTOR (phosphor-S2481) (monoclonal ab137133), mTOR (monoclonal ab87540), p-PI3K (phosphor-Y607) (polyclonal ab182651), PI3K (monoclonal ab40755) and actin (polyclonal ab8227) were purchased from Abcam (Cambridge, MA, United States).

Establishment of stable fluorescence-expressing cell lines

HepG2 cells were cultured according to the above protocol and infected with mRFP-GFP-LC3 lentivirus at an MOI of 10 for 48 h to establish a stable mRFP-GFP-LC3-expressing HepG2 cell line, and then infected with mCherry-p62 lentivirus at an MOI of 10 for 48 h to establish a stable mCherry-p62-expressing HepG2 cell line.

Fluorescence staining

Mitochondria and lysosomes were detected using the MitoTracker Green FM and LysoTracker Deep Red staining kit, respectively (Thermo Fisher Scientific, Waltham, MA, United States). Intracellular ROS generation was detected using the DCFH-DA fluorescent probe. Mitochondrial membrane potential was determined by the mitochondrial membrane potential assay kit (JC-1). Pretreated cells in 6-well plates were processed following the protocols and were observed immediately under a fluorescence microscope at an excitation wavelength of 488 nm and emission wavelength of 525 nm.

Histological staining

Histological staining was performed as described previously[20]. Liver samples were fixed, processed, and embedded in paraffin blocks, and then hematoxylin and eosin (H&E) staining was performed. Frozen liver sections were fixed and stained with oil Red O. Images were acquired on an Olympus BX-50 microscope.

Statistical analysis

All data were expressed as the mean ± SEM. Statistical analyses were performed using GraphPad Prism (GraphPad Software, La Jolla, CA, United States). The differences between groups were analyzed by Student's t-test or ANOVA, as appropriate, and $P < 0.05$ was considered statistically significant.

RESULTS

Autophagy was activated by JZG to protect against injury in PA-treated cells

To determine whether autophagy was involved in the progression of NAFLD, HepG2 cells were treated with PA - a main type of saturated free fatty acid which is elevated in obese subjects and can induce NAFLD[21] - at various concentrations and for different time periods. Results showed that the expression of alanine aminotransferase (ALT) increased in a dose- and time-dependent manner and JZG significantly reduced high ALT levels (Figure 1A and B), suggesting that cell trauma was induced by PA and JZG improved hepatic function. These results also indicated that the dose of 0.4 mmol/L may be an appropriate concentration in subsequent experiments and the time points should include 24 h and 48 h.

Western blot analyses showed that PA increased LC3-Ⅱ/actin expression (Figure 1C), indicating the activation of autophagy. However, the expression of LC3-Ⅱ/LC3-Ⅰ was not increased accordingly after long-term PA stimulation (Figure 1C). In the meantime, the expression of p62 was also increased (Figure 1C), suggesting the restriction of autophagic flux. Thus, it was proposed that PA exhibited dual effects on

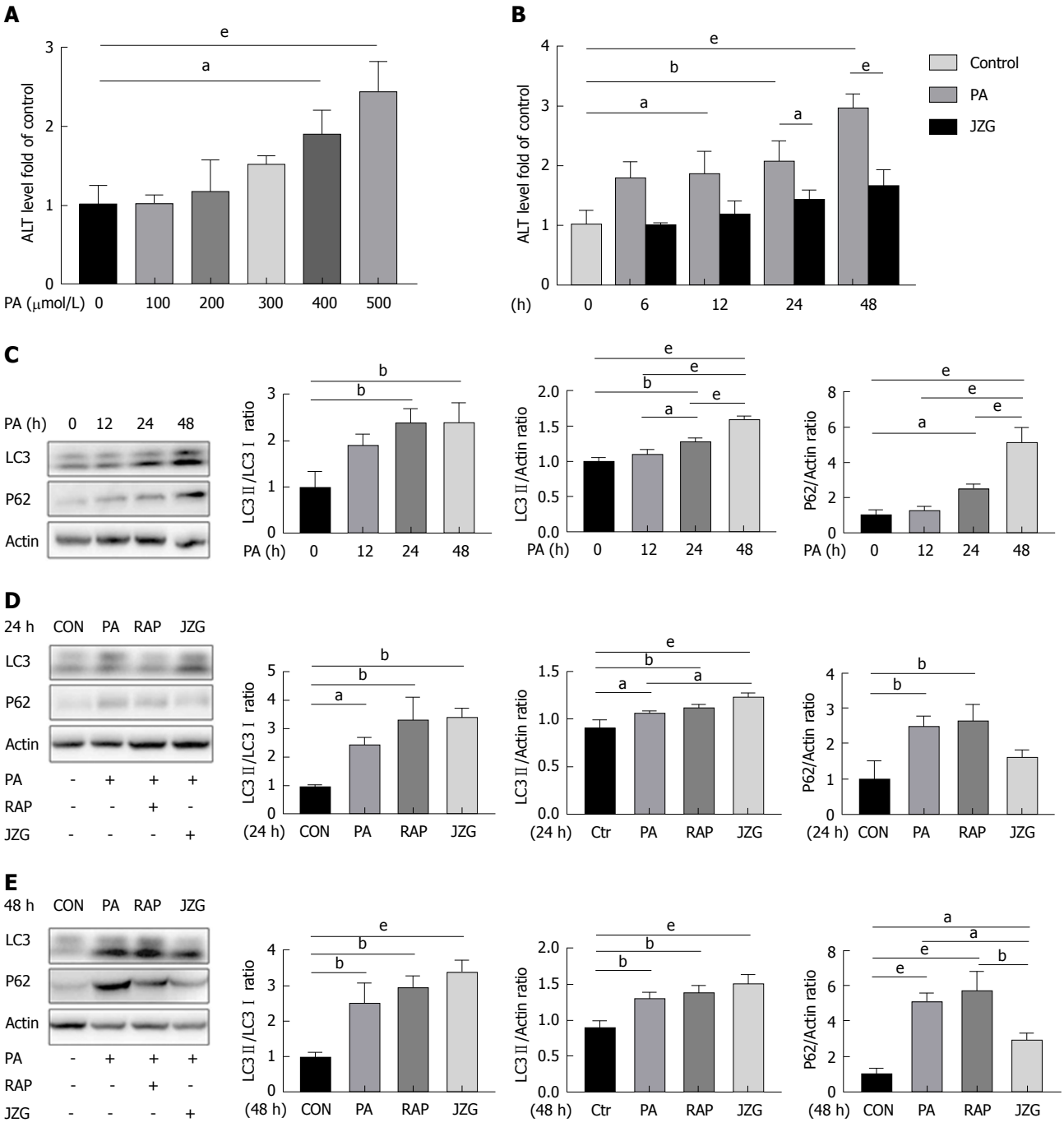

Figure 1 Autophagy was activated by JZG to protect against injury in palmitate-treated cells. A: The expression of ALT in the supernatants of cell cultures was determined by ELISA. HepG2 cells were incubated in culture medium containing PA (0, 0.1, 0.2, 0.3, 0.4 or 0.5 mmol/L); B: The expression of ALT in the supernatants of cell cultures was determined by ELISA. HepG2 cells were treated with 0.4 mmol/L PA with or without JZG (100 μg/mL) for different time periods (0, 6, 12, 24 or 48 h); C: HepG2 cells were treated with 0.4 mmol/L PA for different time periods (0, 12, 24 or 48 h); D: HepG2 cells were treated with 0.4 mmol/L PA and rapamycin (2 μmol/L) or JZG (100 μg/mL) for 24 h; E: HepG2 cells were treated with 0.4 mmol/L PA and rapamycin (2 μmol/L) or JZG (100 μg/mL) for 48 h. Data are expressed as mean ± SEM. $^{a}P < 0.05$, $^{b}P < 0.01$, $^{e}P < 0.001$. ALT: Alanine aminotransferase; ELISA: Enzyme-linked immunosorbent assay; JZG: Jiang Zhi Granule; PA: Palmitate.

autophagy.

A recent study showed that mitochondrial dysfunction caused by elevated mitochondrial stress may block autophagic flux[18]; thus, rapamycin was used in the present study to enhance autophagy at different time points. The outcomes displayed that the expression of LC3-Ⅱ/actin and p62 were both increased but the expression of LC3-Ⅱ/LC3-Ⅰ was not, confirming the dual effects of PA on autophagy (Figure 1D and E).

An increase in LC3-Ⅱ/LC3-Ⅰ expression and a reduction in p62 expression were observed following treatment with JZG for two different time periods (Figure 1D and E), indicating that JZG activated autophagy to protect against PA-induced cell injury.

PI3K-AKT-mTOR pathway was involved in autophagy in JZG-treated cells

As the activation of autophagy can occur due to an

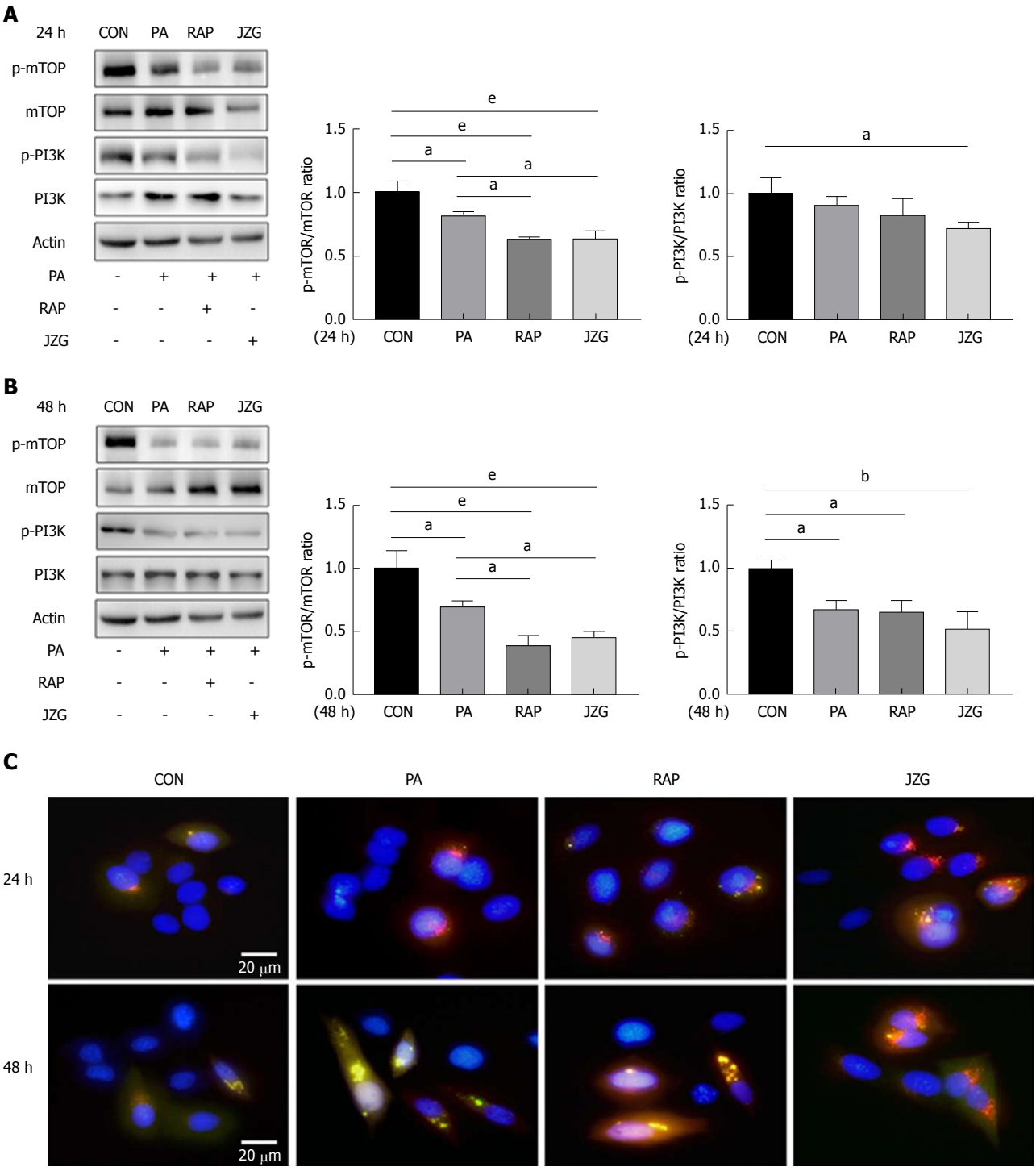

Figure 2 PI3K-AKT-mTOR pathway was involved in autophagy in Jiang Zhi Granule-treated cells. A: HepG2 cells were treated with 0.4 mmol/L PA and rapamycin (2 μmol/L) or JZG (100 μg/mL) for 24 h; B: HepG2 cells were treated with 0.4 mmol/L PA and rapamycin (2 μmol/L) or JZG (100 μg/mL) for 48 h; C: HepG2 cells stably expressing mRFP-GFP-LC3 were pretreated with 0.4 mmol/L PA and rapamycin (2 μmol/L) or JZG (100 μg/mL) for 24 h and 48 h, and then analyzed by fluorescence microscopy. Data are expressed as mean ± SEM. $^{a}P < 0.05$, $^{b}P < 0.01$, $^{e}P < 0.001$. JZG: Jiang Zhi Granule; PA: Palmitate.

increase in autophagy induction and autophagic flux, we first investigated the pathway involved in autophagy induction in JZG-treated cells. The PI3K-AKT-mTOR pathway, a classic signaling pathway that has been identified to be important in autophagy induction, was examined in this study. Western blot analyses revealed that the phosphorylation signaling processes of mTOR and PI3K were inhibited in PA-treated cells, and these results were further confirmed by the addition of rapamycin (Figure 2A and B). As an inhibitor of mTOR, rapamycin did not further depress the phosphorylation of PI3K. Conversely, an additional restraint on both phosphorylation signaling processes was observed in JZG-treated cells (Figure 2A and B), suggesting that

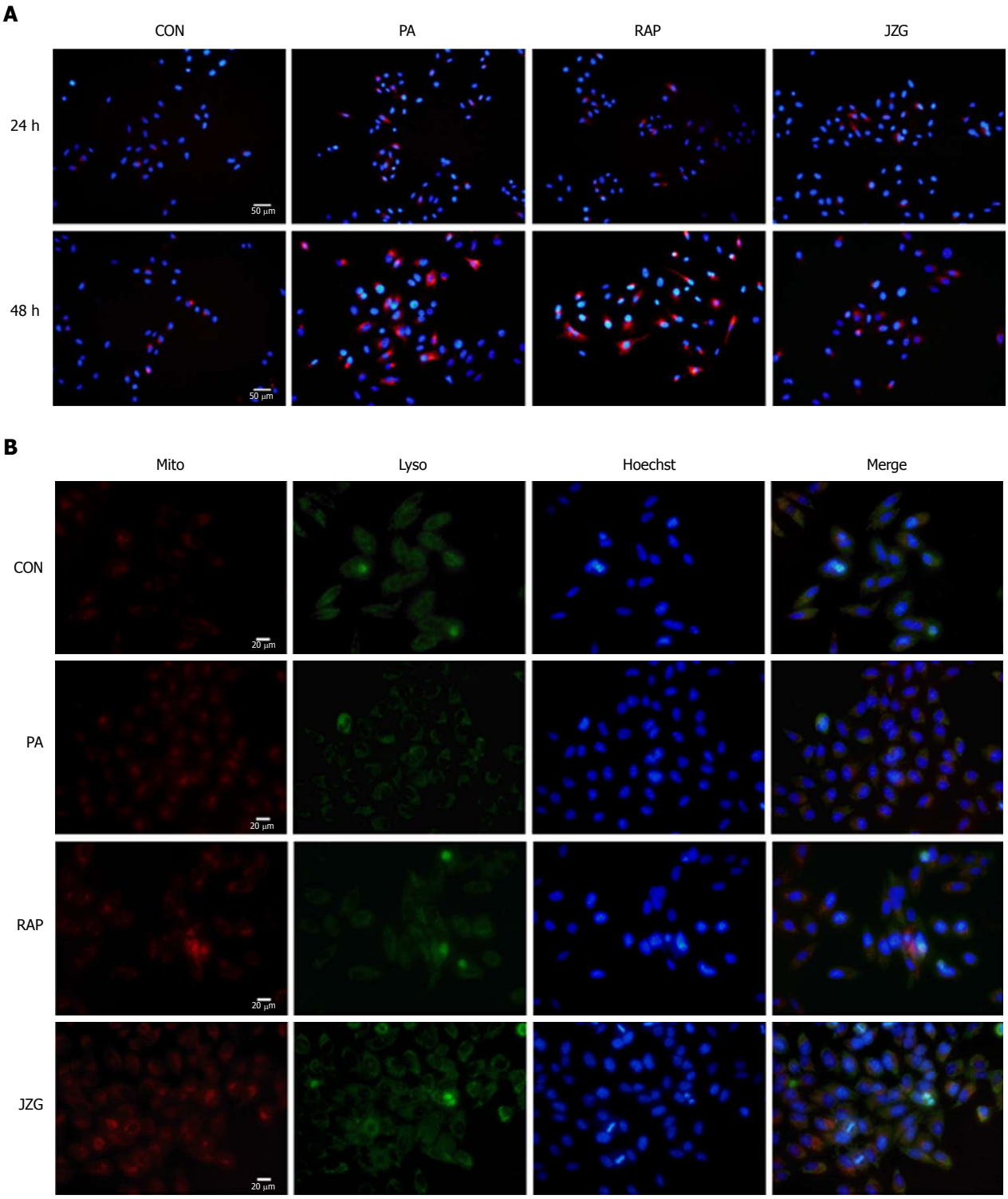

Figure 3 Effects of Jiang Zhi Granule on autophagic flux in palmitate-treated cells. A: HepG2 cells stably expressing mCherry-p62 were pretreated with 0.4 mmol/L PA and rapamycin (2 μmol/L) or JZG (100 μg/mL) for 24 h and 48 h, and then analyzed by fluorescence microscopy; B: HepG2 cells were treated with 0.4 mmol/L PA and rapamycin (2 μmol/L) or JZG (100 μg/mL) for 48 h, and then analyzed by fluorescence microscopy. JZG: Jiang Zhi Granule; PA: Palmitate.

the PI3K-AKT-mTOR pathway is critically involved in autophagy induction in response to PA challenge.

As LC3 is the major constituent of autophagosomes, a stable mRFP-GFP-LC3-expressing HepG2 cell line was established to visualize the progression of autophagosome formation in real time in liver cells. Diffuse cytoplasmic localization of mRFP-GFP-LC3 was observed in the control group, whereas punctate fluorescence was observed in PA-treated cells (Figure 2C), indicating that cytoplasmic LC3 was processed and recruited to autophagosomes. Rapamycin and JZG advanced this process, indicating increased autophagy induction, which confirmed that JZG induced the formation of autophagosomes.

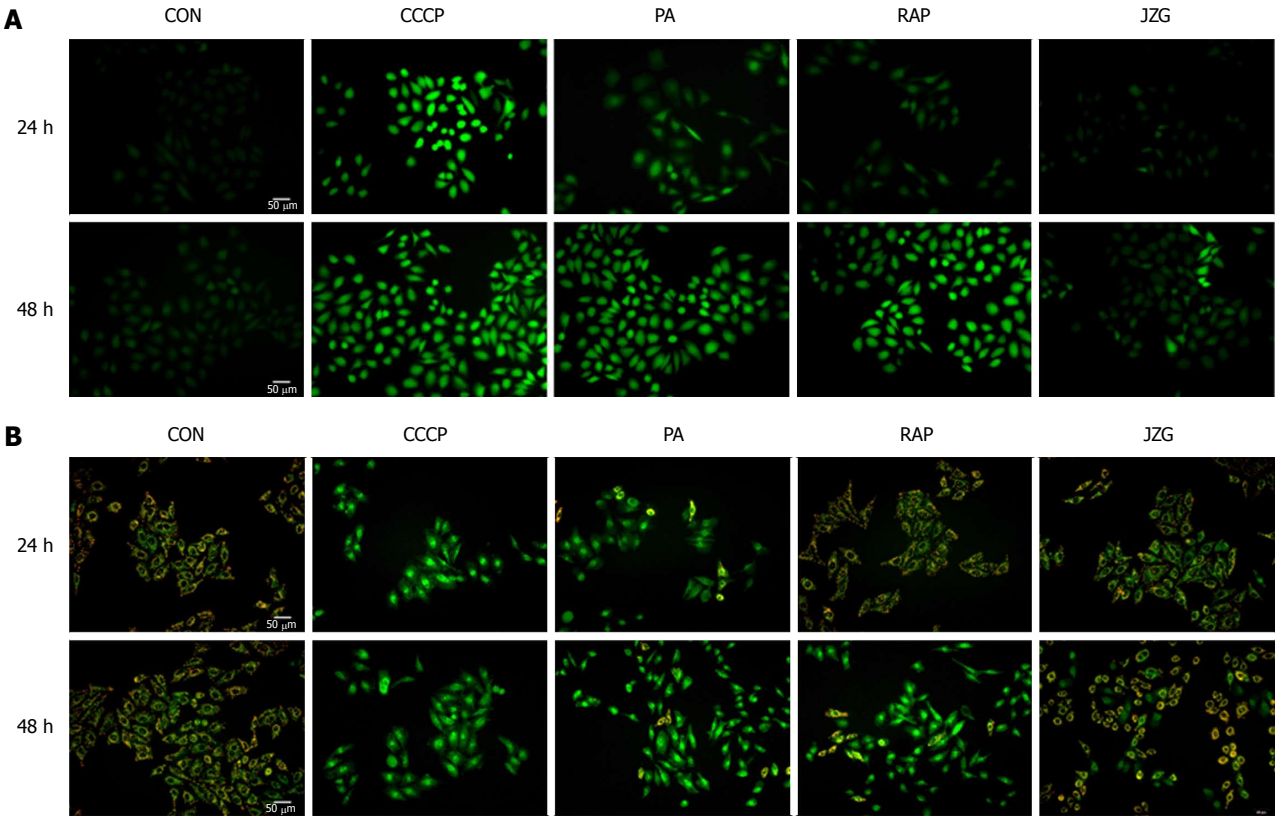

Figure 4 Jiang Zhi Granule protected mitochondrial integrity against oxidative stress. A: The ROS-sensitive fluorescent probe DCFH-DA was used to monitor mitochondrial membrane potential in HepG2 cells pretreated with 0.4 mmol/L PA and rapamycin (2 μmol/L) or JZG (100 μg/mL) for 24 h and 48 h, and the cells were then analyzed by fluorescence microscopy; B: JC-1 was used to monitor mitochondrial membrane potential in HepG2 cells pretreated with 0.4 mmol/L PA and rapamycin (2 μmol/L) or JZG (100 μg/mL) for 24 h and 48 h, and the cells were then analyzed by fluorescence microscopy. JZG: Jiang Zhi Granule; PA: Palmitate; ROS: Reactive oxygen species.

Effects of JZG on autophagic flux in PA-treated cells

To determine the effect of JZG on autophagic flux in PA-treated cells, we first observed this effect in mRFP-GFP-LC3-expressing HepG2 cells. We found that yellow fluorescence - indicating that GFP was not degraded by lysosomal enzymes - was largely seen in HepG2 cells treated with PA for 48 h, whereas red fluorescence was very rare (Figure 2C). These results led us to propose that the colocalization of autophagosomes and lysosomes was prevented and the autophagosomal degradation was blocked. Yellow punctate fluorescence was reduced in JZG-treated cells and red diffuse fluorescence was increased (Figure 2C), suggesting that JZG promoted colocalization.

To confirm these findings, we established another stable mCherry-p62-expressing HepG2 cell line to visualize the cellular expression levels of p62, which inversely correlated with autophagic flux *via* selective incorporation into autophagosomes to be efficiently degraded by autophagy. We found that punctate fluorescence was enhanced in HepG2 cells treated with PA for 48 h and was weak in JZG-treated cells (Figure 3A), confirming the previous findings.

As it has been shown that mitochondrial dysfunction may block autophagic flux[22], we next examined whether the mitochondrial integrity was affected in PA-treated cells. MitoTracker and LysoTracker were used to stain the mitochondria and lysosomes, respectively. The results showed that mitochondrial dysfunction was much more serious in PA-treated cells than in control cells (Figure 3B). A protective effect of JZG on mitochondrial integrity was demonstrated and the colocalization of mitochondria and lysosomes in JZG-treated cells showed that the mitochondrial integrity was related to activation of autophagic flux. Together, these findings suggested that JZG increased the formation of both autophagosomes and autolysosomes and protected against PA-induced mitochondrial dysfunction by activating autophagy.

JZG protected mitochondrial integrity against oxidative stress

As the protective effect of JZG on mitochondrial integrity was demonstrated, we then examined whether oxidative stress was involved in this process. The ROS-sensitive fluorescent probe DCFH-DA was used to monitor cellular oxidative stress. We found that the accumulation of intracellular ROS was considerably increased in PA-treated cells, and JZG significantly reduced the PA-induced increase in ROS production

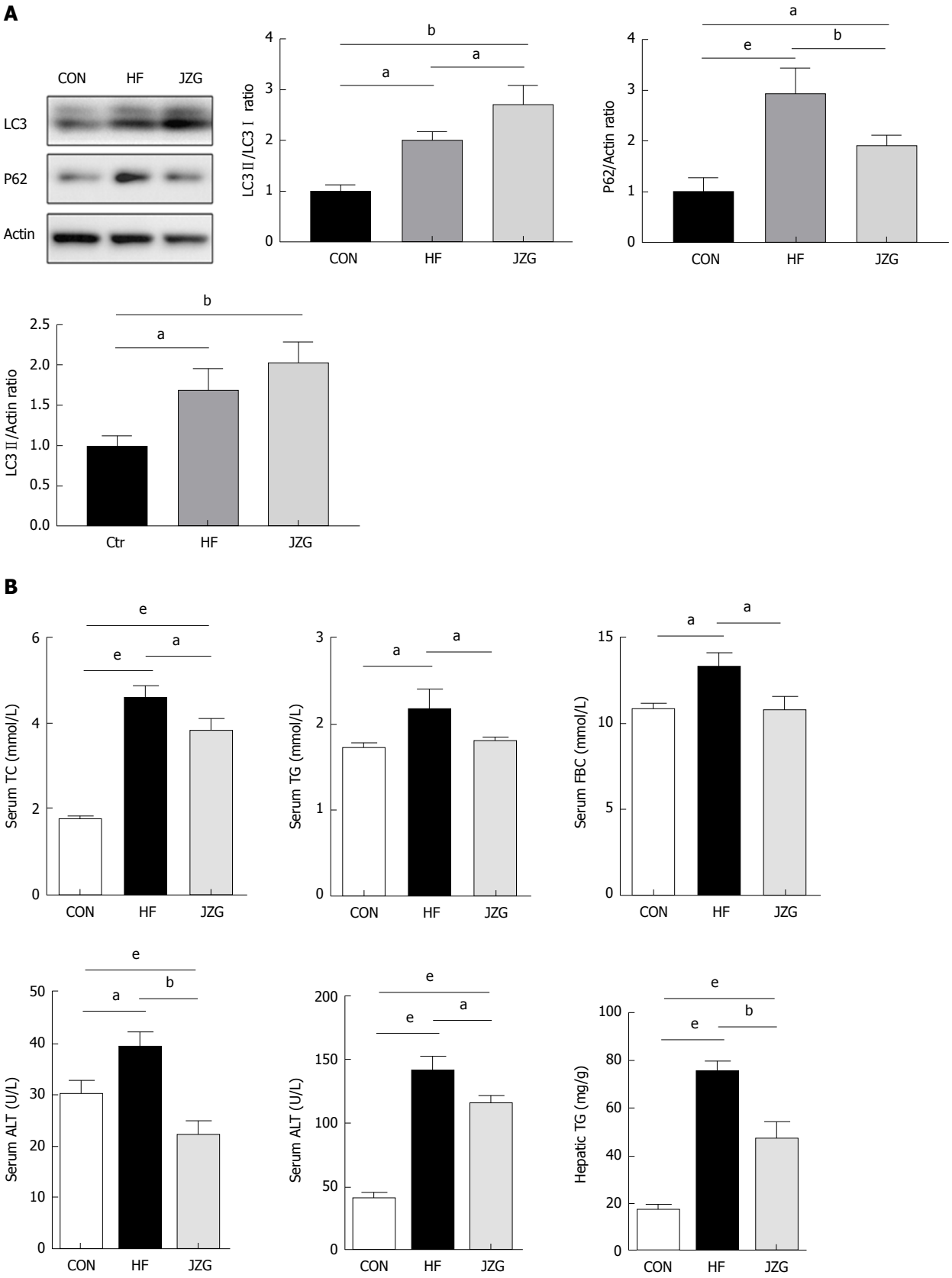
A
CON
HF
JZG
LC3
P62
Actin
LC3 II/LC3 I ratio
P62/Actin ratio
LC3 II/Actin ratio
Ctr
B
Serum TC (mmol/L)
Serum TG (mmol/L)
Serum FBC (mmol/L)
Serum ALT (U/L)
Serum ALT (U/L)
Hepatic TG (mg/g)

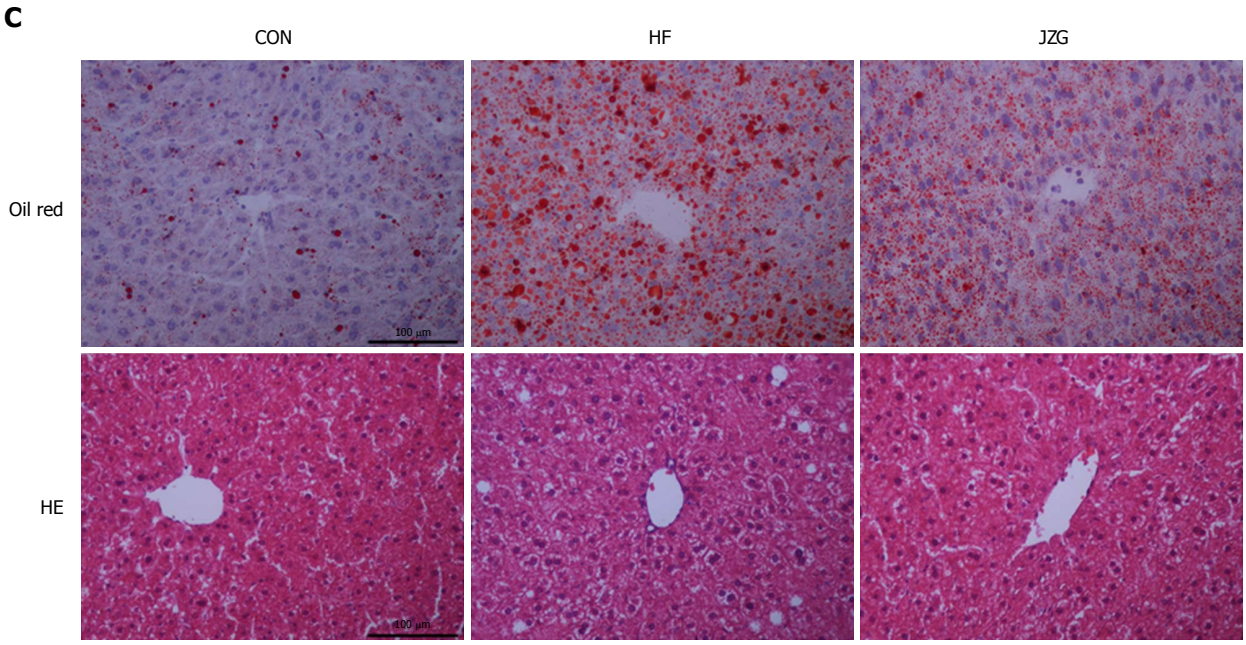

Figure 5 Autophagy was activated by Jiang Zhi Granule to improve non-alcoholic fatty liver disease *in vivo*. A: Autophagy of liver tissue was examined by western blot analyses; B: Biochemical analysis of TG, TC, ALT, AST and FBG using an automatic blood chemistry analyzer; C: Inflammation and lipid content in the liver was detected by HE staining and oil Red O staining. Data are expressed as mean ± SEM. $^{a}P < 0.05$, $^{b}P < 0.01$, $^{e}P < 0.001$. ALT: Alanine aminotransferase; AST: Aspartate aminotransferase; HE: Hematoxylin and eosin; JZG: Jiang Zhi Granule; PA: Palmitate; TC: Total cholesterol; TG: Triglycerides.

(Figure 4A), indicating the potential role of oxidative stress in mitochondrial dysfunction. We also monitored mitochondrial membrane potential with JC-1 to evaluate oxidative damage, and the results revealed a reduction in mitochondrial membrane potential in PA-treated cells, and JZG prevented this PA-induced reduction (Figure 4B), confirming that JZG protected mitochondrial integrity against oxidative stress in PA-induced mitochondrial dysfunction.

Autophagy was activated by JZG to improve NAFLD in vivo

A murine model of NAFLD induced by HFD was employed to assess the potential role of autophagy in metabolic stress-induced liver injury and inflammation. As expected, the HFD increased both the expression of LC3-Ⅱ/actin and p62 (Figure 5A), suggesting the activation of autophagy induction and inhibition of autophagic flux. JZG treatment induced an increase in LC3-Ⅱ/LC3-Ⅰ expression and led to a decrease in p62 expression (Figure 5A), indicating up-regulation of the autophagy pathway in JZG-treated mice.

Biochemical analyses showed that HFD elevated the expression of circulating ALT, aspartate aminotransferase, total cholesterol, triglycerides and fasting blood glucose as well as hepatic triglycerides, and JZG improved the metabolic disorder and associated liver injury (Figure 5B). The results of HE and oil red O staining demonstrated that lipid droplets and inflammation were induced by HFD and JZG ameliorated these conditions (Figure 5C). Together, these findings suggested that JZG had beneficial effects in improving NAFLD *in vivo*.

DISCUSSION

NAFLD, as the leading cause of chronic liver disease, could result in serious liver-related complications and an increase in overall mortality. In previous research, we demonstrated that the Chinese herbal formula, JZG, had beneficial effects in improving hepatic fat accumulation, and in this study, we showed that autophagy is critically involved in this process.

Autophagy occurs when autophagosomes are formed and autophagy induction is attributed to various origins, such as the endoplasmic reticulum, the Golgi apparatus, the mitochondria or the plasma membrane[23,24]. The autophagosomes then become autolysosomes by fusing with lysosomes and degrading the components in cytosols[25,26]. Thus, the upstream event of autophagy induction was presented by LC3-Ⅱ/actin expression in this study, and the downstream event of autophagic flux was presented by the expression of LC3-Ⅱ/LC3-Ⅰ. Stable fluorescence-expressing cell lines of LC3 were established to visualize the whole progression of autophagic flux. Results showed that metabolic stress-induced hepatocyte injury exhibited dual effects on autophagy by activating autophagy induction and blocking autophagic flux.

A series of signaling pathways and regulators which regulate autophagy have been identified in the past decade. In this research, a classic signaling pathway, the PI3K-AKT-mTOR signaling pathway[27], was confirmed to be important in response to PA challenge. As the

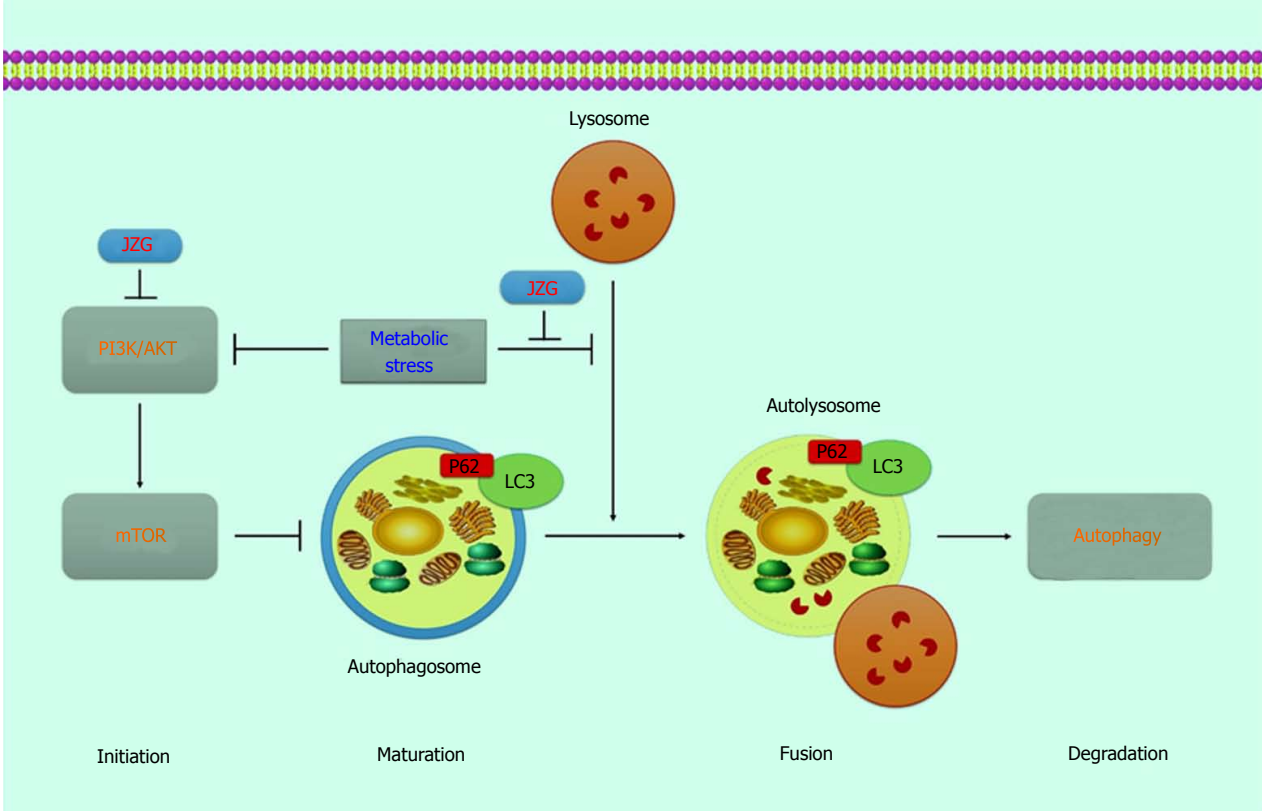

Figure 6 The potential role of autophagy in metabolic stress-induced hepatocyte injury and the protective mechanism of JZG in this process. JZG: Jiang Zhi Granule.

core target in this signaling pathway, mTOR, a master regulator of cellular metabolism, can be stimulated by multiple stimulants, such as nutritional status, hormonal factors and oxygen concentrations[28]. Under these conditions, mTOR complex 1 (mTORC1) will inhibit the ULK complex by phosphorylating Atg13 and ULK1/2, which results in autophagy suppression[29]. However, restraints on both phosphorylation signaling processes of PI3K and mTOR were observed in JZG-treated cells, indicating that the PI3K-AKT-mTOR pathway was involved in autophagy in the JZG-treated cells.

Subsequent studies have shown that SQSTM1/p62 accumulation is correlated with NAFLD and the fusion of isolated hepatic autophagosomes and lysosomes is different in NAFLD patients[30], which suggests that an excessive amount of lipids may contribute to SQSTM1/p62 accumulation by suppressing autophagosomes/lysosome fusion[31,32]. Thus, we examined the SQSTM1/p62 accumulation and the results confirmed previous findings.

Fluorescence staining was performed to connect the mitochondrial integrity with oxidative stress induced by PA. We also found that JZG could activate the autophagy process by either induction of autophagosomes or colocalization of autophagosomes and lysosomes as well as degradation of autolysosomes to protect against metabolic stress-induced hepatocyte injury in NAFLD (Figure 6).

Limitations should be acknowledged. The complex compounds contained in this prescription may have led to multitarget effects, and a series of signaling pathways and regulators were not examined. Beyond that, as p62 could also be degraded by proteasome, further studies on this aspect should be continually conducted to confirm the findings in the future. However, as the current epidemic of obesity and obesity-related NAFLD continues to increase, new approaches for prevention and treatment are urgently needed, and traditional Chinese medicine, as an alternative and complementary medicine, may be an effective addition to the current standardized intervention strategy.

ARTICLE HIGHLIGHTS

Research background

Non-alcoholic fatty liver disease (NAFLD), as the leading cause of chronic liver disease, can result in serious liver-related complications and an increase in overall mortality. However, the pathogenesis of NAFLD is still unknown and no effective therapeutic strategy has been accepted as the standard treatment option. In previous studies, the authors found that JZG had beneficial effects in improving hepatic fat accumulation, metabolic disorder and associated liver injury, and its efficacy in patients with NAFLD was also confirmed.

Research motivation

Autophagy is important in liver diseases, and research has demonstrated that autophagy regulators can improve hepatic function. However, no effective therapeutic strategy has been accepted as the standard option for NAFLD and

its complications. Thus, novel treatments are still urgently needed to prevent or delay the onset as well as the progression of NAFLD.

Research objectives

NAFLD, as the leading cause of chronic liver disease, could result in serious liver-related complications and an increase in overall mortality. And traditional Chinese medicine, as an alternative and complementary medicine, may be an effective addition to the current standardized intervention strategy.

Research methods

The process of autophagy was detected by the expressions of LC3 and SQSTM1/p62. The upstream event of autophagy induction was presented by LC3-Ⅱ/actin expression and the downstream event of autophagic flux was presented by the expressions of LC3-Ⅱ/LC3-Ⅰ and SQSTM1/p62. Stable fluorescence-expressing cell lines were established with mRFP-GFP-LC3 and mCherry-p62 lentivirus to visualize the whole progression of autophagic flux.

Research results

In previous research, the authors had demonstrated that the Chinese herbal formula JZG had beneficial effects in improving hepatic fat accumulation. In this study, autophagy was demonstrated to be critically involved in this process.

Research conclusions

The authors confirmed that metabolic stress-induced hepatocyte injury exhibited dual effects on autophagy, while JZG activated the whole process to provide beneficial effects in NAFLD.

Research perspectives

The exact compounds contained in this prescription are still unknown and the complex compounds might have led to multitarget effects. A systems pharmacology approach to determine the active compounds and action mechanisms might be a good method for the future research.

REFERENCES

1 **Bellentani S**, Marino M. Epidemiology and natural history of non-alcoholic fatty liver disease (NAFLD). *Ann Hepatol* 2009; **8** Suppl 1: S4-S8 [PMID: 19381118]
2 **López-Velázquez JA**, Silva-Vidal KV, Ponciano-Rodríguez G, Chávez-Tapia NC, Arrese M, Uribe M, Méndez-Sánchez N. The prevalence of nonalcoholic fatty liver disease in the Americas. *Ann Hepatol* 2014; **13**: 166-178 [PMID: 24552858]
3 **Wree A**, Broderick L, Canbay A, Hoffman HM, Feldstein AE. From NAFLD to NASH to cirrhosis-new insights into disease mechanisms. *Nat Rev Gastroenterol Hepatol* 2013; **10**: 627-636 [PMID: 23958599 DOI: 10.1038/nrgastro.2013.149]
4 **Tiniakos DG**, Vos MB, Brunt EM. Nonalcoholic fatty liver disease: pathology and pathogenesis. *Annu Rev Pathol* 2010; **5**: 145-171 [PMID: 20078219 DOI: 10.1146/annurev-pathol-121808-102132]
5 **Reiniers MJ**, van Golen RF, van Gulik TM, Heger M. Reactive oxygen and nitrogen species in steatotic hepatocytes: a molecular perspective on the pathophysiology of ischemia-reperfusion injury in the fatty liver. *Antioxid Redox Signal* 2014; **21**: 1119-1142 [PMID: 24294945 DOI: 10.1089/ars.2013.5486]
6 **Jung UJ**, Choi MS. Obesity and its metabolic complications: the role of adipokines and the relationship between obesity, inflammation, insulin resistance, dyslipidemia and nonalcoholic fatty liver disease. *Int J Mol Sci* 2014; **15**: 6184-6223 [PMID: 24733068 DOI: 10.3390/ijms15046184]
7 **Yin XM**, Ding WX, Gao W. Autophagy in the liver. *Hepatology* 2008; **47**: 1773-1785 [PMID: 18393362 DOI: 10.1002/hep.22146]
8 **Cheng Y**, Ren X, Hait WN, Yang JM. Therapeutic targeting of autophagy in disease: biology and pharmacology. *Pharmacol Rev* 2013; **65**: 1162-1197 [PMID: 23943849 DOI: 10.1124/pr.112.007120]
9 **Kim KH**, Lee MS. Autophagy--a key player in cellular and body metabolism. *Nat Rev Endocrinol* 2014; **10**: 322-337 [PMID: 24663220 DOI: 10.1038/nrendo.2014.35]
10 **Johansen T**, Lamark T. Selective autophagy mediated by autophagic adapter proteins. *Autophagy* 2011; **7**: 279-296 [PMID: 21189453]
11 **Stolz A**, Ernst A, Dikic I. Cargo recognition and trafficking in selective autophagy. *Nat Cell Biol* 2014; **16**: 495-501 [PMID: 24875736 DOI: 10.1038/ncb2979]
12 **Christian P**, Sacco J, Adeli K. Autophagy: Emerging roles in lipid homeostasis and metabolic control. *Biochim Biophys Acta* 2013; **1831**: 819-824 [PMID: 23274236 DOI: 10.1016/j.bbalip.2012.12.009]
13 **Singh R**, Kaushik S, Wang Y, Xiang Y, Novak I, Komatsu M, Tanaka K, Cuervo AM, Czaja MJ. Autophagy regulates lipid metabolism. *Nature* 2009; **458**: 1131-1135 [PMID: 19339967 DOI: 10.1038/nature07976]
14 **Lin CW**, Zhang H, Li M, Xiong X, Chen X, Chen X, Dong XC, Yin XM. Pharmacological promotion of autophagy alleviates steatosis and injury in alcoholic and non-alcoholic fatty liver conditions in mice. *J Hepatol* 2013; **58**: 993-999 [PMID: 23339953 DOI: 10.1124/10.1016/j.jhep.2013.01.011]
15 **Song HY**, Zhang L, Pan JL, Yang LL, Ji G. Bioactivity of five components of Chinese herbal formula Jiangzhi granules against hepatocellular steatosis. *J Integr Med* 2013; **11**: 262-268 [PMID: 23867244 DOI: 10.3736/jintegrmed2013034]
16 **Wang M**, Sun S, Wu T, Zhang L, Song H, Hao W, Zheng P, Xing L, Ji G. Inhibition of LXRα/SREBP-1c-Mediated Hepatic Steatosis by Jiang-Zhi Granule. *Evid Based Complement Alternat Med* 2013; **2013**: 584634 [PMID: 23762146 DOI: 10.1155/2013/584634]
17 **Pan J**, Wang M, Song H, Wang L, Ji G. The efficacy and safety of traditional chinese medicine (jiang zhi granule) for nonalcoholic Fatty liver: a multicenter, randomized, placebo-controlled study. *Evid Based Complement Alternat Med* 2013; **2013**: 965723 [PMID: 24369486 DOI: 10.1155/2013/965723]
18 **Matsushita N**, Osaka T, Haruta I, Ueshiba H, Yanagisawa N, Omori-Miyake M, Hashimoto E, Shibata N, Tokushige K, Saito K, Tsuneda S, Yagi J. Effect of Lipopolysaccharide on the Progression of Non-Alcoholic Fatty Liver Disease in High Caloric Diet-Fed Mice. *Scand J Immunol* 2016; **83**: 109-118 [PMID: 26524607 DOI: 10.1111/sji.12397]
19 **Cui W**, Wang M, Maegawa H, Teranishi Y, Kawada N. Inhibition of the activation of hepatic stellate cells by arundic acid via the induction of cytoglobin. *Biochem Biophys Res Commun* 2012; **425**: 642-648 [PMID: 22850540 DOI: 10.1016/j.bbrc.2012.07.126]
20 **Shu X**, Wang M, Xu H, Liu Y, Huang J, Yao Z, Zhang L. Extracts of Salvia-Nelumbinis Naturalis Ameliorate Nonalcoholic Steatohepatitis via Inhibiting Gut-Derived Endotoxin Mediated TLR4/NF-κB Activation. *Evid Based Complement Alternat Med* 2017; **2017**: 9208314 [PMID: 28831287 DOI: 10.1155/2017/9208314]
21 **Kamikubo R**, Kai K, Tsuji-Naito K, Akagawa M. β-Caryophyllene attenuates palmitate-induced lipid accumulation through AMPK signaling by activating CB2 receptor in human HepG2 hepatocytes. *Mol Nutr Food Res* 2016; **60**: 2228-2242 [PMID: 27234712 DOI: 10.1002/mnfr.201600197]
22 **Ruan L**, Zhou C, Jin E, Kucharavy A, Zhang Y, Wen Z, Florens L, Li R. Cytosolic proteostasis through importing of misfolded proteins into mitochondria. *Nature* 2017; **543**: 443-446 [PMID: 28241148 DOI: 10.1038/nature21695]
23 **Hamasaki M**, Shibutani ST, Yoshimori T. Up-to-date membrane biogenesis in the autophagosome formation. *Curr Opin Cell Biol* 2013; **25**: 455-460 [PMID: 23578367 DOI: 10.1016/j.ceb.2013.03.004]
24 **Lamb CA**, Yoshimori T, Tooze SA. The autophagosome: origins unknown, biogenesis complex. *Nat Rev Mol Cell Biol* 2013; **14**: 759-774 [PMID: 24201109 DOI: 10.1038/nrm3696]
25 **Kaur J**, Debnath J. Autophagy at the crossroads of catabolism and anabolism. *Nat Rev Mol Cell Biol* 2015; **16**: 461-472 [PMID: 26177004 DOI: 10.1038/nrm4024]
26 **Madrigal-Matute J**, Cuervo AM. Regulation of Liver Metabolism by Autophagy. *Gastroenterology* 2016; **150**: 328-339 [PMID: 26453774 DOI: 10.1053/j.gastro.2015.09.042]

27 **Liu HY**, Han J, Cao SY, Hong T, Zhuo D, Shi J, Liu Z, Cao W. Hepatic autophagy is suppressed in the presence of insulin resistance and hyperinsulinemia: inhibition of FoxO1-dependent expression of key autophagy genes by insulin. *J Biol Chem* 2009; **284**: 31484-31492 [PMID: 19758991 DOI: 10.1074/jbc.M109.033936]

28 **Levine B**, Kroemer G. Autophagy in the pathogenesis of disease. *Cell* 2008; **132**: 27-42 [PMID: 18191218 DOI: 10.1016/j.cell.2007.12.018]

29 **Kim YC**, Guan KL. mTOR: a pharmacologic target for autophagy regulation. *J Clin Invest* 2015; **125**: 25-32 [PMID: 25654547 DOI: 10.1172/JCI73939]

30 **Fukuo Y**, Yamashina S, Sonoue H, Arakawa A, Nakadera E, Aoyama T, Uchiyama A, Kon K, Ikejima K, Watanabe S. Abnormality of autophagic function and cathepsin expression in the liver from patients with non-alcoholic fatty liver disease. *Hepatol Res* 2014; **44**: 1026-1036 [PMID: 24299564 DOI: 10.1111/hepr.12282]

31 **Koga H**, Kaushik S, Cuervo AM. Altered lipid content inhibits autophagic vesicular fusion. *FASEB J* 2010; **24**: 3052-3065 [PMID: 20375270 DOI: 10.1096/fj.09-144519]

32 **Inami Y**, Yamashina S, Izumi K, Ueno T, Tanida I, Ikejima K, Watanabe S. Hepatic steatosis inhibits autophagic proteolysis via impairment of autophagosomal acidification and cathepsin expression. *Biochem Biophys Res Commun* 2011; **412**: 618-625 [PMID: 21856284 DOI: 10.1016/j.bbrc.2011.08.012]

P- Reviewer: Demonacos C, Marcos R, Osna NA
S- Editor: Gong ZM **L- Editor**: Filipodia **E- Editor**: Huang Y

World Journal of Gastroenterology

Submit a Manuscript: http://www.f6publishing.com

World J Gastroenterol 2018 March 7; 24(9): 1004-1012

DOI: 10.3748/wjg.v24.i9.1004

ISSN 1007-9327 (print) ISSN 2219-2840 (online)

ORIGINAL ARTICLE

Basic Study

Long noncoding RNA RP4 functions as a competing endogenous RNA through miR-7-5p sponge activity in colorectal cancer

Mu-Lin Liu, Qiao Zhang, Xiao Yuan, Long Jin, Li-Li Wang, Tao-Tao Fang, Wen-Bin Wang

Mu-Lin Liu, Long Jin, Li-Li Wang, Tao-Tao Fang, Department of Gastrointestinal Surgery, the First Affiliated Hospital of Bengbu Medical College, Bengbu 233004, Anhui Province, China

Qiao Zhang, Department of General Surgery, the First Affiliated Hospital of Xinxiang Medical University, Xinxiang 453100, Henan Province, China

Xiao Yuan, Wen-Bin Wang, Department of General Surgery, the Fourth Affiliated Hospital of Anhui Medical University, Hefei 230022, Anhui Province, China

ORCID number: Mu-Lin Liu (0000-0003-3930-678X); Qiao Zhang (0000-0001-5413-4547); Xiao Yuan (0000-0002-4299-7377); Long Jin (0000-0002-7765-4091); Li-Li Wang (0000-0003-0439-8119); Tao-Tao Fang (0000-0002-1831-1937); Wen-Bin Wang (0000-0002-9023-6855).

Author contributions: Liu ML, Zhang Q and Yuan X contributed equally to this work; Liu ML and Zhang Q conceived the study and participated in its design and coordination; Yuan X drafted and revised the manuscript; Jin L helped with the statistical analysis; Wang LL and Fang TT performed the experiments; Wang WB conceived the study and revised the manuscript; all authors read and approved the final manuscript.

Supported by Scientific Research Foundation of Anhui Education Department, No. KJ2017A219 to Liu ML; Scientific Research Foundation of Academic Leader of Anhui Province, No. 2016H105 to Liu ML; Education Talent Foundation of Universities of Anhui Education Department, No. gxbjZD2016070 to Liu ML; National Natural Science Foundation of China, No. 81500373 to Wang WB; and Natural Science Foundation of Anhui Province, No. 1608085MH193 to Wang WB.

Institutional review board statement: The study was reviewed and approved by the Ethics Committee of the First Affiliated Hospital of Bengbu Medical College.

Institutional animal care and use committee statement: All procedures involving animals were reviewed and approved by the Institutional Animal Care and Use Committee of SHRM.

Conflict-of-interest statement: The authors declare that there is no conflict of interest related to this study.

Data sharing statement: The datasets supporting the conclusions of this article are included within the article.

Manuscript source: Unsolicited manuscript

Correspondence to: Wen-Bin Wang, PhD, Doctor, Professor, Department of General Surgery, the Fourth Affiliated Hospital of Anhui Medical University, No. 372, Tunxi Road, Hefei 230022, Anhui Province, China. surdoctor@163.com
Telephone: +86-551-62879386
Fax:+86-552-3070260

Received: November 15, 2017
Peer-review started: November 16, 2017
First decision: December 20, 2017
Revised: December 26, 2017
Accepted: January 16, 2018
Article in press: January 16, 2018
Published online: March 7, 2018

Abstract

AIM

To investigate the role of long noncoding RNA (lncRNA) RP4 in colorectal cancer.

METHODS
Lentivirus-mediated lncRNA RP4 overexpression and knockdown were performed in the colorectal cancer cell line SW480. Cell proliferation, tumor growth, and early apoptosis were evaluated by a cell counting kit-8 assay, an *in vivo* xenograft tumor model, and annexin V/propidium iodide staining, respectively. Analysis of the lncRNA RP4 mechanism involved assessment of the association of its expression with miR-7-5p and the *SH3GLB1* gene. Western blot analysis was also performed to assess the effect of lncRNA RP4 on the autophagy-mediated cell death pathway and phosphatidylinositol-3-kinase (PI3K)/Akt signaling.

RESULTS
Cell proliferation, tumor growth, and early apoptosis in SW480 cells were negatively regulated by lncRNA RP4. Functional experiments indicated that lncRNA RP4 directly upregulated *SH3GLB1* expression by acting as a competing endogenous RNA (ceRNA) for miR-7-5p. This interaction led to activation of the autophagy-mediated cell death pathway and de-repression of PI3K and Akt phosphorylation in colorectal cancer cells *in vivo*.

CONCLUSION
Our results demonstrated that lncRNA RP4 is a ceRNA that plays an important role in the pathogenesis of colorectal cancer, and could be a potential therapeutic target for colorectal cancer treatment.

Key words: Colorectal cancer; Long noncoding RNA RP4; SH3GLB1; miR-7-5p; Competing endogenous RNA

Core tip: In the present study, we investigated the role of long noncoding RNA (lncRNA) RP4 in colorectal cancer using an *in vivo* cell model and an *in vivo* xenograft model. Mechanistic analysis suggested that lncRNA RP4 functions in colorectal cancer pathogenesis as a competing endogenous RNA that regulates SH3GLB1 expression by acting as a sponge for miR-7-5p. It could also serve as a potential therapeutic target for colorectal cancer treatment.

Liu ML, Zhang Q, Yuan X, Jin L, Wang LL, Fang TT, Wang WB. Long noncoding RNA RP4 functions as a competing endogenous RNA through miR-7-5p sponge activity in colorectal cancer. *World J Gastroenterol* 2018; 24(9): 1004-1012 Available from: URL: http://www.wjgnet.com/1007-9327/full/v24/i9/1004.htm DOI: http://dx.doi.org/10.3748/wjg.v24.i9.1004

INTRODUCTION

Colorectal cancer is the fourth most common cancer and the fifth most common cause of cancer-related death in China, with an estimated 331300 newly diagnosed patients and 159300 deaths in 2012[1]. Surgical resection followed by adjuvant chemotherapy is the most commonly used strategy for colorectal cancer management. However, although the overall 5-year survival rate of colorectal cancer has improved to 65%, the 5-year survival rate was only 15% in patients presenting with distant metastasis[2], reflecting the poor treatment response in some patients. Therefore, it is necessary to identify effective therapeutic targets to improve treatment and prognosis.

Long noncoding RNAs (lncRNAs), > 200 nucleotides in length, are a recently discovered novel class of genes with regulatory functions but lacking protein-coding ability. Several studies have identified important roles for lncRNAs in a wide range of cellular processes, including X chromosome inactivation, splicing, imprinting, epigenetic control, and gene transcription regulation[3-5]. Moreover, the dysregulated expression of lncRNAs is present in various human diseases, especially in cancers including breast cancer, lung cancer, gastric cancer, and colorectal cancer[6-8]. Indeed, several recent pieces of evidence suggest that lncRNAs are involved in the development and progression of human colorectal cancer and may serve as novel therapeutic targets[9-11]. However, the role of lncRNAs in colorectal cancer is largely unknown.

The dysregulation of lncRNA RP4 has previously been shown by expression profile analysis of a transcriptome microarray. Therefore, the present study investigated the role of lncRNA RP4 in colorectal cancer using an *in vitro* cell model and an *in vivo* xenograft model. Mechanistic analysis suggested that lncRNA RP4 functions in colorectal cancer pathogenesis as a competing endogenous RNA (ceRNA) that regulates *SH3GLB1* expression by acting as a sponge for the microRNA (miRNA) miR-7-5p. It could also serve as a potential therapeutic target for colorectal cancer treatment.

MATERIALS AND METHODS

Ethics statement

This study was conducted in accordance with the ethical standards, the Declaration of Helsinki, and national and international guidelines, and was approved by the authors' institutional review board, which adheres to generally accepted international guidelines for animal experimentation.

Cell culture

The human colorectal cancer cell line SW480 was obtained from the American Type Culture Collection. Cells were maintained as monolayers in cell culture flasks with RPMI1640 medium containing 10% (v/v) fetal bovine serum and 1% antibiotics. They were cultured at 37 ℃ in a humidified atmosphere with 5% CO_2. All cell culture media and additives were purchased from Invitrogen (CA, United States).

Lentiviral short hairpin (sh)RNA particles

Recombinant lentiviral particles expressing lncRNA RP4

Table 1 Sequences of the primers used

Gene	Forward primer (5′-3′)	Reverse primer (5′-3′)
ENST00000565575	ATCCGTTCCAAATCCTGTCGT	TTCAAGCAGAGGCTGTATCGTG
SH3GLB1	CGCTGTCTGAATGACTTTGT	CCTTTCTGCTGCCACTACAC
β-actin	GTGGCCGAGGACTTTGATTG	CCTGTAACAACGCATCTCATATT

or lncRNA RP4 small interfering (si)RNA were obtained from GenePharm Co., Ltd. (Shanghai, China). Cells were grown to approximately 40% confluence and infected with lentiviral particles in complete medium for 48 h. To increase the infection efficiency, cells were co-treated with the cationic polymer polybrene (8 μg/mL in water). Neither shRNA nor polybrene affected cell viability. siRNA and shRNA had no off-target effects, and did not affect cell adherence, shape, or viability at the indicated multiplicity of infection.

Real-time quantitative reverse transcription polymerase chain reaction

Total RNA was extracted from SW480 cells using TRIzol reagent (Invitrogen). RT-PCR was carried out using a One Step SYBR PrimeScript RT-PCR kit (Takara, Dalian, China) and an iQ5 Real-time PCR Detection system (Bio-Rad, Hercules, CA, United States) for evaluation of the expression of lncRNA RP4. The miRNA miR-7-5p was obtained using the PureLink miRNA Isolation Kit (Invitrogen), and the quantification of miRNA expression was performed with a TaqMan MicroRNA Assay Kit (Applied Biosystems, Foster City, CA, United States). The expression of β-actin and *U6* snRNA genes was assessed simultaneously in all samples as an internal control for lncRNA/mRNA and miRNA expression, respectively. Relative gene expression was determined by the $2^{-\Delta\Delta CT}$ method[12]. Oligonucleotide primers specific for lncRNA RP4, *SH3GLB1*, and β-actin are listed in Table 1.

Western blot analysis

Cells were lysed in RIPA buffer, centrifuged at high speed, and then underwent protein quantification using a bicinchoninic acid assay. Cellular proteins were separated by sodium dodecyl sulfate polyacrylamide gel electrophoresis and transferred onto polyvinylidene difluoride membranes. After blocking, the membranes were incubated with anti-total- or -phosphor-PI3K, phospho-Akt, LC3A/B, Bax, and caspase 3 monoclonal primary antibodies (Cell Signaling Technology, Cambridge, MA, United States). β-actin (Santa Cruz Biotechnology, Santa Cruz, CA, United States) was used as the loading control. Appropriate horseradish peroxidase-conjugated secondary antibodies were applied to detect labeled proteins. The protein bands were developed with SuperSignal Ultra Chemiluminescent Substrate (Pierce, Rockford, IL, United States) on X-ray films (Kodak, Tokyo, Japan).

Cell proliferation

SW480 cells (3×10^3 cells) were seeded in 96-well plates in complete medium and infected with lncRNA RP4, lncRNA RP4 siRNA, or control lentivirus particles. Two days later, cell proliferation was evaluated by the cell counting kit-8 method according to the manufacturer's instructions using a microplate reader (Molecular Devices, Sunnyvale, CA, United States) to measure the absorbance.

Nude mouse model of ectopic tumors

Athymic nude (nu/nu) mice at 6 wk old were purchased from Shanghai SLAC Laboratory Animal Co., Ltd. Tumors were generated by the subcutaneous injection of 2×10^6 SW480 cells infected with lncRNA RP4, lncRNA RP4 siRNA, or control lentivirus particles and suspended in 50 μL of PBS into the dorsal region near the thigh. Mice were then weighed and assessed for tumor size every 7 wk by measuring the tumor length and width.

Cell apoptosis analysis

SW480 cells (3×10^5 cells) were seeded in 6-well plates in complete medium and infected with lncRNA RP4, lncRNA RP4 siRNA, or control lentivirus particles. Two days later, cell proliferation was evaluated by flow cytometry (FACScalibur; BD Biosciences, CA, United States) after annexin V/propidium iodide staining (Beyotime institution, Nantong, China).

Statistical analysis

All statistical analyses were carried out using SPSS v18 software (SPSS, Chicago, IL, United States). Data are presented as the mean ± SD. The Student's *t*-test or one-way analysis of variance were used to examine differences between two or multiple groups. Correlation analyses of the expression levels of lncRNA RP4, *SH3GLB1*, and miR-7-5p were performed using Pearson's correlation coefficient. A P-value < 0.05 was considered statistically significant.

RESULTS

lncRNA RP4 regulates proliferation, tumor growth, and early apoptosis in colorectal cancer cells

To investigate the role of lncRNA RP4 in the pathogenesis of colorectal cancer, we performed lentivirus-mediated overexpression and knockdown. As shown in Figure 1A, SW480 cell proliferation was negatively regulated by lncRNA RP4, while early apoptosis was positively regulated by lncRNA RP4 (Figure 1C and D). These results suggested that lncRNA RP4 exerts a negative regulatory role in colorectal cancer cell

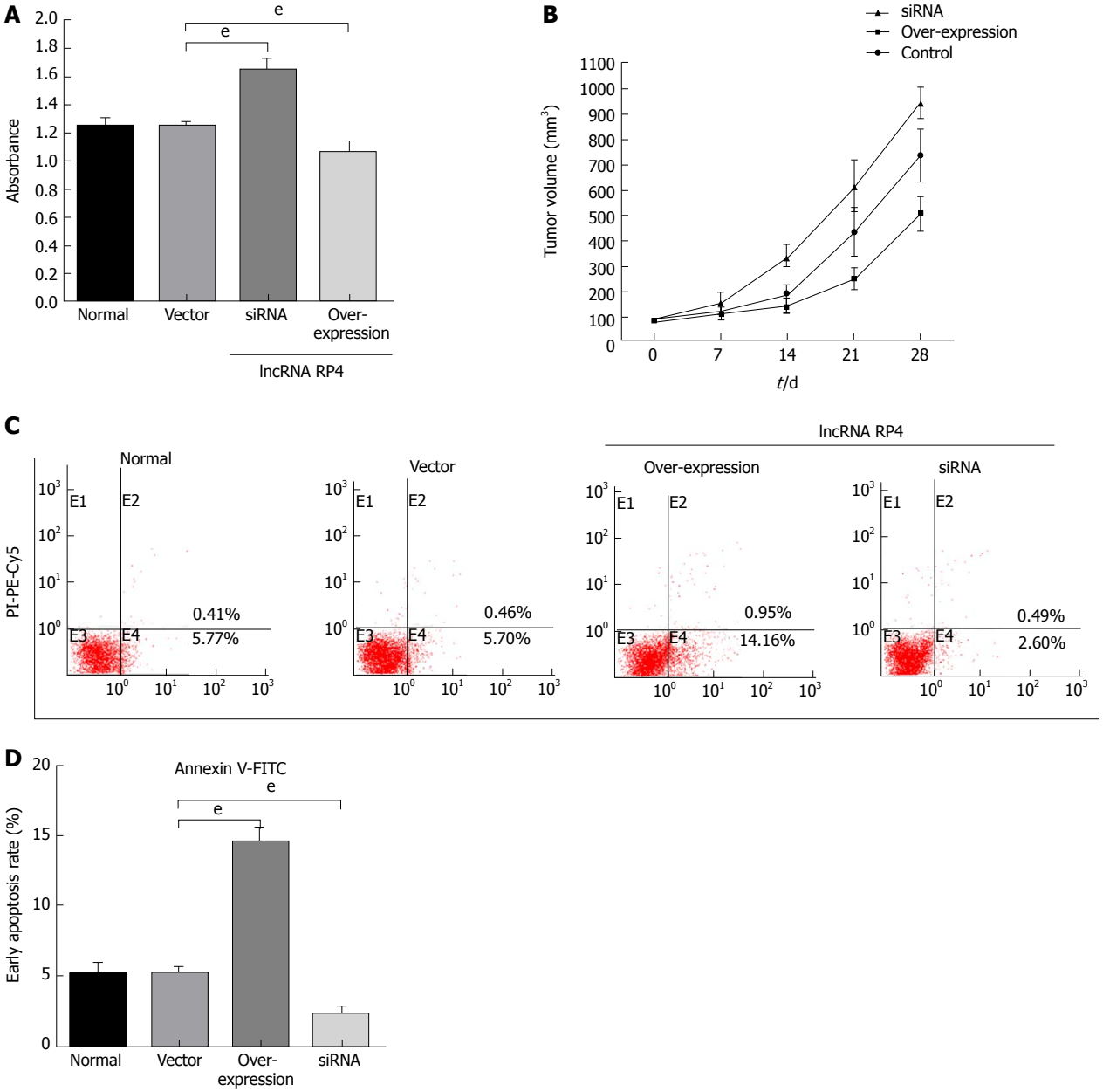

Figure 1 lncRNA RP4 regulates proliferation, tumor growth, and early apoptosis in colorectal cancer cells. Lentivirus-mediated lncRNA RP4 overexpression and knockdown were performed in the colorectal cancer line SW480, and cell proliferation, tumor growth, and early apoptosis were examined. A: Cell proliferation was examined by the CCK-8 assay. lncRNA RP4 overexpression and knockdown were shown to decrease and increase cell proliferation, respectively. B: Tumor growth was evaluated by tumor volume change. lncRNA RP4 overexpression and knockdown were shown to significantly decrease and increase tumor volume, respectively, at weeks 14, 21, and 28. C: Flow cytometry assessment of early apoptosis. lncRNA RP4 overexpression and knockdown increased and decreased early apoptosis, respectively, in colorectal cancer. D: Early apoptosis quantification. $^{e}P < 0.001$ for between-group comparisons.

proliferation and a positive regulatory role in early apoptosis of colorectal cancer cells.

lncRNA RP4 inhibits the growth of colorectal cancer on mice

Compared with the control group, colorectal cancer with lncRNA RP4 siRNA showed a bigger volume, while there was a smaller volume in the group with lncRNA RP4 overexpression (Figure 1B). Consistent with the results in cell line, the results *in vivo* also suggested that lncRNA RP4 plays an inhibitory role in colorectal cell growth.

lncRNA RP4 inhibits the growth of colorectal cancer cells by regulating SH3GLB1

To explore the mechanism of lncRNA RP4-mediated effects in colorectal cancer cells, we examined *SH3GLB1* expression in SW480 cells following lncRNA RP4 overexpression and knockdown. lncRNA RP4 was found to positively regulate *SH3GLB1* expression, and correlation analyses further confirmed the existence of a significant correlation between lncRNA RP4 and

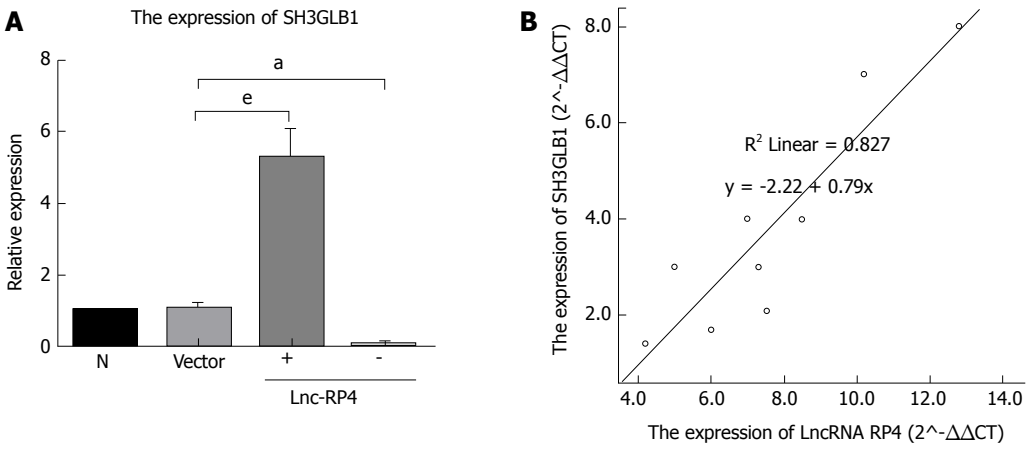

Figure 2 lncRNA RP4 affects the expression of *SH3GLB1* in colorectal cancer cells. Lentivirus-mediated lncRNA RP4 overexpression and knockdown were performed in *SW480* cells, and *SH3GLB1* expression was evaluated by real-time quantitative PCR, followed by association analyses between *SH3GLB1* and lncRNA RP4 levels. A: LncRNA RP4 overexpression and knockdown, respectively, increased and decreased *SH3GLB1* expression in SW480 cells. B: Correlation analyses revealed a linear association between the expression of *SH3GLB1* and lncRNA RP4, with an r^2 value of 0.827. $^aP < 0.05$ and $^eP < 0.001$ for between-group comparisons.

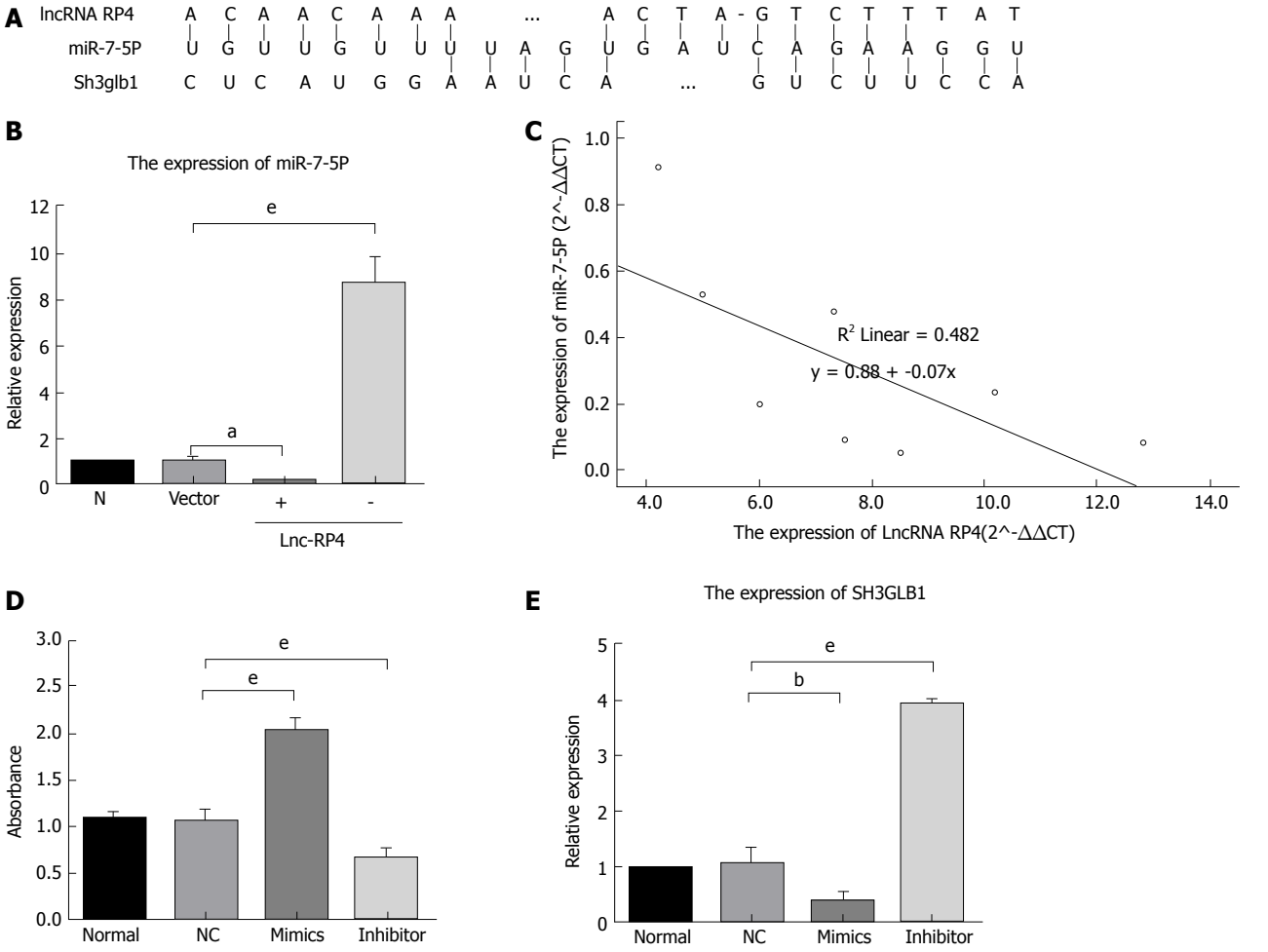

Figure 3 lncRNA RP4 functions as an miR-7-5p decoy in colorectal cancer cells. A: The predicted miR-7-5p binding sites on the *SH3GLB1* and lncRNA RP4 transcript. B: LncRNA RP4 overexpression and knockdown, respectively, decreased and increased the expression of miR-7-5p in SW480 cells. C: Correlation analyses revealed a linear association between the expression of lncRNA RP4 and miR-7-5p, with an r^2 value of 0.482. D: *SW480* cells were transfected with an miR-7-5p mimic and inhibitor, and cell proliferation was evaluated by the CCK-8 assay. miR-7-5p overexpression and knockdown increased and decreased cell proliferation, respectively. E. Real-time quantitative PCR showed that miR-7-5p overexpression and knockdown, respectively, decreased and increased *SH3GLB1* expression level in SW480 colorectal cancer cells. $^aP < 0.05$, $^bP < 0.01$, and $^eP < 0.001$ for between-group comparisons.

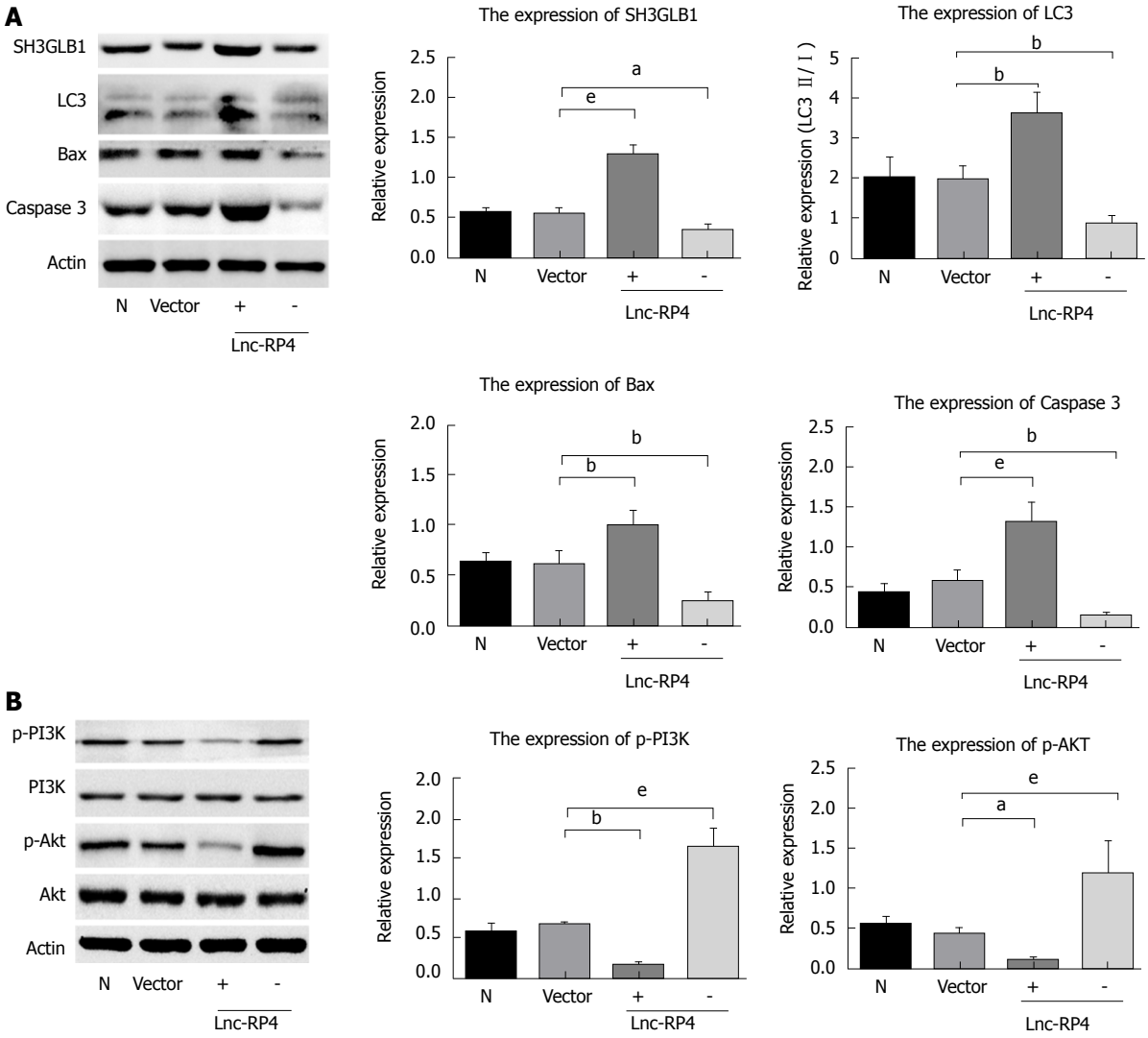

Figure 4 Involvement of the autophagy-mediated cell death pathway and PI3K/Akt signaling pathway in lncRNA RP4-mediated effects in colorectal cancer cells. A: LncRNA RP4 overexpression and knockdown, respectively, decreased and increased expression of the autophagy marker LC3, and apoptosis-related proteins Bax and caspase 3 in SW480 cells, suggesting that it positively regulates autophagy-mediated cell death in colorectal cancer cells. B: LncRNA RP4 overexpression and knockdown, respectively, decreased and increased PI3K and Akt phosphorylation in SW480 cells, indicating that it negatively regulates PI3K/Akt in colorectal cancer cells. C: Schematic of lncRNA RP4 functioning as a decoy by competitively binding miR-7-5p, upregulating the specific repressor SH3GLB1, activating autophagy-mediated cell death, and inhibiting the PI3K/Akt signaling pathway, thereby suppressing colorectal carcinogenesis. $^{a}P < 0.05$, $^{b}P < 0.01$, and $^{e}P < 0.001$ for between-group comparisons.

SH3GLB1 expression (Figure 2).

lncRNA RP4 functions as an miR-7-5p decoy in the regulation of SH3GLB1

Because no direct interaction exists between lncRNA RP4 and *SH3GLB1*, we further analyzed the potential functional mechanism by the introduction of miRNA. lncRNAs were recently reported to act as decoys that sequester miRNAs and prevent them from binding to targets, hence modulating many functional mRNA targets through translation. Bioinformatics analysis (webserver lnCeDB; http://gyanxet-beta.com/lncedb/) predicted potential interactions between lncRNA RP4 and miR-7-5p (Figure 3A), which was confirmed by correlation analysis (Figure 3B and C). We also observed a positive regulatory effect of miR-7-5p on cell proliferation *via* the negative regulation of *SH3GLB1* (Figure 3D and E). These results suggested that lncRNA RP4 functions as an miR-7-5p decoy in colorectal cancer cells.

Involvement of the autophagy-mediated cell death pathway and PI3K/Akt signaling pathway in lncRNA-RP4 mediated effects in colorectal cancer cells

According to previous findings[13,14], autophagy-mediated cell death is involved in the early apoptosis of cancer, while the PI3K/Akt signaling pathway plays a role in cancer cell proliferation and growth[15,16]. Analysis of the effects of lncRNA-RP4 on intracellular signaling revealed that lncRNA-RP4 overexpression and knockdown, respectively, upregulated and downregulated expression levels of the autophagy marker LC3 and apoptosis-related molecules Bax and caspase 3 (Figure 4A). We also observed the negative regulation of PI3K and Akt phosphorylation by lncRNA-RP4 in colorectal cancer cells (Figure 4B). Taken together, we propose a schematic whereby lncRNA RP4 functions as a decoy that competitively binds miR-7-5p, upregulating the specific repressor *SH3GLB1*, activating autophagy-mediated cell death, and inhibiting PI3K/Akt signaling, thereby suppressing colorectal carcinogenesis (Figure 4C).

DISCUSSION

Noncoding regions account for more than 90% of the entire human genome, and are thought to play a critical role in the regulation of physiological function given that only 9% of human genes are protein-coding. As a representative of noncoding regions, approximately 18% of lncRNAs are associated with human tumors and have been shown to act as major contributors in the development and progression of human cancers[17]. Multiple mechanisms have been suggested for the regulatory role of lncRNAs in physiological functions, including trans- and cis-regulatory mechanisms. In a trans-regulatory mechanism, lncRNAs (such as HOTAIR) could affect the transcription of specific genes through their interaction with chromatin-remodeling complexes and complex recruitment to genomic DNA sequences[18]. Some lncRNAs (such as lincRNA-21) also act as cis-regulators by exerting their function on nearby transcripts[19]. Growing evidence has shown that lncRNAs may act as ceRNAs *via* their miRNA response elements for specific miRNA targets, thus blocking the target binding ability of a single miRNA or multiple miRNAs[20,21]. Several lncRNAs have been suggested to function as ceRNAs, including PTENP1[22], H19[23], and CCAT1[24].

In the present study, we investigated the potential role of lncRNA RP4 as a ceRNA of *SH3GLB1* that competes for miRNA-7-5p binding sites, thereby regulating the expression of *SH3GLB1* mRNA targeted by miRNA-7-5p. The overexpression of lncRNA RP4 inhibited colorectal cancer cell proliferation and tumor growth both *in vitro* and *in vivo*, and increased early apoptosis. These findings suggest that lncRNA RP4 plays a critical role in the modulation of colorectal cancer progression.

To further elucidate the role of lncRNA RP4 in colorectal cancer, we analyzed its regulatory mechanism as a ceRNA by bioinformatics analysis and experimental verification. qRT-PCR analysis showed that lncRNA RP4 overexpression downregulated miR-7-5p expression in colorectal cancer cells, while an inverse correlation was detected between lncRNA RP4 and miR-7-5p expression. Additional functional experiments confirmed that miR-7-5p overexpression promoted cell proliferation, while an inverse correlation was detected between miR-7-5p and *SH3GLB1* expression. Consistent with these findings, miR-7-5p has been found to affect cell proliferation, anchorage-independent growth, migration and invasion, apoptosis, and chemosensitivity by targeting specific oncogenic genes in various types of tumor[25-27].

SH3GLB1, a membrane curvature-inducing protein, interacts with BECN1 though UVRAG and regulates the post-Golgi trafficking of membrane-integrated ATG9A during autophagy[28]. In the present study, we found that lncRNA RP4 overexpression upregulated autophagy. Recently, Takahashi *et al*[29] reported that SH3GLB1 is a haploinsufficient tumor suppressor that functions to prevent the acquisition of apoptosis resistance and malignant transformation during *Myc*-driven lymphomagenesis. Our data supported the tumor suppressor role of SH3GLB1 in colorectal cancer. During tumor development and progression, protein interactions between SH3GLB1 and BAX resulted in the activation of caspase 3, thereby inducing apoptosis[30]. Similarly, we showed that lncRP4-induced *SH3GLB1* upregulation increased levels of BAX and caspase 3 in colorectal cancer cells.

Previous studies observed that dysregulated PI3K/Akt signaling in human colorectal cancer is associated with the growth and proliferation pattern of cancer cells[15,16], while the PI3K/Akt pathway negatively regulates autophagy[31,32]. Consistent with this, we

detected reduced PI3K and Akt phosphorylation in lncRP4-overexpressing colorectal cancer cells.

The present study has a number of limitations. First, because of a lack of colorectal cancer tissue, we could not evaluate the expression pattern of lncRNA RP4, miR-7-5p, or *SH3GLB1* in carcinoma tissues and were thus unable to elucidate the clinical significance of lncRP4 in colorectal cancer. The collection of more colorectal cancer tissue will be necessary to overcome this. Second, we did not use small inhibitors of different signaling pathways, yet it is conceivable that the mechanism of lncRNA RP4 involves multiple modalities.

Taken together, our results demonstrate that lncRNA RP4 plays an important role in the progression of human colorectal cancer by functioning as a ceRNA to regulate the expression of *SH3GLB1* through miR-7-5p sponge activity. The pleiotropic effects of lncRNA RP4 on colorectal cancer pathogenesis suggest that is has the potential to be a therapeutic target for colorectal cancer.

ARTICLE HIGHLIGHTS

Research background

Colorectal cancer is the fourth most common cancer and the fifth most common cause of cancer-related death in China. Surgical resection followed by adjuvant chemotherapy, the most commonly used strategy for colorectal cancer management, has poor treatment response in some patients. Therefore, it is necessary to identify effective therapeutic targets to improve treatment and prognosis.

Research motivation

Long noncoding RNAs (lncRNAs), which may serve as novel therapeutic targets, are involved in the development and progression of human colorectal cancer. In our previous study, lncRNA RP4 was found to be dysregulated in colorectal cancer *via* microarray analysis. This indicated that this lncRNA may play an important role in colorectal cancer. Thus, in the present study, lncRNA RP4 was investigated to find out its role in colorectal cancer progression through an *in vitro* cell model and an *in vivo* xenograft model. Besides, the possible mechanisms in the regulation of lncRNA RP4 had not been well described.

Research objectives

To investigate the role of long noncoding (lnc)RNA RP4 in colorectal cancer, and to find out the possible mechanisms of the regulation.

Research methods

Cell counting kit-8 assay *in vitro* and xenograft tumor model *in vivo* were performed to evaluate the role of lncRNA RP4 in the regulation of proliferation. Annexin V/propidium iodide staining was performed to detect the role of lncRNA RP4 in apoptosis. qPCR and Western blot were performed to identify the relationship between lncRNA RP4 and SH3GLB1. And then, Western blot was done to analyse PI3K/Akt signaling pathway and autophagy pathway in the regulation.

Research results

Both cell counting kit-8 assay *in vitro* and xenograft tumor model *in vivo* showed that lncRNA RP4 could inhibit the proliferation and growth of colorectal cancer cells. lncRNA RP4 could promote early apoptosis. lncRNA RP4 was found to positively regulate SH3GLB1 expression, and correlation analyses further confirmed the existence of a significant correlation between lncRNA RP4 and SH3GLB1 expression. We also observed a positive regulatory effect of miR-7-5p on cell proliferation *via* the negative regulation of SH3GLB1.

Research conclusions

Our results demonstrate that lncRNA RP4 plays an important role in the progression of human colorectal cancer by functioning as a ceRNA to regulate the expression of SH3GLB1 through miR-7-5p sponge activity. The pleiotropic effects of lncRNA RP4 on colorectal cancer pathogenesis suggest that is has the potential to be a therapeutic target for colorectal cancer.

Research perspectives

This study suggests that the lncRNA intervention may be a promising treatment strategy for colorectal cancer. The future study might focus on the specific regulatory role of lncRNA RP4 in colorectal cancer *in vivo*, and the therapeutic effect of lncRNA RP4 needs to be validated in clinical practice.

REFERENCES

1 **Chen W**, Zheng R, Zuo T, Zeng H, Zhang S, He J. National cancer incidence and mortality in China, 2012. *Chin J Cancer Res* 2016; **28**: 1-11 [PMID: 27041922 DOI: 10.3978/j.issn.1000-9604.2016.02.08]

2 **Siegel RL**, Miller KD, Jemal A. Cancer statistics, 2016. *CA Cancer J Clin* 2016; **66**: 7-30 [PMID: 26742998 DOI: 10.3322/caac.21332]

3 **Yue M**, Charles Richard JL, Ogawa Y. Dynamic interplay and function of multiple noncoding genes governing X chromosome inactivation. *Biochim Biophys Acta* 2016; **1859**: 112-120 [PMID: 26260844 DOI: 10.1016/j.bbagrm.2015.07.015]

4 **Butler AA**, Webb WM, Lubin FD. Regulatory RNAs and control of epigenetic mechanisms: expectations for cognition and cognitive dysfunction. *Epigenomics* 2016; **8**: 135-151 [PMID: 26366811 DOI: 10.2217/epi.15.79]

5 **Kanduri C**. Long noncoding RNAs: Lessons from genomic imprinting. *Biochim Biophys Acta* 2016; **1859**: 102-111 [PMID: 26004516 DOI: 10.1016/j.bbagrm.2015.05.006]

6 **Tordonato C**, Di Fiore PP, Nicassio F. The role of non-coding RNAs in the regulation of stem cells and progenitors in the normal mammary gland and in breast tumors. *Front Genet* 2015; **6**: 72 [PMID: 25774169 DOI: 10.3389/fgene.2015.00072]

7 **Prensner JR**, Iyer MK, Balbin OA, Dhanasekaran SM, Cao Q, Brenner JC, Laxman B, Asangani IA, Grasso CS, Kominsky HD, Cao X, Jing X, Wang X, Siddiqui J, Wei JT, Robinson D, Iyer HK, Palanisamy N, Maher CA, Chinnaiyan AM. Transcriptome sequencing across a prostate cancer cohort identifies PCAT-1, an unannotated lincRNA implicated in disease progression. *Nat Biotechnol* 2011; **29**: 742-749 [PMID: 21804560 DOI: 10.1038/nbt.1914]

8 **Li W**, Zheng J, Deng J, You Y, Wu H, Li N, Lu J, Zhou Y. Increased levels of the long intergenic non-protein coding RNA POU3F3 promote DNA methylation in esophageal squamous cell carcinoma cells. *Gastroenterology* 2014; **146**: 1714-1726.e5 [PMID: 24631494 DOI: 10.1053/j.gastro.2014.03.002]

9 **Yin D**, He X, Zhang E, Kong R, De W, Zhang Z. Long noncoding RNA GAS5 affects cell proliferation and predicts a poor prognosis in patients with colorectal cancer. *Med Oncol* 2014; **31**: 253 [PMID: 25326054 DOI: 10.1007/s12032-014-0253-8]

10 **Han Y**, Yang YN, Yuan HH, Zhang TT, Sui H, Wei XL, Liu L, Huang P, Zhang WJ, Bai YX. UCA1, a long non-coding RNA up-regulated in colorectal cancer influences cell proliferation, apoptosis and cell cycle distribution. *Pathology* 2014; **46**: 396-401 [PMID: 24977734 DOI: 10.1097/PAT.0000000000000125]

11 **Ding J**, Lu B, Wang J, Wang J, Shi Y, Lian Y, Zhu Y, Wang J, Fan Y, Wang Z, De W, Wang K. Long non-coding RNA Loc554202 induces apoptosis in colorectal cancer cells via the caspase cleavage cascades. *J Exp Clin Cancer Res* 2015; **34**: 100 [PMID: 26362196 DOI: 10.1186/s13046-015-0217-7]

12 **Ji Y**, Strawn TL, Grunz EA, Stevenson MJ, Lohman AW, Lawrence DA, Fay WP. Multifaceted role of plasminogen activator inhibitor-1 in regulating early remodeling of vein bypass grafts.

Arterioscler Thromb Vasc Biol 2011; **31**: 1781-1787 [PMID: 21571686 DOI: 10.1161/ATVBAHA.111.228767]
13 **Santoni M**, Amantini C, Morelli MB, Farfariello V, Nabissi M, Liberati S, Bonfili L, Mozzicafreddo M, Eleuteri AM, Burattini L, Berardi R, Cascinu S, Santoni G. ifferent effects of sunitinib, sorafenib, and pazopanib on inducing cancer cell death: The role of autophagy. *J Clin Oncol* 2013; **6** suppl: 270 [DOI: 10.1200/jco.2013.31.6_suppl.270]
14 **Fulda S**. Autophagy in Cancer Therapy. *Front Oncol* 2017; **7**: 128 [PMID: 28674677 DOI: 10.3389/fonc.2017.00128]
15 **Liu X**, Gomez-Pinillos A, Shah P, Lavilla C, Ferrari AC. Effect of inhibition of the PI3K/Akt/mTOR pathway on AR splicing and downstream targets. *J Clin Oncol* 2013; **6** suppl: 101 [DOI: 10.1200/jco.2013.31.6_suppl.101]
16 **Jeon YW**, Ahn YE, Chung WS, Choi HJ, Suh YJ. Synergistic effect between celecoxib and luteolin is dependent on estrogen receptor in human breast cancer cells. *Tumour Biol* 2015; **36**: 6349-6359 [PMID: 25851346 DOI: 10.1007/s13277-015-3322-5]
17 **Khachane AN**, Harrison PM. Mining mammalian transcript data for functional long non-coding RNAs. *PLoS One* 2010; **5**: e10316 [PMID: 20428234 DOI: 10.1371/journal.pone.0010316]
18 **Bhan A**, Mandal SS. LncRNA HOTAIR: A master regulator of chromatin dynamics and cancer. *Biochim Biophys Acta* 2015; **1856**: 151-164 [PMID: 26208723 DOI: 10.1016/j.bbcan.2015.07.001]
19 **Dimitrova N**, Zamudio JR, Jong RM, Soukup D, Resnick R, Sarma K, Ward AJ, Raj A, Lee JT, Sharp PA, Jacks T. LincRNA-p21 activates p21 in cis to promote Polycomb target gene expression and to enforce the G1/S checkpoint. *Mol Cell* 2014; **54**: 777-790 [PMID: 24857549 DOI: 10.1016/j.molcel.2014.04.025]
20 **Wang K**, Long B, Zhou LY, Liu F, Zhou QY, Liu CY, Fan YY, Li PF. CARL lncRNA inhibits anoxia-induced mitochondrial fission and apoptosis in cardiomyocytes by impairing miR-539-dependent PHB2 downregulation. *Nat Commun* 2014; **5**: 3596 [PMID: 24710105 DOI: 10.1038/ncomms4596]
21 **Tay Y**, Rinn J, Pandolfi PP. The multilayered complexity of ceRNA crosstalk and competition. *Nature* 2014; **505**: 344-352 [PMID: 24429633 DOI: 10.1038/nature12986]
22 **Yu G**, Yao W, Gumireddy K, Li A, Wang J, Xiao W, Chen K, Xiao H, Li H, Tang K, Ye Z, Huang Q, Xu H. Pseudogene PTENP1 functions as a competing endogenous RNA to suppress clear-cell renal cell carcinoma progression. *Mol Cancer Ther* 2014; **13**: 3086-3097 [PMID: 25249556 DOI: 10.1158/1535-7163.MCT-14-0245]
23 **Kallen AN**, Zhou XB, Xu J, Qiao C, Ma J, Yan L, Lu L, Liu C, Yi JS, Zhang H, Min W, Bennett AM, Gregory RI, Ding Y, Huang Y. The imprinted H19 lncRNA antagonizes let-7 microRNAs. *Mol Cell* 2013; **52**: 101-112 [PMID: 24055342 DOI: 10.1016/j.molcel.2013.08.027]
24 **Ma MZ**, Chu BF, Zhang Y, Weng MZ, Qin YY, Gong W, Quan ZW. Long non-coding RNA CCAT1 promotes gallbladder cancer development via negative modulation of miRNA-218-5p. *Cell Death Dis* 2015; **6**: e1583 [PMID: 25569100 DOI: 10.1038/cddis.2014.541]
25 **Kalinowski FC**, Brown RA, Ganda C, Giles KM, Epis MR, Horsham J, Leedman PJ. microRNA-7: a tumor suppressor miRNA with therapeutic potential. *Int J Biochem Cell Biol* 2014; **54**: 312-317 [PMID: 24907395 DOI: 10.1016/j.biocel.2014.05.040]
26 **Kalinowski FC**, Giles KM, Candy PA, Ali A, Ganda C, Epis MR, Webster RJ, Leedman PJ. Regulation of epidermal growth factor receptor signaling and erlotinib sensitivity in head and neck cancer cells by miR-7. *PLoS One* 2012; **7**: e47067 [PMID: 23115635 DOI: 10.1371/journal.pone.0047067]
27 **Giles KM**, Brown RA, Ganda C, Podgorny MJ, Candy PA, Wintle LC, Richardson KL, Kalinowski FC, Stuart LM, Epis MR, Haass NK, Herlyn M, Leedman PJ. microRNA-7-5p inhibits melanoma cell proliferation and metastasis by suppressing RelA/NF-κB. *Oncotarget* 2016; **7**: 31663-31680 [PMID: 27203220 DOI: 10.18632/oncotarget.9421]
28 **Takahashi Y**, Young MM, Serfass JM, Hori T, Wang HG. Sh3glb1/Bif-1 and mitophagy: acquisition of apoptosis resistance during Myc-driven lymphomagenesis. *Autophagy* 2013; **9**: 1107-1109 [PMID: 23680845 DOI: 10.4161/auto.24817]
29 **Takahashi Y**, Hori T, Cooper TK, Liao J, Desai N, Serfass JM, Young MM, Park S, Izu Y, Wang HG. Bif-1 haploinsufficiency promotes chromosomal instability and accelerates Myc-driven lymphomagenesis via suppression of mitophagy. *Blood* 2013; **121**: 1622-1632 [PMID: 23287860 DOI: 10.1182/blood-2012-10-459826]
30 **Fino KK**, Yang L, Silveyra P, Hu S, Umstead TM, DiAngelo S, Halstead ES, Cooper TK, Abraham T, Takahashi Y, Zhou Z, Wang HG, Chroneos ZC. SH3GLB2/endophilin B2 regulates lung homeostasis and recovery from severe influenza A virus infection. *Sci Rep* 2017; **7**: 7262 [PMID: 28779131 DOI: 10.1038/s41598-017-07724-5]
31 **Mans LA**, Querol Cano L, van Pelt J, Giardoglou P, Keune WJ, Haramis AG. The tumor suppressor LKB1 regulates starvation-induced autophagy under systemic metabolic stress. *Sci Rep* 2017; **7**: 7327 [PMID: 28779098 DOI: 10.1038/s41598-017-07116-9]
32 **Wang S**, Li J, Du Y, Xu Y, Wang Y, Zhang Z, Xu Z, Zeng Y, Mao X, Cao B. The Class I PI3K inhibitor S14161 induces autophagy in malignant blood cells by modulating the Beclin 1/Vps34 complex. *J Pharmacol Sci* 2017; **134**: 197-202 [PMID: 28779993 DOI: 10.1016/j.jphs.2017.07.001]

P- Reviewer: Luchini C **S- Editor**: Gong ZM **L- Editor**: Wang TQ
E- Editor: Ma YJ

World Journal of Gastroenterology

Submit a Manuscript: http://www.f6publishing.com

World J Gastroenterol 2018 March 7; 24(9): 1013-1021

DOI: 10.3748/wjg.v24.i9.1013

ISSN 1007-9327 (print) ISSN 2219-2840 (online)

ORIGINAL ARTICLE

Retrospective Study

Quality indicators in pediatric colonoscopy in a low-volume center: Implications for training

Way-Seah Lee, Chun-Wei Tee, Zhong-Lin Koay, Tat-Seng Wong, Fatimah Zahraq, Hee-Wei Foo, Sik-Yong Ong, Shin-Yee Wong, Ruey-Terng Ng

Way-Seah Lee, Chun-Wei Tee, Zhong-Lin Koay, Tat-Seng Wong, Fatimah Zahraq, Hee-Wei Foo, Sik-Yong Ong, Shin-Yee Wong, Ruey-Terng Ng, Department of Paediatrics, University Malaya Medical Centre, Kuala Lumpur 59100, Malaysia

Way-Seah Lee, Paediatric and Child Health Research Group, University Malaya, Kuala Lumpur 50603, Malaysia

ORCID number: Way-Seah Lee (0000-0001-9163-2828); Chun-Wei Tee (0000-0002-1119-2971); Zhong-Lin Koay (0000-0002-8724-9903); Tat-Seng Wong (0000-0002-3076-228X); Fatimah Zahraq (0000-0002-2658-1945); Hee-Wei Foo (0000-0001-7761-0550); Sik-Yong Ong (0000-0001-9647-5788); Shin-Yee Wong (0000-0002-7486-0594); Ruey-Terng Ng (0000-0003-1656-5797).

Author contributions: Lee WS conceived the idea of the research; Lee WS, Ng RT, Ong SY and Foo HW provided the clinical data; Tee CW, Koay ZL, Wong TS and Zahraq F collected the data; Wong SY performed the statistical analysis; Lee WS and Tee CW analyzed the data; Lee WS wrote the first draft; All authors contributed equally to writing of the final draft; All authors authorized the final version of the manuscript.

Supported by Research grant from Ministry of Higher Education, Malaysia, No. UM.C/625/HIR/MOHE/CHAN/13/1.

Institutional review board statement: This study was reviewed and approved by the Ethics Committee of the University Malaya Medical Centre (MEC reference: 902.15).

Informed consent statement: Patients were not required to give informed consent to the study because the analysis performed used anonymous clinical data that were obtained after each patient agreed to treatment by written consent.

Conflict-of-interest statement: All authors declare no conflicts-of-interest related to this article.

Data sharing statement: No additional data are available.

Manuscript source: Unsolicited manuscript

Correspondence to: Way-Seah Lee, MBBS, FRCPCH, MD, Professor, Department of Paediatrics, Level 9, Women's and Children's Block, University Malaya Medical Center, Kuala Lumpur 59100, Malaysia. leews@ummc.edu.my
Telephone: +60-3-79492065
Fax: +60-3-79494704

Received: November 24, 2017
Peer-review started: November 25, 2017
First decision: December 27, 2017
Revised: January 15, 2018
Accepted: January 19, 2018
Article in press: January 19, 2018
Published online: March 7, 2018

Abstract

AIM

To study implications of measuring quality indicators on training and trainees' performance in pediatric colonoscopy in a low-volume training center.

METHODS

We reviewed retrospectively the performance of pediatric colonoscopies in a training center in Malaysia over 5 years (January 2010-December 2015), benchmarked against five quality indicators: appropriateness of indications, bowel preparations, cecum and ileal

examination rates, and complications. The European Society of Gastrointestinal Endoscopy guideline for pediatric endoscopy and North American Society for Pediatric Gastroenterology, Hepatology and Nutrition training guidelines were used as benchmarks.

RESULTS

Median (± SD) age of 121 children [males = 74 (61.2%)] who had 177 colonoscopies was 7.0 (± 4.6) years. On average, 30 colonoscopies were performed each year (range: 19-58). Except for investigations of abdominal pain (21/177, 17%), indications for colonoscopies were appropriate in the remaining 83%. Bowel preparation was good in 87%. One patient (0.6%) with severe Crohn's disease had bowel perforation. Cecum examination and ileal intubation rate was 95% and 68.1%. Ileal intubation rate was significantly higher in diagnosing or assessing inflammatory bowel disease (IBD) than non-IBD (72.9% *vs* 50.0%; P = 0.016). Performance of four trainees was consistent throughout the study period. Average cecum and ileal examination rate among trainees were 97% and 77%.

CONCLUSION

Benchmarking against established guidelines helps units with a low-volume of colonoscopies to identify area for further improvement.

Key words: Pediatric colonoscopies; Quality indicators; Performance

Core tip: Competency in colonoscopy is an essential component in the training for pediatric gastroenterology worldwide. We measured the performance of pediatric colonoscopy from a low-volume training center on quality indicators against established guidelines. The unit, which performed an average of 30 colonoscopies each year, performed well in clear indication for colonoscopy, good bowel preparation, safety and high rate of cecal examination (95%) but needs improvement for ileal intubation (at 68%). Benchmarking against established guidelines helps units with a low volume of colonoscopies to identify area for improvement.

Lee WS, Tee CW, Koay ZL, Wong TS, Zahraq F, Foo HW, Ong SY, Wong SY, Ng RT. Quality indicators in pediatric colonoscopy in a low-volume center: Implications for training. *World J Gastroenterol* 2018; 24(9): 1013-1021 Available from: URL: http://www.wjgnet.com/1007-9327/full/v24/i9/1013.htm DOI: http://dx.doi.org/10.3748/wjg.v24.i9.1013

INTRODUCTION

Colonoscopy is an essential diagnostic procedure for the evaluation and treatment of lower gastrointestinal pathologies in children[1-4]. Major indications for colonoscopy in children include rectal bleeding, investigation of diarrhea, failure to thrive and perianal lesions, and as initial diagnostic evaluation for inflammatory bowel disease (IBD)[5-10].

Approximately 20%-30% of IBD patients have onset of disease in childhood[11]. A study from Australia showed that IBD was the diagnosis in 58% of children who had initial diagnostic colonoscopy[5]. The percentage is much lower in Asia, ranging from 10.9% in Taiwanese children[8] to 19.6% in Korean children[7]. The incidence of IBD is increasing worldwide[12,13]. The incidence in Asia, including Malaysia, is increasing as well, although it is still relatively uncommon as compared to North America and Western Europe[13,14].

Competency in colonoscopy has become an essential component in the training syllabus for both adult and pediatric gastroenterology worldwide[15,16]. In adult colonoscopy, cecal intubation and detection for adenoma are considered as standard quality measures[15]. In children, however, routine screening for adenomas is generally not recommended[15]. On the other hand, ileal intubation is essential for accurate diagnosis of IBD, particularly Crohn's disease (CD)[17]. Thus, appropriate indication for colonoscopy, complete examination including inspection of cecum and terminal ileum, adequate bowel preparation and free of complications are all important quality indicators in pediatric colonoscopy[16].

In areas where the prevalence of IBD is low, such as Malaysia, the volume of pediatric colonoscopies performed may be limited[7-10,18]. The reported cecum examination and ileal intubation rates vary. In Hong Kong, the cecal and ileal intubation rates were 97.6% and 75.6%[10]. In Taiwan, the ileal intubation rate was 77.5%[8]. In Australia, where the incidence of IBD is high, Singh *et al*[5] reported that the cecal and ileal intubation rates were 96.3% and 92.4%, respectively.

A study on quality indicators published previously showed that performance benchmarked against quality indicators varies in different centers[16]. To the best of our knowledge, however, no study on performance benchmarked against quality indicators from low-volume centers has been published previously.

We aimed to ascertain the performance of our unit when benchmarked against established quality indicators in pediatric colonoscopy covering the following areas: indications, quality of bowel preparation, safety and complications, cecal examination and terminal ileum intubation rates. We also assessed the implications of our performance to ascertain opportunities for improvements to the training program in this training center.

MATERIALS AND METHODS

This was a retrospective review on all pediatric colonoscopies performed between January 2010 and

December 2015 at the Paediatric Gastroenterology Unit, University Malaya Medical Centre (UMMC), Malaysia. The present study was approved by the institutional ethics review committee (MEC reference: 902.15). During the study period, the unit was staffed by one full-time consultant and a part-time visiting consultant. They were assisted by fellows-in-training, who spent the first 18 mo of a 3-year fellowship training program in the unit.

Data collection

Cases were retrieved from hospital and the unit database. The following data were collected: demographics and clinical features; indications for colonoscopy; laboratory data; degree of bowel preparation; extent of colonoscopic examination; and complications. Colonoscopic and pathological diagnoses were ascertained. Cases were excluded if the data were incomplete.

Quality indicators

The following areas were used as quality indicators: (1) appropriateness of indications; (2) quality of bowel preparation and extent of colonoscopic examination, including (3) cecum examination and (4) ileal intubation; and (5) safety (including anesthesia and sedation) and complications. Factors affecting extent of examination and the performances of trainees were also analyzed.

Indications and preparations for colonoscopy

In our unit, each referral for colonoscopy was screened and decided by a consultant. Generally, the indications for colonoscopy followed the established guidelines[3,4], and has been reported previously[18]. For the purpose of the present study, the European Society of Gastrointestinal Endoscopy (ESGE) guideline for pediatric endoscopy was used as a benchmark[4].

Sedation and anesthesia

In our unit, colonoscopies were usually performed under general anesthesia. In adolescents, sedation (generally a combination of midazolam and pethidine) was used occasionally at the discretion of the anesthetist.

Bowel preparation

Bowel preparation has been standardized throughout the study period. Two days prior to colonoscopy, each patient was allowed a low residue diet. On the night before the procedure, each patient had bowel cleansing with polyethylene glycol solution and glycerin rectal enema. The degree of bowel preparation observed during colonoscopy was not standardized. It was judged by the endoscopist as poor, fair, good or excellent[6].

Extent of colonoscopy

The extent of the colonoscopy was confirmed by visual identification of the colonic wall appearance, and the anatomy the cecum and terminal ileum. The biopsy of the terminal ileum was also used as an additional confirmation. The recommendation by North American Society for Pediatric Gastroenterology, Hepatology and Nutrition (NASPGHAN) guidelines for training in pediatric gastroenterology was used as a benchmark[19]. The NASPGHAN guidelines recommends a cecum and ileal examination rate of between 90%-95%[19].

Performance

For the purpose of the present study, analysis on performance was confined to colonoscopies where an inspection of ileum was intended. This included cases where intubation of terminal ileum was indicated (*i.e.,* in diagnosing or assessing IBD), feasible (acceptable quality of bowel preparation where full examination was feasible) or safe (benefit of ileal intubation outweighs the risk of full examination, such as bowel perforation).

Performance by trainees

Analysis on the performance by trainees was confined to trainees who had completed a minimum of 12 mo training in the unit during the study period. Number of colonoscopies performed, cecum examination and ileal intubation rates were noted. In colonoscopies where trainees encountered technical difficulties during the procedure and were subsequently taken over by the consultant, the procedures were logged as performed by the consultant.

Statistical analysis

Data were collected and managed by using a statistical software program (SPSS version 20.0; SPSS Inc., IBM Corp., Armonk, NY, United States). Descriptive data were described in percentage, mean and median. Categorical data were analyzed using a two-tailed χ^2 test.

RESULTS

During the 6-year study period, 194 colonoscopies were performed in the unit. Data on 17 procedures were incomplete and were excluded from analysis. Of the remaining 177 colonoscopies, 56 were repeated procedures. Thus, 121 patients who had 177 colonoscopies were analyzed. The results are presented in two parts: (1) indications, colonoscopic findings and diagnosis of 121 patients who had first colonoscopy; and (2) quality indicators of 177 colonoscopies performed.

Volume of procedures

There was a steady increase in the number of colonoscopies performed each year during the study period (Figure 1). On average, 30 colonoscopies were performed each year during the study period, ranging from 19 procedures per year in the first 2 years to 58 procedures in 2015. Among the procedures, 15% (27/177) were logged as performed by consultants, while the remaining 85% (150/177) were performed

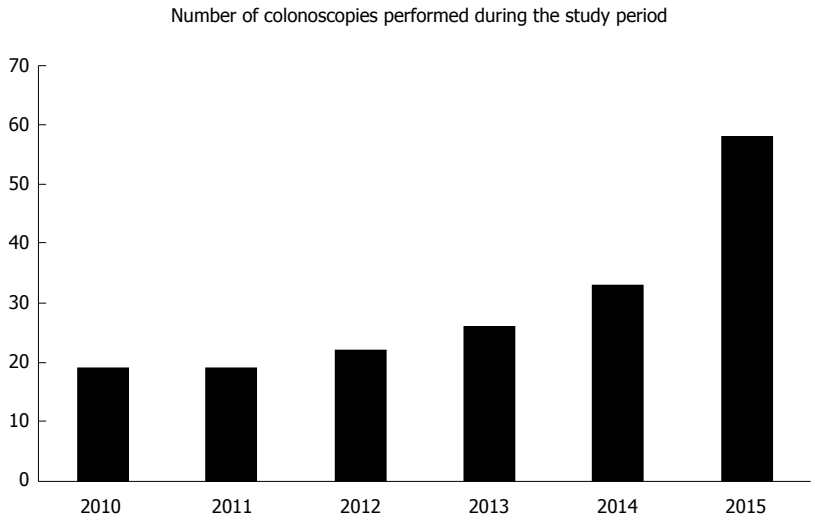

Figure 1 Number of colonoscopies performed each year during the study period.

by trainees supervised by a consultant.

Epidemiology, demographic features in 121 patients

There was a male preponderance (males = 74, 61%) in the 121 patients who had first colonoscopy (Table 1). The median (± SD) age was 7.5 (± 4.5) years. Eighty-one (67%) patients also had concomitant esophago-gastro-duodenoscopy (EGDS).

Indications for first colonoscopy in 121 patients

The most common indication was confirming the diagnosis of IBD (36/121, 30%; Table 1). Others were investigation of anemia or rectal bleeding (25/121, 21%). Investigation of abdominal pain was the indication in 17% (21/121). Most of the repeat colonoscopies were for disease assessment in IBD.

Colonoscopic findings in 121 patients

A positive finding was noted in 68 (56.2%) colonoscopies, while the remaining 53 (43.8%) had a normal colonoscopic finding. Indications for colonoscopy for the 53 patients with a negative finding were: excluding IBD (n = 18); disease assessment of pre-existing IBD (n = 4); assessment of abdominal pain (n = 8); ascertainment of lower gastrointestinal bleeding (n = 10); and, miscellaneous (n = 13).

Diagnosis in 121 patients

In addition to 16 patients who had colonoscopic assessment of preexisting IBD, a new clinical diagnosis or institution of new therapeutic measures was made in another 87 patients following colonoscopy. Thus, a total of 103 patients had a positive diagnosis. The diagnostic yield was 85%.

The colonoscopic diagnoses are shown in Table 1. Overall, 50 (41%) patients had a diagnosis of IBD (newly diagnosed, n = 34; diagnosis confirmed elsewhere, n = 16; Figure 2). Of these, 30 patients had CD and 20 had ulcerative colitis, respectively. Another 22 (18%) patients had focal inflammation of the rectum (IBD-unclassified) or solitary rectal ulcer syndrome.

Trend for diagnosis of IBD in 121 patients

The number of new cases of IBD seen in the unit during the study period is shown in Figure 2. There was an increasing trend in the number of new IBD cases, especially for CD.

Sedation and anesthesia in 177 colonoscopies

Vast majority (165/177, 93.2%) of the procedures were performed under general anesthesia. The remaining 12 procedures (6.8%) were performed under sedation, being administered by anesthetist. No major events related to anesthesia or sedation were observed during the study period.

Bowel preparation in 177 colonoscopies

Bowel preparation was judged to be good by the endoscopist in 87% (155/177) of the patients, moderate in 0.6% (1/177) and bad in 12% (21/177) patients.

Cecum and terminal ileum intubation in 177 colonoscopies

Information on the extent of colonoscopy was available in all 177 procedures (Table 1). The overall ileal intubation rate was 54.2% (96/177). Cecum was examined in an additional 22.0% (39/177). Thus, the cecum was reached in 76.3% (135/177) of patients. The extents of colonoscopy of the remaining 42 procedures are shown in Table 1.

In 36 patients, full colonoscopic examination and ileal intubation were not intended. They were not indicated in 18 cases, including those for confirmation or surveillance of graft-versus-host disease (n = 10), confirmation of rectal metastasis (n = 2), tissue biopsy for malabsorption (1 each for food protein-induced

Table 1 Indications, diagnoses and quality indicators in 121 children who had 177 colonoscopies

	n	%
Sex, males	74	61
Age in yr, median ± SD	7.5 ± 4.5	
Concomitant esophagogastroduodenoscopy	81	67
Indications, *n* = 121[1]		
Suspected of inflammatory bowel disease, new patients	36	30
Per rectal bleeding/investigations of anemia	25	21
Investigation of gastrointestinal symptoms	21	17
Assessment of inflammatory bowel disease, diagnosed elsewhere	16	13
Suspected of colonic polyps	7	6
Exclusion of graft-versus-host disease or colonic malignancies	7	6
Assessment of failure to thrive/malabsorption	4	3.3
Others	10	8
Colonoscopic diagnosis, *n* = 121		
Crohn's disease	30	25
Ulcerative colitis	20	17
Non-specific colitis or solitary rectal ulcer syndrome	22	18
Infective colitis	9	7
Colonic polyps	8	7
Graft-versus-host disease	5	4
Malabsorption	2	2
Allergic colitis	2	2
Miscellaneous diagnosis	5	4
No diagnosis	18	15
Extent of colonoscopic examination, 177 colonoscopies		
Terminal ileum	96	54
Cecum	38	21
Ascending colon	9	5
Transverse colon	13	7
Descending colon	12	7
Sigmoid colon	7	4
Rectum	1	0.6
Reached cecum but no terminal ileum intubation	134	76
Ileal intubation not intended, 177 colonoscopies[2]	36	
Not indicated	18	
Distorted anatomy due to previous surgery	1	
External stricture	2	
Previous colostomy in Crohn's disease	4	
Large polyp at rectum	2	
Risk of perforation outweighs benefit of full examination due to Severe colitis	5	
Poor bowel preparation	4	
Full colonoscopic examination intended, 177 colonoscopies[2]	141	
Ileal intubation	96	68
Cecum examination	134	95

[1]Some patients had more than one indication; [2]Not intended include not indicated, not feasible or the risks of full examination outweigh the benefit of full examination.

enterocolitis syndrome and autoimmune enteropathy), trichuriasis (*n* = 2), and assessment of previously confirmed solitary rectal ulcer syndrome (*n* = 2). Risk of perforation was judged to outweigh benefit of full examination in 5 patients. All had IBD with severe colitis and friable mucosal wall (ulcerative colitis, *n* = 3; CD, *n* = 2). Poor bowel preparation prevented a complete examination in 4 patients. A large rectal polyp obstructing the lumen (*n* = 1) and excessive bleeding in a patient with a large rectal polyp (*n* = 1) prevented a complete colonoscopy in 2 patients.

Of the remaining 141 patients in whom inspection of the terminal ileum was intended, the cecum examination and ileal intubation rates were 95.0% (134/141) and 68.1% (96/141), respectively. Overall, 45.8% of colonoscopies did not include an inspection of terminal ileum, and 31.9% did not reach terminal ileum when it was intended. Similarly, 24.3% of the procedures did not reach the cecum, and 5.0% failed to reach cecum when it was intended.

Factors affecting complete examination

Rate of complete examination was not significantly affected by the age of patients [ileal intubation rate; < 5 years (35/141) *vs* ⩾ 5 years (106/141) = 62.9% *vs* 69.8%; *P* = 0.44]. However, the ileal intubation rate was significantly higher when the indication for the colonoscopy was for the diagnosis or assessment of

Table 2 Colonoscopic performance by trainees

	Trainee A	Trainee	Trainee C	Trainee D	Average
Duration of training in mo	18	18	24	18	19.5
Number of colonoscopies performed during training period	19	17	44	36	29
Number of colonoscopies where intubation of terminal ileum was intended	16	13	39	28	24
Intubation of terminal ileum	12 (75)	10 (77)	34 (87)	18 (64)	77%
Examination of cecum and terminal ileum	16 (100)	13 (100)	38 (97)	26 (93)	97%

Data are presented as *n* or *n* (%), unless otherwise indicated. Note: In colonoscopies where trainees encountered technical difficulties during the procedure and were subsequently taken over by the consultant, the procedures were logged as performed by the consultant.

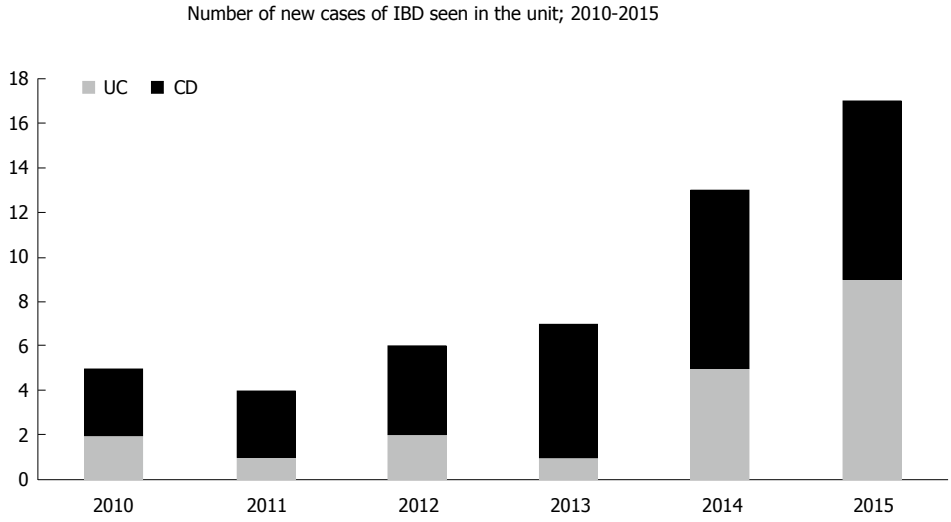

Figure 2 Number of new cases of pediatric inflammatory bowel disease seen in the unit during the study period. CD: Crohn's disease; IBD: Inflammatory bowel disease; UC: Ulcerative colitis.

IBD (73.0% *vs* 50%; $P = 0.016$).

Performance by trainees

During the study period, four trainees completed a minimum of 12-mo training in pediatric colonoscopy in the unit (Table 2). Part of the training period of another three trainees fell outside the study period and were not included in the analysis. The average number of colonoscopies performed was 29. The overall cecum examination rate was 97%, while the overall ileal intubation rate was 77%. There was a consistent performance by the trainees (Table 2).

Complications in 177 colonoscopies

A 7-year-old boy with CD who had gross delay in referral, severe malnutrition and severe mucosal ulcerations had iatrogenic perforation of the colon during the procedure. The patient had an uneventful recovery after colostomy and repair. Another patient with rectal polyp developed bleeding while it was removed during colonoscopy. The bleeding stopped after cauterization. No blood transfusion was required. No other complications were noted in the remaining 175 procedures, either associated with the procedure, anesthesia or sedation.

DISCUSSION

To the best of our knowledge, the present study is the first of its kind on performance benchmarked against established quality indicators in pediatric colonoscopy from a center where the volume of colonoscopy is low. During the study period, the number of colonoscopies performed in the center each year ranged from 19 to 58, with an average of 30. It was conducted in a setting with a low but rapidly increasing incidence of IBD.

Our results reveal that of the five quality indicators which were benchmarked against, the performance was high in four indicators. Most of the indications for colonoscopy performed in the unit were appropriate, following the recommendations of ESGE guidelines. Performances were good in bowel preparation, patient safety and complications. The cecum examination rate reached the expected rate at 95% by NASPGHAN, but was somewhat limited in ileal intubation rate at 68.1%. The performance of all trainees was consistently good in cecum examination but variable in ileal intubation.

There are several important implications on the results of the present study. Firstly, the indications for colonoscopies in the present study were mostly appropriate according to established guidelines[4]. The overall diagnostic yield was 85%. Previously, we observed that 99.7% of all EGDS and colonoscopies performed in the unit were appropriate[18]. The most common indications for colonoscopy were diagnosing or assessing IBD and ascertaining the cause of anemia. There was an increasing trend in the number of newly-diagnosed IBD cases during the study period. Investigation of abdominal symptoms, mainly abdominal pain, was the indication in only 17% of the patients[4].

In adult colonoscopy, screening for colon cancer is the main quality indicator[19]. Surrogate measures, such as colonic adenoma detection and complete examination of the colon, have been found to correlate with high-quality colonoscopy[20]. Pediatric colonoscopy, on the other hand, is fundamentally a different procedure with different indications, technical requirement, and different quality indicators[21]. The most important difference between adult and pediatric colonoscopies are the size of the patients and indications[21].

Screening for IBD is an important indication in pediatric colonoscopy. Differentiating between ulcerative colitis and CD is important in the diagnosis of IBD. Thus, examination of the cecum and terminal ileum are important quality indicators in pediatric colonoscopy[22]. In particular, intubation of the terminal ileum and sampling biopsy is essential for confirming the diagnosis of CD[23,24]. Pediatric endoscopy training guidelines suggest the cecal intubation rate to be at least 90% to 95%, with a comparable terminal ileum intubation rate[16,19].

Based on these quality indicators, the performances of centers vary. In Australia where screening for IBD was the major indication for colonoscopy, the reported cecum and ileal examination rates were 96.3% and 92.4%, respectively[5]. In Taiwan, the reported ileal intubation rate was 77.5%, while in China it was 81.7%[8,9]. The ileal intubation rates in the multicenter consortium review from the United States ranged from 30% to 90%[16].

After excluding procedures where either complete colonoscopy was not indicated, unsafe or not feasible, the cecum examination and ileal intubation rates in the present study were 95% and 68.1%, respectively. The cecum examination was comparable to the NASPGHAN pediatric gastroenterology training guidelines[19], but the ileal intubation rate was somewhat lower. Nevertheless, these figures were comparable with those reported in the region and the United States multicenter consortium study[8,16].

Bowel preparation was noted to be good in the majority of the cases (87%). Colonic perforation was observed in 1 patient who had severe long-standing CD prior to referral. The perforation rate was 0.5%. We reported two perforations in 66 colonoscopies previously[18].

The present study showed that all the trainees have a satisfactory cecum intubation rate, although the ileal intubation rate needs to be improved. To achieve cecal intubation examination and ileal intubation rate of 90%-95%, NASPGHAN guidelines for training in pediatric gastroenterology recommended 120 colonoscopies for pediatric trainees[19]. In this center, each trainee performed about 12-20 colonoscopies in children each year during their training. Before starting pediatric colonoscopy under supervision, the trainees were required to undergo training in adult colonoscopy, performing at least 50 colonoscopies in adult patients.

The implication of this is that the trainees would not have adequate training opportunity of reaching the recommended 120 colonoscopies in pediatric colonoscopy if the entire training was spent in this unit alone. Trainees spent between 18 mo to 24 mo of training in this center. The trainees usually start the training in endoscopic procedures with the adult gastroenterologists before being allowed to perform pediatric colonoscopy. The final year of the training is usually spent in a center of excellence for training in Australia or United Kingdom, where there is abundant opportunity for pediatric colonoscopy. Thus, even though the ileal intubation rate of the trainees noted in the present study did not reach the intended goal suggested by the NASPGHAN training guidelines[19], it is expected that their performance will be enhanced further once the oversea training is completed.

Another potential way to enhance colonoscopic skills is simulated colonoscopy training[25]. Studies involving trainees in adult colonoscopy showed improved performances during patient-based colonoscopy[25]. However, to date, no such study has been published involving training in pediatric colonoscopy.

Other important quality indicators which were not included in the present study were documentation of American Society of Anesthesiologist Physical Status Classification System (ASA) risk assessment and procedure duration. ASA risk assessment was routinely checked by the anesthetist. It was documented separately but was not captured in the present study. Additional potential measures of high-quality pediatric colonoscopy which have been mentioned but not included in this study are minimization of air insufflation, ease of patient sedation, duration of procedure, performance of mucosal biopsy sampling, patient recovery time and ongoing procedural competency assessment[22].

An obvious limitation to this study is its retrospective nature. The data was only collected from one center. However, our center is the only training center for pediatric gastroenterology in the whole country; we are unable to benchmark our performance against other centers. Nevertheless, with the exception of a somewhat lower ileal intubation rate, the performance in other quality indicators is excellent.

In conclusion, there is an increasing trend in the number of colonoscopies performed each year in this center. This is due to the increasing number of newly-diagnosed IBD cases during the study period. The performance of pediatric colonoscopy in this center was excellent in four of the five quality indicators benchmarked. The ileal intubation rate needs to be improved. A period of training in a center with a large volume of IBD will enhance the skills and performance of colonoscopy among the trainees of pediatric gastroenterology in Malaysia.

ARTICLE HIGHLIGHTS

Research background

The incidence of inflammatory bowel disease is on the rise worldwide, including in Asia. The gold standard for the diagnosis of inflammatory bowel disease is histologic confirmation from tissue biopsies obtained during esophago-gastro-duodenoscopy and colonoscopy. In particular, differentiating Crohn' s disease from ulcerative colitis is dependent upon inspection and biopsy of the terminal ileum. Thus, intubation of the terminal ileum is considered as an important quality indicator in pediatric colonoscopy. Current guidelines by the North American Society of Pediatric Gastroenterology, Hepatology and Nutrition recommend the cecum examination and terminal ileum of 95%. This target should be used by pediatric gastroenterology centers worldwide to benchmark their performance.

Research motivation

Current literature showed that reported ileal intubation rate in pediatric colonoscopy from centers around Asia ranged from 75.6% to 77.5%. The performance of our unit, from an area where the incidence of inflammatory bowel disease is currently low but is on the rise, is unknown. Thus, we were motivated to benchmark our performance against current recommendation to identify areas for improvement to enhance the quality of our training program.

Research objectives

The main objective was to benchmark the performance of our unit, in particular the completeness of colonoscopic examination, *i.e.* cecal examination and ileal intubation, against current recommended guidelines. We also evaluated other indicators such as appropriateness of indications, level of bowel preparation, as well as safety and complications of the procedures encountered.

Research methods

We conducted a retrospective analysis on all the pediatric colonoscopies performed in a pediatric gastroenterology training center in Malaysia over a period of 6 years. We included the following indicators: appropriateness of indications; quality of bowel preparation; safety and complications; as well as cecal examination and terminal ileum intubation rates. The performances of trainees in the cecal and ileal examination rates were ascertained separately.

Research results

We found that of the 177 colonoscopies performed, the diagnostic yield was 85%, quality of bowel preparation was good in 87%, while one of 177 procedures was complicated by perforation during the procedure. The overall cecum examination rate was 76.3% and ileal intubation rate was 54.2%. After excluding colonoscopy where full colonoscopic examination was either not indicated, not feasible because of poor bowel preparation or unsafe (severe colitis), the cecum examination rate was 95.0% and ileal intubation rate was 68.1%. Among four trainees who completed a minimum of 12 mo training, the overall cecum rate was 97% while the overall ileal intubation rate was 77%. The performance of all trainees was consistent. Thus, the cecum examination rate of our unit was satisfactory but the rate of terminal ileum intubation needs further improvement. To improve the rate of ileal intubation, the trainees would spend part of their training program in a center of excellence with adequate volume of pediatric colonoscopy.

Research conclusions

The present study was the first attempt by a pediatric gastroenterology unit in Asia to benchmark its performance in pediatric colonoscopy against established international guidelines. Our study suggests that such a benchmark is both applicable and desirable. The study allows our unit to identify areas for further improvement. Trainees from our unit now routinely spend part of their training in a center of excellence to enhance their skills in colonoscopy.

Research perspectives

Benchmarking against established guidelines has been adopted as part of quality assurance of our unit. We plan to conduct a prospective study to include other indicators of good practice not included in this retrospective review. These include anesthetic risk assessment, duration of procedure, ease of sedation, quality of mucosal biopsy sampling and patient recovery time.

REFERENCES

1 **Teague RH**, Salmon PR, Read AE. Fibreoptic examination of the colon: a review of 255 cases. *Gut* 1973; **14**: 139-142 [PMID: 4540492]

2 **Hassall E**, Barclay GN, Ament ME. Colonoscopy in childhood. *Pediatrics* 1984; **73**: 594-599 [PMID: 6718114]

3 **ASGE Standards of Practice Committee**, Lightdale JR, Acosta R, Shergill AK, Chandrasekhara V, Chathadi K, Early D, Evans JA, Fanelli RD, Fisher DA, Fonkalsrud L, Hwang JH, Kashab M, Muthusamy VR, Pasha S, Saltzman JR, Cash BD; American Society for Gastrointestinal Endoscopy. Modifications in endoscopic practice for pediatric patients. *Gastrointest Endosc* 2014; **79**: 699-710 [PMID: 24593951 DOI: 10.1016/j.gie.2013.08.014]

4 **Thomson M**, Tringali A, Dumonceau JM, Tavares M, Tabbers MM, Furlano R, Spaander M, Hassan C, Tzvinikos C, Ijsselstijn H, Viala J, Dall'Oglio L, Benninga M, Orel R, Vandenplas Y, Keil R, Romano C, Brownstone E, Hlava Š, Gerner P, Dolak W, Landi R, Huber WD, Everett S, Vecsei A, Aabakken L, Amil-Dias J, Zambelli A. Paediatric Gastrointestinal Endoscopy: European Society for Paediatric Gastroenterology Hepatology and Nutrition and European Society of Gastrointestinal Endoscopy Guidelines. *J Pediatr Gastroenterol Nutr* 2017; **64**: 133-153 [PMID: 27622898 DOI: 10.1097/MPG.0000000000001408]

5 **Singh HK**, Withers GD, Ee LC. Quality indicators in pediatric colonoscopy: an Australian tertiary center experience. *Scand J Gastroenterol* 2017; **52**: 1453-1456 [PMID: 28936881 DOI: 10.1080/00365521.2017.1380224]

6 **Wahid AM**, Devarajan K, Ross A, Zilbauer M, Heuschkel R. Paediatric gastrointestinal endoscopy: a qualitative study. *Eur J Gastroenterol Hepatol* 2016; **28**: 25-29 [PMID: 26473298 DOI: 10.1097/MEG.0000000000000488]

7 **Lee YW**, Chung WC, Sung HJ, Kang YG, Hong SL, Cho KW, Kang D, Lee IH, Jeon EJ. Current status and clinical impact of pediatric endoscopy in Korea. *Korean J Gastroenterol* 2014; **64**: 333-339 [PMID: 25530584]

8 **Wu CT**, Chen CA, Yang YJ. Characteristics and Diagnostic Yield of Pediatric Colonoscopy in Taiwan. *Pediatr Neonatol* 2015; **56**: 334-338 [PMID: 25850637 DOI: 10.1016/j.pedneo.2015.01.005]

9 **Lei P**, Gu F, Hong L, Sun Y, Li M, Wang H, Zhong B, Chen M, Cui Y, Zhang S. Pediatric colonoscopy in South China: a 12-year experience in a tertiary center. *PLoS One* 2014; **9**: e95933 [PMID: 24759776 DOI: 10.1371/journal.pone.0095933]

10 **Tam YH**, Lee KH, Chan KW, Sihoe JD, Cheung ST, Mou JW. Colonoscopy in Hong Kong Chinese children. *World J Gastroenterol* 2010; **16**: 1119-1122 [PMID: 20205284 DOI: 10.3748/wjg.v16.i9.1119]

11 **Ruel J**, Ruane D, Mehandru S, Gower-Rousseau C, Colombel JF. IBD across the age spectrum: is it the same disease? *Nat Rev*

Gastroenterol Hepatol 2014; **11**: 88-98 [PMID: 24345891 DOI: 10.1038/nrgastro.2013.240]

12 **Ng SC**, Tang W, Ching JY, Wong M, Chow CM, Hui AJ, Wong TC, Leung VK, Tsang SW, Yu HH, Li MF, Ng KK, Kamm MA, Studd C, Bell S, Leong R, de Silva HJ, Kasturiratne A, Mufeena MN, Ling KL, Ooi CJ, Tan PS, Ong D, Goh KL, Hilmi I, Pisespongsa P, Manatsathit S, Rerknimitr R, Aniwan S, Wang YF, Ouyang Q, Zeng Z, Zhu Z, Chen MH, Hu PJ, Wu K, Wang X, Simadibrata M, Abdullah M, Wu JC, Sung JJ, Chan FK; Asia–Pacific Crohn's and Colitis Epidemiologic Study (ACCESS) Study Group. Incidence and phenotype of inflammatory bowel disease based on results from the Asia-pacific Crohn's and colitis epidemiology study. *Gastroenterology* 2013; **145**: 158-165.e2 [PMID: 23583432 DOI: 10.1053/j.gastro.2013.04.007]

13 **Malmborg P**, Hildebrand H. The emerging global epidemic of paediatric inflammatory bowel disease--causes and consequences. *J Intern Med* 2016; **279**: 241-258 [PMID: 26355194 DOI: 10.1111/joim.12413]

14 **Hilmi I**, Jaya F, Chua A, Heng WC, Singh H, Goh KL. A first study on the incidence and prevalence of IBD in Malaysia--results from the Kinta Valley IBD Epidemiology Study. *J Crohns Colitis* 2015; **9**: 404-409 [PMID: 25744112 DOI: 10.1093/ecco-jcc/jjv039]

15 **Walsh CM**, Ling SC, Mamula P, Lightdale JR, Walters TD, Yu JJ, Carnahan H. The gastrointestinal endoscopy competency assessment tool for pediatric colonoscopy. *J Pediatr Gastroenterol Nutr* 2015; **60**: 474-480 [PMID: 25564819 DOI: 10.1097/MPG.0000000000000686]

16 **Thakkar K**, Holub JL, Gilger MA, Shub MD, McOmber M, Tsou M, Fishman DS. Quality indicators for pediatric colonoscopy: results from a multicenter consortium. *Gastrointest Endosc* 2016; **83**: 533-541 [PMID: 26253014 DOI: 10.1016/j.gie.2015.06.028]

17 **Levine A**, Koletzko S, Turner D, Escher JC, Cucchiara S, de Ridder L, Kolho KL, Veres G, Russell RK, Paerregaard A, Buderus S, Greer ML, Dias JA, Veereman-Wauters G, Lionetti P, Sladek M, Martin de Carpi J, Staiano A, Ruemmele FM, Wilson DC; European Society of Pediatric Gastroenterology, Hepatology, and Nutrition. ESPGHAN revised porto criteria for the diagnosis of inflammatory bowel disease in children and adolescents. *J Pediatr Gastroenterol Nutr* 2014; **58**: 795-806 [PMID: 24231644 DOI: 10.1097/MPG.0000000000000239]

18 **Lee WS**, Zainuddin H, Boey CC, Chai PF. Appropriateness, endoscopic findings and contributive yield of pediatric gastrointestinal endoscopy. *World J Gastroenterol* 2013; **19**: 9077-9083 [PMID: 24379634 DOI: 10.3748/wjg.v19.i47.9077]

19 **Leichtner AM**, Gillis LA, Gupta S, Heubi J, Kay M, Narkewicz MR, Rider EA, Rufo PA, Sferra TJ, Teitelbaum J; NASPGHAN Training Committee; North American Society for Pediatric Gastroenterology. NASPGHAN guidelines for training in pediatric gastroenterology. *J Pediatr Gastroenterol Nutr* 2013; **56** Suppl 1: S1-S8 [PMID: 23263531 DOI: 10.1097/MPG.0b013e31827a78d6]

20 **Rex DK**. Quality in colonoscopy: cecal intubation first, then what? *Am J Gastroenterol* 2006; **101**: 732-734 [PMID: 16635220 DOI: 10.1111/j.1572-0241.2006.00483.x]

21 **Rex DK**. Colonoscopy. *Gastrointest Endosc* 2013; **78**: 444-449 [PMID: 23948194 DOI: 10.1016/j.gie.2013.06.025]

22 **Kay M**, Wyllie R. It's all about the loop: quality indicators in pediatric colonoscopy. *Gastrointest Endosc* 2016; **83**: 542-544 [PMID: 26897046 DOI: 10.1016/j.gie.2015.08.058]

23 **Sawczenko A**, Sandhu BK. Presenting features of inflammatory bowel disease in Great Britain and Ireland. *Arch Dis Child* 2003; **88**: 995-1000 [PMID: 14612366]

24 **Batres LA**, Maller ES, Ruchelli E, Mahboubi S, Baldassano RN. Terminal ileum intubation in pediatric colonoscopy and diagnostic value of conventional small bowel contrast radiography in pediatric inflammatory bowel disease. *J Pediatr Gastroenterol Nutr* 2002; **35**: 320-323 [PMID: 12352520]

P- Reviewer: Choi YS **S- Editor**: Gong ZM **L- Editor**: Filipodia **E- Editor**: Huang Y

World Journal of Gastroenterology

Submit a Manuscript: http://www.f6publishing.com

World J Gastroenterol 2018 March 7; 24(9): 1022-1034

DOI: 10.3748/wjg.v24.i9.1022

ISSN 1007-9327 (print) ISSN 2219-2840 (online)

ORIGINAL ARTICLE

Retrospective Study

Prognostic value of lymph nodes count on survival of patients with distal cholangiocarcinomas

Hua-Peng Lin, Sheng-Wei Li, Ye Liu, Shi-Ji Zhou

Hua-Peng Lin, Sheng-Wei Li, Department of Hepatobiliary Surgery, The Second Affiliated Hospital of Chongqing Medical University, Chongqing 400010, China

Ye Liu, Department of Neonatal, Children's Hospital Chongqing Medical University, Chongqing 400016, China

Shi-Ji Zhou, Department of Gastrointestinal Surgery, The Second Affiliated Hospital of Chongqing Medical University, Chongqing 400010, China

ORCID number: Hua-Peng Lin (0000-0002-8632-0069); Sheng-Wei Li (0000-0002-9748-8190); Ye Liu (0000-0002-8077-2961); Shi-Ji Zhou (0000-0002-2145-0786).

Author contributions: Zhou SJ and Lin HP conducted the analyses and wrote the manuscript; all other authors contributed to the idea of the manuscript and approved the final version.

Supported by the National Natural Science Foundation of China, No. 81301975; and the Chongqing Natural Science Foundation, No. cstc2016jcyjA016.

Institutional review board statement: This article does not contain any studies with human participants or animals performed by any of the authors.

Informed consent statement: As this study is based on a publicly available database without identifying patient information, informed consent was not needed.

Conflict-of-interest statement: All authors declare no conflicts-of-interest related to this article.

Data sharing statement: No additional data are available.

Manuscript source: Unsolicited manuscript

Correspondence to: Shi-Ji Zhou, MD, PhD, Doctor, Surgeon, Surgical Oncologist, Department of Gastrointestinal Surgery, The Second Affiliated Hospital of Chongqing Medical University, 74 Linjiang Road, Yuzhong District, Chongqing 400010, China. zhoushiji@hospital.cqmu.edu.cn
Telephone: +86-23-63693626
Fax: +86-23-63693533

Received: December 23, 2017
Peer-review started: December 23, 2017
First decision: January 17, 2018
Revised: January 30, 2018
Accepted: February 8, 2018
Article in press: February 8, 2018
Published online: March 7, 2018

Abstract

AIM

To evaluate the prognostic value of the number of retrieved lymph nodes (LNs) and other prognostic factors for patients with distal cholangiocarcinomas, and to determine the optimal retrieved LNs cut-off number.

METHODS

The Surveillance, Epidemiology and End Results database was used to screen for patients with distal cholangiocarcinoma. Patients with different numbers of retrieved LNs were divided into three groups by the X-tile program. X-tile from Yale University is a useful tool for outcome-based cut-point optimization. The Kaplan-Meier method and Cox regression analysis were utilized for survival analysis.

RESULTS

A total of 449 patients with distal cholangiocarcinoma met the inclusion criteria. The Kaplan-Meier survival analysis for all patients and for N1 patients revealed no significant differences among patients with different retrieved LN counts in terms of overall and cancer-specific survival. In patients with node-negative distal cholangiocarcinoma, patients with four to nine retrieved LNs had a significantly better overall (P = 0.026) and cancer-specific survival (P = 0.039) than others. In the subsequent multivariate analysis, the number of retrieved LNs was evaluated to be independently associated with survival. Additionally, patients with four to nine retrieved LNs had a significantly lower overall mortality risk [hazard ratio (HR) = 0.39; 95% confidence interval (CI): 0.20-0.74] and cancer cause-specific mortality risk (HR = 0.32; 95%CI: 0.15-0.66) than other patients. Additionally, stratified survival analyses showed persistently better overall and cancer-specific survival when retrieving four to nine LNs in patients with any T stage of tumor, a tumor between 20 and 50 mm in diameter, or a poorly differentiated or undifferentiated tumor, and in patients who were $\leqslant$ 70-years-old.

CONCLUSION

The number of retrieved LNs was an important independent prognostic factor for patients with node-negative distal cholangiocarcinoma. Additionally, patients with four to nine retrieved LNs had better overall and cancer-specific survival rates than others, but the reason and mechanism were unclear. This conclusion should be validated in future studies.

Key words: Distal cholangiocarcinomas; Lymph node count; Survival analysis; SEER

Core tip: The prognostic value of retrieved lymph node (LN) counts is still under debate for patients with distal cholangiocarcinomas. The aim of the present study was to evaluate the prognostic value of the number of retrieved lymph nodes and other prognostic factors for patients with distal cholangiocarcinomas and to determine the optimal retrieved LNs cut-off number. A total of 449 patients with distal cholangiocarcinoma were included in this study. The univariate and multivariate analyses revealed that the number of retrieved LNs was independently associated with survival. And, patients with four to nine retrieved LNs had a better overall and cancer-specific survival rate than others.

Lin HP, Li SW, Liu Y, Zhou SJ. Prognostic value of lymph nodes count on survival of patients with distal cholangiocarcinomas. *World J Gastroenterol* 2018; 24(9): 1022-1034 Available from: URL: http://www.wjgnet.com/1007-9327/full/v24/i9/1022.htm
DOI: http://dx.doi.org/10.3748/wjg.v24.i9.1022

INTRODUCTION

Cholangiocarcinoma constitutes approximately 15% of hepatobiliary tumors and 3% of gastrointestinal tumors[1]. According to its anatomic location, cholangiocarcinoma is classified as intrahepatic, perihilar or distal malignancy. Distal cholangiocarcinoma comprise approximately 30% of all cholangiocarcinoma; it is a relatively uncommon disease. The only optimal treatment for distal cholangiocarcinoma is surgical resection, as a result of the insensitivity of cholangiocarcinoma to radiation and chemotherapy[2]. Additionally, complete tumor resection of distal cholangiocarcinoma always relies on pancreaticoduodenectomy, which is a complicated operation with high morbidity and mortality[3]. Hence, the postoperative prognosis of patients with distal cholangiocarcinoma has attracted great interest in several studies[4,5]. Lymph node (LN) status was determined to be a strong predictor for the prognosis of patients with distal cholangiocarcinoma[6]. Patients without LN metastasis had a better prognosis than those with LN involvement. Thus, an adequate number of retrieved LNs is vital to distinguish N0 patients from N1 ones. The appropriate cut-off of retrieved LNs counts should be determined.

Currently, the number of LNs that should be retrieved is still under debate. Several studies evaluated the prognostic value of retrieved LN counts and tried to determine the benchmark number of examined LNs[6-9]. Nevertheless, most of them were designed retrospectively with a small sample size, and cases that met their inclusion criteria comprised both perihilar and distal cholangiocarcinomas. The differences in biological and pathological features, as well as surgical strategies and prognoses, between perihilar and distal cholangiocarcinomas lead to a different influence of retrieving LN counts on survival.

The American Joint Committee on Cancer (AJCC) staging system suggested a different appropriate number of retrieved LNs for perihilar and distal cholangiocarcinomas. For distal cholangiocarcinoma, the number that AJCC suggested was 12. However, this suggestion lacks verification because the retrieved LN counts in most previous studies did not reach 12. Additionally, in the study of Kawai *et al*[10], patients with more than 12 retrieved LNs only had a moderately better survival rate than patients with a smaller number of retrieved LNs in a univariate analysis, not a multivariate analysis. A subgroup study of Kiriyama *et al*[11], using a cohort of N0 patients, found that patients with more than 10 retrieved LNs had a better survival. This subgroup analysis was based on a small sample

size with a univariate analysis, and the cancers of the involved cases were all stages Ⅰ and Ⅱ. Therefore, the appropriate cut-off number of retrieved LNs is still unconfirmed.

Our study was performed to evaluate the interactions between the number of retrieved LNs and the prognosis of patients with distal cholangiocarcinoma; additionally, this study determined the appropriate retrieved LN cut-off number. To obtain a larger sample size, the Surveillance, Epidemiology and End Results (SEER) database was used for the selection of patients with at least one retrieved LN.

MATERIALS AND METHODS

Data source

SEER is a public dataset that collects survival and incidence data of various types of cancers and covers more than 25% of the United States' population. SEER data include tumor characteristics such as primary tumor site, TNM staging of tumor, tumor size, type of treatment and cause of death, and demographic characteristics such as race of patients, age of diagnosis, sex, *etc*. Our study used the latest 11 years' data from SEER (from 2004-2014). We downloaded the data from SEER with SEER*Stat Software (version 8.3.4; https://seer.cancer.gov/seerstat/).

Patients

Our study was designed to be a retrospective study. The inclusion criteria were (1) patients greater than 20 years in age; (2) patients diagnosed with distal cholangiocarcinoma according to the term "006-BileDuctsDistal" of "CS SCHEMA v0204+"; (3) patients with histology code of 8010, 8020, 8070, 8140, 8144, 8160, 8162, 8163, 8260, 8480, 8490 or 8560; (4) patients with diagnoses that were not confirmed by a death certificate or autopsy; (5) patients with active follow-up; (6) patients from a time span of 2004 to 2014 according to the term "year of diagnosis"; (7) patients with only one tumor who had survived more than 1 mo; (8) patients without distant metastasis (the M0 patients); (9) patients who received intent surgery in terms of the combination of "Surg Prim Site" and "Reason no cancer-directed surgery"; (10) patients who did not receive preoperative radiotherapy according to the terms of "Radiation" and "Surg/Rad Seq"; and (11) patients with at least one retrieved LN according to the terms "Regional Nodes Examined". Demographics of patients such as race, age at diagnosis and marital status, and tumor characteristics such as tumor size, laterality of tumor, grade and stage of tumor were all extracted for subsequent analysis. The terms "SEER cause-specific death classification" and "SEER other cause of death classification" were used to distinguish our two endpoints: all-cause mortality and cancer cause-specific mortality.

Statistical analysis

Statistical analyses were conducted with SPSS (version 23.0; IBM Corp., Armonk, NY, United States). The demographic data of patients were compared by *t* tests (for continuous variables) and chi-square tests (for proportion variables). A *P*-value of < 0.05 was defined to be statistically significant. Patients with different numbers of retrieved LNs were divided into three groups.

The cut-off number of retrieved LNs for grouping was determined by the X-tile program (http://www.tissuearray.org/rimmlab/). X-tile from Yale University is a useful tool for outcome-based cut-point optimization. The strategies of the X-tile program for grouping included that it would try each number between the range of the retrieved LN counts as the cut-off; then, the χ^2 score and *P*-value were calculated with this number as the cut-off[12,13]. Eventually, the number with a maximum χ^2 score and a minimum *P*-value would be suggested to be the final cut-off.

The Kaplan-Meier method (univariate analysis) with log-rank tests and Cox regression analysis (multivariate analysis) were utilized for survival analysis. The overall survival and cancer-specific survival were compared between patients with the different categories of retrieved LNs counts. Then, we performed stratified survival analyses for the number of retrieved LNs, in terms of the confounders that were evaluated to be independently associated with survival in the multivariate analysis.

RESULTS

Patient and demographics details

A total of 449 patients with distal cholangiocarcinoma (2004-2014) met the inclusion criteria for this research. The majority of them were white and male. The distributions of age and the diagnosis year were averaged. Nearly 70% of the patients were married. The size of the tumor was less than 50 mm in most patients. Patient and tumor characteristics are shown in Table 1.

The retrieved LN counts ranged from one to sixty-three. More than half of the patients had > 10 LNs retrieved, and 22.7% of patients had > 20 LNs retrieved. There were 226 N0 patients and 223 N1 patients. Most patients underwent extensive surgery and postoperative chemotherapy; the number of patients who received adjuvant radiotherapy was less.

Impact of the number of retrieved LNs on survival rates

We divided patients with different numbers of retrieved LNs into three groups, by use of the X-tile program. Then, the retrieved LN count was converted from continuous variables into categorical variables to study its impact on survival. As shown in Figure 1, the cut-off numbers for grouping in all patients were 3 and 6, the

Table 1 Characteristics of patients and tumors

Variable	No. of patients, *n* (%) of *n* = 449
Race	
White	321 (71.5)
Black	35 (7.8)
Other	93 (20.7)
Sex	
Male	286 (63.7)
Female	163 (36.3)
Age at diagnosis, in yr	
⩽ 60	128 (28.5)
60-70	171 (38.1)
> 70	150 (33.4)
Marital status	
Married	302 (67.3)
Divorced	33 (7.3)
Separated or single	58 (12.9)
Widowed	40 (8.9)
Unknown	16 (3.6)
Year of diagnosis	
2004-2010	110 (24.5)
2011-2012	160 (35.6)
2013-2014	179 (39.9)
Tumor size, in mm	
⩽ 20	203 (45.2)
20-50	191(42.5)
> 50	15 (3.3)
Unknown	40 (8.9)
Grade	
Well differentiated	54 (12.0)
Moderately differentiated	204 (45.4)
Poorly differentiated	158 (35.2)
Undifferentiated	3 (0.7)
Unknown	30 (6.7)
Stage	
Ⅰ A	44 (9.8)
Ⅰ B	60 (13.7)
Ⅱ A	89 (19.8)
Ⅱ B	161 (35.9)
Ⅲ	95 (21.2)
T stage	
T1	49 (10.9)
T2	85 (18.9)
T3	220 (49.0)
T4	95 (21.2)
pN stage	
pN0	226 (50.3)
pN1	223 (49.7)
Surgery type	
Local excision	102 (22.7)
Extensive surgery	347 (77.3)
Adjuvant radiotherapy	
No/Unknown radiotherapy	298 (66.3)
Beam radiation	151 (33.7)
Adjuvant chemotherapy	
No/Unknown chemotherapy	204 (45.4)
Chemotherapy performed	245 (54.6)
No. of LNs retrieved	
1-10	196 (43.7)
11-20	151 (33.6)
> 20	102 (22.7)

LNs: Lymph nodes.

cut-off numbers for N0 patients were 4 and 9, and the cut-off numbers for N1 patients were 4 and 16.

In the Kaplan-Meier survival analysis, no significant difference was observed among the three categories of retrieved LN counts for all and N1 patients with distal cholangiocarcinomas. For patients with node-negative distal cholangiocarcinomas, there was a significantly better overall and cancer-specific survival in patients with 4-9 retrieved LNs than in patients with 1-3 or > 9 retrieved LNs. Additionally, we compared overall and cancer-specific survival among each number of retrieved LNs. Because of space limitations, we could only put part of the results into the table (Table 2).

There was a similar trend of survival rate as the retrieved LN count increased in all, N0 and N1 patients; patients with seven retrieved LNs had the best survival rate compared with the others. In N0 patients, patients with seven or nine retrieved LNs had a significantly higher survival rate compared with other patients; this result was confirmed in analysis regarding retrieved LN counts as categorical variables.

Survival analyses in all patients and patients with node-negative distal cholangiocarcinoma

The results of survival analysis for all patients in the present study were similar to previous studies. As shown in Figure 1 and Table 3, retrieved LN counts were not associated with survival in all patients (P = 0.233). Factors such as tumor size and T and N stages that were significant in univariate analysis were entered into a multivariate model. N stage was shown to be independently associated with overall survival [hazard ratio (HR) = 1.40; 95% confidence interval (CI): 1.05-1.86]. In terms of cancer-specific survival, T stage [(HR = 1.45; 95%CI: 1.02-2.07)] was shown to be an independent risk factor of survival, along with N stage (HR = 1.42; 95%CI: 1.05-1.92).

For N0 patients, univariate analysis showed that retrieved LN counts, age at diagnosis, and grade of tumor were associated with overall survival. After those factors were entered into multivariate analysis, retrieved LN counts and grade of tumor were determined to be independent risk factors of overall survival. Patients with four to nine retrieved LNs had a significantly lower all-cause mortality risk than other patients (HR = 0.39; 95%CI: 0.20-0.74). In terms of cancer-specific survival, tumor size, grade of tumor, T stage and retrieved LN counts were evaluated to be associated with survival in both univariate and multivariate analyses. There was a significant decrease in terms of cancer cause-specific mortality risk (HR = 0.32; 95%CI: 0.15-0.66) for patients with four to nine retrieved LNs (Table 4).

Stratified analyses for the number of retrieved LNs in patients with node-negative distal cholangiocarcinoma

To further study the interactions between retrieved LN counts and prognoses of patients with node-negative distal cholangiocarcinoma, we performed survival analysis stratified by size, grade, T stage of tumor and age of patients. For patients ⩽ 70-years-old, retrieving four to nine LNs resulted in a significantly

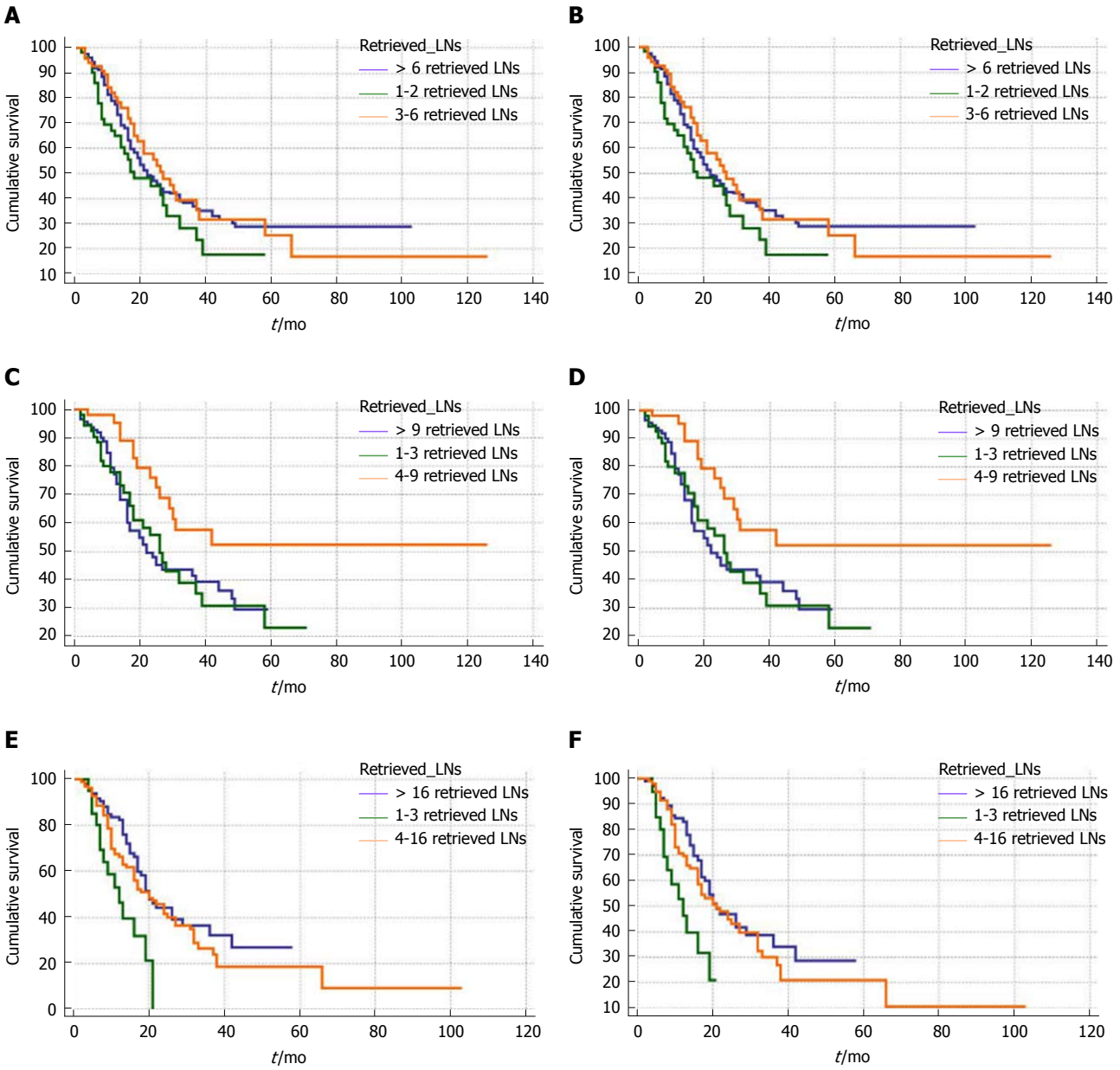

Figure 1 Kaplan-Meier survival curves of all patients in terms of (A) overall survival and (B) cancer-specific survival. There was no significant difference in terms of overall survival (P = 0.233) and cancer-specific survival (P = 0.141) among the three groups. Kaplan-Meier survival curves of patients with node-negative distal cholangiocarcinoma in terms of (C) overall survival and (D) cancer-specific survival. Patients with four to nine retrieved LNs had a better overall (P = 0.026) and cancer-specific (P = 0.008) survival than patients with one to three retrieved LNs and patients with more than nine retrieved LNs. Kaplan-Meier survival curves of N1 patients in terms of (E) overall survival and (F) cancer-specific survival. There was no significant difference in terms of overall survival (P = 0.053) and cancer-specific survival (P = 0.0564) among the three groups. LNs: Lymph nodes.

better survival rate than retrieving one to three LNs in terms of overall survival (Figure 2A) and cancer-specific survival (Figure 3A). Additionally, no significant difference between patients with one to three retrieved LNs and > 9 retrieved LNs in terms of overall and cancer-specific survival was observed.

Subsequently, the above results were confirmed in multivariate survival analyses after adjusting for all confounders (Table 5). As shown in Figures 2 and 3 and Table 5, similar results were found for patients with any T stage of tumor, tumor size between 20 and 50 mm, and tumors that were poorly defined or undifferentiated. The prognostic effect of retrieved LN counts was not present when analyses were limited to well or moderately differentiated tumors, tumors $\leqslant$ 20 mm, and patients greater than 70 years in age.

DISCUSSION

Nodal status is a well-studied indicator for the prognosis of patients with distal cholangiocarcinoma. In addition to the stage of LNs, the prognostic value of positive node counts and lymph node ratios has been evaluated in several studies[6,10,11]. While the prognostic value of the number of retrieved LNs is still under debate, the optimal cut-off number of retrieved LNs

Table 2 Impact of the number of retrieved LNs on survival rates

Retrieved LNs counts	No.	3-yr OS	95%CI	3-yr CSS	95%CI
For all patients					
1	26	29.51%	10.90-51.07	29.51%	10.90-51.07
3	23	35.33%	13.50-58.23	43.64%	18.10-66.88
5	18	46.55%	16.40-72.36	51.20%	17.95-77.03
7	22	63.31%	35.24-81.81	63.31%	35.24-81.84
9	16	57.29%	27.94-78.40	66.20%	32.37-86.00
11	16	37.09%	11.27-63.72	40.46%	12.19-67.77
13	11	28.41%	4.52-59.96	28.41%	4.52-59.96
15	13	16.46%	0.90-50.11	16.46%	0.90-50.11
17	15	15.80%	0.82-49.22	17.01%	0.84-51.90
19	9	34.29%	4.81-68.55	34.29%	4.81-68.55
21	12	47.62%	19.35-71.52	47.62%	19.35-71.52
23	5	33.86%	5.73-66.35	33.86%	5.73-66.35
25	15	37.50%	9.37-66.61	37.50%	9.37-66.61
For N0 patients					
1	17	40.38%	14.15-65.68	40.38%	14.15-65.68
3	18	43.65%	17.20-67.68	47.01%	18.51-71.34
5	11	30.00%	1.23-71.92	37.50%	1.10-80.80
7	16	76.15%	42.67-91.65	76.15%	42.67-91.65
9	5	66.67%	5.41-94.52	66.67%	5.41-94.52
11	9	50.79%	15.67-78.07	59.26%	18.59-84.95
13	4	37.50%	1.10-80.80	37.50%	1.10-80.80
15	6	26.67%	0.97-68.61	26.67%	0.97-68.61
17	4	-	-	-	-
19	2	-	-	-	-
21	6	55.56%	7.34-87.61	55.56%	7.34-87.61
23	1	-	-	-	-
25	7	42.00%	7.01-75.34	52.50%	8.42-84.55
For N1 patients					
1	9	14.29%	0.71-46.49	14.29%	0.71-46.49
3	5	33.33%	0.90-77.41	33.33%	0.90-77.41
5	7	53.57%	13.20-82.50	53.57%	13.20-82.50
7	6	55.56%	7.34-87.61	55.56%	7.34-87.61
9	11	45.00%	13.88-72.41	58.33%	18.02-84.41
11	7	25.00%	1.23-64.59	25.00%	1.23-64.59
13	7	41.67%	5.60-76.65	41.67%	5.60-76.65
15	7	35.71%	1.41-77.98	35.71%	1.41-77.98
17	11	17.05%	0.84-51.92	18.94%	0.87-55.82
19	7	26.67%	0.97-68.61	26.67%	0.97-68.61
21	6	43.64%	11.29-72.96	43.64%	11.29-72.96
23	4	-	-	-	-
25	8	28.57%	4.11-61.15	28.57%	4.11-61.15

CI: Confidence interval; CSS: Cancer-specific survival; LNs: Lymph nodes; OS: Overall survival.

is also unconfirmed. Several studies of other diseases revealed the difference in retrieved LNs' influence on survival between N0 and N1 patients[8,14,15]. Nevertheless, for N0 patients, more LNs retrieved significantly improved survival. Therefore, studies of distal cholangiocarcinoma on retrieved LN counts should be performed in a cohort of N0 patients for whom the prognostic value of retrieved LN counts has never been systematically studied.

Our study screened 449 patients with distal cholangiocarcinoma in a population-based database; a total of 226 patients with node-negative distal cholangiocarcinoma were among them. Retrieved LN counts did not show its prognostic value in the whole cohort and N1 patients. However, in patients with node-negative distal cholangiocarcinoma, patients with four to nine retrieved LNs were determined to have a significantly better prognosis than patients with $\leqslant$ 3 retrieved LNs in terms of overall and cancer-specific survivals. Additionally, tumor size, grade and T stage of tumor were evaluated to be independent risk factors of cancer-specific survival. Therefore, retrieving at least four LNs would be optimal for patients with node-negative distal cholangiocarcinoma.

More retrieved LNs could promote the accuracy of LNs staging to avoid the under-staging effect, thus to improve survival of patients with distal cholangiocarcinoma. Studies on cholangiocarcinoma demonstrated there were micrometastases in approximately 5% of LNs which were diagnosed as negative nodes[16]. The more LNs that were resected and retrieved meant less micrometastases were left, therefore the survival of patients with more retrieved LNs counts could be improved. Additionally, more retrieved LNs represented adequate surgical, pathological and institutional care[17]. What's more, anatomic studies determined that more

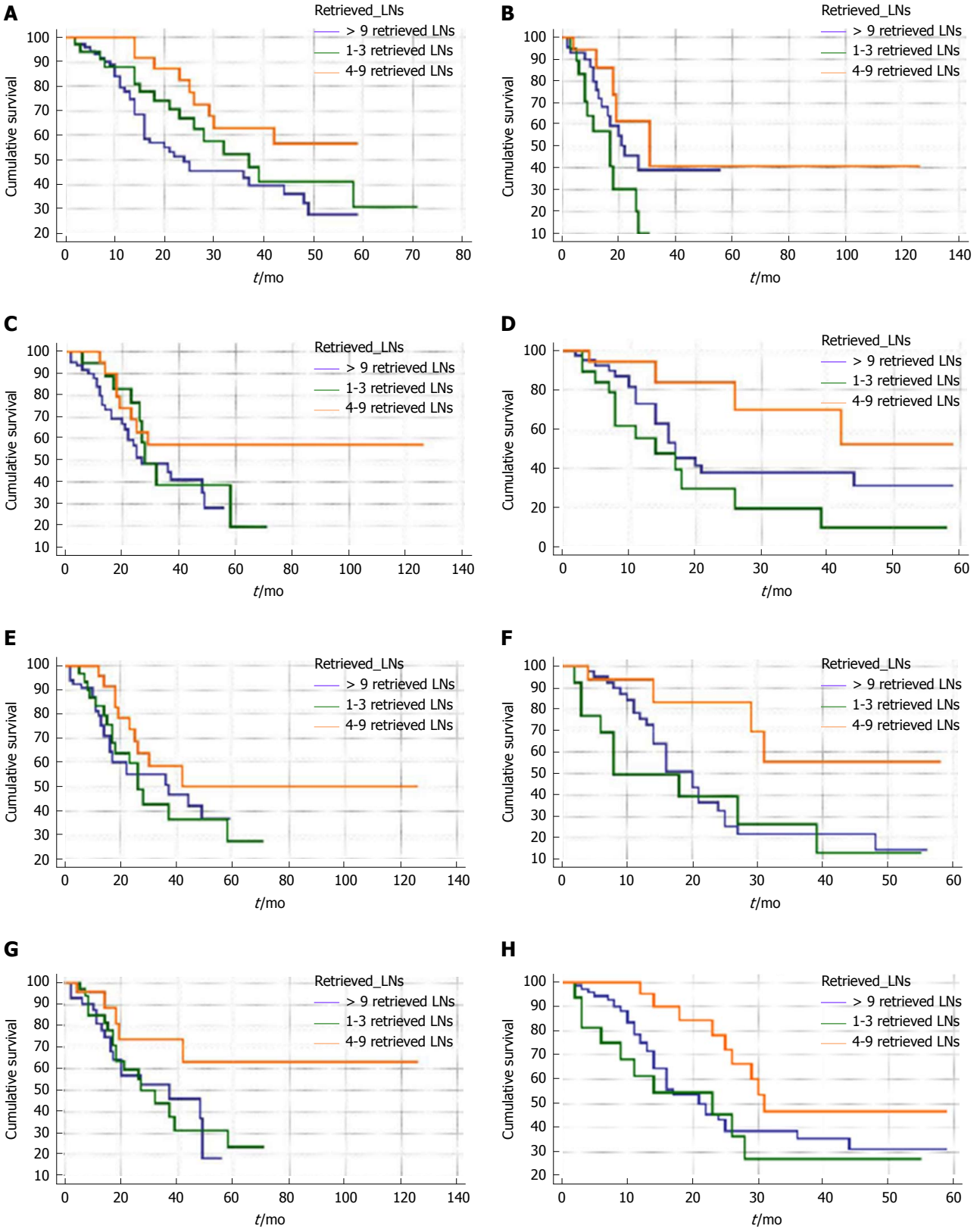

Figure 2 Kaplan-Meier survival curves of stratified analyses in (A) patients ⩽ 70-years-old, (B) > 70-years-old, (C) with tumors of ⩽ 20 mm, (D) with tumors of 20 to 50 mm, (E) with tumors defined as well or moderately differentiated, (F) with tumors defined as poorly or undifferentiated, (G) with tumors of T1/T2 stage, and (H) with tumors of T3/T4 stage in terms of overall survival. Patients with four to nine retrieved LNs had a significantly better overall survival than patients with one to three retrieved LNs and patients with more than nine retrieved LNs in the group of patients ⩽ 70-years-old (P = 0.029), with tumors of 20 to 50 mm (P = 0.018), with tumors defined as poorly or undifferentiated (P = 0.030), and with tumors of T3/T4 stage (P = 0.041). LNs: Lymph nodes.

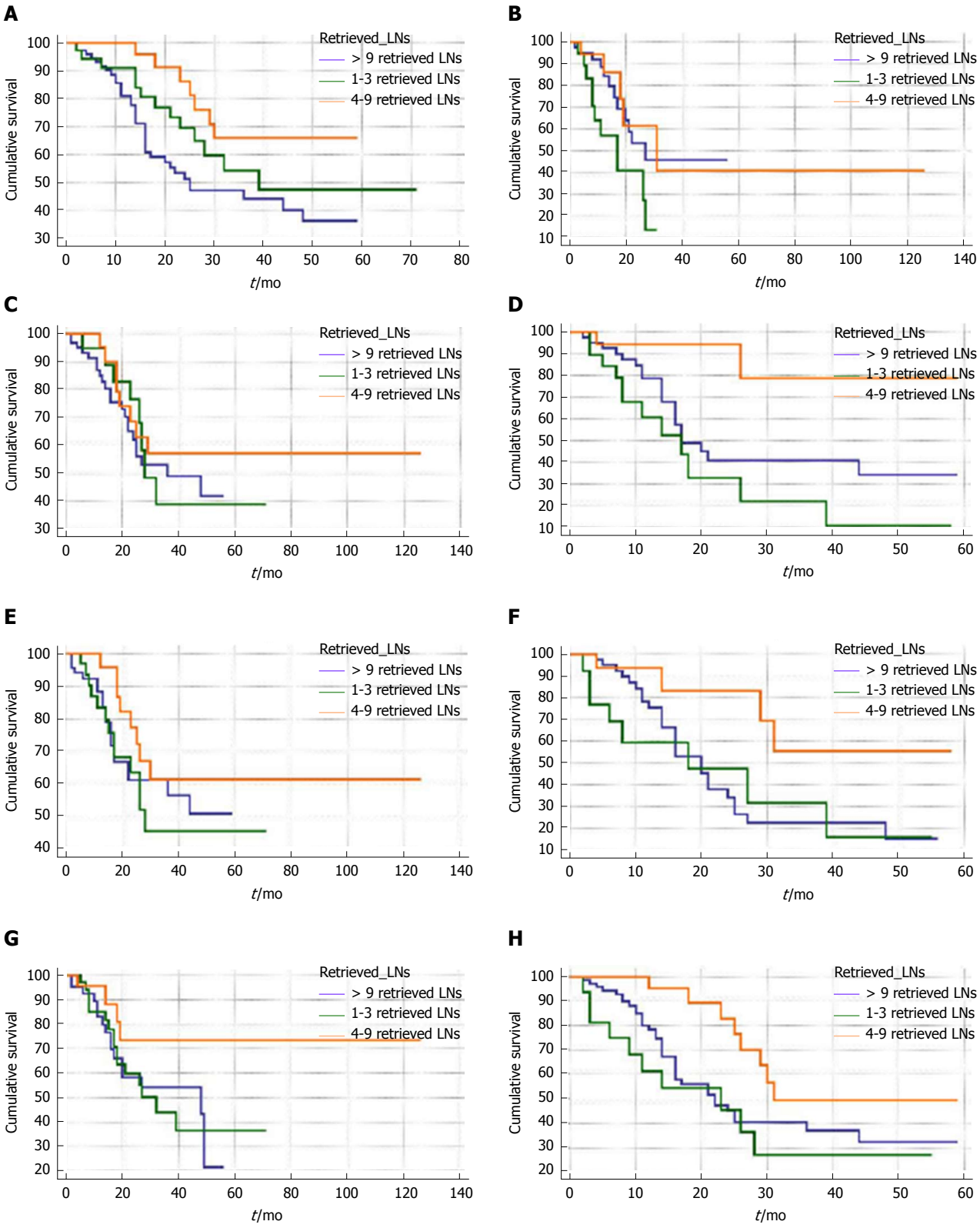

Figure 3 Kaplan-Meier survival curves of stratified analyses in (A) patients ⩽ 70-years-old, (B) > 70-years-old, (C) with tumors of ⩽ 20 mm, (D) with tumors of 20 to 50 mm, (E) with tumors defined as well or moderately differentiated, (F) with tumors defined as poorly or undifferentiated, (G) with tumors of T1/T2 stage, and (H) with tumors of T3/T4 stage in terms of cancer-specific survival. Patients with four to nine retrieved LNs had a significantly better cancer-specific survival than patients with one to three retrieved LNs and patients with more than nine retrieved LNs in the group of patients ⩽ 70-years-old (P = 0.025), with tumors of 20 to 50 mm (P = 0.0.006), with tumors defined as poorly or undifferentiated (P = 0.049), and with tumors of T3/T4 stage (P = 0.041). LNs: Lymph nodes.

Table 3 Univariate and multivariate survival analyses of factors associated with overall and cancer-specific survival of all patients with distal cholangiocarcinoma

Variables	Overall survival					Cancer-specific survival				
	Univariate analysis			Multivariate analysis		Univariate analysis			Multivariate analysis	
	3-yr OS	χ^2	*P* value	HR (95%CI)	*P* value	3-yr OS	χ^2	*P* value	HR (95%CI)	*P* value
Race		2.22	0.329				1.95	0.377		
White	33.3%					36.1%				
Black	34.8%					36.9%				
Other	38.9%					42.1%				
Sex		0.44	0.507				0.54	0.463		
Male	35.3%					38.3%				
Female	37.7%					40.9%				
Age at diagnosis, in yr		1.89	0.387				0.48	0.783		
⩽ 60	31.2%					35.8%				
60-70	39.1%					41.4%				
> 70	30.7%					36.8%				
Marital status		5.02	0.285				5.98	0.201		
Married	37.3%					39.6%				
Divorced	-					-				
Separated or single	31.4%					35.3%				
Widowed	34.1%					-				
Unknown	-									
Year of diagnosis		1.82	0.402				3.25	0.197		
2004-2010	37.3%					41.4%				
2011-2012	30.9%					33.2%				
2013-2014	-					-				
Tumor size, in mm		8.04	0.045		0.230		8.76	0.032		0.249
⩽ 20	40.8%			Reference		44.0%			Reference	
20-50	29.9%			1.25 (0.94-1.67)		33.2%			1.23 (0.91-1.68)	
> 50	0.0%			1.67 (0.86-3.23)		0.0%			1.76 (0.91-3.43)	
Unknown	37.7%			0.95 (0.57-1.58)		46.3%			0.96 (0.56-1.65)	
Grade		6.77	0.079				6.92	0.074		
Well differentiated	48.6%					52.4%				
Moderately differentiated	32.6%					38.9%				
Poorly or undifferentiated	30.3%					32.6%				
Unknown	43.2%					43.2%				
T stage		5.57	0.018		0.270		11.16	< 0.001		0.037
T1/T2	44.3%			Reference		51.6%			Reference	
T3/T4	29.6%			1.19 (0.87-1.64)		32.6%			1.45 (1.02-2.07)	
N stage		10.64	0.001		0.020		12.27	< 0.001		0.022
N0	44.5%			Reference		47.4%			Reference	
N1	26.9%			1.40 (1.05-1.86)		30.3%			1.42 (1.05-1.92)	
Surgery type		1.20	0.272				0.73	0.393		
Local excision	44.0%					45.3%				
Extensive surgery	34.4%					37.9%				
Adjuvant radiotherapy		0.16	0.683				0.79	0.372		
No/Unknown radiotherapy	39.9%					44.3%				
Beam radiation	29.5%					30.5%				
Adjuvant chemotherapy		1.10	0.293				2.92	0.087		
No/Unknown chemotherapy	41.2%					47.5%				
Chemotherapy performed	32.2%					33.3%				
No. of LNs retrieved		2.91	0.233				3.90	0.141		
1-2	23.6%					29.9%				
3-6	35.6%					39.4%				
> 6	36.0%					39.0%				

CI: Confidence interval; HR: Hazard ratio; LNs: Lymph nodes; OS: Overall survival.

resected LNs could improve the underlying tumor-host interactions and reset the immunological balance to improve survival[18].

The AJCC system suggested the optimal number of retrieved LNs of patients with distal cholangiocarcinoma should be 12. Whereas study of Sasaki *et al*[6] demonstrated there was no difference between patients with ⩾ 12 retrieved LNs and < 12 retrieved LNs in terms of overall survival. A subgroup analysis in the study of Kiriyama *et al*[11] revealed that patients with stage Ⅰ or Ⅱ tumors who had more than 10 LNs retrieved had a better survival rate than others. While 83.2% of patients in their study retrieved more than 12 LNs, the number of patients with < 10 retrieved LNs was very small (n = 22), and their results were based on a univariate analysis. Therefore, selection

Table 4 Univariate and multivariate survival analyses of factors associated with overall and cancer-specific survival of patients with node-negative distal cholangiocarcinoma

Variable	Overall survival					Cancer-specific survival				
	Univariate analysis			Multivariate analysis		Univariate analysis			Multivariate analysis	
	3-yr OS	χ^2	*P* value	HR (95%CI)	*P* value	3-yr OS	χ^2	*P* value	HR (95%CI)	*P* value
Race		0.82	0.663				0.13	0.939		
White	44.3%					46.8%				
Black	49.4%					49.4%				
Other	40.4%					44.0%				
Sex		1.32	0.250				0.77	0.377		
Male	39.5%					46.0%				
Female	47.0%					49.8%				
Age at diagnosis, in yr		3.85	0.049		0.056		2.73	0.097		
≤ 70	49.8%			Reference		51.8%				
> 70	31.4%			1.51 (0.98-2.33)		35.7%				
Marital status		6.30	0.177				6.52	0.163		
Married	42.9%					48.5%				
Divorced	-					-				
Separated or single	31.8%					39.6%				
Widowed	46.9%					46.9%				
Unknown	-					-				
Year of diagnosis		3.41	0.181				4.05	0.131		
2004-2010	50.0%					52.1%				
2011-2012	36.5%					41.4%				
2013-2014	48.8%					54.0%				
Tumor size, in mm		7.47	0.058				9.11	0.027		0.036
≤ 20	47.3%					49.6%			Reference	
20-50	36.9%					40.0%			1.57 (0.98-2.53)	
> 50	0.0%					0.0%			3.08 (1.16-8.21)	
Unknown	46.8%					60.8%			0.72 (0.30-1.71)	
Grade		9.65	0.021		0.014		12.56	0.005		0.003
Well differentiated	56.8%			Reference		63.3%			Reference	
Moderately differentiated	43.5%			1.59 (0.84-2.99)		51.8%			1.44 (0.70-2.97)	
Poorly or undifferentiated	26.0%			2.35 (1.24-4.46)		30.5%			2.90 (1.43-5.88)	
Unknown	57.0%			0.76 (0.27-2.16)		57.0%			1.14 (0.37-3.50)	
T stage		1.35	0.244				4.63	0.031		0.030
T1/T2	48.7%					58.4%			Reference	
T3/T4	37.1%					38.7%			1.69 (1.05-2.71)	
Surgery type		0.10	0.748				0.23	0.631		
Local excision	45.7%					48.2%				
Extensive surgery	44.1%					47.0%				
Adjuvant radiotherapy		1.64	0.199				1.53	0.215		
No/Unknown radiotherapy	48.2%					53.2%				
Beam radiation	35.5%					37.2%				
Adjuvant chemotherapy		1.31	0.251				1.48	0.222		
No/Unknown chemotherapy	46.3%					53.8%				
Chemotherapy performed	38.5%					42.1%				
No. of LNs retrieved		7.24	0.026		0.013		6.47	0.039		0.008
1-3	35.1%			Reference		40.9%			Reference	
4-9	52.3%			0.39 (0.20-0.74)		60.0%			0.32 (0.15-0.66)	
> 9	39.3%			0.85 (0.53-1.36)		44.9%			0.62 (0.36-1.07)	

CI: Confidence interval; CSS: Cancer-specific survival; HR: Hazard ratio; LNs: Lymph nodes; OS: Overall survival.

bias should be kept in mind when interpreting their results. The fact that retrieving more than 10 or 12 LNs is an indicator of better prognosis is still disputable.

The present study denoted that retrieving more than nine LNs did not indicate a better prognosis in patients with node-negative distal cholangiocarcinoma, but an increase in terms of all-cause mortality risk and cancer cause-specific mortality risk was observed compared with retrieving four to nine LNs. For patients with distal cholangiocarcinoma, retrieving too many LNs did not obtain better outcomes. This result was contrary to the prevailing dogma that a better prognosis was always associated with higher retrieved LN counts.

There were several hypotheses for the reason why more retrieved LNs represented a worse prognosis. Necrosis represented an aggressive biology of tumor and a decreased survival rate; it had a close association with LN hyperplasia. LN hyperplasia always resulted in increases in the size and number of detectable LNs; therefore, more retrieved LNs (detectable LNs) were related to a worse prognosis[19-21]. The other hypothesis was that there might be a difference at the molecular level between tumors with more and less detectable LNs. Tumors with more detectable LNs, *i.e.*

Table 5 Stratified analyses of overall and cancer-specific survival according to the number of retrieved LNs for N0 patients

Variable	4-9 retrieved LNs (1-3 retrieved LNs as the reference)				> 9 retrieved LNs (1-3 retrieved LNs as the reference)			
	Overall survival		Cancer-specific survival		Overall survival		Cancer-specific survival	
	HR (95%CI)	*P* value	HR (95%CI)	*P* value	HR (95%CI)	*P* value	HR (95%CI)	*P* value
Age, in yr								
≤ 70	0.33 (0.13-0.86)	0.023	0.34 (0.13-0.89)	0.030	1.02 (0.49-2.14)	0.940	0.93 (0.46-1.88)	0.848
> 70	0.32 (0.11-0.98)	0.047	0.33 (0.11-1.04)	0.059	0.63 (0.26-1.49)	0.294	0.40 (1.55-1.04)	0.059
Tumor size, in mm								
≤ 20	0.55 (0.21-1.46)	0.232	0.61 (0.22-1.68)	0.340	1.34 (0.60-2.97)	0.472	0.96 (0.41-2.23)	0.921
20-50	0.22 (0.07-0.69)	0.010	0.12 (0.03-0.55)	0.007	0.54 (0.24-1.21)	0.134	0.48 (0.21-1.12)	0.090
> 50	-	-	-	-	-	-	-	-
Grade								
Well or moderately differentiated	0.56 (0.24-1.30)	0.180	0.47 (0.18-1.20)	0.114	0.99 (0.49-2.01)	0.994	0.74 (0.34-1.62)	0.454
Poorly or undifferentiated	0.23 (0.07-0.79)	0.020	0.26 (0.07-0.89)	0.032	0.69 (0.31-1.58)	0.389	0.75 (0.32-1.78)	0.514
T stage								
T1/T2	0.30 (0.11-0.85)	0.024	0.30 (0.09-0.94)	0.039	0.79 (0.39-1.59)	0.501	0.76 (0.36-1.59)	0.467
T3/T4	0.34 (0.13-0.85)	0.022	0.31 (0.12-0.79)	0.016	0.66 (0.31-1.41)	0.285	0.65 (0.30-1.39)	0.267

CI: Confidence interval; HR: Hazard ratio; LNs: Lymph nodes.

more retrieved LNs, might belong to another subset of distal cholangiocarcinoma that acts biologically more aggressively[19]. Additionally, routine histologic techniques for retrieving LNs may ignore the micrometastases, leading to the under-staging of LNs. Hence, without the application of immunohistochemical techniques that was determined to increase the detection rate of micrometastases, more retrieved LNs could not promote the accuracy of LN staging or improve patient survival. And, we wanted to know if more retrieved LNs reflected extended lymphadenectomy that may result in increasing postoperative complications. However, because of the limitation of the SEER database, we could not compare the background data in the > 9 retrieved LNs group with that in four to nine retrieved LN groups.

There were several limitations in our study. First, although a population-based database was utilized to screen patients, the total number of patients involved in our study was still not large enough compared with congener studies for other diseases. Second, information for adjuvant chemotherapy and radiotherapy in survival analysis did not contain the details of the protocols, and the SEER database did not provide data. Third, disease-free survival could not be calculated because of the lack of information about local recurrence in the SEER. Fourth, patients who received preoperative radiation were excluded. There might be patients who received radiation in some other centers that were not recorded in the SEER, so the down-staging effect of radiation could not be entirely ruled out. Fifth, the number of lymph nodes retrieved may depend upon the type of surgical procedures. And, the lymph nodes distant from the lesion (for example, nodes from Whipple's procedure) may not have the same predicting value as these from local or limited resection specimen. However, the detailed operation methods were unknown because of the limitation of the SEER, *i.e.* we could not know how many patients underwent pancreatoduodenectomy or segmental bile duct resection. Sixth, the number of lymph nodes retrieved may rely on lymph node dissection skill in each individual institution (grossing by resident *vs* practicing pathologists or pathologist assistant). But, the SEER database only provided the information of the region where the patients were from, and the classes of hospital were unknown. Therefore, such institution bias should be taken into consideration when interpreting our results. Seventh, we could only compare survival among the groups of patients with four to nine lymph nodes and others based upon pathological stage and not clinical stage due to the limitation of SEER (the SEER database only provided the information of pathological stage for patients with resectable distal cholangiocarcinomas). Eighth, the AJCC staging system utilized in the present study was the 6th edition, which was not the most commonly used one nowadays (due to limitations of SEER). Finally, we could not get the data referring to the surgical margin status in SEER; surgical margin status was an important prognostic factor in patients with resected distal cholangiocarcinoma.

In conclusion, the number of retrieved LNs did not show its prognostic value in the whole group of patients (a mixture of N0 and N1 patients) and N1 patients. However, the number of retrieved LNs was an independent prognostic factor of overall and cancer-specific survival for patients with node-negative distal cholangiocarcinoma. Patients with four to nine retrieved LNs had better overall and cancer-specific survival rates than others, but the reason and mechanism were unclear. The future studies should consider more operation- and adjuvant therapy-related parameters into their analysis to evaluate our results.

ARTICLE HIGHLIGHTS

Research background

Lymph node (LN) status was determined to be a strong predictor for the prognosis of patients with distal cholangiocarcinoma. However, the prognostic

value of the retrieved LNs counts in distal cholangiocarcinoma is still under debate.

Research motivation

The benchmark number of retrieved LNs has been determined in many gastrointestinal carcinomas, in addition to the distal cholangiocarcinomas. Previous studies regarding the retrieved LNs counts in distal cholangiocarcinomas were limited by their small sample size, and the patients in those studies comprised both perihilar and distal cholangiocarcinomas. The present study tried to determine the interactions between the retrieved LNs counts and the prognosis in patients with only distal cholangiocarcinomas, and a population-based database was used for patients' selection that provided a sufficient sample size.

Research objectives

We aimed to evaluate the prognostic value of the number of retrieved LNs for patients with distal cholangiocarcinomas and to determine the optimal retrieved LNs cut-off number.

Research methods

The Surveillance, Epidemiology and End Results (SEER) database was used to screen for patients with distal cholangiocarcinoma. The retrieved LNs counts were transformed from continuous variables to categorical variables, and the cut-off was defined by the X-tile program. The overall and cancer-specific survival was compared between the different categories of retrieved LNs counts by the means of the Kaplan-Meier method and Cox regression analysis. Then, we performed stratified analyses by the clinical factors that were evaluated to be independently associated with survival in the Cox regression analysis, among patients within the different LNs groups.

Research results

A total of 449 patients with distal cholangiocarcinoma were included in the present study. The Kaplan-Meier survival analysis for all patients and for N1 patients revealed no significant differences among patients with different retrieved LN counts in terms of overall and cancer-specific survivals. In patients with node-negative distal cholangiocarcinoma, patients with four to nine retrieved LNs had a significantly better overall (P = 0.026) and cancer-specific (P = 0.039) survival than others. In the subsequent multivariate analysis, the number of retrieved LNs was evaluated to be independently associated with survival. Additionally, patients with four to nine retrieved LNs had a significantly lower overall mortality risk (hazard ratio (HR): 0.39; 95% confidence interval (CI): 0.20-0.74) and cancer cause-specific mortality risk (HR: 0.32; 95%CI: 0.15-0.66) than other patients. Additionally, stratified survival analyses showed persistent better overall and cancer-specific survival when retrieving four to nine LNs in patients with any T stage of tumor, a tumor between 20 and 50 mm in diameter, or a poorly differentiated or undifferentiated tumor and in patients who were $\leqslant$ 70-years-old.

Research conclusions

The number of retrieved LNs was an important independent prognostic factor for patients with node-negative distal cholangiocarcinoma. Additionally, patients with four to nine retrieved LNs had a better overall and cancer-specific survival rate than patients with less than four or more than nine retrieved LNs.

Research perspectives

Although our study revealed retrieving four to nine LNs in patients with node-negative distal cholangiocarcinoma had better overall and cancer-specific survival rates than others, the reason and mechanism for that were unclear. The future studies should consider more operation- and adjuvant therapy-related parameters into their analysis to evaluate our results.

REFERENCES

1 **Siegel R**, Naishadham D, Jemal A. Cancer statistics, 2012. *CA Cancer J Clin* 2012; **62**: 10-29 [PMID: 22237781 DOI: 10.3322/caac.20138]

2 **Komaya K**, Ebata T, Shirai K, Ohira S, Morofuji N, Akutagawa A, Yamaguchi R, Nagino M; Nagoya Surgical Oncology Group. Recurrence after resection with curative intent for distal cholangiocarcinoma. *Br J Surg* 2017; **104**: 426-433 [PMID: 28138968 DOI: 10.1002/bjs.10452]

3 **Gouma DJ**, van Geenen RC, van Gulik TM, de Haan RJ, de Wit LT, Busch OR, Obertop H. Rates of complications and death after pancreaticoduodenectomy: risk factors and the impact of hospital volume. *Ann Surg* 2000; **232**: 786-795 [PMID: 11088073 DOI: 10.1097/00000658-200012000-00007]

4 **Murakami Y**, Uemura K, Hayashidani Y, Sudo T, Hashimoto Y, Ohge H, Sueda T. Prognostic significance of lymph node metastasis and surgical margin status for distal cholangiocarcinoma. *J Surg Oncol* 2007; **95**: 207-212 [PMID: 17278119 DOI: 10.1002/jso.20668]

5 **Murakami Y**, Uemura K, Sudo T, Hashimoto Y, Nakashima A, Kondo N, Sakabe R, Ohge H, Sueda T. Prognostic factors after surgical resection for intrahepatic, hilar, and distal cholangiocarcinoma. *Ann Surg Oncol* 2011; **18**: 651-658 [PMID: 20945107 DOI: 10.1245/s10434-010-1325-4]

6 **Oshiro Y**, Sasaki R, Kobayashi A, Murata S, Fukunaga K, Kondo T, Oda T, Ohkohchi N. Prognostic relevance of the lymph node ratio in surgical patients with extrahepatic cholangiocarcinoma. *Eur J Surg Oncol* 2011; **37**: 60-64 [PMID: 21094016 DOI: 10.1016/j.ejso.2010.10.011]

7 **Schwarz RE**, Smith DD. Lymph node dissection impact on staging and survival of extrahepatic cholangiocarcinomas, based on U.S. population data. *J Gastrointest Surg* 2007; **11**: 158-165 [PMID: 17390167 DOI: 10.1007/s11605-006-0018-6]

8 **Ito K**, Ito H, Allen PJ, Gonen M, Klimstra D, D'Angelica MI, Fong Y, DeMatteo RP, Brennan MF, Blumgart LH, Jarnagin WR. Adequate lymph node assessment for extrahepatic bile duct adenocarcinoma. *Ann Surg* 2010; **251**: 675-681 [PMID: 20224368 DOI: 10.1097/SLA.0b013e3181d3d2b2]

9 **Pomianowska E**, Westgaard A, Mathisen Ø, Clausen OP, Gladhaug IP. Prognostic relevance of number and ratio of metastatic lymph nodes in resected pancreatic, ampullary, and distal bile duct carcinomas. *Ann Surg Oncol* 2013; **20**: 233-241 [PMID: 22893118 DOI: 10.1245/s10434-012-2592-z]

10 **Kawai M**, Tani M, Kobayashi Y, Tsuji T, Tabuse K, Horiuchi T, Oka M, Yamaguchi K, Sakata Y, Shimomura T, Yamaue H. The ratio between metastatic and examined lymph nodes is an independent prognostic factor for patients with resectable middle and distal bile duct carcinoma. *Am J Surg* 2010; **199**: 447-452 [PMID: 19596119 DOI: 10.1016/j.amjsurg.2009.01.019]

11 **Kiriyama M**, Ebata T, Aoba T, Kaneoka Y, Arai T, Shimizu Y, Nagino M; Nagoya Surgical Oncology Group. Prognostic impact of lymph node metastasis in distal cholangiocarcinoma. *Br J Surg* 2015; **102**: 399-406 [PMID: 25611179 DOI: 10.1002/bjs.9752]

12 **Xiao J**, Ye ZS, Wei SH, Zeng Y, Lin ZM, Wang Y, Teng WH, Chen LC. Prognostic significance of pretreatment serum carcinoembryonic antigen levels in gastric cancer with pathological lymph node-negative: A large sample single-center retrospective study. *World J Gastroenterol* 2017; **23**: 8562-8569 [PMID: 29358864 DOI: 10.3748/wjg.v23.i48.8562]

13 **Qureshi YA**, Sarker SJ, Walker RC, Hughes SF. Proximal Resection Margin in Ivor-Lewis Oesophagectomy for Cancer. *Ann Surg Oncol* 2017; **24**: 569-577 [PMID: 27573522 DOI: 10.1245/s10434-016-5510-y]

14 **Bagante F**, Tran T, Spolverato G, Ruzzenente A, Buttner S, Ethun CG, Groot Koerkamp B, Conci S, Idrees K, Isom CA, Fields RC, Krasnick B, Weber SM, Salem A, Martin RC, Scoggins C, Shen P, Mogal HD, Schmidt C, Beal E, Hatzaras I, Vitiello G, IJzermans JN, Maithel SK, Poultsides G, Guglielmi A, Pawlik TM. Perihilar Cholangiocarcinoma: Number of Nodes Examined and Optimal Lymph Node Prognostic Scheme. *J Am Coll Surg* 2016; **222**: 750-759.e2 [PMID: 27113512 DOI: 10.1016/j.jamcollsurg.2016.02.012]

15 **Mao K**, Liu J, Sun J, Zhang J, Chen J, Pawlik TM, Jacobs LK, Xiao Z, Wang J. Patterns and prognostic value of lymph node dissection for resected perihilar cholangiocarcinoma. *J Gastroenterol Hepatol* 2016; **31**: 417-426 [PMID: 26250532 DOI:

10.1111/jgh.13072]
16 **Mantel HT**, Wiggers JK, Verheij J, Doff JJ, Sieders E, van Gulik TM, Gouw AS, Porte RJ. Lymph Node Micrometastases are Associated with Worse Survival in Patients with Otherwise Node-Negative Hilar Cholangiocarcinoma. *Ann Surg Oncol* 2015; **22** Suppl 3: S1107-S1115 [PMID: 26178761 DOI: 10.1245/s10434-015-4723-9]
17 **Johnson PM**, Porter GA, Ricciardi R, Baxter NN. Increasing negative lymph node count is independently associated with improved long-term survival in stage IIIB and IIIC colon cancer. *J Clin Oncol* 2006; **24**: 3570-3575 [PMID: 16877723 DOI: 10.1200/jco.2006.06.8866]
18 **Zheng WF**, Ji TT, Lin Y, Li RZ. The prognostic value of lymph nodes count on survival of patients with node-negative gastric cancer. *Oncotarget* 2016; **7**: 43680-43688 [PMID: 27270656 DOI: 10.18632/oncotarget.9845]
19 **Mersin H**, Yildirim E, Bulut H, Berberoğlu U. The prognostic significance of total lymph node number in patients with axillary lymph node-negative breast cancer. *Eur J Surg Oncol* 2003; **29**: 132-138 [PMID: 12633555 DOI: 10.1053/ejso.2002.1285]
20 **Camp RL**, Rimm EB, Rimm DL. A high number of tumor free axillary lymph nodes from patients with lymph node negative breast carcinoma is associated with poor outcome. *Cancer* 2000; **88**: 108-113 [PMID: 10618612]
21 **Moorman PG**, Hamza A, Marks JR, Olson JA. Prognostic significance of the number of lymph nodes examined in patients with lymph node-negative breast carcinoma. *Cancer* 2001; **91**: 2258-2262 [PMID: 11413513]

P- Reviewer: Antonini F, Nah YW, Xu RL **S- Editor**: Wang XJ
L- Editor: Filipodia **E- Editor**: Huang Y

World Journal of Gastroenterology

Submit a Manuscript: http://www.f6publishing.com

World J Gastroenterol 2018 March 7; 24(9): 1035-1045

DOI: 10.3748/wjg.v24.i9.1035

ISSN 1007-9327 (print) ISSN 2219-2840 (online)

ORIGINAL ARTICLE

Clinical Practice Study

Phenotypic and genotypic characterization of inflammatory bowel disease in children under six years of age in China

You-Hong Fang, You-You Luo, Jin-Dan Yu, Jin-Gan Lou, Jie Chen

You-Hong Fang, You-You Luo, Jin-Dan Yu, Jin-Gan Lou, Jie Chen, Department of Gastroenterology, Children's Hospital, Zhejiang University School of Medicine, Hangzhou 310052, Zhejiang Province, China

ORCID number: You-Hong Fang (0000-0003-3686-1016); You-You Luo (0000-0002-0185-1371); Jin-Dan Yu (0000-0002-3390-1660); Jin-Gan Lou (0000-0001-9142-5378); Jie Chen (0000-0002-3603-3213).

Author contributions: Chen J, Fang YH and Luo YY designed the research; Fang YH, Luo YY, Yu JD, Lou JG and Chen J performed the research; Fang YH analyzed the data; Fang YH and Chen J wrote the paper.

Supported by Zhejiang Province Medical Platform Backbone, No. 2017KY436.

Institutional review board statement: This study was reviewed and approved by the Ethics Committee of the Children's Hospital of Zhejiang University School of Medicine.

Conflict-of-interest statement: The authors have no financial relationships to disclose.

Data sharing statement: No additional data are available.

Manuscript source: Unsolicited manuscript

Correspondence to: Jie Chen, MD, Attending Doctor, Chief Doctor, Department of Gastroenterology, Children's Hospital, Zhejiang University School of Medicine, 3333 Bin Sheng Road, Hangzhou 310052, Zhejiang Province, China. hzcjie@zju.edu.cn

Telephone: +86-571-87061007

Received: December 12, 2017
Peer-review started: December 12, 2017
First decision: January 18, 2018
Revised: January 31, 2018
Accepted: February 8, 2018
Article in press: February 8, 2018
Published online: March 7, 2018

Abstract

AIM

To analyze clinical differences between monogenic and nonmonogenic very-early-onset inflammatory bowel disease (VEO-IBD) and to characterize monogenic IBD phenotypically and genotypically *via* genetic testing.

METHODS

A retrospective analysis of children aged 0 to 6 years diagnosed with VEO-IBD in a tertiary hospital in southern China from 2005 to 2017 was performed. Clinical data for VEO-IBD patients were collected, and genetic characteristics were analyzed using whole exome sequencing or target gene panel sequencing.

RESULTS

A total of 54 VEO-IBD patients were included in this study. A diagnosis of Crohn's disease (CD) or CD-like intestinal manifestations accounted for 72.2% of the VEO-IBD cases. Nine patients (16.7%) were identified by genetic testing as having monogenic IBD. The median age of diagnosis in the monogenic group was younger than that of the nonmonogenic IBD group, at 18 mo (interquartile range (IQR): 4 to 78) and 43.5 mo (IQR: 3 to 173), respectively; the *P*-value was 0.021. The incidence of perianal disease in the monogenic group was higher than that in the

nonmonogenic group (P = 0.001). However, there were no significant differences between weight-for-age and height-for-age Z-scores between the two groups, and similar laboratory results were obtained for the two groups. Five patients were found to have *IL10* receptor mutation, two patients had chronic granulomatous disease, one patient had common variable immunodeficiency disease, and one patient had X-linked inhibitor of apoptosis protein deficiency.

CONCLUSION

A high proportion of monogenic IBD was observed in the VEO-IBD group, especially with disease onset before the age of 6 mo. Monogenic IBD and nonmonogenic IBD exhibited similar clinical features. Furthermore, next-generation sequencing played an important role in the diagnosis of monogenic IBD, and *IL10* receptor mutation was predominant in this cohort.

Key words: Monogenic; Very-early-onset inflammatory bowel disease; Primary immunodeficiency diseases; *IL10*; *IL10R*

Core tip: This study is the largest study to analyze clinical differences between monogenic and non-monogenic very-early-onset inflammatory bowel disease (VEO-IBD) in China. Moreover, we characterized monogenic IBD phenotypically and genotypically through genetic testing (whole exome sequencing and targeted gene panel sequencing). We found a high proportion of monogenic IBD in the VEO-IBD group, with the most common monogenic IBD being *IL10R* mutation. Monogenic IBD and nonmonogenic IBD showed similar clinical features. Next-generation sequencing played an important role in the diagnosis of monogenic IBD.

Fang YH, Luo YY, Yu JD, Lou JG, Chen J. Phenotypic and genotypic characterization of inflammatory bowel disease in children under six years of age in China. *World J Gastroenterol* 2018; 24(9): 1035-1045 Available from: URL: http://www.wjgnet.com/1007-9327/full/v24/i9/1035.htm DOI: http://dx.doi.org/10.3748/wjg.v24.i9.1035

INTRODUCTION

Very-early-onset inflammatory bowel disease (VEO-IBD) refers to an IBD diagnosis established before the 6th year of life, including a subset of patients with disease onset before the age of 2 years, known as infantile-onset IBD (IO-IBD)[1]. VEO-IBD is rare, with an estimated incidence of 4.37 and a prevalence of 14 per 100000 children[2-4]. These patients present with abdominal pain, intestinal bleeding, diarrhea and malnutrition, similar to adults with IBD. In addition, growth failure is often observed[5,6]. However, VEO-IBD is considered to be a unique entity, and compared to adults with IBD, VEO-IBD children are more likely to present with extensive and treatment-resistant disease.

These patients may require the combined use of immunosuppressant and biologic agents and even early intestinal surgery. Although the IBD classification was recently modified to address the younger age group, this step may not be sufficient to accommodate the heterogeneous phenotypes of VEO-IBD[7]. The etiology of IBD is related to genetic and environmental factors as well as to the intestinal microbiome. Furthermore, VEO-IBD, especially IO-IBD, presents with IBD-like intestinal inflammation and shows a close association with primary immunodeficiency diseases (PIDs), defined as monogenic IBD[3].

More than 50 VEO-IBD-related genes have been reported to date, including those associated with *IL10* and *IL10* receptor mutation, immune dysregulation, polyendocrinopathy, enteropathy X-linked (IPEX) syndrome and X-linked inhibitor of apoptosis (XIAP) deficiency[3]. Nonetheless, the exact incidence of monogenic IBD remains unknown[8] due to variations in the genetic background of this disease. Most reports regarding monogenic IBD are based on small populations or case reports, with only a small number of genes investigated. To the best of our knowledge, this study reports the largest cohort of genetically screened patients with VEO-IBD from China.

MATERIALS AND METHODS

Study subjects

This study was approved by the Ethics Committee of the Children's Hospital of Zhejiang University School of Medicine. A total of 54 pediatric patients diagnosed with VEO-IBD in the Gastroenterology Department of Children's Hospital of Zhejiang University School of Medicine from October 2005 to May 2017 were included in this study. According to Porto criteria[9], Crohn's disease (CD) and CD-like intestinal inflammation present as noncontiguous aphthous or linear ulcers, primarily in the ileum or colon. Histologically, the disease is characterized by chronic focal inflammation with or without granulomas and perianal or fistulating disease. Ulcerative colitis (UC) or UC-like intestinal inflammation presents as continuous mucosal inflammation of the colon starting from the rectum, without small bowel involvement and without CD features. Patients with a definitive diagnosis of IBD with inflammation limited to the colon but without the typical features of UC and CD are classified as IBD of an unclassified type (IBDU).

The clinical characteristics of the pediatric patients, including sex, first symptom(s), time of onset of symptom(s), clinical features, surgical history, medication

history and family history, were collected from medical records.

The following were criteria for genetic testing: (1) patients with disease onset before 6 mo of age; (2) patients with disease onset beyond 6 mo accompanied with severe perianal disease, severe malnutrition or growth failure, or resistance to treatment.

Whole exome sequencing and targeted gene panel sequencing

Genomic DNA was isolated from peripheral blood of the patients. For whole exome sequencing (WES), whole exome library preparation was based on modifications of a protocol using the Agilent SureSelect XT Human All Exon Kit. Sequencing was performed using the Illumina HiSeq 2500 platform.

For targeted gene panel sequencing (TGPS), target sequences were enriched using customized capture probe chips (SureSelect Inherited Disease Panel; Agilent Technologies), which included 4,503 genes known to cause inherited disorders. DNA probes were designed for exons and flanking 10 bp intronic sequences. Briefly, 1 μg of genomic DNA was fragmented into 200-300 bp lengths by the Covaris Acoustics system. The DNA fragments were subsequently processed by end-repairing, A-tailing and adaptor ligation, 4-cycle pre-capture polymerase chain reaction (PCR) amplification, and targeted sequence capture. The captured DNA fragments were eluted and amplified by 15-cycle postcapture PCR. The final products were sequenced with 150-bp paired-end reads using the Illumina HiSeq X Ten platform according to the standard manual.

Raw data were processed by the Illumina pipeline (version 1.3.4) for image analysis, error estimation, base calling and generating the primary sequence data. For quality control, Cutadapt (https://pypi.python.org/pypi/cutadapt) and FastQC (https://www.bioinformatics.babraham.ac.uk/projects/fastqc/) were used to remove 3′-/5′- adapters and low-quality reads, respectively. Clean short reads were mapped to the human genome (hg19) using Burrows Wheeler Aligner software (http://sourceforge.net/projects/bio-bwa/). SOAPsnp software (http: //soap.genomics.org.cn/) and SAM tools Pileup software (http://sourceforge.net/projects/samtools/) were used to detect single-nucleotide polymorphisms and small insertions and deletions.

Variants were annotated using ANNOVAR software (http://www.openbioinformatics.org/annovar/), which includes function implications (gene region, functional effect, mRNA GenBank accession number, amino acid change, cytoband) and allele frequencies in dbSNP, 1000 genomes (http://www.1000genomes.org), ESP6500 (http://evs.gs.washington.edu/EVS/) and ExAc (http://exac.broadinstitute.org/). Damaging missense mutations were predicted by SIFT (http://sift.bii.a-star.edu.sg/), PolyPhen-2 (http://genetics.bwh.harvard.edu/pph2/) and MutationTaster (http://www.mutationtaster.org/). Interpretation of variants was based on recommended standards from the American College of Medical Genetics and Genomics[1,2], and all variants were categorized as pathogenic, likely pathogenic, variants of unknown significance, likely benign or benign.

To validate the variants based on next-generation sequencing (NGS) and WES, PCR amplification and Sanger sequencing were performed for the sequence centers on variant genes.

Statistical analysis

The categorical variables were presented as number (percentage). The continuous variables of normal distribution were presented as mean ± SD, otherwise as median ± interquartile range (IQR). The normality test was performed by Shapiro-Wilk test. The difference in variables with normal/abnormal distribution between nonmonogenic and monogenic IBD were estimated by Student's *t*-test and Mann-Whitney test, respectively. The differences in categorical variables between non-monogenic and monogenic IBD were assessed using the chi-square test; however, if total sample size was less than 40 or the number in one cell was less than 5, Fisher's exact test was used for testing the difference. $P < 0.05$ was considered to be a statistically significant difference. All statistical analyses were conducted with SPSS 22.0 statistical software (SPSS Inc., IBM Corp., Armonk, NY, United States).

RESULTS

General characteristics of VEO-IBD patients

From October 2005 to May 2017, 136 pediatric patients were diagnosed with IBD at our hospital, among which 54 were diagnosed with VEO-IBD; thus, VEO-IBD patients accounted for 39.7% of pediatric IBD patients in our cohort. Among the 54 VEO-IBD patients, 37 were males and 17 females, for a male to female ratio of 2.18:1. Thirty-one VEO-IBD patients (57.4%) had disease onset before the age of 2 years.

Of the 54 patients with VEO-IBD, 72.2% had a diagnosis of CD or CD-like intestinal manifestations, 7.4% had a diagnosis of UC or UC-like intestinal manifestations, and 20.4% had a diagnosis of IBDU. Only one patient was the offspring of a consanguineous union, and his older sister also had similar symptoms during the neonatal period, though without a definitive diagnosis. None of the remaining patients had a positive family history of IBD or PID.

The median age of disease onset was 14 mo (IQR: 0 to 72 mo), and the median age of diagnosis was 35.5 mo (IQR: 3 to 173 mo). The median time to diagnosis was 9 mo (IQR: 0.4 to 104 mo). The Z-scores for median weight-for-age, height-for-age and body mass index -for-age were -1.69 (IQR: -4.69 to 2.2), -1.41 (IQR: -6.43 to 2.51) ($n = 51$) and 14 (IQR: 0 to 72) respectively.

Mortality

The overall mortality rate was 11.1% (6/54). The

Table 1 Clinical features of dead very-early-onset inflammatory bowel disease patients

Patient	Sex	Age of disease onset	Chief complaints	Perianal diseases	EIMs	Colonoscopy features	Disease cause death	Genetic diagnosis
1	M	Neonate	Diarrhea	Perianal abscess and fistula	Arthritis, oral ulcers	Pancolitis, ulcers and hyperplasia	Lymphoma	NA
2	M	2 mo	Diarrhea, bloody stools	None	None	Proctitis, linear and aphthous ulcers	Suspension of treatment	NA
3	M	1 yr 5 mo	Diarrhea, bloody stools	Perianal abscess	None	Pancolitis and terminal ilium ulcers and hyperplasia	Suspension of treatment	NA
4	F	3 yr 10 mo	Abdominal pain	None	None	Pancolitis, ulcers and cobble stone appearance of colon	Sepsis, multiple organ failure	NA
5	M	4 yr 11 mo	Diarrhea, bloody stools, fever, malnutrition	None	Rash, oral erosion	Pancolitis, erosion, ulcers and multiple hyperplasia lesions	Intestinal bleeding	NA
6	M	2 mo 13 d	Diarrhea, fever	Perianal abscess	None	Proctitis, longitudinal ulcer	Sepsis and shock	CGD

EIMs: Extraintestinal manifestations.

Table 2 General data of very-early-onset inflammatory bowel disease patients

	Monogenic IBD	Nonmonogenic IBD	*P* value
Patients	9	45	
Sex, M/F	8/1	28/17	
Median age of disease onset, in mo	1 (0, 72)	19.5 (0, 72)	0.008[a]
Median age of disease diagnosis, in mo	18 (4, 78)	43.5 (3, 173)	0.021[a]
Duration before diagnosis, in mo	6 (2, 29)	9 (0, 104)	0.668

[a]$P < 0.05$. IBD: Inflammatory bowel disease.

clinical conditions of these 6 patients are listed in Table 1. Among the 6 patients, 4 had a diagnosis of CD and 2 a diagnosis of IBDU. Moreover, 2 of the patients had disease onset before 2 years of age.

Clinical characteristics

Nine patients (16.7%) were diagnosed with monogenic IBD; among them, 6 were diagnosed with CD and 3 with IBDU. We also compared the clinical manifestations of monogenic and nonmonogenic IBD patients. The monogenic group was predominately male, with a male to female ratio of 8:1. Four patients had disease onset during the neonatal period, and two patients presented with symptoms before 1 year of age. The median age of disease onset for the monogenic patients was earlier than that for the nonmonogenic patients at 1 mo (IQR: 0 to 72) and 19.5 mo (IQR: 0 to 72) respectively (P = 0.008). Similarly, the median age of diagnosis for the monogenic group was earlier than that for the nonmonogenic group, at 18 mo (IQR: 4 to 78) and 43.5 mo (IQR: 3 to 17) respectively (P = 0.021). However, there was no significant difference in the median time from disease onset to diagnosis between the two groups (P = 0.668; Table 2).

The incidence of perianal disease in the monogenic group was higher than that in the nonmonogenic group (P = 0.001); when comparing weight-for-age and height-for-age Z-scores, no significant differences between the two groups were found. Moreover, laboratory findings were similar between the two groups. Mesalazine was more commonly used in the monogenic than in the nonmonogenic group (P = 0.009). A greater number of patients underwent intestinal surgery in the monogenic group than in the nonmonogenic group; however, this difference was not statistically significant at P = 0.050. To date, more patients in the nonmonogenic group have died compared to the monogenic group (P = 0.000; Table 3).

Genetics

A total of 16 patients underwent WES or TGPS, 6 and 12 respectively (2 patients were tested by both WES and TGPS). Two patients underwent genetic testing (*IL10RA*) at another hospital. Nine patients were diagnosed with monogenic IBD. Seven of these patients were diagnosed by TGPS, and two were diagnosed by both methods. Five patients were diagnosed with *IL10R* mutation, two patients were diagnosed with chronic granulomatous disease (CGD) with *CYBB* mutation, and one patient was diagnosed with XIAP deficiency. One patient was diagnosed with common variable immune deficiency (CVID) with *TNFRSF13B* mutation. The clinical information for the 9 monogenic patients are listed in Table 4, and the genetic phenotypes of the 18 patients are provided in Table 5.

IL10 and IL10R mutations

Patient 1 was a male offspring from a consanguineous union, with disease onset during the neonatal period. The first manifestation was a perianal abscess followed by recurrent fever, bloody stools, anal fistula and anal abscess formation, and skin infections. Colonoscopic findings included strictures of the colon near the splenic flexure, extensive polypoid hyperplasia, irregular ulcers,

Table 3 Comparison of clinical features of monogenic and nonmonogenic inflammatory bowel disease groups

	Nonmonogenic IBD	Monogenic IBD	*P* value
Diagnosis			
CD, %	75.0	50.0	
IBD-U, %	18.2	40.0	
UC, %	6.8	10.0	
Abdominal pain, *n*	25	2	0.142
Diarrhea, *n*	36	8	1.000
Bloody stools, *n*	26	8	0.131
Malnutrition, *n*	19	5	0.489
Growth failure, *n*	14	4	0.461
Oral ulcers, *n*	3	1	0.529
Persistent fever, *n*	3	0	1.000
Perianal diseases, *n*	9	7	0.001[a]
Body weight Z-score	-1.54 (-4.69, 2.20)	-2.04 (-3.66, 0.96)	0.303
Height Z-score	-1.38 (-6.43, 2.51)	-1.76 (-4.92, 0.46)	0.597
WBC, as $^{a}10^{9}$	15.04 ± 1.72	12.53 ± 1.72	0.382
HGB, in g/L	103.02 ± 2.57	106.67 ± 5.00	0.496
PLT, as $^{a}10^{12}$	454.60 ± 28.40	421.89 ± 54.97	0.632
CRP, in mg/L	51.16 ± 8.43	20.22 ± 2.43	0.668
ESR, in mm/h	29.22 ± 4.70	21.00 ± 4.56	0.923
ALB, in g/L	33.80 ± 1.10	36.60 ± 1.77	0.283
Steroid, *n*	36	6	0.399
Antibiotics, *n*	29	7	0.484
Mesalazine, *n*	32	2	0.009[a]
Immunosuppressants, *n*	25	8	0.075
Nutrition, *n*	33	5	0.425
Infliximab, *n*	14	4	0.461
Surgery, *n*	6	4	0.050
Death, *n*	5	1	0.000[a]

[a]$P < 0.05$. IBD: Inflammatory bowel disease.

and inflammatory tags. Esophagogastroduodenoscopy was normal. Preliminary immune tests and the serum IL10 level were normal. The patient underwent a colostomy at the age of 1 year and 1 mo due to recurrent diarrhea and perianal abscesses. At 2 years and 5 mo of age, he underwent transverse partial colectomy, small bowel internal fistula resection and anastomosis. The pathological evaluation revealed transmural inflammatory infiltrate and linear serpentine ulcerations. The patient also underwent incision, drainage and seton placement for multiple abscesses. He was resistant to treatment with antibiotics, steroids, total parenteral nutrition (TPN), enteral nutrition (EN) and infliximab. At the time of writing this manuscript, he is in clinical remission on a combination treatment of azathioprine and thalidomide. Genetic testing by both TGS and WES revealed the following homozygous *IL10RB* mutation: Chr21:34660499: c.737G>A, p.W246X. This mutation has not been reported in HGMDpro.

Patient 2 was a female with VEO-IBD of neonatal onset, with first symptoms of recurrent watery diarrhea and blood and mucous in stools followed by a perianal abscess, fistula formation and recurrent fever. The patient was initially treated with elemental formula due to suspected cow's milk allergy. She had her first colostomy at 1 year and 11 mo of age. Colonoscopy showed a cobble stone appearance and linear ulcerations in the colon. The pathological evaluation revealed classic CD features (strictures, transmural inflammatory infiltrate, linear serpentine ulcerations and noncaseating granulomas). Preliminary immune tests were normal, and the serum IL10 level was slightly elevated. She was resistant to treatment with steroids, mesalazine, antibiotics, immunosuppressants and infliximab. At 3 years and 1 mo of age, she underwent repair for a small bowel perforation, pancolectomy and ileal pouch-anal anastomosis. TGPS revealed the following compound heterozygous *IL10RA* mutations: Chr11:117864125: c.537G>A, p.T179T and Chr11:117860269: c.301C>T, p.R101W. The two mutations were derived from the mother and father, respectively. Both mutations are reported in HGMDpro[10,11].

Patient 3 was a male with disease onset at 1 mo of age. The patient had symptoms of recurrent diarrhea with mucous and blood, oral ulcers, anal fistula, obvious malnutrition and growth failure. Initial immune tests were normal, and the IL10 level was elevated at 85.5 pg/mL (normal range from 2.6 to 4.9 pg/mL). Colonoscopy showed deep ulcers in the rectum. The pathology evaluation showed nonspecific inflammation of the colon. The traditional treatments of antibiotics, TPN, EN and steroids were unsuccessful. Genetic testing at an outside hospital detected the following compound heterozygous *IL10RA* mutations: Chr11:117860269, c.301C>T, p.R101W, Chr11:117993268: c.470A>G, p.Y157C. The two mutations were from his mother and father, respectively. His older sister is a hereditary carrier.

Table 4 Clinical characteristics of monogenic very-early-onset inflammatory bowel disease patients

Patient	Sex	Disease onset	Z-score of height	Z-score of body weight	Chief complaints	Others	Disease locations and behavior	Clinical and genetic diagnosis	Intestinal surgery	Treatment	Prognosis
1	M	< 1 mo	0.22	-1.18	Diarrhea, bloody stools	Pyoderma	L2, P, B2B3	CD, IL10RB mutation	Colostomy	Steroid, IFX, thalidomide, 6-MP/MTX/AZA	Remission
2	F	4 mo	-1.76	-0.96	Diarrhea, bloody stools	Pyoderma	L2,L4b, P, B2B3	CD, IL10RA mutation	Intestinal perforation repair, colostomy and J-POUCH	Steroid, mesalazine, IFX, MTX/CsA	Remission
3	M	1 mo+	-0.79	-2.21	Diarrhea, bloody stools	Elevation of ALT	L2, P, B2	CD, IL10RA mutation	None	None	Waiting HSCT
4	M	1 mo+	-3.11	-3.66	Diarrhea, bloody stools	None	L2, P, B1	IBDU, IL10RA mutation	None	Antibiotics	Give up
5	M	11 d	-4.92	-3.38	Diarrhea, bloody stools	NEC	L2,L4b, P, B1	CD, IL10RA mutation	None	Steroids, AZA	Give up
6	M	< 1 mo	0.46	-1.08	Diarrhea, bloody stools	Epilepsy	L2, P, B1	IBDU, CGD	None	None	Remission
7	M	< 1 mo	-0.84	-2.04	Persistent fever	Intestinal malrotation, elevation of ALT	L2, P, B1	IBDU, CGD	None	None	Dead
8	M	9 mo	-4.63	-2.95	Diarrhea, bloody stools	Hepatosplenomegaly	L2, B1	CD, CVID	Intestinal resection and anastomosis	Steroid, 6MP, mesalazine, thalidomide	Partial remission
9	M	5 yr 11 mo	-2.2	-1.57	Abdominal pain, diarrhea, bloody stools	None	L2, L4b	CD, XIAP deficiency	None	DXM, IFX, 6MP/AZA	Remission

6-MP: 6-mercaptopurine; ALT: Alanine aminotransferase; AZA: Azathioprine; CGD: Chronic granulomatous disease; CsA: Cyclosporin A; CVID: Common variable immunodeficiency; HSCT: Hematopoietic stem cell transplantation; IFX: Infliximab; IL10R: Interleukin 10 receptor; MTX: Methotrexate; XIAP: X-linked inhibitor of apoptosis protein.

At the time of this writing, he is awaiting hematopoietic stem cell transplantation (HSCT). The pathogenic mutation c.301C>T is reported in HGMDpro[10], and c.470A>G was predicted by software mentioned in the methods section to be the likely pathogenic gene.

Patient 4 was a male with first symptoms of recurrent perianal abscess followed by watery diarrhea with scant fresh blood, rash and severe malnutrition. Immune tests were normal, and the IL10 level was 47.2 pg/mL. Colonoscopy showed multiple irregular ulcers at the sigmoid colon and rectum with polypoid hyperplasia and ulcers of the anus. Pathological examination revealed nonspecific findings. TGPS revealed the following homozygous mutation of *IL10RA*: Chr11:117860269: c.301C>T, p.R101W. The mutation was verified in his mother. The mutation is reported in HGMDpro to be pathogenic[10].

Patient 5 was a male with disease onset during the neonatal period. He initially presented with bloody diarrhea and was diagnosed with necrotizing enterocolitis; however, his symptoms persisted after surgery. This patient subsequently presented with a perianal fistula and severe malnutrition. Colonoscopy showed polypoid hyperplasia at the colon and ulcers at the rectum. This patient was treated with mesalazine and enemas. Genetic testing at an outside hospital revealed the following compound heterozygous *IL10RA* mutations: Chr11:117860269: c.301C>T, p.R101W, c.350G>A, p.R117H. The two mutations are reported in the literature to be pathogenic[10,12].

CGD

Patient 6 was a male with disease onset during the neonatal period. He presented with recurrent diarrhea, bloody stools and a perianal abscess. Preliminary immune tests were normal. Colonoscopy showed pancolitis and a perianal abscess. TGPS revealed the following hemizygotic mutation of *CYBB*: ChrX:37658209: c.676C>T, p.R226X. The mutation originates from his mother and is reported in HGMDpro to be pathogenic. The mutation is a termination mutation, which can alter the function of the encoded protein[13].

Patient 7 was a male diagnosed with intestinal malrotation during the neonatal period. He presented with pneumonia, perianal abscess and liver dysfunction; he developed diarrhea and fever during hospitalization. The immunoglobulin level and CD3 (46.81%), CD4 (29.86%), natural killer cell (7.79%), CD4/CD8 (1.86) levels were normal. Colonoscopy showed a longitudinal ulcer at the rectum. Soon thereafter, the patient developed multiple organ failure due to severe infection. TGPS

Table 5 Genetic testing of very-early-onset inflammatory bowel disease patients

Patient	Sex	Age of disease onset	WES/TGPS	Genetic mutation	Location of mutation	Mutation of parents	Homo/Heterozygote	SIFT score/ prediction	Polyphen2 score/ prediction	MutationTaster score/ prediction
1	M	Neonate	Both	*IL10RB*	Chr21:34660499 c.737G>A p.W246X	Heterozygotic mutation of parents c.737G>A	Homozygote	-	-	6/D
2	F	4 mo	TGPS	*IL10RA*	Chr11:117860269 c.301C>T p.R101W	Heterozygotic mutation of father c.301C>T	Compound heterozygote	0/D	1/D	101/D
					Chr11:117864125 c.537G>A p.T179T	mother c.537G>A		1/T	-	-
3	M	1 mo+	TGPS	IL10RA	Chr11:117860269 c.301C>T p.R101W	Heterozygotic mutation of father c.301C>T	Compound heterozygote	0/D	1/D	101/D
					Chr11:117864058 c.470A>G p.Y157C (rs1027503096)	mother c.470A>G		0.001/D	1/D	194/N
4	M	1 mo+	TGPS	IL10RA	Chr11:117860269 c.301C>T p.R101W	Heterozygotic mutation of parents c.301C>T	Homozygote	0/D	1/D	101/D
5	M	Neonate	TGPS	IL10RA	Chr11:117860269 c.301C>T p.R101W	Heterozygotic mutation of father c.301C>T	Compound heterozygote	0/D	1/D	101/D
					c.350G>A p.R117H (rs199989396)	mother c.350G>A		0.011/D	1/D	29/D
6	M	Neonate	TGPS	CYBB	ChrX:37658209 c.676C>T p.R226X (rs137854592)	Heterozygotic mutation of mother c.676C>T	Hemizygotic mutation	-	-	6/D
7	M	Neonate	TGPS	CYBB	ChrX:37642741 c.142-2A>G splicing	Heterozygotic mutation of mother c.142-2A>G	Hemizygotic mutation	-	-	-
8	M	9 mo	Both	TNFRSF13B	Chr17:16843819 c.452C>T p.P151L (rs200037919)	Heterozygotic mutation of father c.452C>T	Compound heterozygote	0.568/T	0.005/B	98/N
					Chr17:16852132 c.365G>A p.R122Q (rs755343222)	mother c.365G>A		0.485/T	0.136/B	43/N
9	M	5 yr 11 mo	TGPS	XIAP	ChrX:123022501 c.910G>T p.G304X	No mutation in parents	Hemizygotic mutation	-	-	6/D
10	F	5 yr 9 mo	TGPS	IL10RB	Chr21:34652146 c.421G>A p.E141K (rs387907326)	Heterozygotic mutation in father c.421G>A	Heterozygote	0.026/D	0.946/D	56/D
11	F	4 mo	WES	-						
12	M	8 mo	WES	-						
13	F	3 yr 3 mo	TGPS	-						
14	F	4 yr	TGPS	-						
15	M	1 yr 10 mo	WES	-						
16	F	4 yr 8 mo	WES	-						

TGPS: Targeted gene panel sequencing; WES: Whole exome sequencing.

revealed the following hemizygotic mutation of *CYBB*: ChrX:37642741: c.142-2A>G splicing. The mutation is reported as pathogenic in HGMDpro[14].

CVID

Patient 8 was a male who presented with jaundice and recurrent respiratory infections during the neonatal period. Immunoglobulin (Ig)G and IgM levels were below normal. He was treated with antibiotics and intravenous immunoglobulin. He gradually developed splenomegaly. At the age of 9 mo, this patient presented with recurrent bloody stools. Colonoscopy showed ulcers and polypoid hyperplasia, which eventually spread to involve the entire colon. Pathological examination of the intestinal biopsy showed nonspecific inflammatory changes. The patient underwent laparotomy, which revealed intestinal swelling and with fissure ulcers, and ulcers involving the tunica muscularis. Treatments with steroids, TPN, EN, mesalazine, infliximab and multiple immunosuppressants were unsuccessful. Both WES and TGPS showed the following compound heterozygous mutations in *TNFRSF13B*: Chr17:16843819: c.452C>T, p.P151L and Chr17:16852132:c.365G>A, p.R122Q. These mutations are reported to be associated with CVID, though they have not been reported in HGMDpro. Further tests are required to determine the effects of these mutations.

XIAP deficiency

Patient 9 was a male, aged 5 years and 11 mo, who presented with recurrent bloody stools, fever and abdominal pain. He had been diagnosed with hemophagocytic syndrome at 4 years of age. Colonoscopy showed blunting and flattening of villi at the terminal ileum. The entire colon showed irregular deep ulcers and aphthous ulcers. Capsule endoscopy revealed sporadic jejunal ulcers. Immune tests were normal. He did not respond to exclusive enteral nutrition therapy and oral steroids. He was treated with infliximab and 6-Mercaptopurine and is currently in clinical remission. His colonoscopy findings have also improved. TGPS revealed the following mutation associated with XIAP deficiency: ChrX:123022501: c.910G>T, p.G304X. The mutation was not acquired from his parents. This mutation has not been reported in HGMDpro.

DISCUSSION

VEO-IBD children are generally recognized as having more severe clinical symptoms, more extensive intestinal inflammation, higher rates of treatment resistances and rapid disease progression compared to patients with adolescence- or adult-onset IBD[15-17]. In contrast, several studies have reported that VEO-IBD patients are not prone to a more severe clinical course compared to those with adolescence-onset IBD[18]. However, geographic and/or ethnic differences can affect genetic background and therefore cause conflicting results among studies. Monogenic IBD typically presents early, with severe clinical features and is resistant to traditional therapy; a portion of VEO-IBD patients even require HSCT[19].

In the study by Jochen Kammermeier *et al*[16], a high rate of IBDU (71%) in patients younger than 2-years-old was observed, among whom 29% were offspring from consanguineous unions, 18% had a positive family history of IBD in a first-degree relative, and 31% were diagnosed with monogenic IBD. In that study, high rates of consanguineous unions and positive family history of IBD resulted in high rates of monogenic IBD, exhibiting a more severe clinical course than traditional IBD[16]. Abdulrahman Al-Hussaini *et al*[20] analyzed 352 IBD patients in Saudi Arabia and found that 21.6% were diagnosed with IBD before the age of 6 years and 9% before the age of 3 years, and the consanguinity rate was significantly higher in the infantile or toddler-onset CD subgroup (57.1%).

In our study, the percentage of VEO-IBD patients among cases of pediatric IBD was similar to that reported by Oren Ledder *et al*[17]. Monogenic IBD patients showed earlier disease onset than nonmonogenic IBD patients, and CD was the predominant diagnosis in both groups. Nonetheless, IBDU was more common in the monogenic group, which suggests that most of the monogenic IBD patients had disease limited to the colon. The results of laboratory tests were similar between the two groups. Moreover, patients in the monogenic group did not show a propensity to be prescribed infliximab and immunosuppressants earlier than those in the nonmonogenic group.

According to the diagnostic guidelines for pediatric IBD by the European Society of Paediatric Gastroenterology, Hepatology and Nutrition[9], CD is likely to be the diagnosis when colonoscopy shows classic or nonclassic CD features with small bowel involvement or the presence of fistula/perianal disease. IBDU classification is reserved for patients with inflammation limited to the colon, in the absence of features suggestive of either UC or CD. If the initial immune work-up is normal, further investigation may be considered by physicians to be unnecessary. However, monogenic IBD, including IL10/R and XIAP deficiencies, CGD, and IPEX syndrome, presents with such features as perianal/fistulating disease, linear serpentine ulcerations, and even non-caseating granulomas[21-23], and these patients are likely to be diagnosed with IBDU or CD. It is recognized that onset of disease before 6 mo of age, growth stunting (height-for-age Z-score < 3), extensive disease and epithelial abnormalities are significantly more prevalent in monogenic IBD[16], which may indicate the need for immune tests and even genetic screening in this group of patients[3].

PID can present as IBD-like symptoms with intestinal manifestations and can be diagnosed by immune tests. CGD is characterized by genetic defects in components of the phagocyte reduced nicotinamide

adenine dinucleotide phosphate (NADPH) oxidase (phox) complex, which can be detected by the neutrophil oxidative burst assay. High levels of IgG may indicate FOXP3 deficiency[16,24]. However, Wiskott-Aldrich syndrome, hyper-IgE syndrome and *IL10* or *IL10R* mutations are not detected by basic immunodeficiency screening tests and require specific functional analyses. Defects in gene *IL10RA* and *IL10RB* can be detected by assays that determine whether exogenous IL10 will suppress lipopolysaccharide-induced peripheral blood mononuclear cell cytokine secretion or IL10-induced STAT3 phosphorylation[22]. Flow cytometry can detect functional defects in muramyl dipeptide signaling in patients with XIAP deficiency[25].

Given the large number of potential candidate genes and overlapping phenotypes, single-gene sequencing and immune tests are becoming less appropriate in children with suspected monogenic IBD. NGS techniques have significantly improved in recent years, with lower cost and diagnosis time. Although WES is suitable for novel gene discovery, it offers less reliable gene coverage in the diagnostic setting compared to TGPS[8]. TGPS and WES were both used in our study, with 16 VEO-IBD patients with suspected immune deficiency undergoing WES and/or TGPS, which revealed 9 cases of monogenic IBD (*IL10RA, IL10RB, XIAP* and *CYBB*). Among the 9 patients, 4 had disease onset during the neonatal period, and 4 had symptoms within 1 year of age. The phenotypes of the patients were in accordance with the genotypes. SIFT, Polyphen2 and MutationTaster were used to predict the innocuousness of the mutated genes.

There were limitations in this study. First, we did not perform functional analyses of novel mutations, and such studies should be performed to confirm the results. However, the novel mutations were all predicted to be pathogenic and likely pathogenic by SIFT, PolyPhen-2 and MutationTaster. Second, not all of the VEO-IBD patients were assessed by genetic testing. In cases in which immune deficiency disease was strongly suspected but could not be diagnosed by initial immune tests, genetic testing was recommended. At our hospital, the identification of monogenic IBD and genetic testing in VEO-IBD patients have only been performed during the last 5 years. Several IO-IBD patients diagnosed in early years who met the criteria for genetic testing had died, and their blood samples were not collected. For this reason, more cases of monogenetic IBD might have been present in our cohort.

In the present study, we identified monogenic IBD in 9 patients, predominantly with *IL10R* mutation; five patients were diagnosed with *IL10R* mutation. Among them, 1 patient was the offspring of a consanguineous union, with a homozygous mutation of *IL10R* which has not been reported in the literature. All remaining patients had compound heterozygous mutations of *IL10R*. *IL10* and *IL10R* mutations have been reported previously. Patients with *IL10* signaling defects primarily present with IBD symptoms within 3 mo of life, with severe perianal disease (abscess, fistula formation, fissure, tags) and susceptibility to infections. In addition, they are usually resistant to traditional therapies, though HSCT can induce sustained remission of intestinal inflammation[19,26,27]. Defects in *IL10* signaling are associated with extraintestinal inflammation, such as folliculitis and arthritis, as well as a predisposition toward B-cell lymphoma[28].

In the report of Zhiheng Huang *et al*[27], 42 IO-IBD patients among the Han population in China had *IL10R* mutations, 41 patients had *IL10RA* mutations, and only 1 patient had an *IL10RB* mutation; thus, *IL10RA* was predominant in the Han population. In another report from China, Xiao *et al*[19] described 4 patients with *IL10RA* mutation and 1 with *IL10RB* mutation among 13 VEO-IBD patients. In the present study and in other studies from Asia[26], monogenic IBD is predominately due to mutations in *IL10R* and *XIAP* and CGD, whereas mutations in *EPCAM, TTC37, SKIV2LLRBA* and *TTC7A* have been reported in Western countries[16]. These findings suggest that *IL10R* mutation is the most common cause of monogenic IBD in the Han population. Further multicenter studies are warranted.

The genetic background of VEO-IBD patients is not clear, especially among different ethnicities. Due to the heterogeneity of VEO-IBD with overlapping phenotypes between different genotypes, TGSP is appropriate for rapid recognition of monogenic IBD in VEO-IBD patients with the signs and features of monogenic IBD. This approach may help guide a more appropriate treatment strategy. For example, sustained remission after HSCT can be achieved with *IL10R*/*IL10* mutation[12], XIAP deficiency[29] and FOXP3 deficiency[30].

In conclusion, using WES and TGPS, we identified underlying PID gene mutations in pediatric patients with VEO-IBD in a Chinese population. There was a high proportion of monogenic IBD in the VEO-IBD group, especially with disease onset before 6 mo of age. *IL10R* mutation was predominant in our cohort.

ARTICLE HIGHLIGHTS

Research background

Very-early-onset inflammatory bowel disease (VEO-IBD) patients show a close association with primary immunodeficiency diseases, defined as monogenic IBD. More than 50 VEO-IBD related genes have been reported to date. Nonetheless, the incidence of monogenic IBD in Chinese population remains unknown.

Research motivation

Most reports regarding monogenic IBD were based on small population or case report, with only a small number of genes investigated. This study reports the largest cohort of genetically screened patients with VEO-IBD from China.

Research objectives

The objective of this research is to characterize monogenic IBD phenotypically and genotypically *via* genetic testing and to analyze clinical differences between

monogenic and nonmonogenic VEO-IBD patients.

Research methods

A retrospective analysis of children aged 0 to 6 years diagnosed with VEO-IBD in a tertiary hospital in southern China from 2005 to 2017 was performed. Clinical data for VEO-IBD patients were collected, and their genetic characteristics were analyzed using whole exome sequencing or target gene panel sequencing.

Research results

Nine patients (16.7%) were identified to have monogenic IBD by genetic testing. Five patients were shown to have *IL10R* mutation, two patients had chronic granulomatous disease, one patient had common variable immunodeficiency disease, and one patient had X-linked inhibitor of apoptosis deficiency.

Research conclusions

A high proportion of monogenic IBD was observed among the VEO-IBD group, especially with disease onset before the age of 6 mo. *IL10RA* was the predominant mutation in this cohort. Monogenic IBD and nonmonogenic IBD demonstrated similar clinical features. Next-generation sequencing played an important role in the diagnosis of monogenic IBD.

Research perspectives

Next-generation sequencing revealed a high proportion of monogenic IBD in our VEO-IBD cohort. Multicenter prospective studies are expected to determine the incidence of monogenic IBD in the Chinese VEO-IBD population and to investigate the genetic characteristics of monogenic IBD in China.

REFERENCES

1 **Muise AM**, Snapper SB, Kugathasan S. The age of gene discovery in very early onset inflammatory bowel disease. *Gastroenterology* 2012; **143**: 285-288 [PMID: 22727850 DOI: 10.1053/j.gastro.2012.06.025]

2 **Benchimol EI**, Fortinsky KJ, Gozdyra P, Van den Heuvel M, Van Limbergen J, Griffiths AM. Epidemiology of pediatric inflammatory bowel disease: a systematic review of international trends. *Inflamm Bowel Dis* 2011; **17**: 423-439 [PMID: 20564651 DOI: 10.1002/ibd.21349]

3 **Uhlig HH**, Schwerd T, Koletzko S, Shah N, Kammermeier J, Elkadri A, Ouahed J, Wilson DC, Travis SP, Turner D, Klein C, Snapper SB, Muise AM; COLORS in IBD Study Group and NEOPICS. The diagnostic approach to monogenic very early onset inflammatory bowel disease. *Gastroenterology* 2014; **147**: 990-1007.e3 [PMID: 25058236 DOI: 10.1053/j.gastro.2014.07.023]

4 **Heyman MB**, Kirschner BS, Gold BD, Ferry G, Baldassano R, Cohen SA, Winter HS, Fain P, King C, Smith T, El-Serag HB. Children with early-onset inflammatory bowel disease (IBD): analysis of a pediatric IBD consortium registry. *J Pediatr* 2005; **146**: 35-40 [PMID: 15644819 DOI: 10.1016/j.jpeds.2004.08.043]

5 **Moeeni V**, Day AS. Impact of Inflammatory Bowel Disease upon Growth in Children and Adolescents. *ISRN Pediatr* 2011; **2011**: 365712 [PMID: 22389775 DOI: 10.5402/2011/365712]

6 **Kim S**, Koh H. Nutritional aspect of pediatric inflammatory bowel disease: its clinical importance. *Korean J Pediatr* 2015; **58**: 363-368 [PMID: 26576179 DOI: 10.3345/kjp.2015.58.10.363]

7 **Levine A**, Griffiths A, Markowitz J, Wilson DC, Turner D, Russell RK, Fell J, Ruemmele FM, Walters T, Sherlock M, Dubinsky M, Hyams JS. Pediatric modification of the Montreal classification for inflammatory bowel disease: the Paris classification. *Inflamm Bowel Dis* 2011; **17**: 1314-1321 [PMID: 21560194 DOI: 10.1002/ibd.21493]

8 **Kammermeier J**, Drury S, James CT, Dziubak R, Ocaka L, Elawad M, Beales P, Lench N, Uhlig HH, Bacchelli C, Shah N. Targeted gene panel sequencing in children with very early onset inflammatory bowel disease--evaluation and prospective analysis. *J Med Genet* 2014; **51**: 748-755 [PMID: 25194001 DOI: 10.1136/jmedgenet-2014-102624]

9 **Levine A**, Koletzko S, Turner D, Escher JC, Cucchiara S, de Ridder L, Kolho KL, Veres G, Russell RK, Paerregaard A, Buderus S, Greer ML, Dias JA, Veereman-Wauters G, Lionetti P, Sladek M, Martin de Carpi J, Staiano A, Ruemmele FM, Wilson DC; European Society of Pediatric Gastroenterology, Hepatology, and Nutrition. ESPGHAN revised porto criteria for the diagnosis of inflammatory bowel disease in children and adolescents. *J Pediatr Gastroenterol Nutr* 2014; **58**: 795-806 [PMID: 24231644 DOI: 10.1097/MPG.0000000000000239]

10 **Mao H**, Yang W, Lee PP, Ho MH, Yang J, Zeng S, Chong CY, Lee TL, Tu W, Lau YL. Exome sequencing identifies novel compound heterozygous mutations of IL-10 receptor 1 in neonatal-onset Crohn's disease. *Genes Immun* 2012; **13**: 437-442 [PMID: 22476154 DOI: 10.1038/gene.2012.8]

11 **Yanagi T**, Mizuochi T, Takaki Y, Eda K, Mitsuyama K, Ishimura M, Takada H, Shouval DS, Griffith AE, Snapper SB, Yamashita Y, Yamamoto K. Novel exonic mutation inducing aberrant splicing in the IL10RA gene and resulting in infantile-onset inflammatory bowel disease: a case report. *BMC Gastroenterol* 2016; **16**: 10 [PMID: 26822028 DOI: 10.1186/s12876-016-0424-5]

12 **Engelhardt KR**, Shah N, Faizura-Yeop I, Kocacik Uygun DF, Frede N, Muise AM, Shteyer E, Filiz S, Chee R, Elawad M, Hartmann B, Arkwright PD, Dvorak C, Klein C, Puck JM, Grimbacher B, Glocker EO. Clinical outcome in IL-10- and IL-10 receptor-deficient patients with or without hematopoietic stem cell transplantation. *J Allergy Clin Immunol* 2013; **131**: 825-830 [PMID: 23158016 DOI: 10.1016/j.jaci.2012.09.025]

13 **Curnutte JT**, Hopkins PJ, Kuhl W, Beutler E. Studying X inactivation. *Lancet* 1992; **339**: 749 [PMID: 1347621]

14 **Roos D**. The genetic basis of chronic granulomatous disease. *Immunol Rev* 1994; **138**: 121-157 [PMID: 8070813]

15 **Ruel J**, Ruane D, Mehandru S, Gower-Rousseau C, Colombel JF. IBD across the age spectrum: is it the same disease? *Nat Rev Gastroenterol Hepatol* 2014; **11**: 88-98 [PMID: 24345891 DOI: 10.1038/nrgastro.2013.240]

16 **Kammermeier J**, Dziubak R, Pescarin M, Drury S, Godwin H, Reeve K, Chadokufa S, Huggett B, Sider S, James C, Acton N, Cernat E, Gasparetto M, Noble-Jamieson G, Kiparissi F, Elawad M, Beales PL, Sebire NJ, Gilmour K, Uhlig HH, Bacchelli C, Shah N. Phenotypic and Genotypic Characterisation of Inflammatory Bowel Disease Presenting Before the Age of 2 years. *J Crohns Colitis* 2017; **11**: 60-69 [PMID: 27302973 DOI: 10.1093/ecco-jcc/jjw118]

17 **Ledder O**, Catto-Smith AG, Oliver MR, Alex G, Cameron DJ, Hardikar W. Clinical patterns and outcome of early-onset inflammatory bowel disease. *J Pediatr Gastroenterol Nutr* 2014; **59**: 562-564 [PMID: 24979317 DOI: 10.1097/MPG.0000000000000465]

18 **Gupta N**, Bostrom AG, Kirschner BS, Cohen SA, Abramson O, Ferry GD, Gold BD, Winter HS, Baldassano RN, Smith T, Heyman MB. Presentation and disease course in early- compared to later-onset pediatric Crohn's disease. *Am J Gastroenterol* 2008; **103**: 2092-2098 [PMID: 18796101 DOI: 10.1111/j.1572-0241.2008.02000.x]

19 **Xiao Y**, Wang XQ, Yu Y, Guo Y, Xu X, Gong L, Zhou T, Li XQ, Xu CD. Comprehensive mutation screening for 10 genes in Chinese patients suffering very early onset inflammatory bowel disease. *World J Gastroenterol* 2016; **22**: 5578-5588 [PMID: 27350736 DOI: 10.3748/wjg.v22.i24.5578]

20 **Al-Hussaini A**, El Mouzan M, Hasosah M, Al-Mehaidib A, ALSaleem K, Saadah OI, Al-Edreesi M. Clinical Pattern of Early-Onset Inflammatory Bowel Disease in Saudi Arabia: A Multicenter National Study. *Inflamm Bowel Dis* 2016; **22**: 1961-1970 [PMID: 27104817 DOI: 10.1097/MIB.0000000000000796]

21 **Marciano BE**, Rosenzweig SD, Kleiner DE, Anderson VL, Darnell DN, Anaya-O'Brien S, Hilligoss DM, Malech HL, Gallin JI, Holland SM. Gastrointestinal involvement in chronic granulomatous disease. *Pediatrics* 2004; **114**: 462-468 [PMID: 15286231]

22 **Glocker EO**, Kotlarz D, Boztug K, Gertz EM, Schäffer AA, Noyan F, Perro M, Diestelhorst J, Allroth A, Murugan D, Hätscher

N, Pfeifer D, Sykora KW, Sauer M, Kreipe H, Lacher M, Nustede R, Woellner C, Baumann U, Salzer U, Koletzko S, Shah N, Segal AW, Sauerbrey A, Buderus S, Snapper SB, Grimbacher B, Klein C. Inflammatory bowel disease and mutations affecting the interleukin-10 receptor. *N Engl J Med* 2009; **361**: 2033-2045 [PMID: 19890111 DOI: 10.1056/NEJMoa0907206]

23 **Worthey EA**, Mayer AN, Syverson GD, Helbling D, Bonacci BB, Decker B, Serpe JM, Dasu T, Tschannen MR, Veith RL, Basehore MJ, Broeckel U, Tomita-Mitchell A, Arca MJ, Casper JT, Margolis DA, Bick DP, Hessner MJ, Routes JM, Verbsky JW, Jacob HJ, Dimmock DP. Making a definitive diagnosis: successful clinical application of whole exome sequencing in a child with intractable inflammatory bowel disease. *Genet Med* 2011; **13**: 255-262 [PMID: 21173700 DOI: 10.1097/GIM.0b013e3182088158]

24 **Uzel G**, Sampaio EP, Lawrence MG, Hsu AP, Hackett M, Dorsey MJ, Noel RJ, Verbsky JW, Freeman AF, Janssen E, Bonilla FA, Pechacek J, Chandrasekaran P, Browne SK, Agharahimi A, Gharib AM, Mannurita SC, Yim JJ, Gambineri E, Torgerson T, Tran DQ, Milner JD, Holland SM. Dominant gain-of-function STAT1 mutations in FOXP3 wild-type immune dysregulation-polyendocrinopathy-enteropathy-X-linked-like syndrome. *J Allergy Clin Immunol* 2013; **131**: 1611-1623 [PMID: 23534974 DOI: 10.1016/j.jaci.2012.11.054]

25 **Ammann S**, Elling R, Gyrd-Hansen M, Dückers G, Bredius R, Burns SO, Edgar JD, Worth A, Brandau H, Warnatz K, Zur Stadt U, Hasselblatt P, Schwarz K, Ehl S, Speckmann C. A new functional assay for the diagnosis of X-linked inhibitor of apoptosis (XIAP) deficiency. *Clin Exp Immunol* 2014; **176**: 394-400 [PMID: 24611904 DOI: 10.1111/cei.12306]

26 **Suzuki T**, Sasahara Y, Kikuchi A, Kakuta H, Kashiwabara T, Ishige T, Nakayama Y, Tanaka M, Hoshino A, Kanegane H, Abukawa D, Kure S. Targeted Sequencing and Immunological Analysis Reveal the Involvement of Primary Immunodeficiency Genes in Pediatric IBD: a Japanese Multicenter Study. *J Clin Immunol* 2017; **37**: 67-79 [PMID: 27747465 DOI: 10.1007/s10875-016-0339-5]

27 **Huang Z**, Peng K, Li X, Zhao R, You J, Cheng X, Wang Z, Wang Y, Wu B, Wang H, Zeng H, Yu Z, Zheng C, Wang Y, Huang Y. Mutations in Interleukin-10 Receptor and Clinical Phenotypes in Patients with Very Early Onset Inflammatory Bowel Disease: A Chinese VEO-IBD Collaboration Group Survey. *Inflamm Bowel Dis* 2017; **23**: 578-590 [PMID: 28267044 DOI: 10.1097/MIB.0000000000001058]

28 **Neven B**, Mamessier E, Bruneau J, Kaltenbach S, Kotlarz D, Suarez F, Masliah-Planchon J, Billot K, Canioni D, Frange P, Radford-Weiss I, Asnafi V, Murugan D, Bole C, Nitschke P, Goulet O, Casanova JL, Blanche S, Picard C, Hermine O, Rieux-Laucat F, Brousse N, Davi F, Baud V, Klein C, Nadel B, Ruemmele F, Fischer A. A Mendelian predisposition to B-cell lymphoma caused by IL-10R deficiency. *Blood* 2013; **122**: 3713-3722 [PMID: 24089328 DOI: 10.1182/blood-2013-06-508267]

29 **Marsh RA**, Rao K, Satwani P, Lehmberg K, Müller I, Li D, Kim MO, Fischer A, Latour S, Sedlacek P, Barlogis V, Hamamoto K, Kanegane H, Milanovich S, Margolis DA, Dimmock D, Casper J, Douglas DN, Amrolia PJ, Veys P, Kumar AR, Jordan MB, Bleesing JJ, Filipovich AH. Allogeneic hematopoietic cell transplantation for XIAP deficiency: an international survey reveals poor outcomes. *Blood* 2013; **121**: 877-883 [PMID: 23131490 DOI: 10.1182/blood-2012-06-432500]

30 **Barzaghi F**, Passerini L, Bacchetta R. Immune dysregulation, polyendocrinopathy, enteropathy, x-linked syndrome: a paradigm of immunodeficiency with autoimmunity. *Front Immunol* 2012; **3**: 211 [PMID: 23060872 DOI: 10.3389/fimmu.2012.00211]

P- Reviewer: Ishige T, Sandberg KC **S- Editor**: Wang XJ
L- Editor: Filipodia **E- Editor**: Huang Y

World Journal of Gastroenterology

Submit a Manuscript: http://www.f6publishing.com

World J Gastroenterol 2018 March 7; 24(9): 1046-1055

DOI: 10.3748/wjg.v24.i9.1046

ISSN 1007-9327 (print) ISSN 2219-2840 (online)

ORIGINAL ARTICLE

Randomized Controlled Trial

Effect of polyglycolic acid sheet plus esophageal stent placement in preventing esophageal stricture after endoscopic submucosal dissection in patients with early-stage esophageal cancer: A randomized, controlled trial

Ning-Li Chai, Jia Feng, Long-Song Li, Sheng-Zhen Liu, Chen Du, Qi Zhang, En-Qiang Linghu

Ning-Li Chai, Jia Feng, Long-Song Li, Sheng-Zhen Liu, Chen Du, Qi Zhang, En-Qiang Linghu, Department of Gastroenterology, Chinese PLA General Hospital, Beijing 100853, China

ORCID number: Ning-Li Chai (0000-0003-0583-4189); Jia Feng (0000-0001-6839-3531); Long-Song Li (0000-0003-4593-7668); Sheng-Zhen Liu (0000-0001-6495-2818); Chen Du (0000-0003-4790-6056); Qi Zhang (0000-0002-6550-9217); En-Qiang Linghu (0000-0002-6311-5265).

Author contributions: Chai NL and Feng J contributed equally to this article; Linghu EQ contributed to study conception and design; Chai NL and Feng J contributed to data acquisition, analysis, and interpretation; Li LS and Liu SZ drafted the manuscript; Du C and Zhang Q contributed to editing and revising the article; all authors read and approved the manuscript.

Institutional review board statement: The study was reviewed and approved by the Ethics Committee of Chinese PLA General Hospital.

Clinical trial registration statement: This study is registered on http:// www.chictr.org.cn (No. chictr-inr-16008709).

Informed consent statement: All study participants provided written informed consent prior to study enrolment.

Conflict-of-interest statement: The authors have no conflicts of interest to disclose.

Data sharing statement: No additional data are available.

Manuscript source: Unsolicited manuscript

Correspondence to: En-Qiang Linghu, MD, PhD, Chief Doctor, Department of Gastroenterology, Chinese PLA General Hospital, 28 Fuxing Road, Beijing 100853, China. 0572013@fudan.edu.cn
Telephone: +86-10-55499292
Fax: +86-10-55499292

Received: September 20, 2017
Peer-review started: September 21, 2017
First decision: September 27, 2017
Revised: January 2, 2018
Accepted: January 16, 2018
Article in press: January 16, 2018
Published online: March 7, 2018

Abstract

AIM

To assess the effect of polyglycolic acid (PGA) plus stent placement compared with stent placement alone in the prevention of post-endoscopic submucosal dissection (ESD) esophageal stricture in early-stage esophageal cancer (EC) patients.

METHODS

Seventy EC patients undergoing ESD were enrolled in this randomized, controlled study. Patients were allocated randomly at a 1:1 ratio into two groups as follows: (1) PGA plus stent group (PGA sheet-coated stent placement was performed); and (2) Stent group (only stent placement was performed). This study was

registered on http://www.chictr.org.cn (No. chictr-inr-16008709).

RESULTS

The occurrence rate of esophageal stricture in the PGA plus stent group was 20.5% (n = 7), which was lower than that in the stent group (46.9%, n = 15) (P = 0.024). The mean value of esophageal stricture time was 59.6 ± 16.1 d and 70.7 ± 28.6 d in the PGA plus stent group and stent group (P = 0.174), respectively. Times of balloon dilatation in the PGA plus stent group were less than those in the stent group [4 (2-5) *vs* 6 (1-14), P = 0.007]. The length (P = 0.080) and diameter (P = 0.061) of esophageal strictures were numerically decreased in the PGA plus stent group, whereas no difference in location (P = 0.232) between the two groups was found. Multivariate logistic analysis suggested that PGA plus stent placement (P = 0.026) was an independent predictive factor for a lower risk of esophageal stricture, while location in the middle third (P = 0.034) and circumferential range = 1/1 (P = 0.028) could independently predict a higher risk of esophageal stricture in EC patients after ESD.

CONCLUSION

PGA plus stent placement is more effective in preventing post-ESD esophageal stricture compared with stent placement alone in EC patients with early-stage disease.

Key words: Esophageal cancer; Endoscopic submucosal dissection; Polyglycolic acid plus stent placement; Esophageal stricture

Core tip: This study determines the effect of polyglycolic acid (PGA) plus stent placement compared with stent placement alone in the prevention of post-endoscopic submucosal dissection (ESD) esophageal stricture in early-stage esophageal cancer (EC) patients. Our findings confirm that PGA plus stent placement is more effective in preventing post-ESD esophageal stricture compared with stent placement alone in EC patients with early-stage disease.

Chai NL, Feng J, Li LS, Liu SZ, Du C, Zhang Q, Linghu EQ. Effect of polyglycolic acid sheet plus esophageal stent placement in preventing esophageal stricture after endoscopic submucosal dissection in patients with early-stage esophageal cancer: A randomized, controlled trial. *World J Gastroenterol* 2018; 24(9): 1046-1055 Available from: URL: http://www.wjgnet.com/1007-9327/full/v24/i9/1046.htm DOI: http://dx.doi.org/10.3748/wjg.v24.i9.1046

INTRODUCTION

Esophageal cancer (EC) is one of the most common carcinomas with high mortality and has been identified as the sixth leading cause of cancer-related death worldwide[1]. Based on 2015 global cancer statistics, an estimated 455800 new EC cases and 400200 deaths occurred in 2012. In the United States, approximately 16940 new EC cases and 15690 deaths will be seen in 2017[2,3]. Endoscopic submucosal dissection (ESD), performed as an endoscopic resection technique, has been widely utilized in the treatment of EC patients with early-stage disease, due to its minimal invasiveness and high rate of *en bloc* resection[4,5]. However, more than 30% of EC patients after ESD still experience postoperative esophageal stricture, which is characterized by dysphagia, dramatically decreasing the quality of life[6,7].

To prevent post-ESD esophageal stricture, various treatments have been implemented, such as polyglycolic acid (PGA) sheet, stent placement, and esophageal balloon dilatation[8]. Among these, PGA sheet, a biodegradable suture material, could be used to prevent post-ESD esophageal stricture because of its advantages of reinforcing suture and minimal scar contracture, although the limitation of instability between the PGA sheet and wound surface after long-term pasting still exists[9-11]. Another popular method is stent placement, which is frequently used with covered self-expandable metal material, and has been verified to have curative effects on refractory stricture to some extent, although its complications, such as translocation and promotion of granulation tissue proliferation, still affect its clinical outcomes in EC patients[12,13].

Although some studies on the applications of combinations of two or three treatments in the prevention of esophageal stricture after ESD have been performed, no study has explored the effect of the combination of PGA and stent placement in the prevention of post-ESD esophageal stricture[9,14]. Therefore, the aim of this study was to assess the effect of PGA plus stent placement compared with stent placement alone in the prevention of post-ESD esophageal stricture in early-stage EC patients.

MATERIALS AND METHODS

Patients

A total of 70 early-stage EC patients receiving ESD at Department of Gastroenterology, China PLA General Hospital from July 2016 to May 2017 were consecutively enrolled in this randomized controlled study. The inclusion criteria were as follows: (1) Circumferential range above 3/4; (2) Longitudinal length above 3 cm; (3) Lesion depth no more than M2; and (4) Tumor lesion could be completely removed. The exclusion criteria were as follows: (1) Patients with coagulative dysfunction, hepatic failure, renal failure, or cardiopulmonary dysfunction; (2) Patients complicated with malignant hematological disease or other solid tumors; (3) Patients who had a previous history of esophagectomy or radiation therapy; (4) Patients

who were unable to complete the ESD operation; (5) Pregnant or lactating women; (6) Patients who could not be followed regularly; and (7) Patients who refused to participate in this study.

This study was approved by the Ethics Committee of China PLA General Hospital (approval No. S2016-059-01), and all participants provided written informed consent. This study was registered on http://www.chictr.org.cn (Chinese Clinical Trial Registry conducted by World Health Organization; registration No. chictr-inr-16008709).

Randomization

The randomization code was generated by a statistician using the blocked randomization method with block length set as four because of the need for allocation balance between the two groups (1:1 ratio). The documents were subsequently sent and kept in Shanghai Qeejen Bio-tech Company (a medical and statistical service company). After screening, when a patient was eligible for the study, a call was made to the Qeejen Company, and a unique subject identification number was provided from the randomized module.

Treatment

After the randomization, patients were allocated to the PGA plus stent treatment group or stent treatment group at a 1:1 ratio. In the PGA plus stent group, the patients received PGA sheet-coated stent placement to prevent esophageal stricture post ESD operation; in the stent group, the patients received only stent placement to prevent esophageal stricture post ESD operation.

ESD procedure

After intravenous anesthesia, patients with tracheal intubation and oropharyngeal tube placement underwent endoscope (Olympus, Japan) insertion to the area of the tumor lesion. Subsequently, the lesion margins were stained with iodine, and the submucosa was labeled. Then, the lesion dissections were performed, and endoscopic submucosal tunnel dissection was used for lesion stripping, followed by hemostasis.

Combination of PGA membrane and stent

According to the ESD wound length (Figure 1A), the length of stent (Derman Science, China, 1.7 cm of diameter, stainless steel, silicone rubber membrane) was selected (Figure 1B), followed by PGA sheet selection (NEOVEIL, Japan, 100 mm × 100 mm × 0.15 mm) (Figure 1C). Subsequently, the stent was coated with the PGA sheet (Figure 1D), and the covered place was designed to the ESD wound site after stent release. Then, this stent covered with a PGA sheet was mounted on the conveyer for the esophageal stent ring supporter (Figure 1E and F) and inserted under endoscopic observation (Figure 1G).

Stent placement

The length of the ESD wound was measured, and then the appropriate length of metal coated stent was selected (Derman Science, China, 1.7 cm of diameter, stainless steel, silicone rubber membrane), which was beyond the top and bottom edge of the lesion by more than 2 cm. Subsequently, the guide wire was placed under the endoscope, and then the endoscope was pulled out and the conveyer was inserted for the esophageal stent ring supporter along with the guide wire for the stent placement. After stent placement, the endoscope was inserted again to observe the stent position. A chest X-ray was performed after the stent placement, and the stent position was recorded.

Stent removal

In the PGA plus stent group, the stent was removed by endoscopy at 4 wk, whereas in the stent group, the stent was removed at 8 wk after operation. Endoscopic evaluation of the ESD wound was performed (Figure 2A-C). The time to remove the stent between the two groups was different because PGA is a biodegradable suture material, which would be degraded after a period of time. According to a preliminary study with a small sample size, we found that when PGA plus stent placement was used to prevent post-ESD esophageal stricture in early-stage EC patients, the PGA was degraded at approximately 3 or 4 wk after ESD, and therefore, the previous clinical experiences suggested that removing PGA plus stent placement at 4 wk might be a good choice in EC patients.

Assessment

The primary endpoint was esophageal stricture occurrence after ESD operation, which was defined as diameter of stricture section below 1 cm (endoscopy could not pass through) under endoscopy. The secondary endpoints were as follows: time to esophageal stricture; location, length, and diameter of esophageal stricture; and balloon dilatation times for the esophageal stricture.

Follow-up

All patients were followed through clinic visits or telephone interviews. Each patient was asked if dysphagia or other symptoms occurred at each visit or call, and if distinct dysphagia was determined, endoscopy was performed to examine the esophageal stricture. Chest X-ray examination was performed every 2 wk to monitor the position of esophageal stent, and if a stent shifted more than 2 cm, endoscopy was performed to adjust the stent to the original place.

Balloon dilatation

All patients with esophageal stricture received endoscopic balloon dilation treatment (balloon diameter: 8 mm/10 mm/12 mm/15 mm, Boston Scientific, United States). The esophageal stricture section was repeatedly

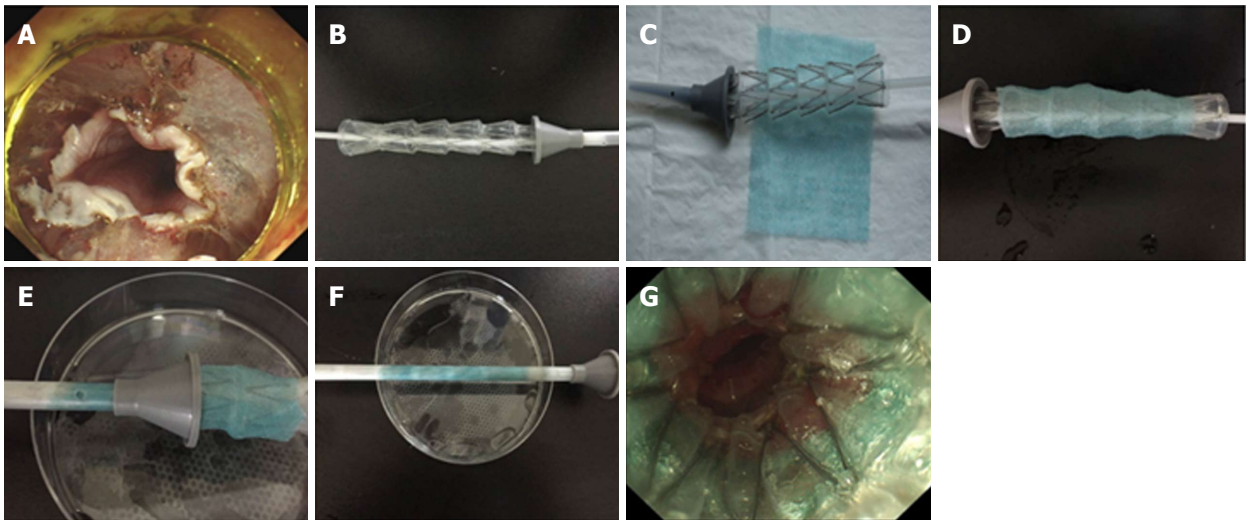

Figure 1 Combination of polyglycolic acid sheet and stent. A: Measurement of endoscopic submucosal dissection wound length; B: Adjustment of stent length; C: Polyglycolic acid sheet selection based on lesion length; D: Stent coating with polyglycolic acid (PGA) sheet; E-F: Stent covered with PGA sheet mounted on the stent support; G: Insertion of stent covered with PGA sheet under endoscopic observation.

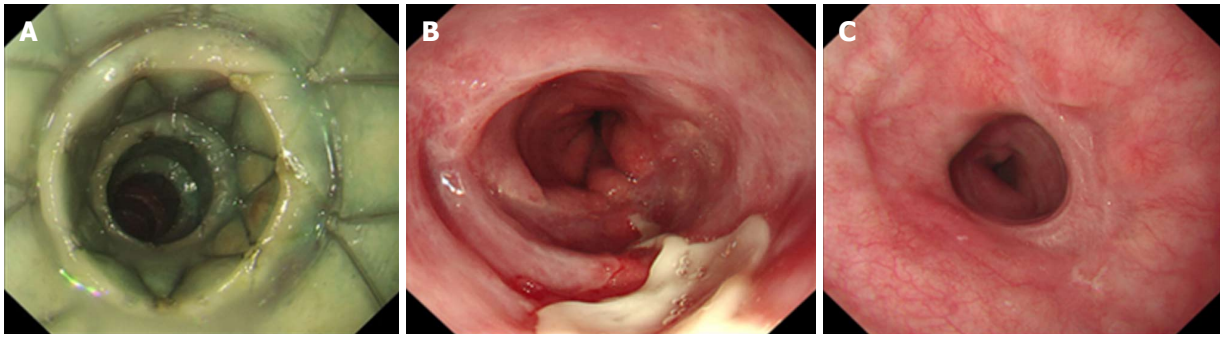

Figure 2 The management of one of the study patients. A: Stent covered with polyglycolic acid sheet inserted after 1 wk; B: Stent removed after 4 wk with a portion of wound not healed; C: No formation of esophageal stricture observed after 2 mo.

dilated until the endoscope could successfully pass through at each endoscopic examination, and balloon dilation was performed every week until the endoscope could pass through the section before dilation.

Statistical analysis

Statistical analyses were performed using SPSS 22.0 (IBM, United States) and OFFICE 2010 (Microsoft, United States). Data are mainly presented as mean value ± SD, median value (range), or count (percentage). The comparison between two groups was determined by *t*-test, Chi-square test, or Wilcoxon rank sum test. Factors affecting esophageal stricture occurrence were evaluated by univariate logistic regression analysis, and all factors with a *P*-value below 0.1 were further detected by multivariate logistic regression analysis. $P < 0.05$ was considered significant.

RESULTS

Study flow

In the current study, 109 EC patients were screened for eligibility, while 39 cases were excluded as follows: 21 patients for exclusions and 10 patients who refused to participate in this study (Figure 3). Subsequently, the remaining 70 patients were randomized at a 1:1 ratio into two groups as follows: PGA plus stent group and stent group. In the PGA plus stent group, one case withdrew during the study due to a lesion depth > M2 post-ESD operation, and 34 (97%) cases completed the entire study. In the stent group, there were three total withdrawals; three patients with lesion depth more than M2 after ESD operation withdrew, and 32 (91%) cases completed the entire study. Ultimately, a total of 66 EC patients completed the final analysis. After the operation, the stent was removed by endoscopy at 4 wk in the PGA plus stent group, and it was removed at 8 wk in the stent group. During the study, stent displacement was adjusted by endoscopy. Chest X-ray examination was performed every 2 wk. Endoscopy was performed to check the esophageal stricture. All patients with esophageal stricture received endoscopic balloon dilation treatment.

Baseline characteristics

As shown in Table 1, no difference in patients'

Table 1 Baseline characteristics *n* (%)

Parameter	PGA + stent group (*n* = 34)	Stent group (*n* = 32)	*P* value
Patients characteristic			
Age (yr)	62.74 ± 8.38	59.91 ± 8.80	0.186
Gender (Male/Female)	22/12	18/14	0.482
Tumor lesion feature			
Location			0.145
Upper third	0 (0)	0 (0)	
Middle third	12 (35)	17 (53)	
Lower third	22 (65)	15 (47)	
Tissue depth			0.331
M1	20 (59)	15 (47)	
M2	14 (41)	17 (53)	
Longitudinal length (cm)	5.97 ± 2.68	6.06 ± 2.12	0.878
Circumferential range			0.684
3/4	12 (35)	14 (44)	
4/5	8 (24)	8 (25)	
1/1	14 (41)	10 (31)	

Data are presented as mean ± SD or count (with or without percentage). Comparison was performed by *t*-test or Chi-square test. $P < 0.05$ was considered significant. PGA: Polyglycolic acid.

Table 2 Comparison of esophageal stricture features in polyglycolic acid + stent and stent groups

Parameter	PGA + stent group (*n* = 7)	Stent group (*n* = 15)	*P* value
Length (cm)	0.97 + 0.59	1.47 + 0.59	0.080
Diameter (cm)	0.37 + 0.17	0.51 + 0.14	0.061
Location (distance from the incisors, cm)	31.71 + 3.20	29.07 + 5.20	0.232
Balloon dilatation times	4 (2-5)	6 (1-14)	0.007

Data are presented as mean ± SD or median (range). Comparison was performed by *t*-test or Wilcoxon rank sum test. $P < 0.05$ was considered significant. PGA: Polyglycolic acid.

characteristics and tumor lesion features between the PGA plus stent group and stent group were observed ($P > 0.05$ for all). The numbers of patients with tumor location at the upper, middle, and lower third were 0 (0%), 12 (35%), and 22 (65%), respectively, in the PGA plus stent group, while 0 (0%), 17 (53%), and 15 (47%) in the stent group ($P = 0.145$). In terms of tissue depth ($P = 0.331$), there were 20 (59%) patients with M1 and 14 (41%) patients with M2 in the PGA plus stent group and 15 (47%) patients with M1 and 17 (53%) patients with M2 were in the stent group. The mean value of longitudinal length was 5.97 ± 2.68 cm in the PGA plus stent group and 6.06 ± 2.12 cm in the stent group ($P = 0.878$). Other baseline characteristics are presented in Table 1.

Comparison of post-ESD stricture in the two groups

The occurrence rate of patients with esophageal stricture in the PGA plus stent group was 20.5% ($n = 7$), which was lower than that in the stent group (46.9%, $n = 15$) ($P = 0.024$, Figure 4A). Regarding time to esophageal stricture, the mean value was 59.6 ± 16.1 d and 70.7 ± 28.6 d in the PGA plus stent group and stent groups, respectively ($P = 0.174$, Figure 4B).

Comparison of esophageal stricture features in the two groups

T-test or Wilcoxon rank sum test was used to compare esophageal stricture features between the PGA plus stent and stent groups (Table 2). The balloon dilatation times for esophageal stricture in the PGA plus stent group were less than those in the stent group [4 (2-5) *vs* 6 (1-14), $P = 0.007$]. Length ($P = 0.080$) and diameter ($P = 0.061$) of esophageal stricture were numerically decreased in the PGA plus stent group compared with the stent group, whereas there was no difference in location ($P = 0.232$) between the two groups (Table 2).

Comparison of tumor lesion features in patients with esophageal stricture

As presented Table 3, comparison of tumor lesion features in patients with esophageal stricture between the PGA plus stent and stent groups was performed. No difference was observed in location ($P = 0.899$), tissue depth ($P = 0.823$), longitudinal length ($P = 0.360$), or circumferential range ($P = 0.181$) in patients with

Table 3 Comparison of tumor lesion features in patients with esophageal stricture *n* (%)

Parameter	PGA + stent group (*n* = 7)	Stent group (*n* = 15)	*P* value
Location			0.899
Upper third	0 (0)	0 (0)	
Middle third	4 (57)	9 (60)	
Lower third	3 (43)	6 (40)	
Tissue depth			0.823
M1	2 (29)	5 (33)	
M2	5 (71)	10 (67)	
Longitudinal length (cm)	7.71 + 3.50	6.60 + 2.10	0.360
Circumferential range			0.181
3/4	0 (0)	4 (27)	
4/5	1 (14)	4 (27)	
1/1	6 (86)	7 (47)	

Data are presented as mean ± SD or count (percentage). Comparison was determined by *t*-test or Chi-square test. $P < 0.05$ was considered significant. PGA: Polyglycolic acid.

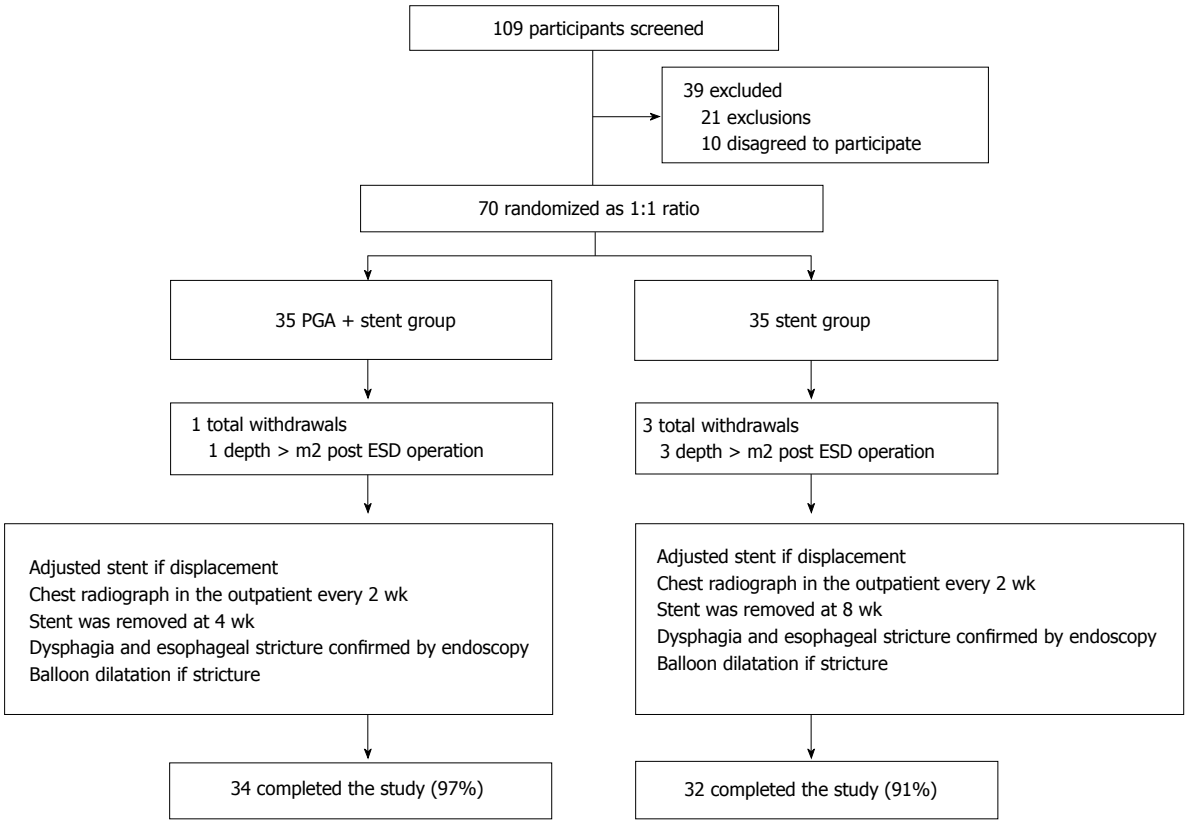

Figure 3 Study flow. ESD: Endoscopic submucosal dissection.

esophageal stricture between the two groups (Table 3).

Analysis of factors affecting esophageal stricture occurrence

Factors affecting esophageal stricture occurrence were determined by univariate logistic regression analysis (Table 4). PGA plus stent placement ($P = 0.027$) was correlated with a lower possibility of esophageal stricture occurrence, whereas circumferential range = 1/1 ($P = 0.008$) and tissue depth M2 ($P = 0.017$) were associated with a higher probability of esophageal stricture occurrence. Location in the middle third ($P = 0.083$) and longitudinal length ⩾ 6 cm ($P = 0.059$) were two factors that appeared to be correlated with a higher risk of esophageal stricture but without statistical significance. All factors with a *P*-value not above 0.1 were further detected by multivariate logistic regression analysis. PGA plus stent placement ($P = 0.026$) was an independent predictive factor for a lower risk of esophageal stricture, whereas location in the middle third ($P = 0.034$) and circumferential range = 1/1 ($P = 0.028$) could independently predict a

Table 4 Logistic analysis of factors affecting esophageal stricture occurrence

Parameter	Univariate logistic regression				Multivariate logistic regression			
	P value	OR	95%CI		*P* value	OR	95%CI	
			Lower	Higher			Lower	Higher
PGA + stent (*vs* stent alone)	0.027	0.294	0.099	0.868	0.026	0.197	0.047	0.820
Age ⩾ 62 yr	0.298	1.733	0.615	4.887	-	-	-	-
Location - middle third (*vs* lower third)	0.083	2.528	0.886	7.214	0.034	5.148	1.135	23.344
Longitudinal length ⩾ 6 cm	0.059	2.779	0.963	8.019	0.092	3.826	0.801	18.270
Circumferential range = 1/1 (*vs* others)	0.008	4.333	1.457	12.888	0.028	5.113	1.194	21.892
Tissue depth M2 (*vs* M1)	0.017	3.750	1.264	11.123	0.069	3.284	0.912	11.822

Data are presented as *P*-value, OR (odds ratio), and 95%CI. Factors affecting esophageal stricture occurrence were determined by univariate logistic regression analysis, while all factors with a *P*-value less than 0.1 were further detected by multivariate logistic regression analysis. *P*-value < 0.05 was considered significant. PGA: Polyglycolic acid.

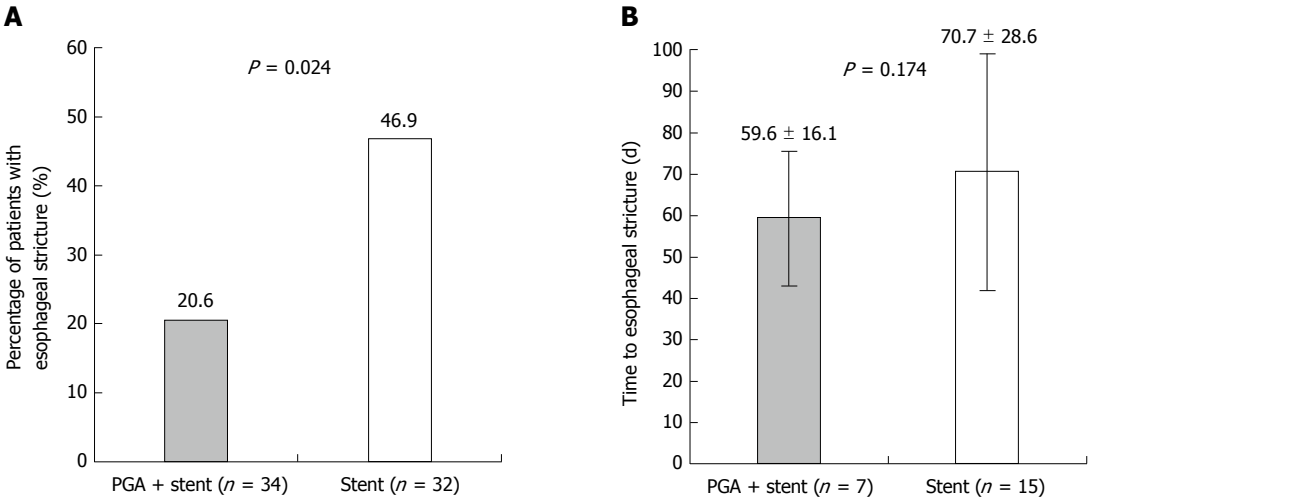

Figure 4 Comparison of post-endoscopic submucosal dissection stricture in polyglycolic acid plus stent and stent groups. A: Patients in the polyglycolic acid (PGA) plus stent group had a lower occurrence rate of esophageal stricture than that in the stent group; B: No difference in time to esophageal stricture was observed between the PGA plus stent and stent groups. Comparison of post-endoscopic submucosal dissection stricture in the PGA plus stent and stent groups was performed by *t*-test. *P* < 0.05 was considered significant.

higher risk of esophageal stricture in EC patients after ESD.

DISCUSSION

In the current study, we found that: (1) the occurrence rate of esophageal stricture in the PGA plus stent group was lower compared with the stent group, and the balloon dilatation times of esophageal stricture in the PGA plus stent group were less compared with the stent group; and (2) PGA plus stent placement could independently predict a lower occurrence rate of esophageal stricture, while location in the middle third and circumferential range = 1/1 were independent predictive factors for a higher possibility of post-ESD esophageal stricture occurrence in EC patients.

ESD, which is considered an effective method to completely resect mucosal lesions, has been popularly applied in EC patients with early-stage disease, although due to the physiological characteristics of the esophageal cavity, esophageal stricture frequently occurs after ESD[4,15,16]. Recent data indicate that the appearance of several fibroblasts and the shrinking of the natural muscle layer are present in the formation of post-ESD esophageal stricture, which suggests that fiber proliferation, scar formation, and wound contracture might contribute to the formation of post-ESD esophageal stricture[17].

Stenting has been regarded as a useful way to prevent post-ESD esophageal stricture, although a high recurrence rate still exists in most patients after removing the stent, and some patients with long-term stent placement experience several complications, such as displacement and granulation tissue hyperplasia[18,19]. In clinical practice, stent insertion has been reported to decrease the dysphagia score and the mean diameter of esophageal stricture[20]. PGA sheet, a polymer with a fiber mesh structure, could: (1) provide abundant cytoskeletons to support cell crawling during the repair process, and inhibit rejection reaction by its strong degradative function, thereby leading to a decreased risk of scar germination and stricture formation; and (2) carry cells and medicines to promote cell repair and wound healing. An interesting study revealed that

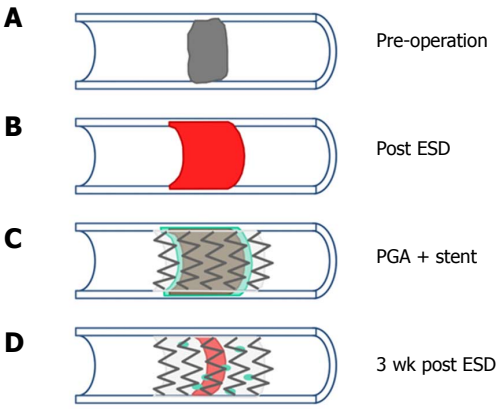

Figure 5 The endoscopic submucosal dissection wound before and after the polyglycolic acid sheet plus stent placement. A: The esophageal lesion before endoscopic submucosal dissection (ESD); B: The mucosal defect after ESD; C: The ESD wound after the PGA sheet plus stent placement; D: The PGA sheet plus stent placement was inserted after 3 wk.

PGA sheets could shield mucosal defects and prevent scarring, reducing postoperative adverse events in patients with colorectal ESD[21]. However, some limitations of PGA sheets still exist, which are easy to fall off for long-term utilization[9,10]. Therefore, both stents and PGA can decrease the risk of esophageal stricture to some extent. However, there remain several limitations. No study on the effects of the combined application of PGA and stent has been reported. Our study compared the occurrence rate of post-ESD esophageal stricture between the PGA plus stent and stent groups and indicated that the percentage of post-ESD esophageal stricture in the PGA plus stent group was lower compared with the stent group. Balloon dilatation, which is one of the most common treatments for esophageal stricture, has been identified to have good short-term efficacy, whereas the long-term curative effect is still far from satisfactory. A previous study suggested that the average usage rate of balloon dilatation is estimated to be 16 times for post-ESD esophageal stricture[22]. The results of our study also found that the balloon dilatation times for esophageal stricture in the PGA plus stent group were less than those in the stent group [4 (2-5) *vs* 6 (1-14) times]. Therefore, these findings indicated that PGA plus stent placement could decrease the risk of esophageal stricture and the balloon dilatation times for esophageal stricture compared with stent placement alone. Possible explanations might be as follows: (1) The stent could provide radial force to fix the PGA sheet, thereby preventing the defluvium of the PGA sheet[18,19]; and (2) The PGA sheet could increase the friction between the stent and wound surface, reducing stent displacement, and also provide cytoskeleton and carry medicine to accelerate cell repair and wound healing. Therefore, the interaction of the PGA sheet with the stent could decrease the occurrence rate of post-ESD esophageal stricture[9,11]. However, seven patients still reported the formation of esophageal stricture in the PGA plus stent group. This occurrence might be explained by the fact that during the process of wound repair, epithelial cells usually crawl from the edge of the wound to the central area. Because of the long-term repair, the PGA sheet might be degraded to result in frameless support, leading to its defluvium and increasing the occurrence rate of esophageal stricture in the central area (Figure 5A-D). As to the predictive value, the results of the present study showed that PGA plus stent placement could be an independent factor to predict a lower possibility of esophageal stricture occurrence. The possible reasons are that the stent contributes to fixing the PGA sheet and the PGA sheet increases the friction to reduce stent displacement, thereby preventing the occurrence of post-ESD esophageal stricture[9,11,18,19]. Although there is no report on the effects of PGA plus stent in the prevention of post-ESD esophageal stricture in EC patients, further studies investigating other combined treatments, such as PGA plus stent plus corticosteroids, are greatly needed. Furthermore, the results of our study also found that shorter length (P = 0.080) and diameter (P = 0.061) were observed in the PGA plus stent group compared with the stent group, which suggests that the interaction of PGA and stent might decrease the severity of the degree of esophageal stricture.

In clinical practice, glucocorticoids have established their value in inhibiting the inflammatory response, repressing collagen synthesis, and promoting collagen decomposition, thereby preventing the formation of post-ESD esophageal stricture[23,24]. Although glucocorticoid injection is a good way to decrease the occurrence of systemic adverse reactions, it still leads to several complications in EC patients after ESD, including perforation, bleeding, and mediastinal abscess[23,25]. Therefore, a PGA sheet infiltrated with a glucocorticoid (triamcinolone acetonide) might decrease the occurrence of post-ESD esophageal stricture while reducing adverse reactions. Furthermore, to optimize the methods to prevent esophageal stricture, we explored the combined application of PGA, stent, and glucocorticoid in three EC patients after ESD (Figure 6A-C). After stent removal, no formation of esophageal stricture occurred and good effectiveness was achieved during a 3 mo follow-up (Figure 6D and E). However, further study with a larger sample size and a longer follow-up period is necessary.

One limitation in the present study was that the total number of recruited EC patients was relatively small, which might cause lower statistical efficiency compared with a study with a large sample size. Therefore, a study with a larger sample size is needed to further confirm the efficacy of PGA plus stent placement in preventing esophageal stricture.

In conclusion, PGA plus stent placement is more effective in preventing post-ESD esophageal stricture compared with stent placement alone in EC patients

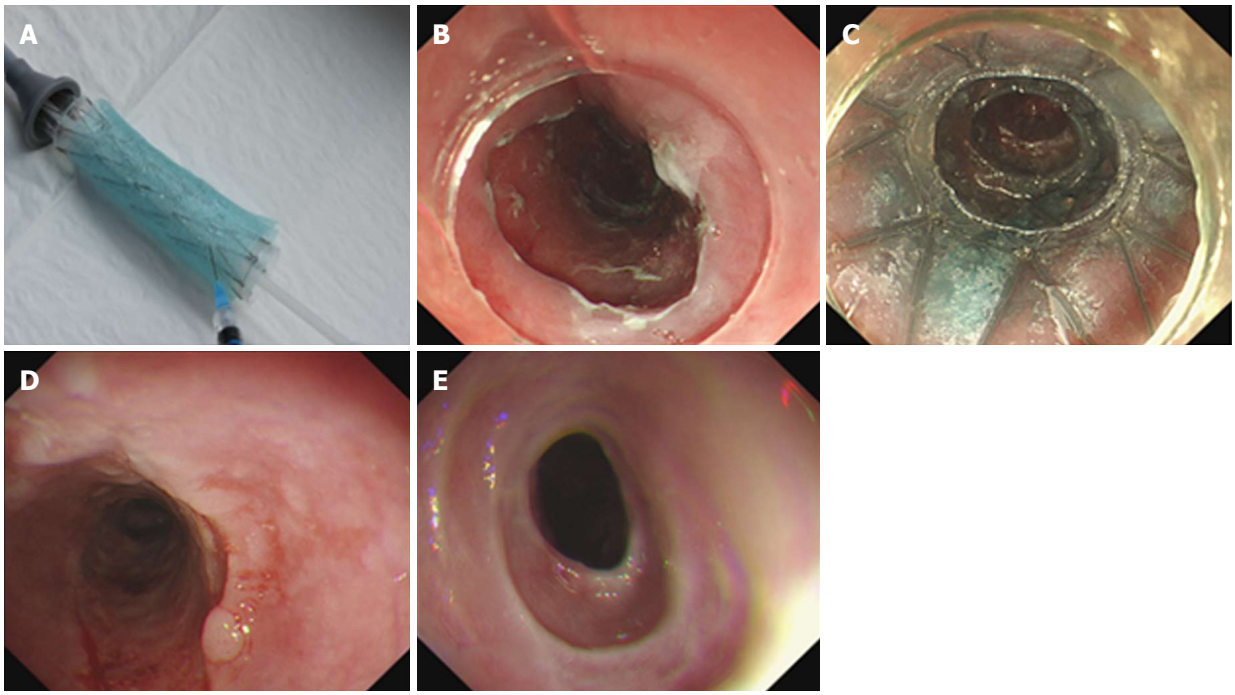

Figure 6 The management of one of the study patients. A: Stent covered with polyglycolic acid (PGA) sheet was injected with glucocorticoid before insertion; B: The mucosal defect after endoscopic submucosal dissection (ESD); C: The combination of PGA, stent, and glucocorticoid was applied after 1 wk; D: The endoscopic appearance of the esophagus 4 wk after ESD; E: The endoscopic appearance of the esophagus 3 mo after ESD.

with early-stage disease.

ARTICLE HIGHLIGHTS

Research background

Esophageal cancer (EC) is one of the most common carcinomas with high mortality, and more than 30% of EC patients after endoscopic submucosal dissection (ESD) still experience postoperative esophageal stricture, which dramatically decreases the quality of life.

Research motivation

The applications of combinations of two or three treatments in the prevention of esophageal stricture after ESD have been investigated in some studies. However, no study explored the effect of the combination of PGA and stent placement in the prevention of post-ESD esophageal stricture.

Research objectives

This study aimed to assess the effect of PGA plus stent placement *vs* stent placement alone in the prevention of post-ESD esophageal stricture in early-stage EC patients.

Research methods

About 70 EC patients undergoing ESD were enrolled in this study. Patients were allocated randomly at a 1:1 ratio into a PGA plus stent group (PGA sheet-coated stent placement was performed) and a stent group (only stent placement was performed). All patients were followed, and if dysphagia or other symptoms occurred, endoscopy was performed to examine the esophageal stricture.

Research results

The occurrence rate of esophageal stricture in the PGA plus stent group was lower than that in the stent group. Times of balloon dilatation in the PGA plus stent group were less than those in the stent group. Multivariate logistic analysis suggested that PGA plus stent placement was an independent predictive factor for a lower risk of esophageal stricture, while location in the middle third and circumferential range = 1/1 could independently predict a higher risk of esophageal stricture in EC patients after ESD.

Research conclusions

PGA plus stent placement is more effective in preventing post-ESD esophageal stricture *vs* stent placement alone in early-stage EC patients.

Research perspectives

The total number of recruited EC patients in the present study was relatively small. And a study with a larger sample size is needed to further confirm the efficacy of PGA plus stent placement in preventing esophageal stricture.

REFERENCES

1 **Mohammed F**. Esophageal cancer. *N Engl J Med* 2004; **350**: 1363-1364; author reply 1363-1364 [PMID: 15044652 DOI: 10.1056/NEJMc033106]
2 **Torre LA**, Bray F, Siegel RL, Ferlay J, Lortet-Tieulent J, Jemal A. Global cancer statistics, 2012. *CA Cancer J Clin* 2015; **65**: 87-108 [PMID: 25651787 DOI: 10.3322/caac.21262]
3 **Scott DL**, Wolfe F, Huizinga TW. Rheumatoid arthritis. *Lancet* 2010; **376**: 1094-1108 [PMID: 20870100 DOI: 10.1016/S0140-6736(10)60826-4]
4 **Ning B**, Abdelfatah MM, Othman MO. Endoscopic submucosal dissection and endoscopic mucosal resection for early stage esophageal cancer. *Ann Cardiothorac Surg* 2017; **6**: 88-98 [PMID: 28446997 DOI: 10.21037/acs.2017.03.15]
5 **Yu JP**, Liu YJ, Tao YL, Ruan RW, Cui Z, Zhu SW, Shi W. Prevention of Esophageal Stricture After Endoscopic Submucosal Dissection: A Systematic Review. *World J Surg* 2015; **39**: 2955-2964 [PMID: 26335901 DOI: 10.1007/s00268-015-3193-3]
6 **Shi KD**, Ji F. Prophylactic stenting for esophageal stricture prevention after endoscopic submucosal dissection. *World J Gastroenterol* 2017; **23**: 931-934 [PMID: 28246466 DOI: 10.3748/wjg.v23.i6.931]
7 **Jain D**, Singhal S. Esophageal Stricture Prevention after Endoscopic Submucosal Dissection. *Clin Endosc* 2016; **49**: 241-256 [PMID: 26949124 DOI: 10.5946/ce.2015.099]

8 **ASGE Technology Committee.**, Maple JT, Abu Dayyeh BK, Chauhan SS, Hwang JH, Komanduri S, Manfredi M, Konda V, Murad FM, Siddiqui UD, Banerjee S. Endoscopic submucosal dissection. *Gastrointest Endosc* 2015; **81**: 1311-1325 [PMID: 25796422 DOI: 10.1016/j.gie.2014.12.010]

9 **Sakaguchi Y**, Tsuji Y, Ono S, Saito I, Kataoka Y, Takahashi Y, Nakayama C, Shichijo S, Matsuda R, Minatsuki C, Asada-Hirayama I, Niimi K, Kodashima S, Yamamichi N, Fujishiro M, Koike K. Polyglycolic acid sheets with fibrin glue can prevent esophageal stricture after endoscopic submucosal dissection. *Endoscopy* 2015; **47**: 336-340 [PMID: 25314328 DOI: 10.1055/s-0034-1390787]

10 **Kim YJ**, Park JC, Chung H, Shin SK, Lee SK, Lee YC. Polyglycolic acid sheet application to prevent esophageal stricture after endoscopic submucosal dissection for recurrent esophageal cancer. *Endoscopy* 2016; **48**: E319-E320 [PMID: 27706540 DOI: 10.1055/s-0042-117224]

11 **Iizuka T**, Kikuchi D, Yamada A, Hoteya S, Kajiyama Y, Kaise M. Polyglycolic acid sheet application to prevent esophageal stricture after endoscopic submucosal dissection for esophageal squamous cell carcinoma. *Endoscopy* 2015; **47**: 341-344 [PMID: 25412087 DOI: 10.1055/s-0034-1390770]

12 **Yamasaki T**, Tomita T, Takimoto M, Ohda Y, Oshima T, Fukui H, Watari J, Miwa H. Esophageal stricture after endoscopic submucosal dissection treated successfully by temporary stent placement. *Clin J Gastroenterol* 2016; **9**: 337-340 [PMID: 27687827 DOI: 10.1007/s12328-016-0685-0]

13 **Vleggaar FP**. Stent placement in esophageal cancer as a bridge to surgery. *Gastrointest Endosc* 2009; **70**: 620-622 [PMID: 19788979 DOI: 10.1016/j.gie.2009.03.025]

14 **Nagami Y**, Shiba M, Tominaga K, Ominami M, Fukunaga S, Sugimori S, Tanaka F, Kamata N, Tanigawa T, Yamagami H, Watanabe T, Fujiwara Y, Arakawa T. Hybrid therapy with locoregional steroid injection and polyglycolic acid sheets to prevent stricture after esophageal endoscopic submucosal dissection. *Endosc Int Open* 2016; **4**: E1017-E1022 [PMID: 27652294 DOI: 10.1055/s-0042-111906]

15 **Nagami Y**, Ominami M, Shiba M, Minamino H, Fukunaga S, Kameda N, Sugimori S, Machida H, Tanigawa T, Yamagami H, Watanabe T, Tominaga K, Fujiwara Y, Arakawa T. The five-year survival rate after endoscopic submucosal dissection for superficial esophageal squamous cell neoplasia. *Dig Liver Dis* 2017; **49**: 427-433 [PMID: 28096057 DOI: 10.1016/j.dld.2016.12.009]

16 **Kanai N**, Yamato M, Ohki T, Yamamoto M, Okano T. Fabricated autologous epidermal cell sheets for the prevention of esophageal stricture after circumferential ESD in a porcine model. *Gastrointest Endosc* 2012; **76**: 873-881 [PMID: 22867446 DOI: 10.1016/j.gie.2012.06.017]

17 **Nonaka K**, Miyazawa M, Ban S, Aikawa M, Akimoto N, Koyama I, Kita H. Different healing process of esophageal large mucosal defects by endoscopic mucosal dissection between with and without steroid injection in an animal model. *BMC Gastroenterol* 2013; **13**: 72 [PMID: 23617935 DOI: 10.1186/1471-230X-13-72]

18 **Wagh MS**, Forsmark CE, Chauhan S, Draganov PV. Efficacy and safety of a fully covered esophageal stent: a prospective study. *Gastrointest Endosc* 2012; **75**: 678-682 [PMID: 22243830 DOI: 10.1016/j.gie.2011.10.006]

19 **Shah MB**, Jajoo K. Endoscopic retrieval of a migrated esophageal stent in the cecum. *Endoscopy* 2010; **42** Suppl 2: E245-E246 [PMID: 20931463 DOI: 10.1055/s-0030-1255604]

20 **Cheng YS**, Li MH, Chen WX, Chen NW, Zhuang QX, Shang KZ. Temporary partially-covered metal stent insertion in benign esophageal stricture. *World J Gastroenterol* 2003; **9**: 2359-2361 [PMID: 14562413 DOI: 10.3748/wjg.v9.i10.2359]

21 **Tsuji Y**, Ohata K, Gunji T, Shozushima M, Hamanaka J, Ohno A, Ito T, Yamamichi N, Fujishiro M, Matsuhashi N, Koike K. Endoscopic tissue shielding method with polyglycolic acid sheets and fibrin glue to cover wounds after colorectal endoscopic submucosal dissection (with video). *Gastrointest Endosc* 2014; **79**: 151-155 [PMID: 24140128 DOI: 10.1016/j.gie.2013.08.041]

22 **Yamaguchi N**, Isomoto H, Nakayama T, Hayashi T, Nishiyama H, Ohnita K, Takeshima F, Shikuwa S, Kohno S, Nakao K. Usefulness of oral prednisolone in the treatment of esophageal stricture after endoscopic submucosal dissection for superficial esophageal squamous cell carcinoma. *Gastrointest Endosc* 2011; **73**: 1115-1121 [PMID: 21492854 DOI: 10.1016/j.gie.2011.02.005]

23 **Hanaoka N**, Ishihara R, Takeuchi Y, Uedo N, Higashino K, Ohta T, Kanzaki H, Hanafusa M, Nagai K, Matsui F, Iishi H, Tatsuta M, Ito Y. Intralesional steroid injection to prevent stricture after endoscopic submucosal dissection for esophageal cancer: a controlled prospective study. *Endoscopy* 2012; **44**: 1007-1011 [PMID: 22930171 DOI: 10.1055/s-0032-1310107]

24 **Nagami Y**, Shiba M, Tominaga K, Minamino H, Ominami M, Fukunaga S, Sugimori S, Tanigawa T, Yamagami H, Watanabe K, Watanabe T, Fujiwara Y, Arakawa T. Locoregional steroid injection prevents stricture formation after endoscopic submucosal dissection for esophageal cancer: a propensity score matching analysis. *Surg Endosc* 2016; **30**: 1441-1449 [PMID: 26123341 DOI: 10.1007/s00464-015-4348-x]

25 **Hashimoto S**, Kobayashi M, Takeuchi M, Sato Y, Narisawa R, Aoyagi Y. The efficacy of endoscopic triamcinolone injection for the prevention of esophageal stricture after endoscopic submucosal dissection. *Gastrointest Endosc* 2011; **74**: 1389-1393 [PMID: 22136782 DOI: 10.1016/j.gie.2011.07.070]

P- Reviewer: Sato Y, Rodrigo L **S- Editor**: Wang JL
L- Editor: Wang TQ **E- Editor**: Huang Y

World Journal of Gastroenterology

Submit a Manuscript: http://www.f6publishing.com

World J Gastroenterol 2018 March 7; 24(9): 1056-1062

DOI: 10.3748/wjg.v24.i9.1056

ISSN 1007-9327 (print) ISSN 2219-2840 (online)

CASE REPORT

Four cancer cases after esophageal atresia repair: Time to start screening the upper gastrointestinal tract

Floor WT Vergouwe, Madeleine Gottrand, Bas PL Wijnhoven, Hanneke IJsselstijn, Guillaume Piessen, Marco J Bruno, René MH Wijnen, Manon CW Spaander

Floor WT Vergouwe, Marco J Bruno, Manon CW Spaander, Department of Gastroenterology and Hepatology, Erasmus MC University Medical Center, Rotterdam 3000 CA, Netherlands

Floor WT Vergouwe, Hanneke IJsselstijn, René MH Wijnen, Department of Pediatric Surgery, Erasmus MC University Medical Center - Sophia Children's Hospital, Rotterdam 3000 CB, Netherlands

Madeleine Gottrand, Department of Pediatrics, Jeanne de Flandre Children's Hospital - Univ. Lille, CHU Lille, Lille 59000, France

Bas PL Wijnhoven, Department of Surgery, Erasmus MC University Medical Center, Rotterdam 3000 CA, Netherlands

Guillaume Piessen, Department of Digestive and Oncological Surgery, Claude Huriez Hospital - Univ. Lille, CHU Lille, Lille 59000, France

ORCID number: Floor WT Vergouwe (0000-0002-8599-4264); Madeleine Gottrand (0000-0002-2908-6931); Bas PL Wijnhoven (0000-0003-4738-3697); Hanneke IJsselstijn (0000-0001-5824-3492); Guillaume Piessen (0000-0001-8243-8310); Marco J Bruno (0000-0001-9181-5499); René MH Wijnen (0000-0001-7266-9713); Manon CW Spaander (0000-0002-9103-9757).

Author contributions: Vergouwe FWT, Gottrand M, Wijnhoven BPL and Piessen G collected clinical data; Vergouwe FWT, IJsselstijn H and Spaander MCW designed the manuscript; Vergouwe FWT, IJsselstijn H and Spaander MCW interpreted the data and drafted the manuscript; Gottrand M, Wijnhoven BPL, Piessen G, Bruno MJ and Wijnen RMH interpreted the data and critically revised the manuscript; all authors gave their final approval of the version of the article to be published.

Informed consent statement: Informed consent was waived since all handling to the subjects was part of standard clinical care.

Conflict-of-interest statement: All authors have no conflicts of interest to declare.

Manuscript source: Unsolicited manuscript

Correspondence to: Manon CW Spaander, MD, PhD, Associate Professor, Department of Gastroenterology and Hepatology, Erasmus MC University Medical Center, P.O. Box 2040, Rotterdam 3000 CA, Netherlands. v.spaander@erasmusmc.nl
Telephone: +31-10-7035643
Fax: +31-10-7035172

Received: October 26, 2017
Peer-review started: October 28, 2017
First decision: November 22, 2017
Revised: December 4, 2017
Accepted: January 24, 2018
Article in press: January 24, 2018
Published online: March 7, 2018

Abstract

Esophageal atresia (EA) is one of the most common congenital digestive malformations and requires surgical correction early in life. Dedicated centers have reported survival rates up to 95%. The most frequent comorbidities after EA repair are dysphagia (72%) and gastroesophageal reflux (GER) (67%). Chronic GER after EA repair might lead to mucosal damage, esophageal stricturing, Barrett's esophagus and eventually esophageal adenocarcinoma. Several long-term follow-up studies found an increased risk of

Barrett's esophagus and esophageal carcinoma in EA patients, both at a relatively young age. Given these findings, the recent ESPGHAN-NASPGHAN guideline recommends routine endoscopy in adults born with EA. We report a series of four EA patients who developed a carcinoma of the gastrointestinal tract: three esophageal carcinoma and one colorectal carcinoma in a colonic interposition. These cases emphasize the importance of lifelong screening of the upper gastrointestinal tract in EA patients.

Key words: Adenocarcinoma; Esophageal atresia; Esophageal cancer; Screening; Barrett's esophagus; Squamous cell carcinoma

Core tip: Esophageal atresia (EA) is a common congenital malformation that requires surgical correction early in life. Improved perioperative care and surgical techniques have increased the survival rate. Gastroesophageal reflux and stasis are common after surgical repair and may be associated with an increased esophageal cancer risk. However, data on incidence and risk factors for esophageal carcinogenesis after EA repair are scarce. The recent ESPGHAN-NASPGHAN guideline recommends routine endoscopy in adults born with EA. Here we report four cancer cases at a relatively young age after EA repair: three esophageal carcinoma and one colorectal carcinoma in a colonic interposition.

Vergouwe FW, Gottrand M, Wijnhoven BP, IJsselstijn H, Piessen G, Bruno MJ, Wijnen RM, Spaander MC. Four cancer cases after esophageal atresia repair: Time to start screening the upper gastrointestinal tract. *World J Gastroenterol* 2018; 24(9): 1056-1062 Available from: URL: http://www.wjgnet.com/1007-9327/full/v24/i9/1056.htm DOI: http://dx.doi.org/10.3748/wjg.v24.i9.1056

INTRODUCTION

With a prevalence of 2.43 per 10000 births, esophageal atresia (EA) with or without a tracheoesophageal fistula (TEF) is one of the most common congenital digestive malformations[1]. Surgical correction needs to be performed shortly after birth. Due to advanced surgical techniques and improved perioperative care, survival rate has increased up to 95% in dedicated centers[2,3]. Follow-up studies have shown that most EA patients have a favourable long-term outcome despite persistant digestive and respiratory problems. Common gastrointestinal symptoms after EA repair are dysphagia and gastroesophageal reflux (GER) in up to 72% and 67% of the patients, respectively[4,5]. Chronic GER after EA repair might lead to mucosal damage, esophageal stricturing, Barrett's esophagus and eventually esophageal adenocarcinoma (EAC)[5-8]. Data on incidence and risk factors for esophageal carcinogenesis after EA repair are scarce[8-10]. The recent ESPGHAN-NASPGHAN guideline recommends routine endoscopy in adults born with EA[11]. Until now, eight cases of esophageal cancer in young EA patients have been described: five esophageal squamous cell carcinoma (ESCC) and three EAC[10,12-15]. Here we report four EA patients who developed a carcinoma of the gastrointestinal tract: three esophageal carcinoma and one colorectal carcinoma in a colonic interposition. These cases emphasize the importance of lifelong screening and surveillance of the upper gastrointestinal tract in EA patients.

CASE REPORT

Case 1

Patient A presented for the first time with esophageal carcinoma at age 45 years. He was born with EA Gross type C (with a distal TEF) which was surgically repaired with closing of the fistula and end-to-end anastomosis of the esophagus. In childhood he had undergone a number of esophageal dilations to treat an anastomotic stricture.

At the age of 37 years he developed progressive dysphagia. Upper endoscopy showed proximal esophagitis and a stenotic anastomosis, which then was dilated. No biopsies were taken. Eight years later, dysphagia for solid foods reoccurred with complaints of heartburn and weight loss of 6 kg in six months (BMI 21.6 kg/m^2). He was a tobacco smoker (at least 27 pack years) and used 3-4 alcoholic beverages per day. Upper endoscopy showed a non-stenotic anastomosis at 30 cm from the incisors with a ¾ circular growing easily bleeding lesion from 33-42 cm from the incisors. Biopsies showed chronic inflammation. A chest CT scan revealed a stenotic esophagus extending from the aortic arch to the cardia with a malignant appearance and mediastinal lymph nodes (pre- and subcarinal). Due to the strong suspicion of esophageal cancer an esophageal resection with gastric tube reconstruction was performed. Pathology results confirmed the diagnosis of a squamous cell carcinoma (SCC) of the distal esophagus (pT2N0M0) which did not need further treatment.

Fifteen years later, at the age of 60 years, he again developed dysphagia and odynophagia with 7 kg weight loss (BMI 23.2 kg/m^2). Endoscopy revealed a circular tumor (17-21 cm from incisors) in the remaining cervical native esophagus eroding the constructed gastric tube and trachea. Biopsies showed a well-differentiated SCC. One suspicious supraclavicular and two mediastinal FDG-positive lymph nodes were seen on PET-CT scan images and tumor invasion in the left thyroid gland was suspected (Figure 1). Given the long interval between the two malignancies, this new

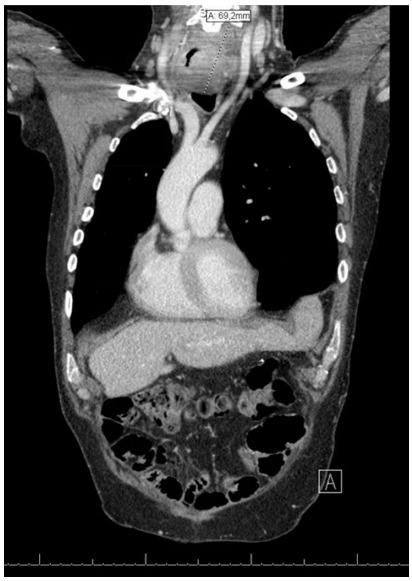

Figure 1 Chest computed tomography scan (CT scan) (case 1, tumor 2) demonstrating a tumor mass in the cervical native esophagus with suspected tumor invasion in the left thyroid gland.

tumor (T4bN2M0) was most likely a second primary tumor in the remaining cervical esophagus. In a multidisciplinary team discussion it was decided to treat with induction chemotherapy (carboplatin/paclitaxel). Initially the tumor responded well, but four months later he suffered from progressive disease with fistula formation to the trachea which was a contraindication for additional radiotherapy. An esophageal stent was placed to manage progressive dysphagia and palliative radiotherapy (13 × 3 Gy) was started to manage neuropathic pain caused by tumor invasion with imminent spinal cord compression. He died two days later.

Case 2

Patient B was a 42-year old man born with VACTERL association (acronym: vertebral anomalies, anal atresia, cardiac anomalies, TEF, renal anomalies, and limb defects)[16] including EA Gross type A (long gap without TEF), anorectal malformation, coccyx agenesis and vertebral anomalies. Continuity of the esophagus was restored with a delayed end-to-end anastomosis.

At 37 years of age he presented with dysphagia. Upper endoscopy revealed a stenotic anastomosis at 30 cm from the incisors, which could be easily dilated. In the next two years he underwent another three esophageal dilation procedures because of recurrent dysphagia. Biopsies revealed chronic and active inflammation with presence of hyphae. At the age of 42 years he presented with progressive dysphagia, without weight loss (BMI 17.6 kg/m^2). He smoked tobacco and drank alcoholic beverages only in the weekend. This time upper endoscopy revealed a circular stenotic ulcerative ESCC in the proximal esophagus (22-29 cm, anastomosis not visible) (Figure 2A). Endoscopic ultrasound findings were suspicious for tumor invasion in the trachea and several potentially malignant regional lymph nodes (T4N2M0). The tumor was considered unresectable due to invasion of surrounding vital structures (cT4b) (Figure 2B), lymph node metastases, previous thoracotomies (both sides) and intra-mediastinal surgery. Induction chemotherapy (paclitaxel/carboplatin) was started to which the tumor evidently had responded after 2 mo. Concomitant chemoradiotherapy was given (28 × 1.8 Gy) with curative intent. Six years after treatment he shows no signs of recurrent or metastatic disease.

Case 3

Patient C presented at the age of 36 years. She was born with an EA Gross type A which was surgically repaired with an end-to-end anastomosis using Livaditis elongation procedure at one month of age. At one year of age she underwent a Nissen fundoplication for severe GER. At the age of 3 years, an anastomotic stricture developed which was treated with repeated esophageal dilations. At the age of 22 years she presented with chronic respiratory symptoms, severe pneumonia, persistent GER, and dysphagia complaints. Upper endoscopy with esophageal biopsies showed no abnormality. In view of the respiratory and gastrointestinal symptoms a duodenal diversion procedure (partial antrectomy with Roux-en-Y gastrojejunal anastomosis) was performed at the age of 23 years.

At 36 years of age she presented with food impaction and weight loss of 4 kg (BMI 14.9 kg/m^2). She did not smoke tobacco and did not drink alcoholic beverages. Upper endoscopy revealed a stenotic ulcerative tumor in the distal esophagus with proximal dilation of the esophagus (25-32 cm from the incisors, gastroesophageal junction at 34 cm, anastomosis not visible). Biopsies revealed a well differentiated SCC. PET-CT scan (Figure 3) and bronchoscopy did not reveal any metastasis. She underwent a subtotal esophagectomy with total gastrectomy and a colonic interposition (pT1bN0M0). Within the following month she required reoperation for a cervical fistula and mediastinitis and underwent two endoscopic dilations of an anastomotic stricture without any evidence of tumor recurrence. Twelve months after surgery she was diagnosed with pleural and bone metastases for which she recently has started palliative chemotherapy.

Case 4

Patient D presented at the age of 47 years. He was born with VACTERL association[16](EA Gross type C, anorectal malformation, congenital urethral valves with bilateral vesicoureteral reflux and hydronephrosis left kidney). At day 5 after birth a thoracotomy was performed with TEF closure, gastrostomy and cervical esophagostomy placement. In addition the

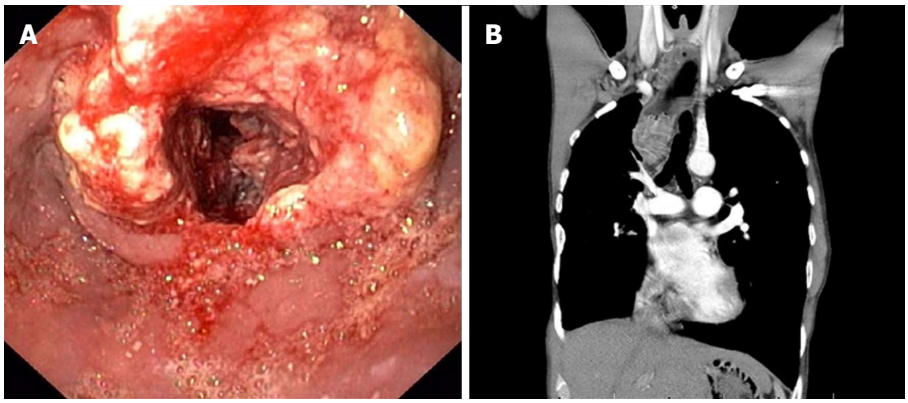

Figure 2 Findings at upper endoscopy and chest computed tomography scan (CT scan) (case 2). A: Upper endoscopy revealing a stenotic ulcerative tumor in the proximal esophagus, 22-29 cm from incisors. Histological examination of esophageal biopsies confirmed the diagnosis esophageal squamous cell carcinoma. B: Chest CT scan showing a tumor mass in the proximal esophagus with suspected tumor invasion in the trachea.

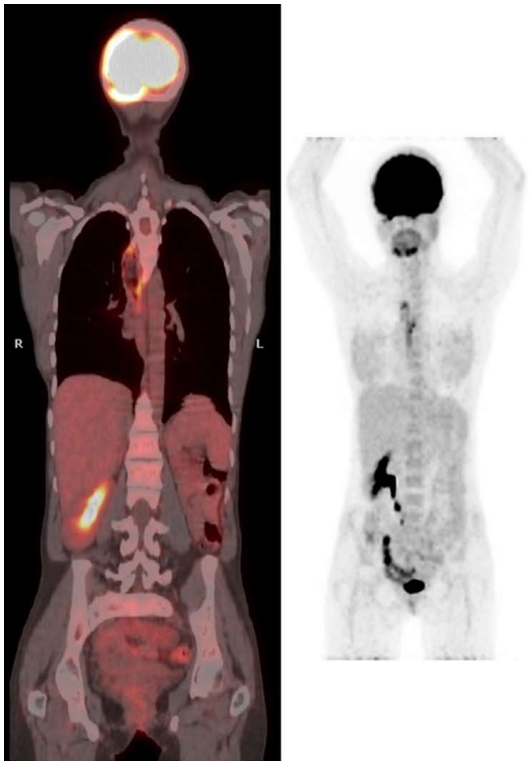

Figure 3 Initial findings at positron emission tomography-computed tomography scan (PET-CT scan) (case 3), showing PET-positive lesion in the distal esophagus without metastasis.

anorectal malformation was corrected. Nine days later a recurrent TEF was ligated. At day 29 the distal esophagus was ligated directly above the stomach and after 7 mo a colonic interposition was constructed. The spleen was congested and therefore resected during this surgery. Revision was needed because of leakage of the proximal anastomosis 19 days later. At 2.5 year of age the gastrostomy was closed. Other medical history included asthmatic bronchitis, bilateral orchidopexy, transurethral resection of urethral valves and nephrectomy of an afunctional infected left kidney.

At presentation the patient suffered from pneumonia with a density in the lower lobe of the right lung. Subsequent PET-scan revealed a PET-positive thickening in the colonic interposition for which he had been referred to our center. He complained about progressive dysphagia without any weight loss (BMI 18.6 kg/m^2). He was a cannabis smoker (2 joints/wk), had quit tobacco smoking just before presentation (a few cigarettes per day) and only sporadically drank alcoholic beverages. Upper endoscopy revealed the proximal and distal anastomosis of the colonic interposition at, respectively, 21 and 47 cm from incisors. From 26-30 cm from incisors a tumor was visible in the colon interposition which could be easily passed with the scope. Histology revealed a moderately differentiated adenocarcinoma. No abnormalities were found at colonoscopy. PET-CT scan showed circumferential thickening of the colonic interposition over a length of 10 cm, not clearly separated from the thyroid and left brachiocephalic vein, a small lesion in the lower right lobe of the lung (PET-negative) and a few locoregional lymph nodes ($\leqslant$ 1 cm, PET-negative) (Figure 4 A and B).

Patient D was treated with induction chemotherapy (capecitabine/oxaliplatin) to enable maximum tumor regression. After six treatments, the colonic interposition was resected and an esophagostomy and jejunal fistula for feeding were created. Pathological examination confirmed the diagnosis of colonic adenocarcinoma with a maximum diameter of 4.1 cm, tumor free resection margins ($\geqslant$ 1 cm) and one of 19 lymph nodes positive for metastasis (ypT2N1). Family history was negative for Lynch Syndrome. Both pentaplex microsatellite instability testing and mismatch repair gene expression analysis for MLH1, MSH2, MSH6 and PMS2 were normal.

After 4 mo continuity was restored by a subcutaneous gastric tube pull-up. At oncological follow-up one year after resection of the colonic interposition patient D did not experience any dysphagia, weight was stable (BMI 19.7 kg/m^2) and ultrasound of the liver and

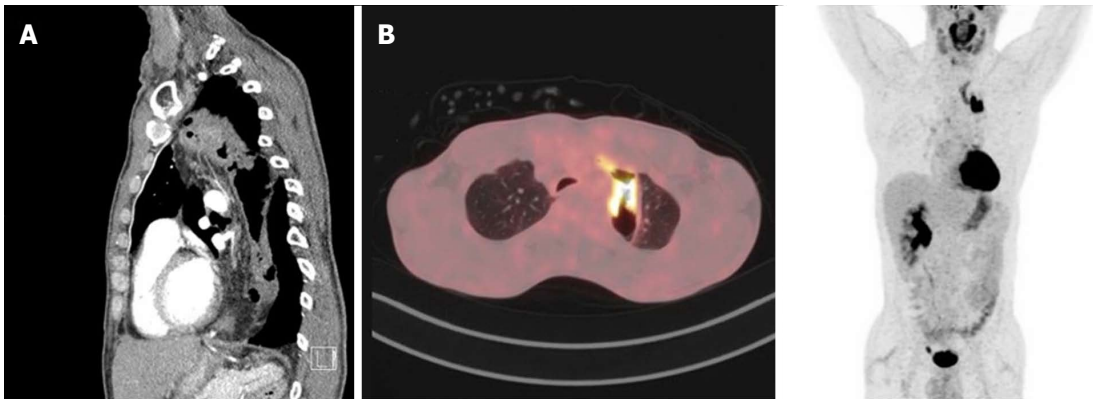

Figure 4 Initial findings at positron emission tomography-computed tomography scan (PET-CT scan) (case 4). A: Chest CT scan image with a circumferential wall thickening of the thoracic colonic interposition over a length of 10 cm, not clearly separated from the thyroid and left brachiocephalic vein. Locoregional suspected lymph nodes (< 1 cm). B: PET-CT scan showing a PET-positive lesion in the thoracic colonic interposition. No PET-positive lesions or lymph nodes.

CEA were normal (2.72 μg/L).

DISCUSSION

We presented four cases of gastrointestinal cancer that have developed more than 30 years after surgical treatment of EA: three esophageal carcinoma and one unusual presentation of colorectal carcinoma in a colonic interposition. These patients' relatively young age, the fact that only few carcinogenic factors were identified and the high incidence of cancer development in a low prevalence disease suggest that EA carries an increased risk for esophageal cancer development and therefore screening and surveillance may be warranted, as recommended in the ESPGHAN-NASPGHAN guideline[11].

Esophageal cancer is the 8th most common cancer worldwide, with an incidence rate of 6.4 and 1.2 per 100000 males and females respectively in developed countries and 10.1 and 4.1 per 100000 males and females, respectively, in less developed countries[17]. ESCC and EAC have different etiologies. ESCC arrises from dysplastic squamous epithelium and is associated with a low socioeconomic status, use of tobacco or alcohol, several dietary factors, and human papilloma virus[18,19]. The main risk factors for EAC are GER, use of tobacco, obesity, and hiatal hernia[18]. Chronic GER might lead to gastric and intestinal metaplasia of the squamous epithelium in the esophagus, known as Barrett's esophagus, which predisposes to dysplasia and EAC. GER is present in up to 67% of the adult EA patients and is likely to contribute to EAC development[5]. However, in literature - and also in our case series - ESCC is more common than EAC in EA patients[10,12-15]. The reason for this high risk of ESCC development has not yet been established. The pathogenesis might be the same as in achalasia, where ESCC is thought to result from stasis, causing bacterial overgrowth with nitrosamine production and subsequent esophageal inflammation, dysplasia and cancer[20,21]. Most of the ESCC in EA patients were found near or at the anastomosis (mid-distal esophagus). It has been suggested, therefore, that frequent dilation procedures with associated mucosal tears, scarring and inflammation may lead to development of ESCC in this patient group[10,12]. Mitomycin-C, an antifibrotic applicant used to prevent recurrence of strictures, may be an additional risk factor for ESCC, but this was not used in any of the patients in present case series[22]. Moreover, genetic predisposition may contribute to esophageal cancer in EA patients and is subject to future studies.

Endoscopic surveillance of EA patients is advocated to detect lesions at an early stage[11]. Those treated with a colonic interposition should not be excluded from surveillance, as carcinoma could arise in the cervical native esophagus or thoracic colon. More data on the actual incidence of esophageal cancer development in adulthood will hopefully become available soon when surveillance programs have been implemented. Together with the identification of risk factors this will help to optimize surveillance strategies in EA patients. Until then, pediatric surgeons and gastroenterologists who are involved in treatment of EA patients should be made aware of the cancer risk and be encouraged to reach consensus on optimal surveillance. When EA patients reach adulthood, they should be transferred to a gastroenterologist for endoscopic surveillance.

ARTICLE HIGHLIGHTS

Case characteristics

At presentation (age 36-47 years) all four patients born with esophageal atresia (EA) complained of progressive dysphagia, and two of them had lost weight.

Clinical diagnosis

Clinical diagnosis was made by upper endoscopy, revealing a for potentially malignant circular stenotic lesion in the esophagus in three cases and a tumor in the colonic interposition in one case.

Differential diagnosis

The differential diagnosis included severe ulcerative esophagitis, benign stenotic anastomosis, and motility disorder.

Laboratory diagnosis

Carcinoembryonic antigen (CEA) was measured (normal) in the patient with a colonic adenocarcinoma in the colonic interposition.

Imaging diagnosis

In addition to upper endoscopy a positron emission tomography-computed tomography scan (PET-CT scan) - in combination with endoscopic ultrasound in one case - was performed, which revealed a stenotic esophagus in three cases; a circumferential thickening of the colonic interposition in one case; potentially malignant lymph nodes in three cases; and suspected tumor invasion in two cases.

Pathological diagnosis

Histology and immunohistochemistry results confirmed the diagnosis of squamous cell carcinoma of the esophagus in three cases and adenocarcinoma of the colonic interposition in one case, in the latter case pentaplex microsatellite instability testing and mismatch repair gene expression analysis for MLH1, MSH2, MSH6 and PMS2 were normal.

Treatment

The esophageal cancer patients underwent (sub)total esophagectomy with reconstruction (curative intent); received induction chemotherapy (paclitaxel/carboplatin) followed by chemoradiotherapy (curative intent); or received palliative radiotherapy or chemotherapy. The patient with colon cancer was treated with induction chemotherapy (capecitabine/oxaliplatin) followed by resection of the colonic interposition with construction of an esophagostoma and jejunal fistula for feeding.

Related reports

Up to two-thirds of EA patients suffer from gastroesophageal reflux, which in the long-term might lead to mucosal damage including Barrett's esophagus and esophageal adenocarcinoma. As dysphagia is common (up to 72%) after EA repair, this symptom may be neglected as an early warning symptom of esophageal cancer in these patients. Up till now, eight esophageal cancer cases have been described in young EA patients.

Term explanation

EA with or without tracheoesophageal fistula (TEF) is a common congenital malformation and requires surgical correction early in life. The Gross classification divides five types of EA: type A (isolated EA), type B (EA with proximal TEF), type C (EA with distal TEF), type D (EA with dual TEF's) or type E (isolated TEF).

VACTERL is an acronym that describes a nonrandom association of birth defects: Vertebral anomalies, Anal atresia, Cardiac anomalies, TEF, Renal anomalies, and Limb defects.

Experiences and lessons

These patients' relatively young age, the fact that only few carcinogenic factors were identified and the high incidence of cancer development in a low prevalence disease suggest that EA carries an increased risk for esophageal cancer development. This emphasizes the importance of lifelong screening and surveillance of the upper gastrointestinal tract in EA patients.

REFERENCES

1 **Pedersen RN**, Calzolari E, Husby S, Garne E; EUROCAT Working group. Oesophageal atresia: prevalence, prenatal diagnosis and associated anomalies in 23 European regions. *Arch Dis Child* 2012; **97**: 227-232 [PMID: 22247246 DOI: 10.1136/archdischild-2011-300597]

2 **Wang B**, Tashiro J, Allan BJ, Sola JE, Parikh PP, Hogan AR, Neville HL, Perez EA. A nationwide analysis of clinical outcomes among newborns with esophageal atresia and tracheoesophageal fistulas in the United States. *J Surg Res* 2014; **190**: 604-612 [PMID: 24881472 DOI: S0022-4804(14)00433-8]

3 **Sulkowski JP**, Cooper JN, Lopez JJ, Jadcherla Y, Cuenot A, Mattei P, Deans KJ, Minneci PC. Morbidity and mortality in patients with esophageal atresia. *Surgery* 2014; **156**: 483-491 [PMID: 24947650 DOI: S0039-6060(14)00109-3]

4 **Rintala RJ**, Pakarinen MP. Long-term outcome of esophageal anastomosis. *Eur J Pediatr Surg* 2013; **23**: 219-225 [PMID: 23737132 DOI: 10.1055/s-0033-1347912]

5 **Vergouwe FW**, IJsselstijn H, Wijnen RM, Bruno MJ, Spaander MC. Screening and Surveillance in Esophageal Atresia Patients: Current Knowledge and Future Perspectives. *Eur J Pediatr Surg* 2015; **25**: 345-352 [PMID: 26302062 DOI: 10.1055/s-0035-1559817]

6 **Huynh Trudeau V**, Maynard S, Terzic T, Soucy G, Bouin M. Dysphagia among adult patients who underwent surgery for esophageal atresia at birth. *Can J Gastroenterol Hepatol* 2015; **29**: 91-94 [PMID: 25803019]

7 **Taylor AC**, Breen KJ, Auldist A, Catto-Smith A, Clarnette T, Crameri J, Taylor R, Nagarajah S, Brady J, Stokes K. Gastroesophageal reflux and related pathology in adults who were born with esophageal atresia: a long-term follow-up study. *Clin Gastroenterol Hepatol* 2007; **5**: 702-706 [PMID: 17544997 DOI: S1542-3565(07)00285-6]

8 **Sistonen SJ**, Koivusalo A, Nieminen U, Lindahl H, Lohi J, Kero M, Kärkkäinen PA, Färkkilä MA, Sarna S, Rintala RJ, Pakarinen MP. Esophageal morbidity and function in adults with repaired esophageal atresia with tracheoesophageal fistula: a population-based long-term follow-up. *Ann Surg* 2010; **251**: 1167-1173 [PMID: 20485152 DOI: 10.1097/SLA.0b013e3181c9b613]

9 **Sistonen SJ**, Koivusalo A, Lindahl H, Pukkala E, Rintala RJ, Pakarinen MP. Cancer after repair of esophageal atresia: population-based long-term follow-up. *J Pediatr Surg* 2008; **43**: 602-605 [PMID: 18405703 DOI: S0022-3468(07)00982-7]

10 **Jayasekera CS**, Desmond PV, Holmes JA, Kitson M, Taylor AC. Cluster of 4 cases of esophageal squamous cell cancer developing in adults with surgically corrected esophageal atresia--time for screening to start. *J Pediatr Surg* 2012; **47**: 646-651 [PMID: 22498376 DOI: S0022-3468(11)00837-2]

11 **Krishnan U**, Mousa H, Dall'Oglio L, Homaira N, Rosen R, Faure C, Gottrand F. ESPGHAN-NASPGHAN Guidelines for the Evaluation and Treatment of Gastrointestinal and Nutritional Complications in Children With Esophageal Atresia-Tracheoesophageal Fistula. *J Pediatr Gastroenterol Nutr* 2016; **63**: 550-570 [PMID: 27579697 DOI: 10.1097/MPG.0000000000001401]

12 **Deurloo JA**, van Lanschot JJ, Drillenburg P, Aronson DC. Esophageal squamous cell carcinoma 38 years after primary repair of esophageal atresia. *J Pediatr Surg* 2001; **36**: 629-630 [PMID: 11283893 DOI: S0022-3468(01)36587-9]

13 **Adzick NS**, Fisher JH, Winter HS, Sandler RH, Hendren WH. Esophageal adenocarcinoma 20 years after esophageal atresia repair. *J Pediatr Surg* 1989; **24**: 741-744 [PMID: 2769539 DOI: S0022346889002757]

14 **Alfaro L**, Bermas H, Fenoglio M, Parker R, Janik JS. Are patients who have had a tracheoesophageal fistula repair during infancy at risk for esophageal adenocarcinoma during adulthood? *J Pediatr Surg* 2005; **40**: 719-720 [PMID: 15852288 DOI: S0022346805000217]

15 **Pultrum BB**, Bijleveld CM, de Langen ZJ, Plukker JT. Development of an adenocarcinoma of the esophagus 22 years after primary repair of a congenital atresia. *J Pediatr Surg* 2005; **40**: e1-e4 [PMID: 16338286 DOI: S0022-3468(05)00647-0]

16 **Solomon BD**, Baker LA, Bear KA, Cunningham BK, Giampietro PF, Hadigan C, Hadley DW, Harrison S, Levitt MA, Niforatos N, Paul SM, Raggio C, Reutter H, Warren-Mora N. An approach to the identification of anomalies and etiologies in neonates with identified or suspected VACTERL (vertebral defects, anal atresia, tracheo-esophageal fistula with esophageal atresia, cardiac anomalies, renal

anomalies, and limb anomalies) association. *J Pediatr* 2014; **164**: 451-457.e1 [PMID: 24332453 DOI: 10.1016/j.jpeds.2013.10.086]

17 **Torre LA**, Bray F, Siegel RL, Ferlay J, Lortet-Tieulent J, Jemal A. Global cancer statistics, 2012. *CA Cancer J Clin* 2015; **65**: 87-108 [PMID: 25651787 DOI: 10.3322/caac.21262]

18 **Kamangar F**, Chow WH, Abnet CC, Dawsey SM. Environmental causes of esophageal cancer. *Gastroenterol Clin North Am* 2009; **38**: 27-57, vii [PMID: 19327566 DOI: S0889-8553(09)00006-5]

19 **Zhang SK**, Guo LW, Chen Q, Zhang M, Liu SZ, Quan PL, Lu JB, Sun XB. The association between human papillomavirus 16 and esophageal cancer in Chinese population: a meta-analysis. *BMC Cancer* 2015; **15**: 1096 [PMID: 25777422 DOI: 10.1186/s12885-015-1096-1]

20 **Sandler RS**, Nyrén O, Ekbom A, Eisen GM, Yuen J, Josefsson S. The risk of esophageal cancer in patients with achalasia. A population-based study. *JAMA* 1995; **274**: 1359-1362 [PMID: 7563560]

21 **Pajecki D**, Zilberstein B, Cecconello I, Dos Santos MA, Yagi OK, Gama-Rodrigues JJ. Larger amounts of nitrite and nitrate-reducing bacteria in megaesophagus of Chagas' disease than in controls. *J Gastrointest Surg* 2007; **11**: 199-203 [PMID: 17390173 DOI: 10.1007/s11605-006-0066-y]

22 **Chapuy L**, Pomerleau M, Faure C. Topical mitomycin-C application in recurrent esophageal strictures after surgical repair of esophageal atresia. *J Pediatr Gastroenterol Nutr* 2014; **59**: 608-611 [PMID: 24590215 DOI: 10.1097/MPG.0000000000000352]

P- Reviewer: De Lusong MAA, Thota PN, Wani HU
S- Editor: Gong ZM **L- Editor**: A **E- Editor**: Huang Y

Published by **Baishideng Publishing Group Inc**
7901 Stoneridge Drive, Suite 501, Pleasanton, CA 94588, USA
Telephone: +1-925-223-8242
Fax: +1-925-223-8243
E-mail: bpgoffice@wjgnet.com
Help Desk: http://www.f6publishing.com/helpdesk
http://www.wjgnet.com

ISSN 1007-9327